Kielce University of Technology

Koszalin University of Technology

National Academy of Sciences of Ukraine

Institute of Engineering Thermophysics

The European Academy of Education and Science

National Technical University of Ukraine

University of Zagreb

University of Žilina

Vilnius Gediminas Technical University

VI International Scientific-Technical Conference

Book of abstracts

ACTUAL PROBLEMS OF RENEWABLE ENERGY, CONSTRUCTION AND ENVIRONMENTAL ENGINEERING

24-27 November 2022, Kielce
(Poland, Ukraine, Croatia, Slovakia, Lithuania)

The time and place of the meeting: 24-27 November 2022
Faculty of Environmental, Geomatic and Energy Engineering
Kielce University of Technology, Poland
al. Tysiąclecia Państwa Polskiego 7, 25-314 Kielce

Beginning of conference: 24 November 2022 in 10:00
Phones for information: +48 41 34 24 850; +48 883 74 12 91
e-mail: apavlenko@tu.kielce.pl, wisge@tu.kielce.pl

Conference languages: Polish, English, Ukrainian

Conference Chairs:

Anatoliy Pavlenko
prof. doctor of science Head of Department of Building Physics and Renewable Energy, Kielce University of Technology

KIELCE 2022

ISBN 978-83-66678-37-8

VI International
Scientific-Technical Conference

Book of abstracts

ACTUAL PROBLEMS OF RENEWABLE ENERGY, CONSTRUCTION AND ENVIRONMENTAL ENGINEERING

The time and place of the meeting: 24-27 November 2022
Faculty of Environmental, Geomatic and Energy Engineering
Kielce University of Technology, Poland
al. Tysiąclecia Państwa Polskiego 7, 25-314 Kielce

Conference Chairs:

Anatoliy Pavlenko
prof. doctor of science Head of Department of Building Physics
and Renewable Energy, Kielce University of Technology

KIELCE 2022

The organizers:

- Kielce University of Technology, Faculty of Environmental, Geomatic and Energy Engineering (Poland)
- Koszalin University of Technology, Faculty of Civil Engineering, Environment and Geodetic Sciences (Poland)
- Institute of Engineering Thermophysics National Academy of Sciences of Ukraine (Ukraine)
- The European Academy of Education and Science (Poland)
- National Technical University of Ukraine "Igor Sikorsky Kyiv Polytechnic Institute" (Ukraine)
- University of Zagreb Faculty of Metallurgy (Croatia)
- University of Žilina Department of Power Engineering (Slovakia)
- Vilnius Gediminas Technical University (Lithuania)

Scientific and organizing committee of the conference:

Co-organizers (Scientific committee):

- Prof. doctor of science ANATOLIY PAVLENKO – Head of Department of Building Physics and Renewable Energy, Kielce University of Technology (Poland)
- Prof. PŚk doctor of science LIDIA DĄBEK – Scientific Director of the Discipline Environmental Engineering, Mining and Energy, Kielce University of Technology (Poland)
- Prof. doctor of science HANNA KOSHLAK – Department of Building Physics and Renewable Energy, Kielce University of Technology (Poland)
- Prof. doctor of science ENGVALL KLAS – KTH (Sweden)
- Prof. doctor of science LADISLAV LAZIĆ – Faculty of Metallurgy University of Zagreb (Croatia)
- Prof. doctor of science MILAN MALCHO – Head of Department of Power Engineering (Slovakia)
- Doctor of science ANDREJ KAPJOR – Department of Power Engineering (Slovakia)
- Prof. doctor of science, Corresponding Member of NAS of Ukraine BORYS BASOK – Head of Department "Thermophysical Basics of Energy-Saving Technologies" Institute of Engineering Thermophysics National Academy of Sciences of Ukraine (Ukraine)
- Doctor of science HELEN SKOP – Smart heat corporation (USA)
- Prof. doctor of science VIOLETA MOTUZIENĖ – Vilnius Gediminas Technical University (Lithuania)
- Prof. doctor of science ZONGMING YANG – Jiangsu University of Science and Technology (China)
- Prof. doctor of science VALERII DESHKO – National Technical University of Ukraine "Igor Sikorsky Kyiv Polytechnic Institute" (Ukraine)

ISBN 978-83-66678-37-8

Regulations:

in the plenary – to 20 min
at the meetings sectional – 10-15 min
speaking – to 5 min

The general program of the ConferenceTime	Time	Place	Moderator
Registration of participants	24 November 2022 10:00-10:45		The Organizing Committee
This opening session, plenary session Anatoliy Pavlenko *Promising renewable energy sources* Borys Basok *Municipal energy of Ukraine current state and trend of post-war development* **Violeta Motuzienė** *Energy Performance Gap in New Existing Buildings*	25 November 2022 11:00-12:00	4.09E	Prof. doctor of science Anatoliy Pavlenko Prof. doctor of science **Violeta Motuzienė** Prof. doctor of science Borys Basok Prof. doctor of science **Ladislav Lazić** Prof. doctor of science Milan Malcho Prof. doctor of science Hanna Koshlak Prof. doctor of science **Lidia Dąbek**
Actu**al problems of building** physics	25 November 2022 12:30-14:00	1.15E	Prof. doctor of science Valerii Deshko
Actual problems of environmental engineering and ecology	25 November 2022 12:30-14:00	1.20E	Prof. doctor of science Hanna Koshlak
Actual problems of thermal and renewable energy	25 November 2022 12:30-14:00	1.08E	Prof. doctor of science **Violeta Motuzienė**
Actual **problems** fundamental heat and mass transfer	25 November 2022 12:30-14:00	1.09E	Prof. doctor of science **Łukasz Orman**
Theoretical foundations of thermal machines	25 November 2022 12:30-14:00	2.19E	Prof. doctor of science Milan Malcho
Actual problems of quantitative assessment of the low-carbon energy and industry	25 November 2022 12:30-14:00	2.20E	Prof. doctor of science Anatoliy Pavlenko
Thermophysics of the interaction of a building with the environment	25 November 2022 12:30-14:00	1.14E	Prof. doctor of science Borys Basok
Continued work of section	26 November 2022 12:30-14:00		The section moderators
Discussion	26 November 2022 14:15-15:30		The section moderators
Summary and the closing of the conference	27 November 2022 16:00	4.09E	The Organizing Committee

Anatoliy Pavlenko – Head of Department of Building Physics and Renewable Energy, Kielce University of Technology, Poland.
Scientific direction of work – thermophysics of dispersed media.
Scientific interest – mathematical modeling of thermophysical processes occurring in liquids in the metastable state.

Dear Colleagues,

I cordially greet all participants of our 6th international conference.

For five years now our Conference traditionally consolidates all those best scientific ideas, that authors present in their speeches.

All these years we examines the questions and problems of modern power engineering, energy technology of power-consuming industry branches, alternative sources of energy, resource conservation, questions of modeling the process of industrial equipment, processes and equipment of various branches of industry, questions of automated control systems and information processing, heat-and mass-exchanging processes and equipment of special technique, questions and problems of electricity and power control.

I see these directions also in the submitted works this year.

Unfortunately, the restrictions associated with the coronavirus did not allow us to traditionally meet for discussion. I think that next year we will be able to do this at our university.

I wish everyone good health and new creative achievements.

Conference Chair
Anatoliy Pavlenko

Ladislav Lazić – professor of University of Zagreb, Faculty of Metallurgy, Department of Mechanical Metallurgy, Laboratory of Thermal Technique and Mechanical Engineering. The main areas of scientific activities: Computation of high-temperature radiative heat transfer, Thermodynamics of fuel utilization and pollutant formation, Design and efficiency of industrial furnaces and heating equipments, CFD approach to combustion modelling and numerical simulation of furnace processes, Finite element technique in simultaneous transient conduction and thermal stress analysis, Techniques in the reduction of NOx emissions and, in particular, Metallurgical archeology.

Dear colleagues, organizers and participants of the Conference,

it is my great pleasure to be a member of the Scientific and organizing committee of the conference for several reasons. The main reason is that in today's world, energy and ecology are in the focus of interest, and I am glad that the organizers of the conference are institutions of countries with whose scientific and educational institutions I have many years of successful cooperation. I regret that due to the Coronavirus Pandemic we will not have the opportunity for personal contact, but we remain in the hope that we will realize this next year.

I greet you from my city of Petrinja, where I live, and from Sisak, where I work, cities that were badly damaged in two strong earthquakes in December last year. However, that did not destroy our hope for recovery.

Violeta Motuzienė – professor at Vilnius Gediminas Technical University, Department of Building Energetics, Lithuania.

Scientific interests – buildings energy efficiency and sustainability, life cycle analysis, indoor environment, ventilation, occupants' behaviour.

Dear participants of the Conference,

It is my pleasure to join this conference as a member of scientific and organizing committee for the first time and welcome you at the conference. In the context of the growing climate change and global energy crisis many countries are facing with great challenges. A transition to clean energy requires moving faster than what we are capable of doing now. Here research can decisively support the energy transition through appropriate transformations and suggest effective pathways to turn polluting global energy systems into zero-emission systems by developing RES solutions. I believe the researches presented at the conference and discussions will have added value into solving above mentioned problems both at regional or global level.

I hope that you will enjoy the conference and wish you all the fruitful discussions at separate sections.

Yury F. Snezhkin – acting head of the Institute, Academician of NAS of Ukraine, doctor of technical sciences, professor, laureate of state prizes of USSR and Ukraine in the field of science and technology.

Dear Colleagues,

on behalf of the Institute of engineering thermophysics of the National Academy of Sciences of Ukraine, we thank the faculty of Environmental, Geomatic and Energy Engineering, Kielce University of Technology for participating in co-founding the VI International Scientific-Technical Conference „ACTUAL PROBLEMS OF RENEWABLE EN CONSTRUCTION AND ENVIRONMENTAL ENGINEERING". We believe the researches presented at the conference and discussions will have value into solving problems both at regional or global level.

Borys Basok – Prof. doctor of science, Corresponding Member of NAS of Ukraine.
Head of Department "Thermophysical Basics of Energy-Saving Technologies" Institute of Engineering Thermophysics National Academy of Sciences of Ukraine.

Dear colleagues!

Dear conference participants!

We are very grateful for the invitation and the opportunity to participate in your conference.

The Institute of Technical Thermal Physics of the National Academy of Sciences of Ukraine this year participates in the conference in a new capacity as a co-organizer, for which we express our gratitude to you. It is a great honor for us and the opportunity to share with you our scientific and engineering achievements, especially because this year our institute celebrated the 75th anniversary of its foundation.

On my behalf, I wish the participants of the conference fruitful work, the exchange of interesting scientific achievements, the establishment of new creative contacts, as well as power and inspiration to realize them.

Separately, heartfelt and sincere gratitude to the Polish people and the leadership of the Republic of Poland for the great help to Ukraine.

Table of Contents

MUNICIPAL ENERGY OF UKRAINE: CURRENT STATE AND TREND OF POST-WAR DEVELOPMENT

Borys Basok, Evgenyi Bazeev

Institute of Engineering Thermophysics of the National Academy of Sciences of Ukraine,
Marii Kapnist street, 2a, Kyiv, 03057, Ukraine
e-mail: basok@ittf.kiev.ua

Today, the economy of Ukraine, including the fuel-energy complex, suffered significant losses in all sectors because of Russia's military aggression, although a critical deficit in energy resources and energy carriers is not felt as much for this moment, therefore we can talk about maintaining the necessary security level of the economy and the life of society. However, challenges and risks have appeared for the sustainable functioning and development of the energy industry. Therefore, it is necessary to evaluate these risks and lay out the foundation for economic reconstruction and modernization, especially the energy sector of the future post-war period, taking into account the fact that part of the building stock is destroyed or damaged. At the same time, it is desirable to use experience in the reconstruction and modernization of the energy sector, relying on the best practices of Western countries, in particular the EU.

It should be noted that the war had a significant negative impact on the work of the Ukrainian energy industry [1]. Due to their economic, humanitarian and geopolitical importance, energy infrastructure facilities have become main targets of Russian terrorism. Nevertheless, the Ukrainian energy system demonstrates high stability, and the energy industry shows extraordinary professionalism in ensuring the stable operation of the industry even in wartime conditions. As of July 2022, according to [1, 2], about 4% of generating capacities were destroyed during hostilities, another 35% of capacities are located in the occupied territories (Fig. 1) [2]. In particular, the Zaporizhzhia Nuclear Power Plant periodically operates in very difficult conditions and is under constant pressure from the Russian occupiers, including its mining, constant shelling, and nuclear-political blackmail. In general, about 50% of thermal electricity generation, 30% of solar generation and more than 90% of wind generation have been destroyed or are in the occupied territories. Gas production decreased by 10-12% during the full-scale military invasion. The main oil refineries were stopped (own production provided about 30% of oil products) causing logistical difficulties with oil products supply. As of mid-June 2022, the direct damage caused to the infrastructure of the Ukrainian energy industry and the oil and gas sector, according to preliminary estimations, counts nearly 47 billion UAH (1.7 billion USD). The total indirect losses of the power sector since the beginning of the war are estimated at 341.8 billion UAH. In the sector of gas production, transit and distribution, the damage estimations reached 61 billion UAH. For the sector of oil production and oil refining – 66 billion UAH.

As of August 10, 2022, 300 Ukraine's communal thermal power facilities were damaged or destroyed due to the Russian Federation war, 158 of them have been already restored. Among these facilities are 10 thermal power plants, three of which have been restored. From October 10 to 20, more than 400 energy facilities in 16 regions of Ukraine were damaged as a result of Russian invaders shelling, 10% of which are in critical condition.

Therefore, current key risks of the proper Ukrainian energy industry functioning are [2]:

- damage/occupation and threat of further destruction or loss of operational control;
- difficulties with pricing and general industry financing;
- difficulties in attracting financial resources and lack of payments for used energy;
- certain dependence of the energy system on imported coal and gas;
- technological, technical and resource limitations.

Approaches for solving the mentioned problems of martial law and the task of post-war development are given in the strategic document published by the National Council for the Recovery of Ukraine from the Consequences of the War – the draft "Ukraine Recovery Plan" [3] for a ten-year period. This Plan provides not only compensation for the war-caused damages but also highlights the issues of accelerated economic growth and improvement of the quality of life in Ukraine. In it, within the framework of 24 working groups proposals, 15 National programs are defined for achieving ambitious goals by 2032. Two of them are related to the development of energy and ensuring the country's energy security, namely: National Program No. 4 "Energy Security", which consists of two parts – 4A "Increasing the stability of the integrated energy system: expanding the interconnection with ENTSO-E, development of oil product pipelines connected to refineries in Europe, development of gas storage facilities" (financing: ~14 billion USD) and 4B "Supporting the transition of the EU to energy with zero carbon emissions: development of carbon-free energy (nuclear and RES), increasing production gas and biofuel, development of the H2 ecosystem" (~114 billion USD).

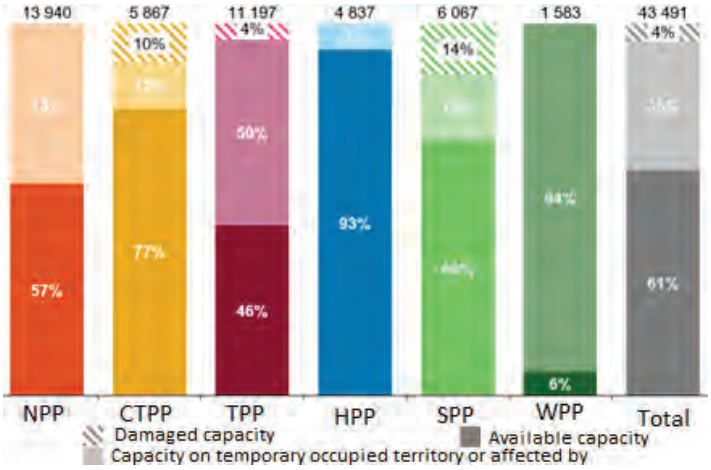

Figure 1. *Distribution of operating capacity in MW (by functional status and location) of power generation facilities as of the beginning of July 2022.*

Another National Program No. 10 "Modernization of Regions and Housing Construction" [4] is also divided into two parts: 10A "Modernization of Regions: Launch of the Housing Modernization Program" (funding: ~70-150 billion USD) and 10B "Increasing Volumes housing construction and infrastructure modernization" (~80-100 billion USD).

Each of the National programs is completed by appendices with a list of specific projects of nationwide or departmental status and a list of necessary legislative initiatives at the level of normative legal acts. Time periods (stages) of implementation of the National Programs: "War Economy" (2022), "Post-war Reconstruction" (2023-2025), "New Economy" (2026-2032). Officially, for the first time, the Ukraine recovery plan was presented at the URC 2022 (Ukraine Recovery Conference) on July 4-5, 2022 in Lugano, Switzerland, where it was thoroughly discussed on 5 panels, including panel discussion No. 5 took place – the restoration of the environment and achieving energy security of Ukraine.

The total financing needs of the "Ukraine Recovery Plan" are estimated at more than 750 billion USD, of which ~2/3 is the support of partners (grants, loans and equity capital). The implementation of the specified plan provides for a significant annual growth of Ukraine's GDP by 7%, forecasted GDP in 2032 – 1.97% of 2021 level, accordingly, in ten years, GDP will almost double. Such high rates of the country development occurred only for five years during independence (2001, 2003-2004, 2006-2007, State Statistics Service of Ukraine). For your information: Ukraine’s GDP in 2021 increased by 3.4% (compared to 2020, State Statistics of Ukraine), with amount of 198.32 billion USD, and according to purchasing power parity – 588.4 billion USD.

The main emphases of the National Energy Program No. 4 are as follows:

1. Ukraine supports plans to ensure Europe's energy security and the transition to a low-carbon economy.
2. The main trend for the recovery of Ukraine in the energy sector is the rapid electrification of the economy thanks to the energy transition, as well as a significant increase in energy efficiency.
3. Main sectoral assumptions: hydrogen – internal consumption of H2 ~0.1-0.2 million tons in 2032, ~0.5 million tons by 2050; industry – electrification of the main industries (for example, metallurgy); residential sector – ~50% of buildings will be thermally modernized by 2032, ~100% by 2050; electrification of heating (electric boilers, heat pumps); transport – electrification of railway transport up to 95%, increasing the share of electric vehicles up to ~15% by 2032, ~80% by 2050, electrification/use of H2 for municipal transport up to ~5% by 2032 and ~100% until 2050; electricity losses will be reduced to 8% by 2032 (according to the National Economic Strategy).
4. Key development catalyst projects: expansion of interconnectors with ENTSO-E up to ~6 GW; increase in nuclear power (2 new units at the Khmelnytskyi NPP, safety and prolongation, load increase); development of 30 GW of wind and solar energy; development of ~3.5 GW of hydro- and hydro-storage power plants; development of ~15 GW of electrolyzers and H2-infrastructure; hub of natural gas in the EU: replenishment of the strategic reserve and provision of connection with the LNG reserves of the EU/Turkey; modernization of the gas transportation network; development of the production of biofuels (bioethanol, biodiesel, biogas/biomethane); post-war expansion of oil refining capacities (reconstruction of the Kremenchug Refinery and construction 1 new refinery, Brody-Adamova Zastava pipeline).

Therefore, the main opportunities for Ukrainian energy industry development are:

- integration with energy systems of EU;
- decarbonization;
- optimization of the energy mix and balancing of the energy system;
- increasing energy efficiency.

A significant increase in nuclear energy, renewable energy sources, the emergence of a new branch of fuel-energy complex (production of H2), a significant decrease in the share of oil and gas, and a significant decrease in the share of coal are predicted. In general, the energy indicators of the recovery plan of Ukraine correspond to similar indicators of the New Energy Strategy for the period till 2030, however, in the materials of the recovery plan, the use of coal has been significantly reduced, in particular, in comparison with the planned volumes of coal usage according to the current energy strategy of Ukraine until 2035 and global trends of coal usage grows and increase of its price. Regarding this, it is necessary to use solid biomass and carbon-rich wastes for centralized heat supply and joint production of electricity with fossil fuels at thermal power plants and cogeneration thermal power plants. Given the actual state of the thermal power industry, the short ten-year period for the implementation of recovery programs (2022-2032), the uncertainty of martial law terms and the actual start of recovery, it seems appropriate to focus on the carefully calculated and planned in the current New energy strategy until 2035 a share of 10...12% of heat and electricity production from coal. Firstly, the potential option of effectively retrofitting coal-fired power generation with innovative CO_2 capture systems (and thereby meeting the requirements of the Glasgow Climate Pact) was somehow not considered in the recovery programs. Secondly, in the dilemma of achieving carbon neutrality of the economy or sustainable socio-economic development of the country (with a high rate of 7% annually), it is necessary to establish and reach a balanced compromise. During the war and in the post-war period, it is important not only (and not so much) to combat global warming, but also the mandatory implementation of other relevant UN goals – elimination of hunger (for example – grain blockade); good health and well-being; clean water and sanitation; available and clean energy; decent work and economic growth; industrialization, innovation and infrastructure; sustainable cities and settlements; responsible consumption and

production. Thirdly, Ukraine belongs to the group of developing countries, moreover, it suffers a lot from the war, and therefore it can fairly count on certain mitigation from the international community and the UN in the scenario of its economic decarbonization.

With regard to National Program No. 10, we note that the modernization of regions and housing, including a large-scale energy efficiency program is a strategic priority. The three blocks of solving the problems of the program are as follows: a large-scale energy efficiency program, better buildings and new city planning, and modernization of other infrastructure.

In general, Ukraine's buildings energy consumption accounts about 40% of final energy (which is almost 1.5 times more than the similar global indicator, according to the IEA), in particular, 31.7% for the residential sector. More than 80% of buildings were built in Ukraine before 1991 and do not meet modern energy efficiency requirements. The average specific indicator of energy consumption by buildings is about 194 kWh/m^2, exceeding the corresponding indicators of European countries by 30-50%.

According to the projects "Long-term strategy of thermo-modernization until 2050", "Renovated buildings, energy independence, high quality of life, new jobs" and "State target program of support for thermo-modernization until 2030" it is expected to achieve in 2030 the indicators given in table. The data are given for an ambitious scenario: a high level of spread of thermal modernization, which by 2030 could be about 35-40% of the building stock, which would approximately correspond to the indicative targets of 3.6% thermal modernization of buildings annually, set in the EU (within the framework of the European Green Course, "Fit for 55 Package", "RepowerEU").

Table 1. *Forecast indicators of thermal modernization of Ukrainian buildings according to the ambitious scenario of the long-term strategy.*

	Unit	Total	Individual houses	Apartment buildings	Public buildings
Newly renovated buildings	piece	2369130	2275000	62630	31500
Gas savings, per year	billion m^3	3.9	1.8	1.5	0.6
General investments	billion EUR	58.8	23.9	25.3	9.6

Therefore, modernization of regions and thermal modernization of housing, including a large-scale energy efficiency program is a strategic priority. We highlighted the maximum estimated funding for the National Program No. 10 stages, in particular: improving the energy efficiency of buildings ~60 billion USD; modernization and optimization of heat supply (centralized and individual) ~$26 billion USD, including 18 billion USD for heat pumps; modernization and optimization of heat supply networks – 3 billion USD; new housing in accordance with best practices – 41 billion USD, including temporary housing and reconstruction of damaged housing; pilot projects for buildings with close to zero energy consumption and centralized cooling systems 3 billion USD.

References

[1] National Council for the Recovery of Ukraine from the War. Working group "Audit of losses incurred as a result of the war". July 2022 (in Ukrainian), https://www.kmu.gov.ua/storage/app/sites/1/recoveryrada/ua/audit-of-war-damage.pdf.

[2] National Council for the Recovery of Ukraine from the War. Working group "Energy security". July 2022 (in Ukrainian), https://www.kmu.gov.ua/storage/app/sites/1/recoveryrada/ua/energy-security.pdf.

[3] Ukraine Recovery Plan, https://recovery.gov.ua/en.

[4] National Council for the Recovery of Ukraine from the War. Working group "Construction, urban planning, modernization of cities and regions of Ukraine". July 2022 (in Ukrainian), https://www.kmu.gov.ua/storage/app/sites/1/recoveryrada/ua/construction-urban-planning-modernization-of-cities-and-regions.pdf.

HYDROGEN ENERGY IN UKRAINE – PROBLEMS AND CHALLENGES

Borys Basok, Evgenyi Bazeev, Vitalii Opryshko

Institute of Engineering Thermophysics of the National Academy of Sciences of Ukraine,
Marii Kapnist str., 2a, Kyiv, 03057, Ukraine
e-mail: basok@ittf.kiev.ua

The recently formulated low-carbon development paradigm and strategy for reducing risks from harmful climate changes, including global warming foresee an increase in the energy efficiency of the economy, an increase of using renewable energy sources (RES) trend, electrification (including the electrification of transport), and the development of hydrogen energy. The new "Green Course" of the EU envisages a complete abandonment of fossil fuels by 2050. For European countries, the low-carbon path of development means reducing the cost of importing hydrocarbon energy resources, increasing energy efficiency, and reducing the risk of mortality from harmful emissions of coal-hydrogen energy. Thus, the climate factor risks becoming a reason for the curtailment of hydrocarbon energy and, at the same time, becoming an incentive for the market promotion of alternative energy sources (AES), RES and hydrogen energy. There are other underestimated risks due to the principle circumstance, namely: a reliable hydrocarbon system will require a dramatic increase in energy costs – from 8% of world GDP to almost 30% by 2035-2050. This can become a key limitation on the way to accelerate energy transition scenarios implementation.

The common view towards the trend of using AES in the energy balance is still not always predetermined. On the one hand, renewable energy sources are perceived as the main energy resource of the future, on the other hand, there is cautious optimism: the share of renewable energy sources in the overall energy balance until the end of the 21st century remains relatively insignificant, hydrocarbon types of fuel will prevail with an increase in the share of natural gas. The key problems of using AES are presented in [1].

The thesis about the relatively insignificant role of RES in the fuel and energy complex is argued by the fundamental physical limitations inherent in such types of energy resources, namely: their low density of energy flow ("dispersed energy") and low primary energy efficiency of production (extraction) (Fig. 1) [1].

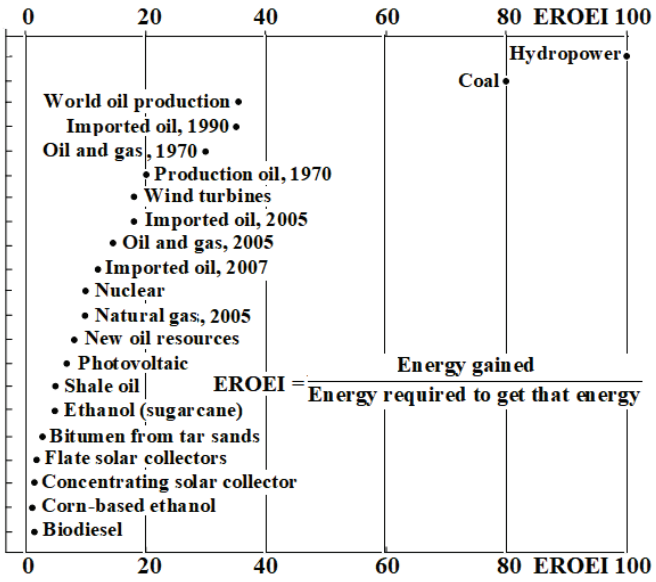

Figure 1. *Energy efficiency of the primary energy resource.*

On a regional scale, the role of such energy resources, appropriately technically and economically justified, can be significant [1].

From the beginning of the 80s, the problem of using hydrogen in the energy industry began to be discussed. Free hydrogen as a type of energy resource is practically absent under terrestrial conditions. There is deep hydrogen-methane degassing due to faults in the earth's crust, which leads to the destruction of the ozone layer in atmospheric heights (Fig. 2) [2]. For example, the flow rate of hydrogen in the tube of one of the ruptures reached 105 m^3 per day (1150 l/s). As can be seen from Figure 2, the concentration of hydrogen is 10-50 ppm [2].

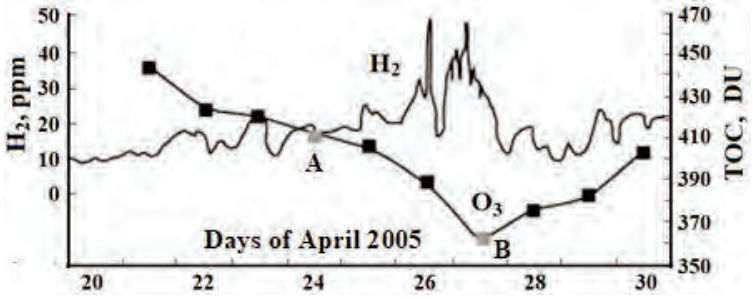

Figure 2. *The concentration of subsoil hydrogen in the Khibiny Mountains (left axis) and the total ozone content (right axis) over the Kola Peninsula in April 2005.*

Black squares are data from the ground ozonometric station Murmansk and gray squares (points A, B) are data from the American Earth Probe satellite. TOC (Total Organic Carbon, the content of organic matter) is the total content of ozone O3. DU – Dobson unit, 1 DU = $21.45 \cdot 10^{-6}$ kg/m^2.

The motivational manifestation for bigger attention to hydrogen use in the energy sector was the idea of its nature, as an efficient and environmentally friendly fuel: the heat of combustion is 140 MJ/kg (natural gas – methane up to 50 MJ/kg). When hydrogen is burned, actually only water is formed. But hydrogen is not an energy resource, it is an intermediate energy carrier, to produce which traditional energy resources are used.

The problem of including hydrogen in the fuel cycle has gained increased relevance and many special and popular works are devoted to this topic. Forecasts of the development of hydrogen energy using "green" hydrogen (gained from the electrolysis of water), and "blue" hydrogen (obtained from natural gas with a concomitant output of CO_2) are considered. The production and usage of this energy carrier in the energy industry require solutions to related problems and possible risks of scientific, technological, economic, legal, and even organizational sides which arise from this [1].

Currently, industrial hydrogen is obtained by converting traditional hydrocarbons – gas, coal, and oil. Increasing the production of hydrogen as a fuel using such technology has led to an increase in CO_2 emissions – an anthropogenic factor increasing the greenhouse effect. To obtain hydrogen by electrolysis of water, it is proposed to use mainly the electricity of nuclear power plants during their load failure. Atomic energy, as well as RES, are relatively environmentally friendly and low-carbon energy resources compared to others. Below is the emission data of energy resources in the equivalent of CO_2 for the complete life energy cycle during the production of 1 kWh of electricity, the data for the range of values of the first column are given in [3], and the second column in [4].

As can be seen, the data from the two literary sources differ significantly, which can be explained by the different depths of the complete energy cycle components analysis, but they convincingly confirm the proposition about the "low-carbon" nature of nuclear energy. All nuclear power plants in the world save a total of 2.0 billion tons of CO_2 per year. FYI, all the forests of the planet annually absorb 2.6 billion tons of CO_2. If the world's average CO_2 emissions figure is 475 g/kWh, then in 2021, Ukraine's nuclear power industry ensured that more than 40 million tons of CO_2 were not released into the environment (approximately 1 ton per capita). Thus, nuclear energy can reasonably be classified as conventionally "green" energy.

Table 1. *The amount of carbon dioxide in the production of energy (1 kWh) from various energy sources.*

Energy resource	CO_2 emissions, g/kW·h, source:	
	[3]	[4]
Coal	860-1290	262-357
Oil	689-890	219-264
Natural gas	460-1234	120-188
Solar photocells	30-279	27-76
Hydropower	16-410	6-65
Biomass	37-116	3-13
Wind energy	11-75	3-13
Atomic energy	9-30	2-6

The possibility of using nuclear power plants for obtaining hydrogen (decarbonization) was supported by the Paris climate agreement. But such technology needs its legal field. It is necessary to unify the provisions regulating relations in the field of production, transportation, and storage of hydrogen obtained at the Nuclear Power Plant (NPP). For this, it is necessary to improve the legal regulation in the field of atomic energy use at the international and national levels, highlighting the fields that require unification [5].

In addition to NPP electricity, the use of electricity from other types of power plants, conventionally "environmentally clean" solar power plants, is being considered for obtaining hydrogen by water electrolysis. Certain hopes of obtaining hydrogen are associated with the development of photocatalysts that split water under the influence of sunlight, and successes in microbiology – the creation of strains of microorganisms that generate hydrogen. But all these fundamentally possible technologies are still far from technically sound engineering solutions. The practical problems of transporting and storing hydrogen have also not been solved yet.

The fundamental problems associated with the use of renewable energy resources and hydrogen, and possible risks from involving them in the existing fuel cycle, are presented in [1].

The existing scientific, technical, technical, economic, and environmental problems inherent in hydrogen energy do not allow us to conclude that the involvement of such an energy carrier as hydrogen in the fuel cycle is a matter of the near future. Several issues need to be resolved for cautious optimism. The production of hydrogen by electrolysis is associated with progress in the development of thermonuclear energy, the terms of which are gradually shifting, although recent successes are impressive.

In Ukraine, despite military challenges, the problem of low-carbon energy development, including hydrogen energy, remains relevant. The management of the Gas Transmission System of Ukraine signed an agreement with the European Hydrogen Mainline on infrastructure integration (transportation of hydrogen by pipeline to end users). 31 gas companies throughout Europe participate in the initiative. Ukraine has great potential and can become the hydrogen hub of Europe. Draft regulation for "fully renewable" hydrogen has recently been published (Commission Delegated Regulation (EU). https://www.euractiv.com/wp-content/uploads/sites/2/2022/05/090166e5ec7b7157.pdf) as an annex to the Directive EU Renewable Energy Directive 2018/2001.

On February 17, 2022, a scientific session of the General Assembly of the National Academy of Sciences of Ukraine (NAS of Ukraine) was held on the problems of forming and implementing a model for the development of a low-carbon economy of Ukraine (Bulletin of the NAS of Ukraine, No. 3. 2022). Among other problems, related to the use of RES, hydrogen in the economy and

energy, namely: problems of the economy in the imperatives of low-carbon development, the impact of energy on the environment, the transformation of Ukraine's energy into an intellectual ecologically safe system, water new energy in the world and Ukraine.

Regarding national research and prospects for the use of hydrogen, we should note that the NAS of Ukraine successfully conducts a wide range of research work on this issue, since 2006 scientific programs have been held, in particular, "Fundamental problems of hydrogen energy" (2006-2010), "Hydrogen in alternative energy and the latest technologies" (2011-2015), "Fundamental aspects of renewable hydrogen energy and fuel cell technologies" (2016-2018), and in 2019-2021 the target program of fundamental of research "Development of scientific principles of obtaining, storing and using hydrogen in autonomous energy supply systems".

At the recently held XXIII international scientific and practical online conference "Renewable energy and energy efficiency in the XXI century" (May 19-20, 2022), the Institute of Renewable Energy of the NAS of Ukraine presented the project of the Hydrogen Strategy of Ukraine until 2050 [6], the main goal of which is the transition to a new clean energy system, that is, the transition to a carbon-free, ecologically safe, circular economy, which corresponds to the development trends of academic economic science. One of the ways to develop the country's hydrogen energy is the production of the so-called "green" hydrogen based on RES, in particular with the help of wind energy [7] by the classic way of electrolysis of water, including seawater. Even the most pessimistic scenario (according to the annual volume of electricity production from insolation and wind energy in 2035 in the amount of 25 billion kW·h by the Energy Strategy of Ukraine until 2035) indicates the annual production of "green" H2 in the estimation of the volume of 5.5 billion nm^3. According to the basic scenario of the Hydrogen Strategy of Ukraine, in 2050, the production of electricity from wind (installed capacity of 460 GW) and insolation (70 GW) will increase to an annual value of 1,500 billion kW·h, which will increase hydrogen production to an annual volume of 330 billion nm^3.

The optimal solution for the inclusion of various energy resources and energy carriers in the energy balance is not to oppose them to each other, but in a reasonable technical-economically and ecologically justified combination, which usually requires deepening and expanding the scientific foundations of the theory and practice of conducting a technical-economic analysis of energy technologies with taking into account modern intellectual and computing capabilities in the innovative digital economy.

References

[1] Arutyunov V.S., Lisichkin G.V., *Energy resources of the 21st century: problems and forecasts. Can renewable energy sources replace fossil fuels?* RUSS CHEM REV, 2017, 86 (8), 777-804, DOI: https://doi.org/10.1070/RCR4723 (russian).

[2] Syvorotkin V.L., *Catastrophic era of hydrogen degassing*. Rare lands. 2018, No. 9, pp. 32-9, http://rareearth.ru/ru/pub/20170810/03395.html (russian).

[3] Rogner H.-H., Khan A., *Comparison of energy sources*. Energy: economics, technology, ecology, 1997, No. 3, pp. 8-14.

[4] Trofymenko A.P., *Ecological impact of atomic energy and its perception by the community*. Works of international conf. "Energy security of Europe. View in the 21st century", May 22-25, Kyiv, 2001, pp. 169-171 (ukrainian).

[5] Lysitsyn-Svetlanov A.G., Romanova V.V., *Legal aspects of nuclear energy regulation as an integral part of the low-carbon energy agenda*. Vestnyk RAS, Vol. 92, No. 2, 2022, pp. 125-130, https://www.elibrary.ru/contents. asp? id=47958164) (russian).

[6] Benmenni M., *Hydrogen strategy of Ukraine (project)*. https://www.ive.org.ua/wp-content/uploads/ Vodneva-Strategia-Cover.pdf (ukrainian).

[7] Kudria S., Ivanchenko I., Tuchynskyi B., Petrenko K., Karmazin O., Riepkin O., *Resource potential for wind-hydrogen power in Ukraine*. International Journal of Hydrogen Energy, Vol. 46, No. 1, 2021, pp. 157-168.

ANALYSIS OF WASTEWATER HEAT RECOVERY IN THE WASTEWATER TREATMENT PLANT AND RECOVERED HEAT USE IN COMMERCIAL BUILDING

Violeta Misevičiūtė, Kęstutis Čiuprinskas, Artur Rogoža

Vilnius Gediminas Technical University, Vilnius, Lithuania

Introduction

About 40% of the heat produced in cities is discharged into the sewer along with the used water [1]. Depending on the purpose of the water, the wastewater temperature ranges from 10°C to 40°C [2], so the wastewater entering the wastewater treatment plant has a significant energy potential, but is treated and discharged to a natural receiver without further treatment. The purpose of this research is to analyze the possibilities of wastewater heat recovery in Vilnius wastewater treatment plant and to assess whether the thermal energy demand of the commercial building can be ensured by using the heat of the treated wastewater in a heat pump.

Object

The largest wastewater treatment plant in Lithuania, Vilnius wastewater treatment plant, was chosen for the research. All wastewater generated in the city of Vilnius is collected and delivered to the wastewater treatment plant, where it is mechanically and biologically cleaned. There are no residential areas near the plant, there are forests and the Neris river in the north and east directions around the plant, and in the west and south it is bordered by the Paneriai forest. The closest heat consumer was selected as the object of recovered heat supply, the store "DEPO", which is located about 2 km in the southeast direction. The heating area of the building is 19087 m^2 and the volume is 190105 m^3. The energy efficiency class B building was built in 2018. The building is supplied with heat from the city district heating networks. The store is open on weekdays from 8 a.m. to 9 p.m., on Saturday – from 8 a.m. to 8 p.m., and on Sunday from 9 a.m. to 6 p.m.

Research methodology

The research is based on data from reports prepared by JSC "Vilniaus vandenys" [3] on the flow rate and temperature of treated wastewater at Vilnius wastewater treatment plant and the calculated heat demand of the store. The heat potential of treated wastewater is determined by different temperature differences. In each case, heat pump duty cycle calculations are performed, the results of which are used in *EnergyPro software* [4] compiled model. With this model, it is checked whether the heat pump will be able to cover the heat demand of the building, what will be its duration of operation and the electricity consumption. The standard heating demand in "DEPO" building is calculated based on the building's energy efficiency certificate issued on 02/28/2018. The demand for hot water preparation is determined according to the rules for installing hot water systems in buildings [5]. The annual store heat needs have been determined: annual heat demand for heating 180 MWh/year, for ventilation 386 MWh/year, and 34 MWh/year for the preparation of hot water.

When calculating the waste heat potential, the minimum hourly wastewater flow determined in the considered period was evaluated. The decrease in wastewater temperature in the heat pump was evaluated in three cases – when the temperature decreases by 2°C, 3°C and 4°C. Since wastewater is treated mechanically and biologically, its physical parameters (specific heat, enthalpy, density, etc.) are selected according to simplified formulas to calculate the thermophysical properties of water [6]. The thermal energy potential is calculated:

$$Q_{pot.} = \frac{Q_h \cdot \rho_n \cdot c_n \cdot \Delta T}{3.6} \cdot 10^{-6} \quad \text{MW} \tag{1}$$

where: $Q_{pot.}$ – heat energy potential of treated wastewater, MW; Q_h – minimum or average hourly flow rate, m^3/h; ρ_n – density of wastewater, kg/m^3; c_n – specific heat of wastewater, kJ/(kg·K); ΔT – difference in wastewater temperatures before and after heat pump, K.

The working agent (refrigerant) of the analyzed heat pump is R1234ze(E). This refrigerant is classified as a refrigerant with a low global warming potential, and its thermodynamic parameters are analogous to R134a [7]. In the calculations, it is assumed that the refrigerant temperature in the condenser is 65°C and in the evaporator -5°C, and the heat pump cycle is represented on the p-h chart of the refrigerant R1234ze(E). The basic scheme of the heat pump is presented in Figure 1. The dotted line in the diagram indicates the boundaries of the thermodynamic system.

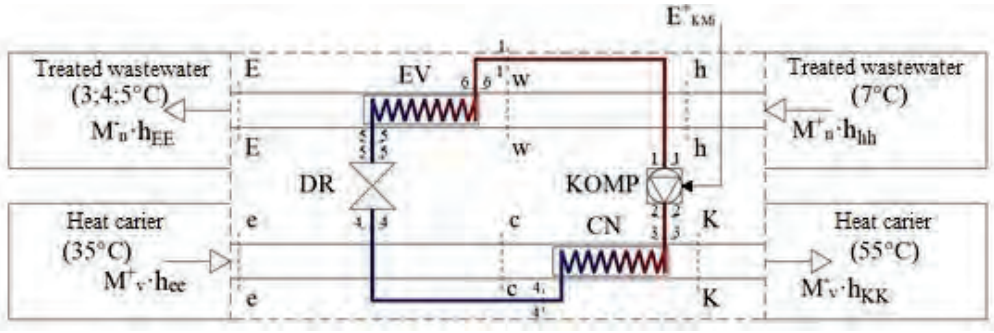

Figure 1. *Principal scheme of the heat pump. Abbreviations: EV – evaporator, KOMP – compressor, CN – condenser, DR – expansion valve, M_v – mass flow of water supplied to the building, M_n – mass flow of treated wastewater, h – enthalpy at the considered point.*

Results

The heat supply to the building was simulated for the period from September 22 until 2020, to September 21, 2021. The change in temperature and discharge of treated wastewater and outdoor air during the considered period was evaluated. The temperature of treated wastewater was assessed to vary from ~3°C to ~20°C during the considered period. The graph shows that the effluent temperature is slightly dependent on the outside air temperature, but does not fall below 7°C. Depending on the daily flow rate, the average and minimum hourly flow rates of treated wastewater also fluctuate. Based on these data, the thermal potential of wastewater treated in the Vilnius wastewater treatment plant was determined at different temperature differences and minimum and average flow rates. At a minimum hourly wastewater flow of 2577 m^3/h and ΔT = 2°C, the thermal potential is equal to 21.63 MW, and double the temperature difference doubles the theoretical thermal potential to 43.27 MW. The total heat load needed for the building was determined using *EnergyPro* software and is equal to 400 kW. Therefore, the thermal power of the heat pump is also 400 kW, the power required for the compressor is 140.11 kW, and the coefficient of performance (COP) of the heat pump in this case is equal to 2.85. The minimum required flow rate determined for treated wastewater is equal to 55.66 m^3/h. The minimum hourly wastewater flow determined by the measurements is 2577 m^3/h, and it exceeds the minimum demand 46 times, so the heat demand of the building is covered by the calculated heat pump throughout the year. The total annual heat demand of the building is equal to 600 MWh, the monthly maximum demand is observed in January and is equal to 115.8 MWh. The lowest heat needs occur during the summer season, when the heat is only used for hot water preparation; this need is equal to 3 MWh. The total amount of electricity consumed by the heat pump is 210.4 MWh. The heat pump operates at a constant, partial, or full load during the heating season without pauses. In total, the heat pump operates for 7464 hours per year and operates at approximately 20% of full load (1503 hours).

Conclusions

In the period from 22 September 2020 to 21 September 2021, the temperature of treated wastewater in the Vilnius city wastewater treatment plant was 7-20°C and the minimum hourly flow rate of treated wastewater was equal to 2577 m^3/h. The theoretical heat potential of treated wastewater is equal to 43.27 MW. The COP of the heat pump, which uses treated wastewater as a heat source to supply heat to the investigated, was determined to be 2.85. After simulation using *EnergyPro* software, it was determined that a heat pump with a thermal power of 400 kW would fully supply the building with thermal energy, i.e. the heat pump would produce 600 MWh of heat and consume 210 MWh of electricity per year.

References

[1] Hepbasli A., Biyik E., Ekren O., Gunerhan H., Araz M. (2014), *A key review of wastewater source heat pump (WWSHP) systems.* Energy Conversion and Management, 88, pp. 700-722, https://doi.org/ 10.1016/j.enconman.2014.08.065.

[2] Somogyi V., Sebestyén V., Domokos E. (2018), *Assessment of wastewater heat potential for district heating in Hungary.* Energy, 163, pp. 712-721, https://doi.org/10.1016/j.energy.2018.07.157.

[3] Report of the JSC 'Vilniaus vandenys'. "Data of non-continuous measurements of monitoring of technological processes of economic entities and monitoring of pollutants emitted/released by pollution sources" 2020. IV quater, 2021 I, II, III quarters.

[4] EMD International. EnergyPRO software, https://www.emd-international.com/energypro/. Accessed 2022-10-17.

[5] Order of the Minister of Energy of the Republic of Lithuania "Regarding the approval of the rules for the installation of hot water systems in buildings" of 2017, July 19, No. 1-196, Vilnius.

[6] Popiel C.O., Wojtkowiak J. (1998), *Simple Formulas for Thermophysical Properties of Liquid Water for Heat Transfer Calculations (from 0°C to 150°C)*. Heat Transfer Engineering, Vol. 19, Issue 3, pp. 87-101, https://doi.org/10.1080/01457639808939929.

[7] Rogoža A., Šiupšinskas G., Bielskus J. (2021), *Case analysis of heat pump integration in district heating system*. Science - Future / Science - Future of Lithuania, 13, pp. 1-6, https://doi.org/10.3846/mla.2021. 15272.

THERMAL COMFORT ANALYSIS IN THE SMART SUSTAINABLE BUILDING

Natalia Krawczyk, Luiza Dębska, Łukasz Orman

Faculty of Environmental, Geomatic and Energy Engineering
Kielce University of Technology, 25-314 Kielce, Poland
e-mail: ldebska@tu.kielce.pl

Introduction

The society spends most of its life in a closed space, this applies to employees' offices, shops and houses. This is also significantly influenced by the trend of sustainable construction, equipped with a BMS system, various types of technological solutions using renewable energy sources.

Many authors are working on research related to thermal comfort. One such example is Becker and Paciuk [1], who examined 205 apartments in the summer and 189 in the winter, turning out that there is a difference between the PMV and the respondents' answers. Another example [2] focuses on 25 buildings with air conditioning. Again, as in research [1], PMV also did not coincide with people's assessment of their real heat sensations. Similarly to the works [3-5].

The aim of this study is to compare the results of the surveys with the actual results for an intelligent building

Methodology

The building that was tested is called Energis. Three rooms were tested for temperatures from 22.9°C to 24.6°C, air humidity from 33.01 to 49.4 and for the content of carbon dioxide ranging from 678 ppm to 2607 ppm. Two methods were used for this purpose. The first one consisted of thermal impressions and humidity surveys, which were supplemented by students and the Testo 400 meter, which collected microclimate data through probes. A total of 37 people were examined, 13 women and 24 men.

Results

Thermal impressions, according to the respondents' assessment, for all tested rooms showed that about 85% of people described their feelings as "pleasantly cool", "comfortable" and "pleasantly warm". On the other hand, about 15% rated their feelings at the moment as "too warm" and "too hot". Another value that appeared in the survey concerned the acceptability of temperature. About 59% of people found it acceptable, and about 38% found it comfortable. Only about 3% of the respondents declared that the temperature during the examination was no longer acceptable. Turning to room temperature preferences, about 62% would not decide to change it at all, as opposed to about 30% who would like it to be cooler or about 5% much cooler. Only about 3% would like the room to be warmer. The answers of the respondents have their overlap with the answers they marked. Because when assessing thermal sensations, the respondents mainly marked "pleasantly cool/warm" and "comfortable", but also values for "too warm/hot", which proves when asked about preferences that this environment could be cooler. The Thermal Sensation Vote (TSV) was compared to the PMV (Predicted Mean Vote) based on the ISO 7730 [6] standard, as was the PPD (Predicted Percentage of Dissatisfied). The TSV indicators for three rooms showed that in one of them people felt comfortable, in another the comfort range included in the ISO 7730 [6] standard of -0.5 to +0.5 was slightly exceeded, and in the last tested room the TSV definitely exceeded the comfort range with a value above +0.75. More interestingly, the values for PMV were low in the room where the TSV was high. In a room where TSV was low, PMV was high. This proves that

there is a significant difference between the real feelings of people and the norm, which assumes that where the environment is good according to the respondents, the PMV according to them is always much higher.

Conclusion

Summing up, according to the respondents, the examined classrooms met their thermal expectations. On the other hand, the Fanger model, which is the basis of the ISO 7730 standard, and the real thermal sensations of people at the moment have no overlap. So the conclusion is that it would be necessary to modify Fanger's model in such a way as to bring it as close as possible to the actual feelings of people.

References

[1] Becker R., Paciuk M., *Thermal comfort in residential buildings – Failure to predict by Standard model.* Building and Environment, pp. 948-960 (2009), http://dx.doi.org/10.1016/j.buildenv.2008.06.011.

[2] Broday E.E., Moret J.A., Xavier A.A.P., *Reginaldo de Oliveira*, International Journal of Industrial Ergonomics 69, pp. 1-8 (2019), https://doi.org/10.1016/j.ergon.2018.09.007.

[3] Mors S.T., Hensen J.L.M., Loomans M.G.L.C., Boerstra A.C., *Adaptive thermal comfort in primary school classrooms: Creating and validating PMV-based comfort chart*s, Building and Environment 46, pp. 2454-2461 (2011), https://doi.org/10.1016/j.buildenv.2011.05.025.

[4] Manu S., Shukla Y., Rawal R., Thomas L.E., de Dear R., *Field studies of thermal comfort across multiple climate zones for the subcontinent: India Model for Adaptive Comfort (IMAC)*, Building and Environment 98, pp. 55-70 (2016), https://doi.org/10.1016/j.buildenv.2015.12.019.

[5] Vilcekova S., Meciarova L., Burdova E.K., Katunska J., Kosicanova D., Doroudiani S., *Indoor environmental quality of classrooms and occupants' comfort in a special education school in Slovak Republic*, Building and Environment 120, pp. 29-40 (2017), http://dx.doi.org/10.1016/j.buildenv. 2017.05.001.

[6] ISO International Organisation for Standardization, Ergonomics of the thermal environment – Analytical determination and interpretation of thermal comfort using calculation of the PMV and PPD indices and local thermal comfort criteria International Standard ISO 7730 2005.

FEATURES OF COMPLEX ASSESSMENT OF ENERGY CONSERVATION MEASURES IN BUILDINGS

Borys Basok[1], Denys Derevinko[1,2], Nataliia Bespala[1], Ihor Bohoiko[2]

[1]Institute of Engineering Thermophysics of the National Academy of Science of Ukraine
2a, Marii Kapnist (Zhelyabova) Str., Kyiv, 03057, Ukraine
[2]National Technical University of Ukraine "Igor Sikorsky Kyiv Polytechnic Institute"
115, Borschahivska str., Kyiv, 03056, Ukraine
e-mail: dereviankodenys@gmail.com

Introduction

The reduction in the consumption of energy resources for heating purposes in buildings can be achieved by using [1, 2]: modern heat-insulating materials and technologies at the stages of design and operation; non-traditional and renewable energy sources (RES) and distributed generation (DG) systems; means of automatic management of heating systems of buildings; various user behavior management programs.

When developing energy conservation measures, buildings should be considered as complex thermal energy systems, which include the internal microclimate, the building envelope, engineering networks, and the external climate. This approach makes it possible to carry out a comprehensive analysis of the energy characteristics of buildings and to implement a reasonable and efficient use of energy resources. Mathematical models can be used to assess efficiency of energy consumption at various stages of a building's life cycle. For a long time, the energy characteristics of buildings were determined for annual/seasonal calculation intervals (stationary calculation) [2].

Results

In accordance with the optimization tasks, the algorithm for determining and evaluation of the energy effects from the implementation of energy conservation measures (ECM's) to improve the energy efficiency of buildings consists of the following main stages (Fig. 1).

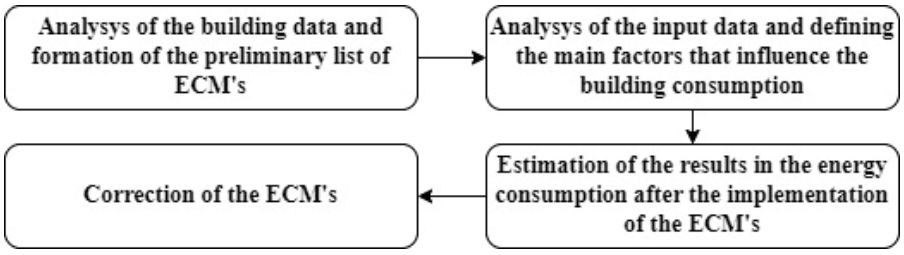

Figure 1. *Algorithm for determining and evaluating of the energy effects from the implementation of measures to improve the energy efficiency of buildings.*

At the first stage, the initial state of the object (building) is analyzed from the point of view of data analyses and preliminary selection of a set of ECM's. For most budget facilities, it is advisable to start the analysis precisely with the possibilities of "passive" energy saving. After choosing a complex of necessary ECM's, it is necessary to identify them, including by the type of obtained energy effects: Energy; Economical; Ergonomic; Environmental; Financial.

Also, it is important to assess the initial conditions, determine the factors that affect the consumption of energy resources by the building. It is necessary to evaluate the initial conditions, identify and account for influencing factors: independent variables and (or) static factors. At this

stage (stage 2), a general analysis of the building's energy consumption over recent years is carried out, from the point of view of identifying the basic trend, possible fluctuations, and factors affecting the level of energy consumption are also assessed.

After forming a list of measures to improve energy efficiency at the first stages, the task of selecting the most appropriate of them, taking into account the condition of the building and other aspects of the implementation of individual measures, appears. At the same time, energy saving purposes can be obtained both by changing parameters that have a strong impact on reducing the use of energy resources, and by changing the duration of equipment operation during the year [3]. In addition, the analysis and calculation of each technical solution should be carried out for the entire life cycle from the beginning of investment in project work to the disposal of equipment.

To form an assessment of the feasibility of implementing energy-saving measures, such measures should first of all be divided into certain groups, for example: measures aimed at increasing the efficiency of an individual heating unit, increasing the thermal resistance of enclosing structures, reducing hot water consumption, increasing the frequency of air exchange.

For each of the groups, the initial energy characteristics (before the implementation of the measures) and the characteristics after the implementation of the measures are calculated. Accordingly, economic and financial indicators (NPV, NPVQ) are calculated.

The next step is the ratio of the initial and final technical factors for each energy efficiency improvement measure in each group, respectively (Fig. 2).

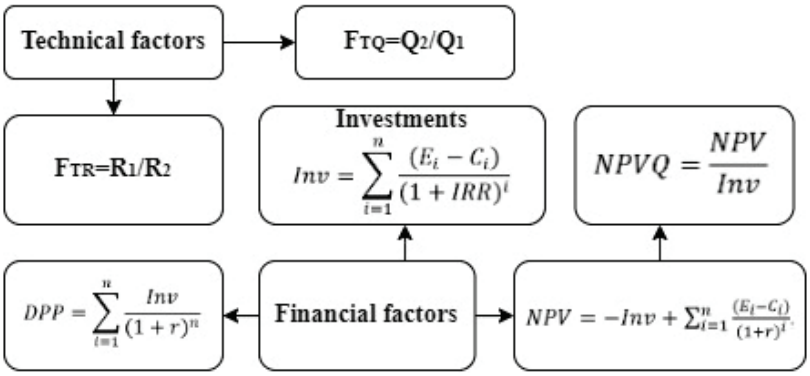

Figure 2. *Technical and financial factors.*

Assessing the feasibility of implementing a particular ECM is carried out graphically based on two indicators – the ratio of initial and final technical parameters and the NPVQ profitability index.

On the basis of the obtained values, a diagram of the dependence of NPVQ on the value of the ratio of technical factors is constructed (Fig. 3a).

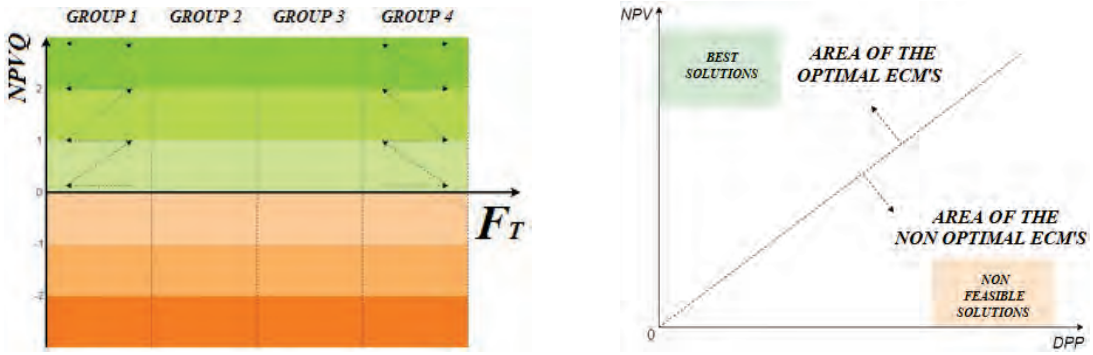

a) b)

Figure 3. *Diagram (a) of dependence of NPVQ and factor of technical efficiency (F_T) and diagram (b) for comparing the effectiveness of ECM's of one group.*

After plotting the pointsinto the diagram corresponding to NPVQ values and the ratio of technical factors (F_{Ti}), a matrix of points is formed that correspond to specific ECM in a certain group. By comparing the positions of the points corresponding to the ECM's relative to the coordinate axes, taking into account the specifics of the implementation of the measures and the value of the technical factors, among several measures of the same group, the one that is the most effective and, accordingly, the most expedient, is chosen.

When two or more measures fall into the zone of greatest efficiency and a choice must be made between them, it is proposed to add the dependence of NPV on the discounted payback period of DPP to the selection criteria. It is also convenient to choose between two such measures by evaluating their parameters graphically using the diagram shown in Figure 3b.

Based on the results of energy audits in buildings of the communal sphere, we will give example of calculating the value of saving energy and changing the technical characteristics of enclosing structures, engineering systems, and climatic conditions before and after the implementation of a number of measures to improve energy efficiency.

Table 1. *Parameters of evaluation of building energy saving measures.*

ECM group	Specific ECM	F_T	NPVQ	NPV, UAH	DPP, years
Increase of thermal resistance	1. Insulation of external walls	0.34	0.12	57 162.6	11.7
	2. Replacement of windows	0.84	0.07	4 560.1	12.3
Increasing the efficiency of the heating system	3. Modernization of IHP	0.067	3.10	1 726 455.7	2.7
	4. Flushing the heating system	0.91	2.7	416 546.1	2.10

The next step is the ratio of the initial and final technical factors for each ECM in each group, respectively.

The diagram (Fig. 4) graphically shows the location of the points corresponding to the measures from Table 1. Based on the position of the points, it can be concluded that measures numbered 1 and 3 in the first and second groups, respectively, will be the most appropriate for implementation.

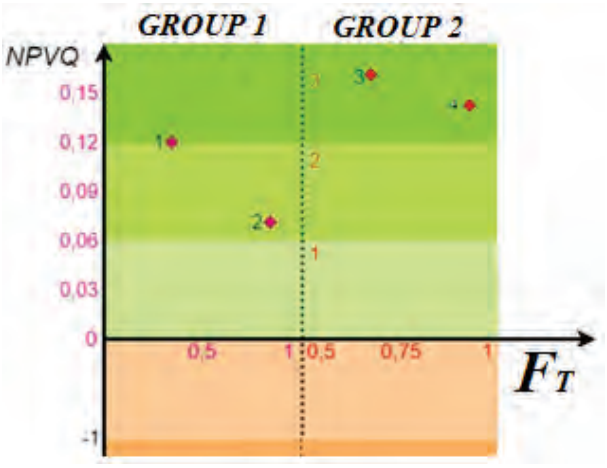

Figure 4. *Diagram of the distribution of measures by the level of feasibility of their implementation.*

However, there are cases when it is quite difficult to draw a clear conclusion, as in the case of the measures of the second group. In such cases, it is worth applying the evaluation method using the ratio of NPV to the discounted payback period of DPP, constructing the diagram in Figure 5.

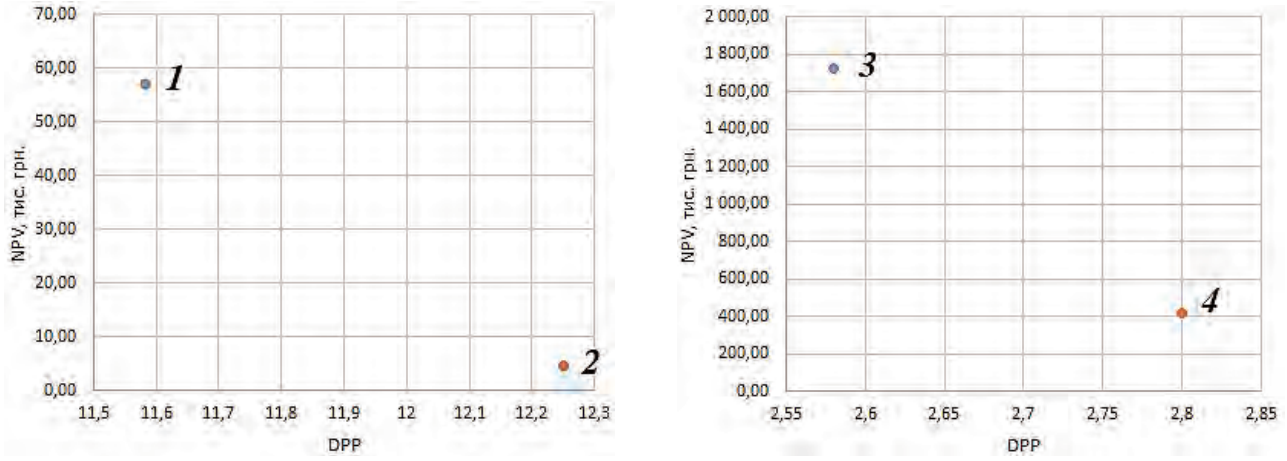

a) b)

Figure 5. *Comparison of measures of the thermal resistance increase group (a) and groups for increasing the efficiency of the heating system (b).*

Assessing the feasibility of implementing a particular measure to improve energy efficiency is carried out graphically based on two indicators – the ratio of initial and final technical parameters and the NPVQ profitability index. Therefore, after analyzing the indicators of the above measures, the most effective in this case is the modernization of the IHU.

Conclusions

The considered dynamic methods of assessing the expediency of implementing measures to improve energy efficiency in communal buildings make it possible to more accurately assess financial indicators during the life cycle of the building. Technical factors should also be taken into account along with economic factors. The algorithm proposed in this work for assessing the feasibility of implementing measures to improve energy efficiency in communal buildings makes it possible to comprehensively evaluate technical and economic indicators when analyzing individual ECM's. This algorithm is based on the application of graphic models of complex presentation of technical and economic indicators. Therefore, its use will help to make a decision on the implementation of exactly such measures to improve energy efficiency, which will allow not only to save money, pay off investments, but also to increase the level of comfort of staying in buildings and to reach the level of minimum requirements of current legal acts.

References

[1] On energy efficiency: Law of Ukraine of 17 December. 2020 No. 4507. URL: http://w1.c1.rada.gov.ua/pls/zweb2/webproc4_1?pf3511=70687 (access date: 21.10.2021).

[2] Dodonov B., *Energy Efficiency Monitoring of Ukraine* 2015. URL: https://www.ua.undp.org/content/ukraine/uk/home/library/environment_energy/energy_efficiency_ukrain e2015.html.

[3] Ministry of Energy and Coal Industry of Ukraine, NEC Ukrenergo, Scientific and Technical Center of Electric Power Industry. Analysis of energy efficiency in developed foreign countries and dependence on their imports. URL: https://ua.energy/wp-content/uploads/2018/01/1.-Efektyvnist_energ_resursiv.pdf.

PROSPECTS FOR THE USE OF CAVITATION MECHANISMS IN ORDER TO REDUCE THE CONSUMPTION OF NATURAL WATER IN MUNICIPAL ENERGY

Bogdan Tselen, Georgiy Ivanytskyi, Anna Nedbaylo, Nataliya Radchenko

Institute of Engineering Thermophysics of the National Academy of Sciences of Ukraine

A way to solve the problem of utilization of acidic condensate of natural gas combustion products and the possibility of its reuse to reduce the consumption of natural water in technological processes and reduce wastewater emissions is proposed.

The advantages and disadvantages of existing methods for the extraction of carbon dioxide from condensate – chemical neutralization, decarbonization, thermal deaeration, vacuum deaeration, ultrasonic and hydrodynamic cavitation – are considered. It has been established that the most effective of these methods for the release of condensate from carbon dioxide are the methods of ultrasonic and hydrodynamic cavitation degassing of liquids. Although the efficiency of ultrasonic cavitation degassing is based on the possibility of the fastest possible extraction of free gas from a liquid and the possibility of degassing virtually any liquid, this method has not yet been widely used due to its significant specific energy costs. It was established that the process of hydrodynamic cavitation degassing of a liquid should be considered as a significant alternative to acoustic cavitation of degassing in the direction of increasing productivity and reducing specific energy consumption.

A new alternative method of condensate neutralization without the use of chemical reagents with low specific energy costs is proposed, based on fundamental research within the framework of the scientific direction of discrete-pulse energy input (DPIE) and the use of such mechanisms as high-frequency hydrodynamic oscillations, accompanied by high circumferential velocity and shear stresses, cavitation, and phase transitions.

Based on the created universal mathematical models of the dynamics of single steam-gas bubbles and the ensemble of bubble dynamics, numerical modeling of the growth of steam-gas bubbles in condensate was carried out. Within the framework of the mathematical model of the dynamics of the ensemble of bubbles, an analytical study of the evolution of the unit of steam-gas bubbles to achieve a critical value of the gas content in them was carried out.

The regularities of influence of DPIE mechanisms on the extraction of carbon dioxide from a liquid by processing liquid on a laboratory stand, which consisted of two main working units – a rotary-pulsation apparatus (RPA) of a special design and a chamber for thermal vacuum treatment of liquid, were investigated. The dependence of the pH change in the condensate of the combustion products of natural gas and model liquid (distilled water saturated with carbon dioxide) on the duration of treatment was obtained. It was established that the main amount of carbon dioxide is removed within 2 minutes of processing. It was also revealed that after processing, the condensate is in an unstable state and its pH continues to grow, which is explained by the course of relaxation processes in the liquid. After 7 hours of exposure, the pH of the condensate stabilizes at 6.5, which corresponds to the almost complete absence of carbon dioxide in it. The resulting condensate according to physicochemical parameters is similar to distilled water with a low content of dissolved carbonic acid.

The use of the proposed method of neutralizing condensate will create conditions for reducing the negative impact on the environment by reducing the amount of effluent (chemically contaminated neutralized condensate and waste from water desalting plants) and rational use of water resources by reducing the need for natural water.

INFLUENCE OF STRUCTURAL CHARACTERISTICS OF POROUS MATERIALS ON HEAT TRANSFER INTENSITY

Andrii Cheilytko

German Aerospace Center (DLR), Institute of Solar Research, Juelich, Germany
e-mail: andrii.cheilytko@dlr.de

Porous materials are widely used in industry. These are polystyrene foam materials, aerated concrete, some highly fire-resistant materials, foam glass, expanded clay. Porous materials have also occupied a niche in innovative technologies: combustion chambers, turbine walls, solar station receivers, thermal storage.

Let's take a closer look at the effect of pore location on the thermal conductivity of the material. Uses the following designations: porosity, $\lambda 1$ – heat transfer coefficient of the material (silica material with a heat transfer coefficient of 0.12 W/(m·K) was chosen as an example), $\lambda 2$ – the thermal conductivity coefficient of the medium (in the example selected air with gas admixtures having a thermal conductivity of 0.019 W/(m·K)). Heat flow is directed from the bottom upwards.

Most of the existing studies of porous structures of materials for thermal protection of elements of industrial power plants take into account the total porosity as the main structural characteristic of the thermal insulation material, and sometimes take into account either the shape of the pores and their number or the type of pores. The analysis of the current literature shows that even the simultaneous consideration of the total porosity of the material, the size and type of pores is not enough to fully characterize the porous structure of the heat-insulating material. It is proposed to pay attention to the following main factors in porous systems: the nature of the structure, the number of structure components, the aggregate state of the structure components and the processes of interaction between the structure components. These complex indicators are convenient for the separation of porous systems as a whole because they allow controlling the thermophysical properties of a particular macroporous material by changing the porosity structure. But these indicators do not allow to find the functional dependence of the thermophysical properties of heat-insulating materials on the porous structure, which does not allow to optimize the thermophysical properties of porous heat-insulating material by creating predictable porous structures. Therefore, we propose the main complex indicators of the porous structure of the heat-insulating material and structures of thermal protection of elements of industrial power plants, which fully reflect the porous structure and make it possible to draw up a regression equation for the dependence of the thermal properties of porous heat-insulating materials on the proposed indicators:

1. Porosity – porosity as a general indicator of the density of thermal insulation material and thermal protection structures.
2. Number of pores – the number of pores for a homogeneous structure in combination with porosity gives a general idea of the distribution of pores in the material. The change in the number of pores over time during the formation of the porous structure of heat-insulating materials expresses the dynamics of the pore formation process.
3. The location of the pores in space – described by the Brave translation system (Brave lattice), in which the pore is the core of the lattice with dimensions smaller than the Wigner-Seitz cell, or the statistical distribution of pores in the volume of the insulating material.
4. Pore shape – a spatial coordinate function describing the shape of the pore. It is possible to accept the description of all pores as spheres with the description of the deformation inherent in this sphere, according to the Poincaré hypothesis, or the overall dimensions of the pore, or the general coefficient of geometric characteristics of the porous structure.

5. Indicators of the gas state in the pores – the temperature gradient on which convection in the pores and the physical properties of the coolant in the pore depend. It can also be represented by the product of Grasgoff number and Prandtl number.
6. Specific surface area porosity.

EXPERIMENTAL STUDY OF THE HEAT FLUX DENSITIES DISTRIBUTION IN DIFFERENT TYPES OF TRIPLE-PANE WINDOWS

Karolina Sadko

Kielce University of Technology, Poland

Introduction

Windows and glazed facades play a major part in the character of a building, providing natural light, solar gains, ability to view the outside and air ventilation. However, they contribute up to 60% of the total heat loss through the building envelope, due to their comparably larger overall heat transfer coefficients [1]. Hence, transparent building partitions with high thermal resistance have a significant potential to substantially increase energy savings. The thermal resistance of the double-pane window filled with air is proving to be 1.7 times lower than of the triple-pane window with the same thickness. It is due to the fact that the central pane in the triple-pane window causes reduction in the velocity of free-convective flow of the fluid in the gap between panes [2]. The fluid rises along the hot pane, changes the direction of flow in the upper part of the window and falls down along the cold pane, creating a primary circulation. Besides, multicellular secondary circulations occur in the gaps of double- and triple-pane windows over the critical values of the Rayleigh number, thus cause short cuts between hot and cold surfaces [3]. Comparing with the double-pane window, the number of multicellular circulation is higher due to the lower temperature gradient in the gaps of triple-pane window. Moreover, the central pane contributes more substantially to the decrease in the radiative heat transfer, acting as a screen [4]. The heat transfer in triple-pane windows is the subject of many scientific papers, however, many simplifications are applied in the mathematical modelling. These are related to assuming mean values for the heat flux density on window surfaces and treating window surfaces as isothermal. For the above reasons, experimental investigations were conducted in order to determine the heat-flux densities at the lower, central and upper part of triple-pane windows on their external and internal surfaces.

Materials and Methods

The research is conducted for four types of window:

1. Air-filled triple-pane window (4float/18Air/6float/18Air/4float). Float glass emissivity $\varepsilon = 0.84$.
2. Argon-filled triple-pane window containing a low-emission coating on the panes surfaces faced to the gaps (4low-e/18Ar/6float/18Ar/4low-e). Low-e glass emissivity $\varepsilon = 0.17$.
3. Argon-filled triple-pane window containing a low-emission coating on the panes surfaces faced to the gaps (4low-e/18Ar/6float/18Ar/4low-e). Low-e glass emissivity $\varepsilon = 0.17$. At the lower part of the inner gap, on the central pane, a heating plate consisting of heating rods with a resistance of 50 Ω is installed. The power supply wire suitable for plugging into the 230 VAC socket is pulled out from the inner side of the window's frame.
4. Argon-filled triple-pane window consisting of heating EGLAS glass, which operate by combining two factors: electric current and a low-emission metal oxides layer on one of the glass surfaces. The power supply wire suitable for plugging into the 230 VAC socket mains is pulled out from the inner side of the window's frame.

Schematic representations of investigated window units are shown in Figure 1.

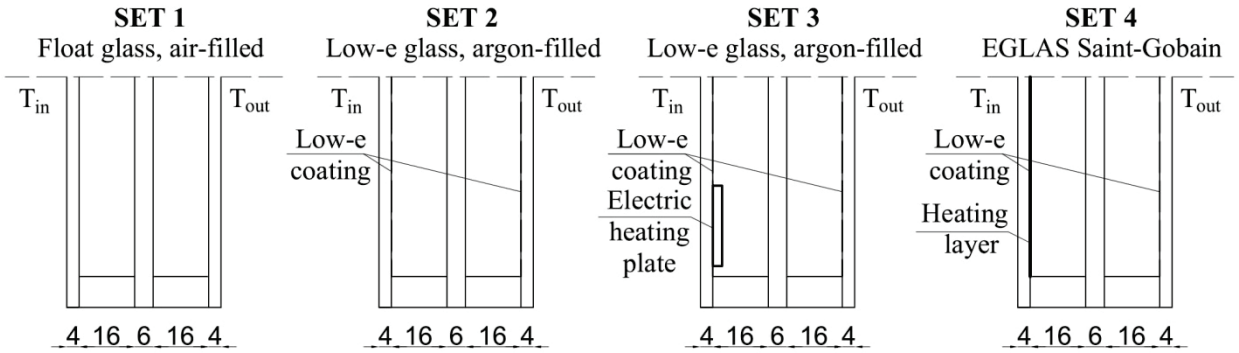

Figure 1. *Schematic representation of investigated triple-pane windows.*

Four investigated windows, each measuring 87.5 × 60.0 cm, are fitted in the 15 cm thick reinforced concrete wall. The building partition is mounted in a climatic chamber by an aluminum frame (warm profile), as shown in Figure 2.

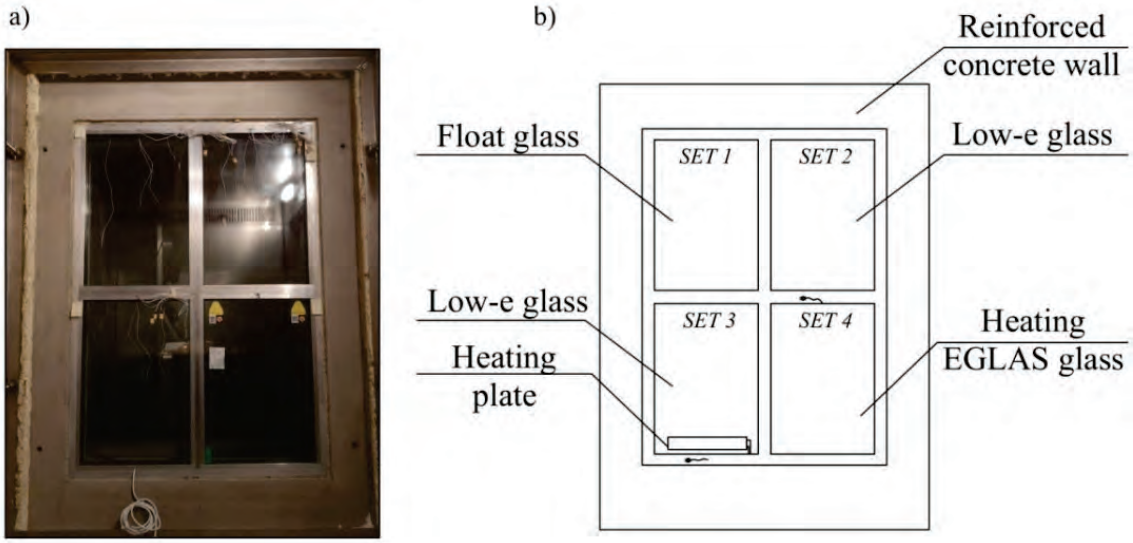

Figure 2. *Details on the setup construction: a) photo of the climatic chamber testing plane; b) location of investigated windows sets.*

Internal temperature of the climatic chamber was set to be constant at T_{in} = 20°C. In order to show the effect of the temperature gradient on the change in the heat flux density, the tests were carried out for three external temperatures of T_{out} = -5°C, 0°C and 5°C, respectively. Three Hukseflux FHF04 foil heat flux density sensors were attached at the lower, central and upper part of each window on their external and internal surface to monitor the heat flow rate. Hukseflux LI19 recorder was used to measure heat flux density and to save results, which are then exported to Microsoft Excel tables. Tests were continuously reporting results at intervals of 2 seconds for a period of 30 minutes.

Results

The aim of the study was to determine the density of heat flux at the lower, central and upper part of each window under different outdoor temperature conditions. Figure 3 presents selected measurement results.

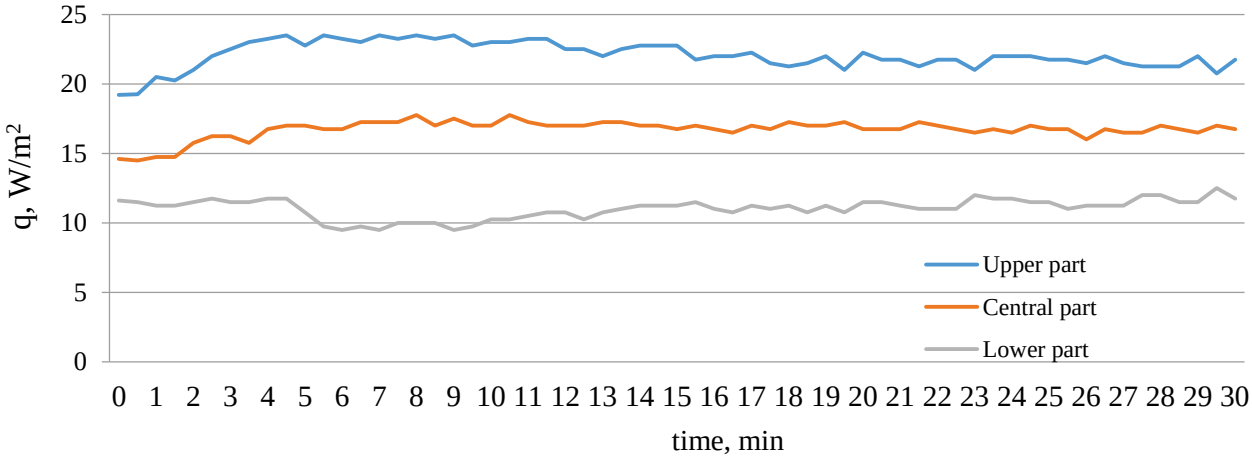

Figure 3. *Mean values of the heat flux density on the external glazing of set 1 (T_{out} = -5 ℃).*

As can be seen in Figure 1, the heat flux densities vary depending on the part of the window. The maximum value in the upper part of the external surface is 23.5 W/m^2 and the minimum value at the lower part of the external surface is 9.5 W/m^2. The average value at the central part is 16.7 W/m^2. The tendency is the same in all examined windows. On the outer surface, the heat flux density increases with height, and on the inner surface it decreases with height.

Conclusions

Summing up, significant differences of heat flux density occur at the lower and upper part of the window surfaces. The maximum values of the heat-flux density on the window's external surface are observed at upper part. However, the maximum values of the heat-flux density on the window's internal surface are measured at the lower part, due to the ascending and descending flows of the gas medium in gaps between panes. Thus, non-uniformity of heat flux densities distribution causes many errors in the mathematical modelling of heat transfer, based on assuming a constant average value of the heat flux density. In addition, results show that locating an additional heat source at the lower part of the internal pane is reasonable.

References

[1] Rezaei S.D., Shannigrahi S., Ramakrishna S., *A review of conventional, advanced, and smart glazing technologies and materials for improving indoor environment*. Solar Energy Materials and Solar Cells 2017, 159, pp. 26-51, https://doi.org/10.1016/j.solmat.2016.08.026.

[2] Basok B., Davydenko B., Isaev S.A., Goncharuk S.M., Kuzhel L.N., *Numerical modeling of heat transfer through a triple-pane window*. Journal of Engineering Physics and Thermophysics 2016, 89, pp. 1277-1283, https://doi.org/10.1007/s10891-016-1492-7.

[3] Basok B., Davydenko B., Novikov V.G., Pavlenko A.M., Novitska M.P., Sadko K., Goncharuk S.M., *Evaluation of heat transfer rates through transparent dividing structures*. Energies 2022, 15, 4910, https://doi.org/10.3390/en15134910.

[4] Arici M., Karabay H., Kan M., *Flow and heat transfer in double, triple and quadruple pane windows*. Energy and Building 2015, 86, p. 394-402, https://doi.org/10.1016/j.enbuild.2014.10.043.

ANALYSIS OF THERMOTECHNICAL PARAMETERS OF AIR-WATER HEAT PUMP AS A PART OF THE RADIATOR SYSTEM OF HEAT SUPPLY OF THE ADMINISTRATIVE BUILDING

Borys Basok[1], Oleksandr Nedbailo[1], Ihor Bozhko[1], Volodymyr Marteniuk[2]

[1]Institute of Engineering Thermophysics of the National Academy of Sciences of Ukraine, bldg. 2, Bulakhovskogo str., Kyiv, 03164, Ukraine

[2]National University of Food Technologies, 68, Volodymyrska str., Kyiv, 01601, Ukraine
e-mail: nan_sashulya@ukr.net

Introduction

According to statistics, people spends up to 90% of the total time in buildings, the climatization of which is comparable to the largest part of the final consumption of all types of energy. In Ukraine, the housing and communal sector uses for more than 40% of this volume, and the efficiency of possible energy-saving measures in this direction, on a national scale, exceeds the possible savings in such technologically energy-intensive industries as metallurgy, chemical industry, etc. [1].

The use of heat pump systems based on renewable energy sources is a real alternative to the use of fossil fuels. More and more attention in the literature has been paid to the issues of efficiency assessment and implementation of heat pump technologies in customer's heat supply systems.

Object, subject, and methods of research

The Institute of Engineering Thermophysics of the National Academy of Sciences of Ukraine has implemented a number of projects aimed on reducing the consumption of thermal energy for the needs of heating of the administrative buildings. Among such projects is the modernization of part of the heating system of building No. 1 of the Institute with the installation of an air-water heat pump [2].

To conduct research on the effectiveness of the heat pump, the temperature of the heat carrier in the forward and return pipelines of both circuits is measured by TSP-002k type thermal sensors and recorded by secondary control devices. To automate the operation of the heat pump, following temperature sensors are used:

- heat carrier in the supply and return circuit of the heat pump with an intermediate heat carrier (supply and return heat carrier from the heat pump);
- heat carrier in the supply and return circuit of heating devices (supply and return heat carrier of the heating system);
- heat carrier in the supply and return circuit of the centralized heat supply system (supply and return heat carrier of the heating system);
- air inside the control room;
- external air.

Experimental studies, the results of which are presented, were conducted during the heating period in 2019 using different modes of operation of the heat supply system of a part of the administrative building using an air-water heat pump in different operating modes. The duration of the study of one of the modes was an average of 15 days.

With the help of the measuring complex, all the main heat supply parameters were determined and recorded automatically in real time at intervals from one to twenty minutes: the temperature of the heat carrier at the inlet and outlet of all circuits, the air in the control room and the environment, as well as the consumption of the heat carrier in each of the circuits.

Regulation of the heat pump operating modes was carried out using a temperature sensor installed on the return pipeline of the heat pump circuit. For a detailed analysis, time intervals of the heat supply system operation were chosen, during which the temperature of the surrounding air changed slightly and the process of heat transfer through the enclosing structures of the building was quasi-stationary [3, 4].

Study results and their discussion

In Figure 1 shows the experimental data that were obtained on January 24, 2019 from 5:00 a.m. to 11:00 a.m. The heat supply system based on the heat pump worked in the mode of heating 4 circuits of the heating devices of building No. 1, the peak electric boiler was turned off.

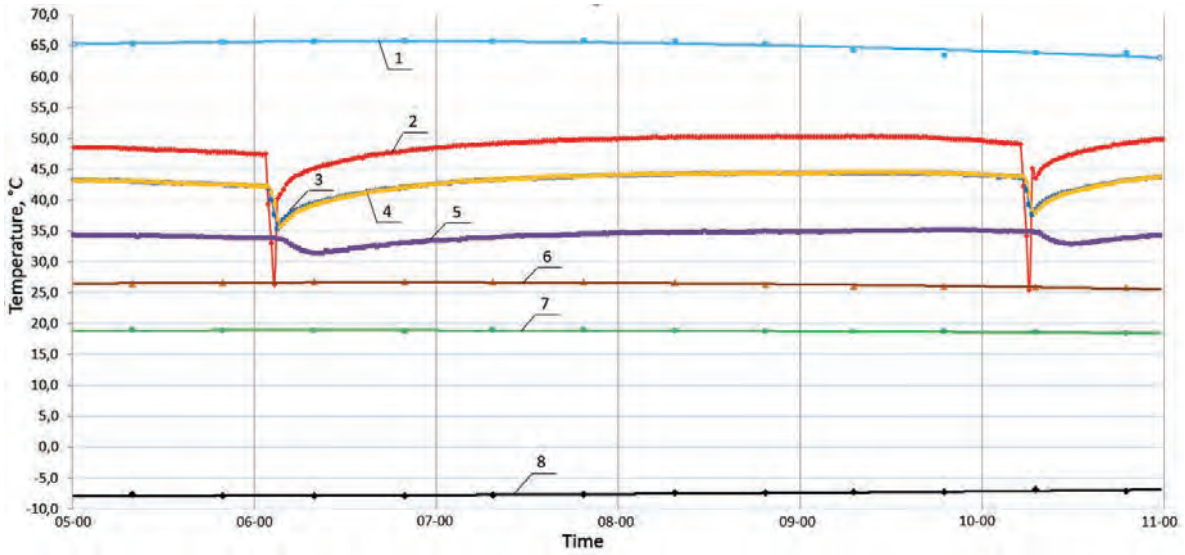

Figure 1. *Dependencies of internal air and heat carrier temperatures in the circuits of the heat supply system of a part of the administrative building 24.01.2019 (hours): 1 – heat carrier supply temperature from the centralized heat supply system; 2 – the temperature of the intermediate heat carrier at the outlet of the heat pump; 3 – the temperature of the intermediate heat carrier at the inlet to the heat pump; 4 – the temperature of the heat carrier on supply to the heating system; 5 – temperature of the return heat carrier from the heating system; 6 – the temperature of the return heat carrier of the centralized heat supply system; 7 – air temperature in the control room; 8 – outdoor air temperature.*

The flow of the heat carrier was:

- heat carrier flow in the centralized heat supply system G_1 = 1.1-1.3 m^3/h;
- heat carrier flow in the circuit of the heat pump G_{TN} = 1.2 m^3/h;
- heat carrier flow in the G_{CO} heating system = 1.4 m^3/h.

As can be seen from Figure 1, the heat pump operates with an on/off interval of about 4 hours, indicating an excessive heat load on the heating system. The temperature of the heat carrier supplied to the heating system is on average 0.5°C lower than the temperature of the return heat carrier of the heat pump circuit. This indicates the insufficiency of the available heat exchange surface and the need to increase it. The outside air temperature ranged from -7.7°C to -7.1°C. The internal air temperature was within 19.0°C ±0.5°C.

Based on the obtained experimental data, the coefficient of performance (COP) of the heat pump was calculated for the above mode of operation of the heat supply system, which was COP_1 = 1.6.

In Figure 2 shows the experimental data obtained on February 25, 2019 from 17:00 to 23:00. The heat supply system based on the heat pump worked in the mode of heating 4 circuits of the heating devices of the building No. 1, the peak electric boiler heated up the heat carrier of the circuit of the heating system of the building. The flow of the heat carrier was:

– heat carrier flow in the centralized heat supply system G_1 = 1.2-1.3 m^3/h;
– heat carrier flow in the circuit of the heat pump G_{TN} = 0.95 m^3/h;
– heat carrier flow in the G_{CO} heating system = 1.75 m^3/h.

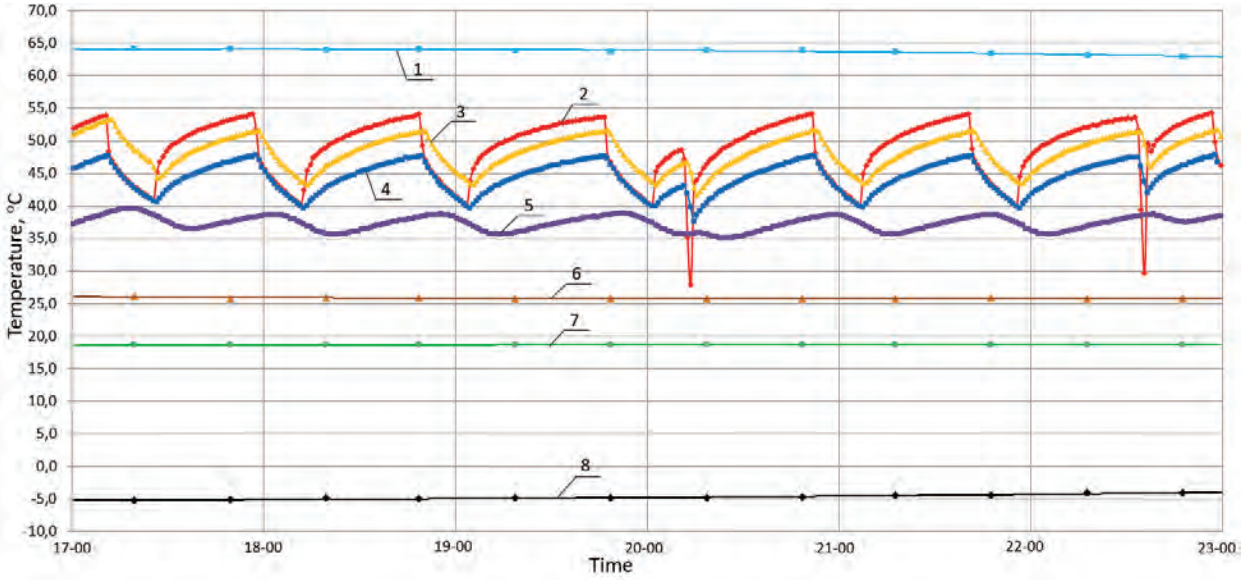

Figure 2. *Dependencies of internal air and heat carrier temperatures in the circuits of the heat supply system of a part of the administrative building 25.02.2019 (hours): 1 – heat carrier supply temperature from the centralized heat supply system; 2 – the temperature of the intermediate heat carrier at the outlet of the heat pump; 3 – the temperature of the intermediate heat carrier at the inlet to the heat pump; 4 – the temperature of the heat carrier supply to the heating system; 5 – temperature of the return heat carrier from the heating system; 6 – the temperature of the return heat carrier to the centralized heat supply system; 7 – air temperature in the control room; 8 – outdoor air temperature.*

The heat pump operation interval in this mode decreased and the on/off period was 1.5 hours. In this operating mode, the temperature of the heat carrier that was supplied to the heating system is on average 3.0-3.5°C higher than the temperature of the return heat carrier of the heat pump circuit due to the operation of the electric boiler. The outside air temperature ranged from -5.3°C to -4.1°C. The internal air temperature was 19.5°C.

Conclusion

Average for the heating period, the COP of the air-water heat pump, when it was integrated into the existing heat supply system of the administrative energy building, was COP = 1.6, which is significantly less than the recommended 2.5-2.7 for proper implementation. However, even with such indicators, a significant saving of thermal energy is achieved, from 10% to 24%, in comparison with the use of a centralized heat supply system.

References

[1] Долінський А.А., Басок Б.І., Базєєв Є.Т., *Енергетична стратегія України: розвиток теплозабезпечення*. Промышленная теплотехника. 2015. Т. 37, No. 2. С. 3-11. https://doi.org/10.31472/ihe.2.2015.01.

[2] Басок Б.І., Бєляєва Т.Г., Коба А.Р., Ткаченко М.В., Недбайло О.М. та інш, *Комплексна модернізація типової системи теплопостачання будівлі на основі використання теплового насосу типу «повітря-вода»*. Промышленная теплотехника. 2009. Т. 31. No. 7. С. 19-21.

[3] Недбайло О.М., *Використання теплового насосу типу «повітря-рідина» в існуючій централізованій системі опалення*. Компрессорное и энергетическое машиностроение. 2010. No. 2(20). С. 32-36.

[4] Басок Б.І., Недбайло О.М., Ткаченко М.В., Божко І.К., Лисенко О.М., Луніна А.О., *Модернізація системи опалення будівлі з використанням теплового насоса типу «повітря-рідина»*. Промышленная теплотехника. 2015. Т. 37. No. 5. С. 68-74. https://doi.org/10.31472/ihe.5.2015.08.

VALIDATION OF THE FANGER MODEL AND ASSESSMENT OF SBS SYMPTOMS IN THE LECTURE ROOM

Natalia Krawczyk, Luiza Dębska, Lidia Dąbek, Grzegorz Majewski, Łukasz Orman

Faculty of Environmental, Geomatic and Energy Engineering
Kielce University of Technology, 25-314 Kielce, Poland
e-mail: ldebska@tu.kielce.pl

Introduction

Thermal comfort is a very important aspect of well-being in closed interiors. It is important to create such parameters of the microclimate that you do not feel any ailments. However, any change in air temperature, humidity or carbon dioxide can make a person start to feel pain in the eyes, dizziness or a runny nose.

Many authors of studies try to discuss this topic – sick building syndrome like [1-3]. On the other hand, the authors of [4] showed in their studies that adequate ventilation will ensure good air exchange, reducing the appearance of infections. In addition, authors from China [5] examined 2370 buildings, confirming that it is the indoor environment that is the factor influencing the appearance of SBS. Another example of research related to SBS as well as productivity was Licina and Yildrim [6], who showed that SBS symptoms were below 20%.

The main purpose of the work is to find out whether the students of the Kielce University of Technology in one of the modern lecture halls may experience such syndromes as dizziness, runny nose, nausea and eye pain.

Methodology

The study was carried out in one of the modern lecture halls belonging to the Kielce University of Technology. In order to conduct the research, a meter called BABUC-A, an Italian manufacturer, was used, and a questionnaire was completed by a group of 69 (age 20-25) people regarding their well-being during the classes, i.e. symptoms related to the sick building syndromes.

Results

Using the BABUC-A meter, internal environmental parameters were obtained for air temperature of 26.2°C, carbon dioxide content of 1223 ppm, and relative humidity of 53.3%. In addition, for the Body Mass Index, the average was 17.71. First, the results regarding the feeling of dizziness were discussed. It turned out that women felt more dizzy than men. Secondly, eye pain was examined. This symptom was confirmed by "I definitely feel" only women (around 10%), while that for "I rather feel" by around 10% for males and females. The rest of the group declared that they "didn't feel anything" or "rather didn't feel anything". Moving on to the next ailment, i.e. the feeling of nausea, it was surprising that the men themselves declared feeling it. Women did not constitute any percentage share. One of the most frequently chosen ailments was a runny nose, as 19% of women and 9% of men indicated that they developed a runny nose after staying in this room. The prevailing conditions that prevailed during the study were definitely not conducive to well-being. Therefore, the answers related to the assessment of thermal sensations and dissatisfaction with the prevailing internal conditions were analysed. The results showed that the actual thermal sensations of people calculated on the basis of surveys (TSV – Thermal Sensation Vote) and the PMV (Predicted Mean Vote) index, calculated on the basis of the ISO 7730 [7] standard, are within the known range of thermal comfort from the ISO 7730 standard of cm from -0.5 to +0.5. However, it should be noted that people nevertheless rated the indoor environment as

good (TSV) as it was -0.15, as opposed to the PMV which was +0.42. Moreover, the PPD (Predicted Percentage of Dissatisfied) indicator was analysed for student surveys and according to the ISO 7730 [7] standard. The feeling of discomfort by students was definitely lower than the data obtained from the ISO 7730 standard.

Conclusion

In the room examined for sick building syndromes, the values for the examined ailments were similarly high for eye pain, dizziness, and runny nose, with the exception of nausea. After analyzing the validation of the Fanger model, discrepancies between the model calculations and the experimental data were noticed. The conclusion that arises after the study is that the possibility of increasing the flow of fresh air could lead to a reduction in the feeling of SBS symptoms.

References

[1] Suzuki N., Nakayama Y., Nakaoka H., Takaguchi K., Tsumura K., Hanazato M., Hayashi T., Mori C., *Risk factors for the onset of sick building syndrome: A cross-sectional survey of housing and health in Japan*, Building and Environment, 202 (2021), Doi: 10.1016/j.buildenv.2021.107976 C.

[2] Hu J., He Y., Hao X., Li N., Su Y., Qu H., *Optimal temperature ranges considering gender differences in thermal comfort, work performance, and sick building syndrome: A winter field study in university classrooms*, Building and Environment, 254 (2022), https://doi.org/10.1016/j.enbuild.2021.111554.

[3] Sun Y., Zhang Y., Bao L., Fan Z., Wang D., Sundell J., *Effects of gender and dormitory environment on sick building syndrome symptoms among college students in Tianjin, China*, Building and Environment 68, 134-139 (2013). Doi: 10.1016/j.buildenv.2013.06.010.

[4] Aguilar A.J., de la Hoz-Torres M.L., Costa N., Arezes P., Martínez-Aires M.D., Ruiz D.P., *Assessment of ventilation rates inside educational buildings in Southwestern Europe: Analysis of implemented strategic measures*, Journal of Building Engineering 51 (2022), https://doi.org/10.1016/j.jobe.2022.104204.

[5] Fan L., Ding Y., *Research on risk scorecard of sick building syndrome based on machine learning*, Building and Environment, 211 (2022), https://doi.org/10.1016/j.buildenv.2021.108710.

[6] Licina D., Yildirim S., *Occupant satisfaction with indoor environmental quality, sick building syndrome (SBS) symptoms and self-reported productivity before and after relocation into WELL-certified office buildings*, Building and Environment, 204 (2021), Doi: 10.1016/j.buildenv.2021.108183.

[7] ISO International Organisation for Standardization, Ergonomics of the thermal environment – Analytical determination and interpretation of thermal comfort using calculation of the PMV and PPD indices and local thermal comfort criteria International Standard ISO 7730.

GAS SYNTHESIS METHOD WITH PREDICTABLE COMPOSITION

Anatoliy Pavlenko[1], Hanna Koshlak[1], Borys Basok[2], Borys Davydenko[2]

[1] Kielce University of Technology
al. Tysiąclecia Państwa Polskiego 7, 25-314 Kielce, Poland
e-mail: apavlenko@tu.kielce.pl

[2] Institute of Engineering Thermophysics of National Academy of Sciences of Ukraine

Worldwide, every year about 20 tons of waste are attributed to each person. The problem of waste disposal is considered to be a major international challenge nowadays. At present, pyrolysis plants, developed and used in various countries, make it possible to neutralize household and industrial waste. Nearly complete absence of air and water pollution is typical of all pyrolysis plants. As a result of this type of destruction, we obtain products with their characteristics depending on the particular method used, as well as the composition of secondary raw materials.

We distinguish two main resulting areas in this paper: waste neutralization and collection of raw materials base. The latter option is the most relevant nowadays. First of all, it is due to the ability to recreate petrochemical products as their natural resource is irreplaceable.

Pyrolysis products were revealed to contain several hundreds of chemical components. More attention is paid to regeneration of individual chemical compounds (levoglucosan and hydroxyacetic aldehyde) or their families (polyphenols) from pyrolysis products. Higher value of individual chemical products, compared to fuel, could make it profitable to extract these products even at low concentrations. An integrated approach to the problem of chemical products extraction and fuels opens up large-scale possibilities in this area.

The purpose of the study is to improve the efficiency of gasification processes of raw materials (biomass, household waste, rubbish, car tyres, etc.) and develop ways of using the synthesised gas in thermal units, processing of synthesised gas into liquid hydrocarbons, hydrogen, fertilizers and other products. The efficiency of processes can be improved by establishing optimal technological regimes for obtaining synthesised gas with predictable composition of chemical components. A mathematical model based on the idea of minimising the system isobaric-isothermal potential has been developed to make such predictions.

The mathematical model will make it possible to determine the synthesis gas composition and temperature during the heat treatment process depending on raw material characteristics and other gasification process parameters. Due to the envisaged non-adiabatic nature of the model it is possible to maintain a constant process temperature by simulating the energy input to the reactor. Thus we can study independent effects of main gasification process parameters such as excess air ratio, biomass moisture and reactor temperature on the synthesis gas composition and yield. In this way, depending on the raw material composition and synthesis gas purpose, we can adjust the pyrolysis process so as to obtain the intended composition of the chemicals in the gas and optimize further pyrolysis gas processing into required products.

If we determine the raw material chemical composition (at least an average) before heat treatment, it is possible to adjust the quantitative parameters of the effect on the raw material to obtain the required pyrolysis gas composition using control functions including process conditions and kinetics of the main reactions.

MOBILE THERMAL ENERGY STORAGE (M-TES)

Volodimir Georgiyovych Demchenko, Alina Vasylievna Konyk

Institute of Engineering Thermophysics of National Academy of Sciences of Ukraine

Introduction

In countries with developed economy, there is a transition to smart energy consumption that is accompanied by the development of technologies with a careful attitude to natural resources and the surrounding environment. Energy-efficient technologies are being used, new equipment, automation and measuring equipment are being created. They reduce the cost of electrical and thermal energy. The main changes concern [1-5] with:

- lowering the heat carrier temperature;
- reduction of heat losses at each stage of heat supply;
- attraction of new non-traditional energy sources;
- creation of decentralized heat supply.

One of the technological solutions used in almost each of these issues is the conservation and accumulation of heat. Nowadays heat storage technologies, special equipment and materials are actively developing [6-8]. The paper is devoted to the development of mobile heat accumulators operating based on latent heat technology [9, 10].

Within the framework of the state order in the Institute of Engineering Thermophysics of National Academy of Sciences of Ukraine design documentation for Mobile Thermal Energy Storage (hereinafter M-TES) for transporting heat from various energy sources has been developed. As a result of the work carried out, M-TES with a heat output of 0.5 MW was manufactured and tested.

The design of the MTA has several of original and at the same time universal solutions presented as objects of patents for inventions:

- design of the battery tank (patent application a2019 11450);
- the composition (formula) of the heat storage material used in the storage tank to increase the storage effect (patent application a2021 07588);
- design of the MTA system as a whole (patent application a2021 01559).

The main purpose of using M-TES is to ensure the collection and primary processing of initial information; create a unified reporting system on performance indicators; improve the quality (completeness, accuracy, reliability, timeliness, consistency) of information; reduce the processing time of information thermal processes, the safety of information and fire safety.

Mobile thermal energy storage

The mobile thermal energy storage is a reliable universal design housed in a standard 20-foot Dry Cube "20DC" container. The container structure is equipped with roller shutters made of AG77 profile, namely, a system for closing technological openings. To insulate the containers in the container, liquid ceramic latex thermal insulation is used.

The container is divided by a partition into two parts an accumulation zone and an individual heating point (IHP).

The accumulation zone consists of 8 heat accumulators (hereinafter referred to as the HA) installed in containers in 2 rows. In the first row 4 heat accumulators are connected in series with each other, in the second row 4 heat accumulators are connected in parallel (Fig. 1). Each HA is equipped with temperature and pressure sensors. Charging and discharging of HA is carried out with the help of ITR.

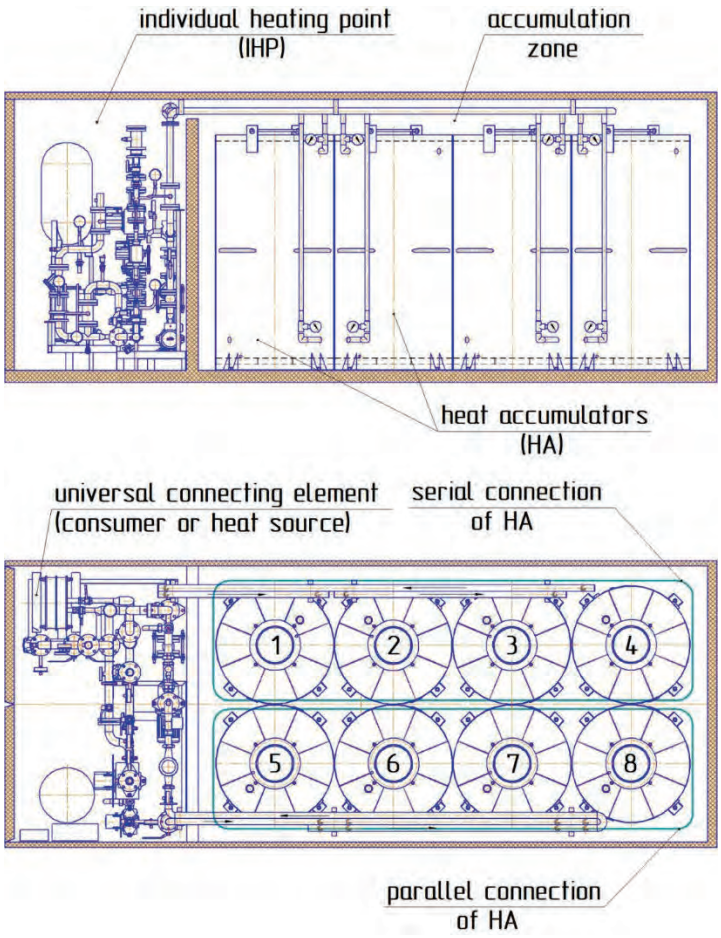

Figure 1. *Mobile thermal energy storage M-TES-0.5 MW.*

The operation of the IHP is carried out through the entrance gate of the container. The ITP is not supposed to have a permanent stay of personnel. For remote monitoring and control the MTE-S is equipped with a PRO-X multifunctional GSM controller (OKO^{TM}, Ukraine), which is usually used for remote monitoring and management at stationary objects simultaneously performing a number of functions.

To ensure adequate operation of the equipment, the M-TES is equipped with a modern automatic control system. The purpose of the automation system is to provide control of the heat supply process with the help of M-TES, access to information about its verification. Therefore, the system must be able to perform the following tasks:

- simplification of data entry;
- providing a secure authentication protocol for logging into the system;
- prevention of user errors when entering data;
- ensuring secure storage of entered data;
- providing open online access and search tools for open data located in the public module and the possibility of downloading them;
- creating an open API for developers to provide secure access to open data and download it in different formats.

To ensure the operation of M-TES the following are automated:

- temperature regulation of supply and return pipelines from the consumer and the storage module;
- management of M-TES charging and discharging processes;
- registration of unauthorized access and fire safety of M-TES;
- geographical location of M-TES.

Technical characteristics of M-TES-0.5 MW

When creating M-TES-0.5 MW, a set of working design documentation was developed. Namely, there are Terms of Reference, Passport, Specifications, a set of working and design documentation. The main technical parameters of these documents are presented in Table 1.

Table 1. *The main technical parameters of documents.*

Parameter, unit of measurement	Value
Mode of operation of M-TES	cyclic
Thermal capacity of M-TES, MW, no more than	0.5
Pressure in tanks and pipelines of the accumulated compartment, MPa, no more than	0.07
Productivity of the coolant of the heating/cooling circuit, m^3/h, up to	2.5
Electric power installed, kW, no more than	8.2
The temperature of the coolant in the heat accumulator circuit when: – charging, °C – discharging, °C	 90 50
The temperature of the direct heat carrier during M-TES charging, °C The temperature of the return heat carrier during M-TES charging, °C	110 60
The temperature of the direct heat carrier during M-TES discharging, °C The temperature of the return heat carrier during M-TES discharging, °C	50 30
The volume of the heat carrier in the heat accumulator, m^3, up to	1.5
The volume of the heat carrier in M-TES as a whole, m^3, up to	12
Overall dimensions of M-TES, no more than: – length, mm – width, mm – height, mm	 6300 3000 3000
Air temperature in the environment during operation, °C	-10...-15

The operation mode of MTA can be intermittent, periodic or cyclical depending on the type of heat source, consumer conditions and the distance between them.

Conclusions

The use of mobile heat accumulators has several of indisputable advantages:

1. There is an opportunity to build flexible heat supply systems for individual consumers, objects of municipal property, critical infrastructure or in cases of emergencies.
2. Use as a heat source of local types of fuels, waste technological heat of enterprises, sources of renewable energy, etc.
3. Reduction of heat losses arising during pipeline transportation as a result of transportation or the occurrence of emergencies.

References

[1] Wirtza M., Kivilipa L., Remmena P., Mullera D. (2020), *5th Generation District Heat-ing: A novel design approach based on mathematical optimization*, Applied Energy, 260, https://doi.org/10.1016/j.apenergy.2019.114158.

[2] Thermal networks, DBN V.2.5-39:2008, Valid with 2009-01-07.

[3] Union European. EU Energy in figures: Statistical pocketbook 2020. 2020. URL, https://op.europa.eu/s/oIDP.

[4] Lunda H., Østergaard P.A., Connolly D., Mathiesen B.V. (2017). *Smart energy and smart energy systems*, Review. Energy, 137, pp. 556-565, https://doi.org/10.1016/j.energy.2017.05.123.

[5] Lund H., Werner S., Wiltshire R., Svendsen S., Thorsen J.E., Hvelplund F., et al. (2014). *4th Generation District Heating (4GDH): integrating smart thermal grids into fu-ture sustainable energy systems*. Energy, 68, pp. 1-11, https://doi.org/10.1016/j.energy.2014.02.089.

[6] Zayeda M.E., Zhaoa J., Lia W., Elsheikhc A.H, Elbannab A.M., Jinga L., Geweda A.E. (2020). *Recent progress in phase change materials storage containers: Geometries, design considerations and heat transfer improvement methods*. Energy Storage, 30, https://doi.org/10.1016/j.est.2020.101341.

[7] Levenberg V.D., Tkach M.R., Holström V.A. (1991), *Heat accumulation*. Technique, 111.

[8] Demchenko V.G., Konyk A.V., *Main aspects of process the heating system, Odessa National University of Food Technologies*, Scientific works, 2020. Issue 1, Tome 84, pp. 48-53. https://doi.org/10.15673/ swonaft.v84i1.1868.

[9] Wang W., Guo S., Li H., et. al. (2014), *Experimental study on the direct/indirect contact energy storage container in mobilized thermal energy system (M-TES)*. Applied Energy, 119, pp. 181-189. https://doi.org/10.1016/j.apenergy.2020.116277.

[10] Du K., Eames P., Kaiser J., Calautit S., Wu Y. (2020), *A state-of-the-art review of the application of Phase Change Materials (PCM) in Mobilized-Thermal Energy Storage (M-TES) for recovering lowtemperature Industrial Waste Heat (IWH)*. Renewable Energy, https://doi.org/10.1016/j.renene. 2020.12.

ENERGY-EFFICIENT HEAT TECHNOLOGIES AND PRODUCTION EQUIPMENT. HEAT FROM RENEWABLE ENERGY SOURCES

Yurii Sniezhkin

Institute of Engineering Thermophysics National Academy of Sciences of Ukraine
e-mail: 1snezhkin@gmail.com

Today, guaranteeing the energy security of an individual country is possible only on the condition that its energy system is achieved and maintained in a state capable of technically reliable, stable, economically efficient and environmentally acceptable provision of energy resources to the economy and the social sphere, despite the existing and expected influence of negative internal and external factors.

Saving energy resources is equivalent to their production, and most often it is the most cost-effective and ecological means of ensuring the growth of energy demand.

Measures to increase energy efficiency and energy saving make it possible to reduce the energy intensity of economic development and the load on infrastructure, thus strengthening the energy security of the country.

In developed countries with high-tech production, a large share of added value in the gross domestic product (GDP) and a high level of energy efficiency, GDP growth occurs with a practically stationary, and in some countries even a decrease in the level of consumption of fuel and energy resources (PER). So, for example, in the German economy, there is also a significant reduction in greenhouse gas emissions. The energy intensity of GDP in Ukraine is much higher, than in the developed countries of the world. Therefore, the strategic direction of the country's development is to reduce the energy intensity of GDP.

The choice of a rational method of transformation (fuel consumption) aimed at increasing the return of energy to the final consumer is the main thing in energy efficiency. The main generalizing criterion of efficiency is the coefficient of use of primary energy. It is defined as the ratio of useful heat to the calorific value of the spent fuel (Table 1) [1].

Table 1. *Coefficient of use of primary fuel energy*

Type of fuel	Coefficient of using
Electric heating	0.27-0.35
Combustion of fuel in a heat generator	0.75-0.95
Steam compression heat pump with an electric drive	0.6-1.35
Steam compression heat pump with a heat engine	1.37-2.3

A comparison of alternative options for heating the coolant according to the degree of use of primary energy shows that direct electric heating is the least energy efficient (K_{EL} = 0.27-0.35), because an average of 70% of primary energy is lost at a thermal power plant during the production of electrical energy for transportation by networks. Heating the coolant in the heat generator by direct combustion of fuel in the boiler room leads to losses of about 15% of primary energy on average. A significant fluctuation of the primary energy coefficient depends on the design of the heat generator and the type of fuel. For steam-compression heat pumps with an electric drive, the

coefficient of primary energy use (K_{HP}) is equal to the product of the conversion coefficient of the heat pump μ and the coefficient of use of primary energy in the production of electricity (K_{EL}):

$$K_{HP} = \mu \cdot K_{EL}$$

The conversion factor of the heat pump μ depends on the difference between the required temperature of the coolant and the temperature of the cold source, the thermodynamic properties of the working substance and the features of the thermodynamic cycle and the technical perfection of the design.

The main factor of the high coefficient of use of the primary energy of the heat pump (HP) is the use of low-potential heat from renewable energy sources (RES), the potential of which exceeds the energy of explored traditional energy resources by 80 times. Prospective low-potential energy sources in Ukraine are geothermal energy, heat of open reservoirs, wastewater, mine water, ventilation emissions, water circulation cycles in energy and industry.

For the first time in Ukraine, the Institute are developed and implemented a heat pump system for hot water supply with a capacity of 1.5 MW, in which the source of low-potential energy is untreated sewage in Kramatorsk. This heat pump system provides a hot water to 4,400 consumers and saves 1.5 million m^3 of gas per year. Heat pump unit conversion factor (HPU) COP = 3.6.

In general, 8-10% of the energy produced in the world is spent on drying processes, during which more than 25 million tons of moisture, which is a greenhouse gas, evaporates [2]. The use of heat pumps in drying processes is quite effective. As already mentioned, when using heat pumps for heating or hot water supply, it is necessary to find a source of low-potential energy. During the drying process, it is present in the dryer itself – it is a spent coolant. That is, the use of heat pump units in drying processes is an almost ideal option for their use.

The heat carrier, passing through the dryer, lowers its temperature and increases the moisture content. The spent heat carrier enters the evaporator, while its temperature decreases, moisture condenses on the surface of the evaporator, giving energy to the working body, and the heat carrier itself is dried. Passing through the condenser, the dry coolant increases its temperature and enters the dryer again. At the same time, moisture does not enter the environment, but condenses in the HP evaporator and is removed from the dryer as a liquid. Energy consumption for the drying process is several times lower, than in traditional dryers. In some cases, they are even smaller, than the theoretical energy consumption for moisture evaporation from an open surface.

For the first time in Ukraine, a grain dryer for seed grain was developed at the Institute. Energy consumption for moisture evaporation is 0.6-0.8 kWh/l. Similarity of grain after drying – 100%. The dryer was introduced in Ukraine.

The institute also developed and implemented in Vietnam a technological line for the production of food powders from tropical fruits. This line uses a four-zone tunnel dryer with a heat pump unit. The drying unit is designed to dehydrate 450 kg per hour of tropical fruits to a moisture content of 6% in order to obtain food powders from the dried material. The tunnel type dryer has four working zones, each zone maintains its own thermal and moisture parameters of the drying agent. The first three zones work according to the traditional scheme with the release of moist air and the supply of fresh air from the atmosphere. The fourth zone has a closed circulation circuit with a heat pump system for drying the heat carrier of the dryer. In the zone, the temperature is maintained at about 60°C and the moisture content of the coolant is 20 g/kg of dry air, which is 10 g/kg lower than in the environment. Energy consumption per 1 kg of evaporated moisture in the dryer was 1.0-1.2 kWh/l. This made it possible, for the first time in the world, to obtain natural food powders from bananas and pineapples in conditions of high humidity of a tropical climate (temperature 32°C, humidity 35%) [3].

The technically achievable potential from the implementation of HPU in Ukraine is 31.3 billion kWh/year, which is equivalent to more than 4.2 billion m^3 of gas.

Geothermal energy is an independent type of renewable energy, that uses the heat of the Earth's interior as a primary resource to obtain electrical energy and heat.

The main advantage of geothermal energy over other renewable energy sources is environmental cleanliness, renewability, the possibility of stable forecasting of reserves, independence from climatic and seasonal changes, stability and controllability.

The coefficient of use of the installed capacity of geothermal power plants in the world is, on average, 72% and in some cases 95%, which is 3-7 times higher, than that of solar, wind and hydraulic plants. Despite the highest capital investments for the use of geothermal energy carriers, the cost of the produced heat is the lowest compared to other renewable energy sources (up to 2.5-3.0 US cents per 1 kWh).

The Institute was a "pioneer" in the development of geothermal energy in Ukraine. At one time, scientists of the institute developed an environmentally safe method of using mineralized geothermal waters, which was called "Ukrainian". According to the developed method, mineralized geothermal water is raised to the surface and in the geothermal heat point, it gives its energy to the communal heat carrier (water), which is used for heating the premises of buildings, and the spent geothermal water is pumped back underground. In this way, the material balance is preserved and the environment is not harmed by mineralized geothermal water.

The Institute has developed a cogeneration geothermal station for using of gas-saturated thermal waters with a gas piston engine. Gas-saturated thermal water with a temperature of 64°C rises to the surface from a depth of 1,850 m. Gas-saturated thermal water is separated into gas and water in a separator. The gas enters the engine where electricity is produced, and the thermal water in the heat exchanger gives off heat to the communal heat carrier (water) and is pumped back into the bowels of the Earth. The thermal capacity of the station is 0.76 MW, the electrical capacity is 60 kW. The station is implemented in the village of Medvedivka, Autonomous Republic of Crimea.

The annual technically achievable energy potential of geothermal waters in Ukraine is approximately 13.5 thousand GWh/year of heat and 2.3 thousand GWh/year of electricity, which is equivalent to a reduction in natural gas consumption by 2.2 billion m^3 per year [4].

Almost 3 billion tons of peat are produced annually in the world, which is approximately 120 times more than its production. According to UN General Assembly Resolution No. 33/148 of 1978, peat is classified as a renewable energy source. Peat contains much less sulfur and ash, and when burned, it almost does not emit toxic substances and, accordingly, does not pollute the environment, compared to coal. The cost of a unit of energy (GJ) when burning peat is the lowest among existing types of fuel (gas, coal, firewood, biomass).

Ukraine has more than 2 billion tons of peat, which is equivalent to replacing 660 billion cubic meters of gas. In 1928, 35% of all energy in Ukraine was obtained from peat. Then cheap gas appeared and the use of peat as a fuel decreased dramatically. Farmers also say that peat is a very high-quality fertilizer and protest against its use as fuel. But the fertilizer in peat is humic substances, the amount of which reaches more than 50%, but they are water-insoluble. Therefore, if peat is used as a fertilizer on acidic soils, then there is no benefit from it. We have developed a technology by which humic substances are extracted from peat (with an alkaline solution), and biomass is added to the processed peat and we obtain a high-quality composite fuel, the heat of combustion of which is 15-17 mJ/kg. For fuel, we developed and approved technical specifications, and for technology we received patents and sold a license for this technology in Vietnam. The technically achievable potential from the introduction of composite fuel in Ukraine is about 1.6 million ton of conventional fuel, which is equivalent to the replacement of more than 1.0 billion m^3 of natural gas [5].

For burning composite and other types of large-fraction organic fuels (cod, wood pellets), the Institute created a water-heating boiler KVU-0.5T. Structurally, the boiler is 3-pass for flue gases and 2-pass for water. The boiler is made from unified components, which greatly simplifies the production technology and reduces its cost. The design of the boiler allows you to replace the water heating drum with a steam one, change the type of fuel and fuel supply, use a retort pallet burner or

a compressed layer burner, which are designed for burning large-fraction solid fuel. Fuel consumption per 1 Gcal is 160-240 kg/h. The working pressure of water is 0.6 MPa. The water temperature at the boiler outlet is 115°C, and at the inlet is 60°C. The efficiency factor is 90%. The weight of the boiler is 3000 kg. The overall dimensions are 2.7 x 1.7 x 2.0 m. The boiler was introduced in Ukraine.

A compressed layer burner device has been developed, which can be used to create boiler units and heat generators, as well as to transfer boilers, furnaces, dryers operating on natural gas, with the aim of replacing it with alternative fuel (coal, wood pellets, pellets, agricultural processing waste). The combustion process is two-stage. The completeness of combustion is up to 1.0. The thermal voltage of the combustion mirror is 3.0-8.0 MW/sq·m. The burner device is manufactured for thermal power depending on the needs of the customer and the type of fuel. The burner is introduced in Ukraine.

The implementation of the technologies and equipment presented above at the country's enterprises will contribute to the diversification of local energy consumption, will make an important contribution to reducing the energy intensity of Ukraine's GDP, and will also provide a number of economic and environmental benefits.

References

[1] Snezhkin Y.F., Chalayev D.M., Shavrin V.S., Dabyzha N.O. (2008), *Heat pumps in the heating and cooling system*. Polygraph-Service LLC (in Ukrainian).

[2] Mujumdar A.S., Kudre T. (2001), *Progress in drying technologies* [Text], Vol. 7, 459.

[3] Sniezhkin Yu.F., Shapar R.O. (ed.) (2021), *Energy efficiency of drying processes: Thematic collection of articles*. Kyiv: Tropea, Vol. 2 (in Ukrainian).

[4] Dolinsky A.A., Rezakova T.A. (2017), *The contribution of geothermal energy to the energy independence of Ukraine*. Industrial heat engineering, Vol. 39, No. 2, pp. 6-11 (in Russian).

[5] Snezhkin Yu.F., Korinchuk D.M. (2022), *Peat is an effective alternative type of fuel*. Thermal physics and thermal energy, Vol. 44, No. 3, pp. 5-15 (in Ukrainian).

APPLICATION OF ENERGY EFFICIENT WINDOWS IN PASSIVE SMART HOUSES

Borys Basok, Borys Davydenko, Liliia Kuzhel, Volodymyr Novikov

Institute of Engineering Thermophysics of National Academy of Sciences of Ukraine

Introduction

For Ukraine, the policy of increasing energy efficiency and energy saving in the housing and communal sector is extremely relevant. In [1] presents a national plan to increase the number of buildings with a minimum level of energy consumption, where much attention is paid to ensuring the energy efficiency of buildings and reducing energy consumption in buildings. These measures will save millions of tons of reference fuel [2].

Thousands of passive buildings are being built around the world. The reason for this trend is that the standards of the passive house are clearly defined, apply in all climatic zones and ensure minimal energy consumption. Important problems arising in the design of passive houses are the reduction of outdoor air infiltration through the building envelope, as well as the elimination of the causes of the formation of "cold bridges". In general, to reduce the energy consumption of buildings, the reduction of heat losses is crucial. An important role in the construction of passive buildings is played by window structures, which should be one of the most important elements of the tightness of the structure of the whole house, and at the same time be characterized by the insignificant heat transfer coefficient.

An experimental "smart" passive house is located on the territory of the **Institute of Engineering Thermophysics of NAS of Ukraine**. A characteristic feature of this house is that its walls are built from different building materials. It uses various insulation technologies, various types of energy-efficient window structures are installed, and a combined heat pump system for heat supply is used. It is fully equipped with monitoring systems that continuously record temperature, humidity, heat flow and other parameters on all surfaces of the building for testing, approbation and research of building materials [2].

Two-chamber double-glazed windows with two low-emission coatings with five-chamber frame profiles were chosen as translucent structures. This choice was made after the analysis of previously obtained experimental data on different types of double-glazed windows with different gas filling of the chambers of the double-glazed window and with different distances between the glasses. Double-glazed windows of this type have the highest thermal resistance and are cost-effective.

Results

To determine the heat loss through the building envelope of the experimental "smart" passive house, a measuring complex was developed and installed, with the help of which the heat flux densities on the facade surfaces and the temperature indicators of these surfaces were determined in real time. Obtained experimental data of heat flux density pulsations and temperature of the inner and outer surfaces of a double-glazed window with two i-coatings (4i-8-4M1-8-4i), and the temperature of the outside air and the air inside the room. Also the resistance to heat transfer of the investigated double-glazed window was determined.

As the results of numerical simulation of the temperature regime of windows with ordinary glass show, about 65% of the heat from the room to the environment is transferred by radiation through the windows [4]. The reduction of the radiant component of the total heat flux is facilitated by the application of a low-emission coating on the inner surfaces of the glasses. To elucidate the effect of a low-e coating on the resistance to heat transfer through windows, a numerical simulation of heat transfer was performed under the condition that there is no low-e coating on the glass, for the case

of one low-e coating on the inner glass and for the case of two low-e coatings: one on the inner glass, and the second on the outer glass.

The results of calculating the distribution of the vertical velocity of the flow of the gaseous medium v_z and temperature over the thickness of the double-glazed window 4i-8-4M1-8-4i in its middle vertical section are shown in Figure 1. The up-and-down flow of the gas medium in the double-glazed unit chambers occurs as a result of natural convection. As can be seen from the figure, under these conditions, the air flow velocity in the chambers does not exceed v_z = 0.008 m/s. In this regard, in double-glazed windows with a distance between glasses of 8 mm, convection does not significantly affect the overall heat transfer. This is also evidenced by the almost rectilinear distribution of temperature over the thickness of the gas layer. Heat is transported primarily by radiation and conduction. The minimum effect of convection is an important advantage of double-glazed windows with a distance of 8 mm between the panes. At the same time, this distance provides the minimum thermal resistance to heat conduction through the gas layer of the double-glazed window.

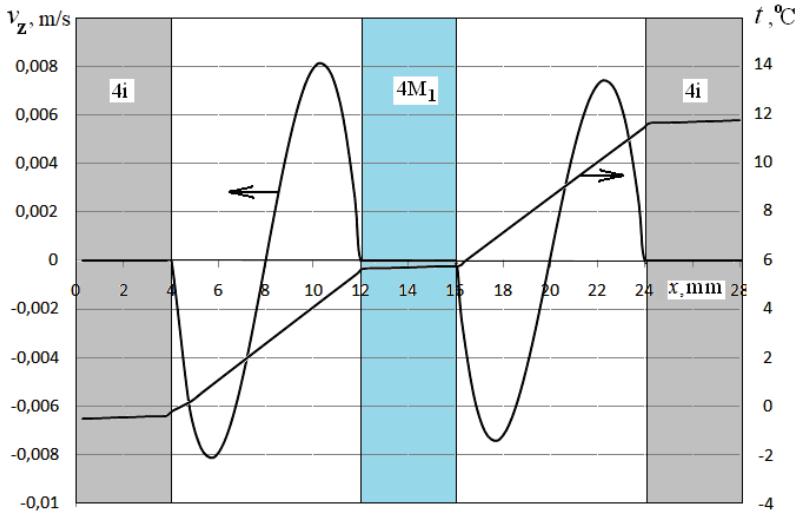

Figure 1. *Vertical velocity distributions in the gas interlayers between panes and temperature across the thickness of a 4i-8-4M1-8-4i double-glazed window with two low-emissivity coatings.*

The results of calculating the distribution of heat fluxes over the outer and inner surfaces of the investigated double-glazed windows are shown in Figure 2.

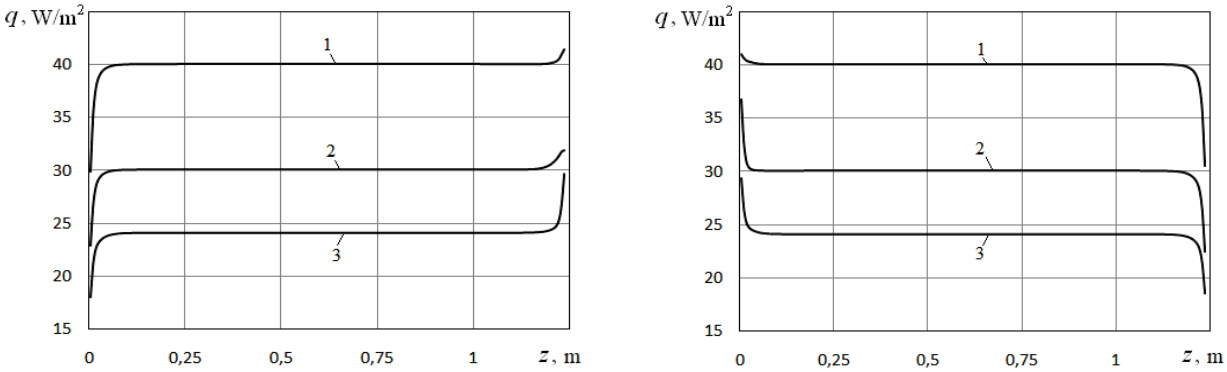

Figure 2. *Distribution of heat flux density over the outer (a) and inner (b) surfaces of double-glazed windows: 1 – 4M1-8-4M1-8-4M1; 2 – 4M1-8-4M1-8-4i; 3 – 4i-8-4M1-8-4i.*

As can be seen from the figure, the distribution of heat flux densities over the surfaces of double-glazed windows is almost uniform except for the areas located near the lower (z = 0) and upper

(z = 1.25 m) ends of the chambers of double-glazed windows, on which the flow of the gaseous medium in the chambers turns and changes its direction. In the middle part of double-glazed windows, the heat flux densities on the inner (Fig. 2a) and outer (Fig. 2b) surfaces practically coincide. For the considered temperature conditions in the case of an uncoated double-glazed window (curves 1, Fig. 2), the heat flux densities are q ~40 W/m^2. For double-glazed windows with one coating (curves 2) q ~30 W/m^2. In the presence of two low-emission coatings (curves 3) q ~24.17 W/m^2.

From the above results, it is possible to evaluate the effect of low-emissivity coatings on the heat transfer resistance of double-glazed windows. The heat transfer resistance between the inner and outer surfaces of an insulating glass unit is calculated using the formula $R_0 = (t_{in} - t_{ex}) / q$. More often, to characterize the heat transfer resistance of an insulating glass unit, the value $R_t = R_0 + 1/\alpha_{in} + 1/\alpha_{out}$ is used, where: α_{in} = 8.6 W/(m^2·K) – heat transfer coefficient on the inner surface; α_{out} = 23 W/(m^2·K) – heat transfer coefficient on the outer surface of the double-glazed window.

A comparison of the heat transfer resistance values for the three considered double-glazed windows is shown in Figure 3. As can be seen from the figure, the minimum resistance R_t = 0.465 (m^2·K)/W has an uncoated double-glazed window. Higher resistance R_t = 0.57 (m^2·K)/W in double glazing with a single coating. The maximum heat transfer resistance R_t = 0.67 (m^2·K)/W is provided by a double-glazed window with two low-emission coatings. Approximately the same value R_t = 0.7 (m^2·K)/W was obtained as a result of experimental studies.

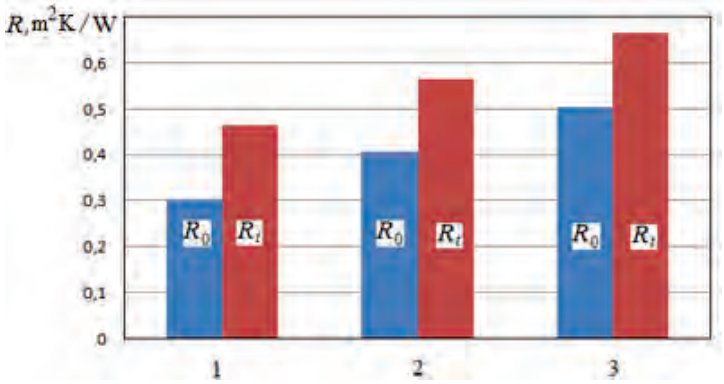

Figure 3. *Influence of a low-emissivity coating on the heat transfer resistance of double-glazed windows: 1 – 4M1-8-4M1-8-4M1; 2 – 4M1-8-4M1-8-4i; 3 – 4i-8-4M1-8-4i.*

Based on the results of experimental studies, as well as theoretical studies, we can conclude that window panes with two low-emission double-glazed windows have thermal performance that meets the requirements of building codes of Ukraine. The presented thermophysical model makes it possible to determine the regularities of the radiation and convective components of the heat flux, as well as the velocity in the gas interlayers of the chambers of double-glazed windows.

References

[1] The Law of Ukraine on Energy Efficiency of Buildings. Available: https://zakon.rada.gov.ua/laws/show/2118-19#Text.

[2] Goncharuk S., Kalinina M., Bozhko I., Kuzhel L., Lysenko O., *Creation of an experimental energy-efficient passive type house "zero energy"*, Industrial Heat Engineering, 2014, Vol. 36, No. 3, pp. 88-95.

[3] Basok B., Belyaeva T., Khybyna M., *Energy efficient passive type houses*. Materials XII International. online conference: Problems of thermophysics and heat energy (October 26-27, 2021). Kyiv: Symonenko OI, 2021, p. 149.

[4] Basok B.I., Davydenko B.V., Isaev S.A., Goncharuk S.M., Kuzhel L.N., *Numerical modeling of heat transfer through a triple-pane window*. Journal of Engineering Physics and Thermophysics. 2016, Vol. 89, No. 5, pp. 1277-1283.

ENERGY-ACTIVE WINDOWS

Boris Basok, Boris Davydenko, Svitlana Goncharuk, Maryna Moroz

Institute of Engineering Thermophysics National Academy of Sciences of Ukraine

Introduction

In Ukraine, the minimum permissible value of the reduced heat transfer resistance for translucent enclosing structures for the first and second temperature zones of building operation is $R_{q\min}$ = 0.9 m^2 K/W (I) and $R_{q\min}$ = 0.7 m^2 K/W (II), respectively [1]. That is why the greatest attention from a thermotechnical point of view should be paid specifically to the windows. After all, the largest percentage of heat losses in a building is carried out through translucent structures due to their relatively low resistance to heat transfer (about 40%, and in some cases much more of the total heat losses of the building). Therefore, the study of the thermal insulation capabilities of window structures and the creation or improvement of the design of energy-saving and energy-active windows is an extremely important problem.

Results

Translucent structures with ventilated glass units are one of the types of energy-active windows. In this case, the heat of the removed air from the room is used by pumping it through the interlayers in the glass unit. A number of studies on this issue have been carried out (for example, [2-5]). Most of the studies are aimed at the established mode of operation under constant boundary conditions. But the temperature of the outside air, wind speed, solar radiation change not only depending on the season, but also during the day. To solve this issue, a method for calculating thermal processes in two-chamber windows with a ventilated inner layer was created, taking into account variable climatic factors [6].

Another type of energy-active window can be a window structure with electric heating. As a rule, the inner surface of the inner glass in the double-glazed unit is heated. For this purpose, a low-emission heat-saving coating applied to the inner surface of the inner glass based on sputtering of certain metal ions is used as a heating resistive element. Electric voltage is applied to equidistant (for example, opposite) corners of the heated glass. From an energy point of view, due to significant heat losses through such a window to the external environment, it can be assumed that using a window with electric heating is not rational. In this regard, thermophysical models were developed and certain experimental studies were carried out to determine the effect of the use of windows with electric heating on the thermal regime of the building premises [7-12]. Appropriate experimental and numerical studies were carried out to obtain the distribution of heat flux and temperature over the surfaces of triple-glazed windows with electric heating [13].

Conclusions

Two types of energy-active window structures were analyzed, namely supply air' ventilated and heated windows.

A method for taking into account the continuous impact of a combination of climatic factors on heat transfer in triple-glazed windows with a ventilated inner chamber with air extracted from the room was created. It allows you to constantly monitor thermal processes through such windows and establish the effectiveness of decisions. Calculations showed that with an air exchange coefficient in the room equal to 1.5, air blowing the inner chamber of a triple-glazed window of a similar design leads to a reduction of annual heat losses by half.

Experimental and numerical studies of heat transfer processes through an energy-saving triple-glazed window with electric heating (4i-10-4M1-10-4i) were carried out. The data showed that 83...85% of the heat released due to electric heating is transferred to the room, and 15...17% – to the external space.

Energy-active windows can be used as a backup heating system for the premises of the building, as well as to create a comfortable temperature and humidity regime in the room.

References

[1] DBN V.2.6-31:2021 Thermal insulation and energy efficiency of buildings. K.: Minregion of Ukraine, 2022. 23 p.

[2] Gloriant F., Joulin A., Tittelein P., Lassue S., *Using heat flux sensors for a contribution to experimental analysis of heat transfers on a tripleglazed supply-air window*. Energy. Vol. 215, 2021, pp. 119-154, DOI: 10.1016/j.energy.2020.119154.

[3] Nourozi B., Ploskić A., Chen Y., Ning-Wei Chiu J., Wang Q., *Heat transfer model for energy-active windows - An evaluation of efficient reuse of waste heat in buildings*, Renewable Energy Vol. 162, 2020, pp. 2318-2329, DOI:10.1016/j.renene.2020.10.043.

[4] Ala-Kotila P., Vainio T., Laamanen J., *The Influence of Building Renovations on IndoorComfort – A Field Test in an Apartment Building*. Energies 2020, 13, 4958, DOI: 10.3390/en13184958.

[5] Southall R., Mcevoy M., *Investigations into the functioning of a supply air window in relation to solar energy as determined by experiment and simulation*. Solar Energy 2006, 80(5), pp. 512-523, DOI: 10.1016/j.solener.2005.04.016.

[6] Basok B.I., Nakorchevskii A.I., *Thermal physics of the influence of solar radiation on buildings*. K.: Scientific opinion, 2016, 223 p.

[7] Kurnitski J., Jokisalo J., Palonen J., Jokiranta K., Seppänen O., *Efficiency of electrically heated windows*. Energy and Buildings, 2004, Vol. 36, No.10, pp. 1003-1010, DOI: 10.1016/j.enbuild.2004.06.007.

[8] Moreau A., Sansregret S., Fournier M., *Modeling and Study of the Impacts of Electrically Heated Windows on the Energy Needs of Buildings*. 6th IASME/WSEAS International Conference on heat transfer, thermal engineering and environment (HTE'08). At: Rhodes, Greece, August 20-22, 2008, pp. 76-83.

[9] Cakó B., Lovig D., Ózdi A., *Measuring the effects of heated windows on thermal comfort*. Pollack Periodica. 2021, Vol. 16(3), pp. 114-119, DOI: 1556/606.2021.00361.

[10] Jammulamadaka H.-S., *Evaluation of Energy Efficiency Performance of Heated Windows*. Graduate Theses, Dissertations, and Problem Reports, 2017, pp. 58-79.

[11] Krukovskyi P.G., Smolchenko D.A., Krukovskyi G.P., Deineko A.I., *Analysis of the heating capacity of electrically heated windows*. Thermophysics and Thermal Power Engineering. 2021, 43(4), pp. 62-67, DOI: 10.31472/ttpe.4.2021.7.

[12] Lee R., Kang E., Lee H., Yoon J., *Heat Flux and Thermal Characteristics of Electrically Heated Windows: A Case Study*. Sustainability. 2022, 14, 481, DOI: 10.3390/su14010481.

[13] Basok B.I., Davydenko B.V., Goncharuk S.M., Pavlenko A.M., *Experimental and numerical studies of heat transfer from a double-glazed window with electric heating of its surface*. The Proceedings of the Institute of Electrodynamics of the NAS of Ukraine. 2022, 62, pp. 12-18, DOI: 10.15407/publishing 2022.62.012.

ORGANIZATION OF EMERGENCY HEAT SUPPLY OF HEALTH CARE FACILITIES AND EVACUATION ASSEMBLY POINTS LOCATED IN EDUCATIONAL INSTITUTIONS OF KYIV

Borys Basok, Maryna Moroz

Department of thermophysical basics of energy-saving technologies Institute
of Engineering Thermophysics National Academy of Sciences of Ukraine,
e-mail: basok@ittf.kiev.ua; morozmarina234@gmail.com

The provision of vital activities in the premises during the heating period depends on the maintenance of the thermal regime through the stable operation of the heat supply systems. Centralized heat supply, which historically began to develop since 1937, is the main way of providing consumers of the city of Kyiv with thermal energy for heating, hot water supply and other needs. The sources of thermal energy generation for centralized heat supply systems are the facilities of KP «KYIVTEPLOENERGO» (CHP-5, CHP-6, «Energia» plant, 4 heat supply stations and 179 boiler houses), Darnytsia CHP (CHP-4, EURO-RECONSTRUCTION LLC) and departmental industrial heating boiler houses, as well as individual heating systems [1].

Due to significant physical wear and tear of heat supply systems in Ukraine, emergency shutdowns often occur, which negatively affects the microclimate of the premises and the stable operation of the life support system and requires additional and significant material costs for their restoration. Unfortunately, in addition to physical wear and tear, the operation of energy infrastructure facilities is negatively affected by war [2]. Therefore, it is relevant to carry out research on the organization of emergency heat supply in emergency-deficit situations in heat supply systems.

Knowing the complexity of the upcoming heating season and the seriousness of the risks associated with it, the Kyiv city government takes additional measures to eliminate emergency situations, including: purchase of transportable boiler installations (TBI); increasing the stock of reserve fuel for CHP; purchase of an additional number of generators; checking the condition of electrical networks and electrical equipment, for stable operation in conditions of increased load.

In order to prevent deaths from hypothermia when the temperature drops significantly and for people to stay in the evacuation collection points in the event of an emergency shutdown of the heat supply, 5-6 educational institutions were selected from each district. New institutions or educational institutions were chosen, which at one time implemented a set of energy-efficient measures, including comprehensive thermal sanitation, reconstruction of DHS and internal engineering systems.

A significant demand during martial law was caused by modular mobile boiler houses installed directly near consumers. In order to ensure the conditions for the provision of medical services in the health care institutions of the city of Kyiv and the organization of collective heating points, the commission on technogenic and ecological safety and emergency situations of the executive body of the Kyiv City Council made a decision on the need to provide such institutions with transportable boiler plants. For uninterrupted operation of the boiler room in the absence of electricity, diesel generators are provided.

Such a boiler plant is a complete, automated technological complex, fully prepared for operation and consisting of a metal structure, an automated water heating boiler on liquid fuel, a water storage tank, a pumping unit with a network and recirculation boiler pump, a plate heat exchanger, electrical equipment, an automation system; control and measuring devices and transportable capacity of diesel fuel. As a rule, unified and standardized containers are used as metal structures (Fig. 1). The transportable boiler room is fully automated and works without permanent maintenance personnel, and the automation system provides emergency protection of the equipment.

Figure 1. *Transportable boiler installations with a diesel generator.*

The TBI is connected to the internal heating system of the building, namely to the supply and return pipelines of the heating system, after the mixing units, elevator units or heat exchangers of the heating system. In order to make such a connection possible, it is necessary to perform reconstruction of the internal heating system, which includes: performing preparatory work for the possibility of operational connection of a transportable boiler room; pipeline laying from the place of installation of TBI to DHS; installation of additional equipment in the existing premises. To prevent the fusion of the heat carrier in emergency modes, the installation of rotary valves with electric drives is provided on the supply and return pipelines of the heating system. For the initial filling of the system when connecting a transportable boiler house, the installation of a feed pump is provided, and to ensure the necessary reserve of coolant – a non-pressurized plastic tank.

As a result of Russia's military aggression, Ukraine's energy sector suffered significant losses and continues to be the main target of Russian aggression. Therefore, local executive authorities and energy supply organizations should coordinate measures to prepare for the heating period, taking into account possible threat scenarios to ensure uninterrupted heat supply in a crisis situation.

References

[1] Kyiv regional state administration. Separate subdivision "Kyiv Regional Expert Center for Energy Efficiency" SE "KYIVOBLBUDINVEST" "Heat supply scheme of the city of Kyiv for the period until 2030", Kyiv, 2020.

[2] The National Council for the Recovery of Ukraine from the Consequences of the War. Project of the Recovery Plan of Ukraine. Materials of the working group "Audit of losses incurred as a result of the war". July 2022, https://www.kmu.gov.ua/storage/app/sites/1/recoveryrada/ua/audit-of-war-damage.pdf.

A REVIEW AND RESEARCH OF THE SYNTHESIS AND APPLICATION OF ZEOLITES FROM FLYASH

Hanna Koshlak, Anna Kaczan

Faculty of Environmental, Geomatic and Energy Engineering
Kielce University of Technology, 25-314 Kielce, Poland

Waste – the main problem of today's communities. Environmental engineering and ecology are struggling with increasingly difficult topics regarding waste and its disposal. A big complication for many years is the use of fly ashes that have been left after burning coal. One of the directions for fly ash that scientists have chosen over time is to use it as a substrate in the syntheses of hydrothermal mesoporous materials, the so-called synthetic zeolites. There are natural zeolites and synthetic zeolites – with strictly defined structure parameters, which allows them to be qualified for specific applications. The formation of zeolites is a complex process that involves the transformation of silicates and aluminates, the formation and dissolution of aluminosilicates, the continuous change of solid phase and gel solution phase, and the formation and growth of zeolite nucleation. Synthetic zeolites are constantly being improved, and thanks to innovative production technologies, new ones will also be created, depending on what they will be used for. The object of the research are fly ashes from the combustion of hard coal in one of the Polish power plants. The subject of the research is the method of synthesis carried out with different mass ratios of fly ash NaOH and the study of the effect of NaOH concentration in the activating solution on the composition of the synthesized sample. Methods of research: the morphology and chemical composition in the micro-area of the main mineral components of the tested materials was determined using a scanning microscope (SEM). In the results fly ash the dominant chemical components were SiO_2 and Al_2O_3, while the main phase components were mullite, quartz and hematite, and a significant share of amorphous substance (glass and unburnt organic substance). The presence of oxide minerals – Al_2O_3, Fe_2O_3, MgO, CaO was established in the mineral composition of bottom ash; silicates and aluminosilicates – with island, ring, chain, layered and spatial structure.

OCCUPANCY IMPACT ON THE INDOOR AIR QUALITY OF THE MONITORED OPEN-OFFICES

Vilūnė Lapinskienė, Violeta Motuzienė, Genrika Rynkun

Vilnius Gediminas Technical University, Lithuania

Introduction

Today, people spend up to 90% of their time in an indoor environment. It is well known that indoor air quality (IAQ) has a significant impact on health, well-being, and human performance. Therefore, to ensure a minimum ventilation rate to guarantee air quality conditions different countries have different requirements [1]. CO_2 is the most common indoor air pollutant and is commonly used as a metric of IAQ [2]. It is commonly assumed that when the CO_2 level is higher than 1000 ppm, it indicates that the room is polluted, which can lead to poor well-being, health, and productivity [3]. As the main source of CO_2 in the room are its occupants, it is obvious that room occupancy is directly related to the CO_2 concentration and demand for ventilation.

Occupancy (demand) based ventilation is a key solution to optimise energy consumption related to ventilation. Here different sophisticated, artificial intelligence-based methodologies are developed and proposed by scientists already for some years. E.g. novel image-based occupancy positioning system for demand-oriented ventilation [4], different neural network based methods [3], etc. But Covid-19 pandemic have brought upfront significant changes in buildings IAQ to minimize spread of viruses [5]. However, even at these conditions, demand-controlled ventilation is considered as a key solution to keep buildings safe and energy efficient, just more novel CO_2-based demand-controlled ventilation strategies can be applied [6].

It was noticed, that occupancy of the office buildings was also significantly changed (decreased) by the pandemic [7]. The goal of this paper is to demonstrate based on long-term measurements of modern office buildings how changes in occupancy within recent years influence IAQ.

Methodology

The research is based on long-term (not less than 3 months) measurements performed in 4 office buildings in Vilnius (Lithuania). All the buildings are built after 2005 and have energy efficiency certificates; they also have mechanical balanced air ventilation systems with heat recovery. The occupancy was measured using TableAir double check motion sensors (PIR) which were mounted under the tables and the CO_2 was measured with the weather station HOBO MX1102A. The data were processed to gain hourly values for occupancy and CO_2 concentrations for all of the measured period and for each week separately. The average weekly occupancies and CO_2 concentration graphs were generated.

Results

The example of one of the analysed buildings' (B_1) open-offices CO_2 concentration variations is presented in Figure 1. The measured period is 33 weeks starting from the end of December 2021. The separate grey lines present weekly variations and black lines present average weekly curve from Monday to Friday. It is obvious that most of the time CO_2 concentrations are much lower than generally recommended by many sources – 1000 ppm. An average peak concentration is less than 700 ppm. So the most of the time room is over-ventilated. This is related to very low occupancies of the room and very similar tendencies are found in other measured buildings showing common problems which can be significantly influenced by changes in user behaviours (remote work).

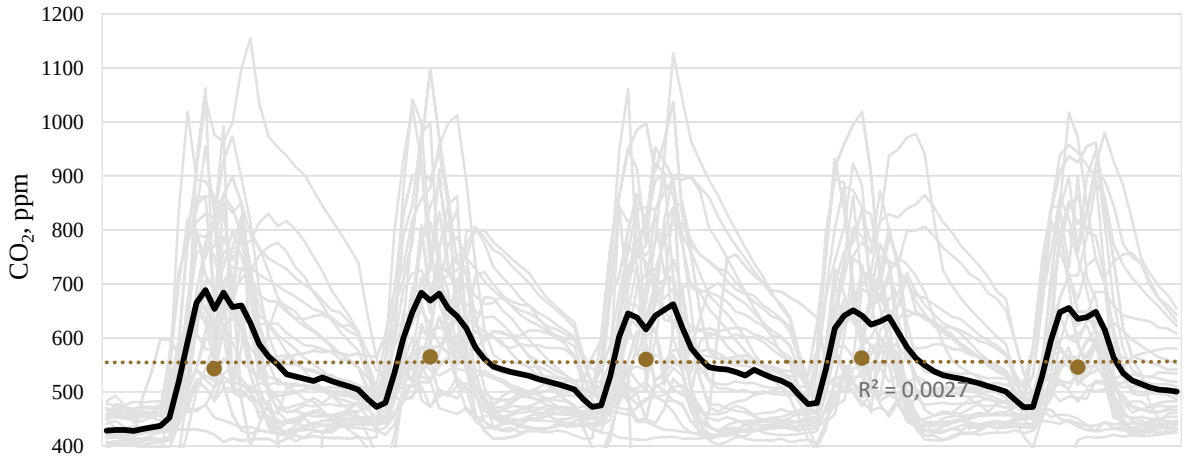

Figure 1. *Weekly CO_2 concentrations variation for open-office of the building B**_1**.*

Conclusions

There is a new tendency in many modern office buildings with balanced mechanical ventilation systems, when ensuring sufficient indoor air quality during building operation is not an issue anymore. Because of changes in buildings occupant's behaviour, e.g. lower occupancies, not all the buildings managers pay attention at the problem of the over-ventilation of such buildings. This causes waste of energy and high energy bills. At the situation when Europe is facing energy crisis, more attention must be paid at actual CO_2 concentrations and real demand for ventilation. Even if ventilation system is not designed as demand controlled, there are different technical cost effective measures that can be applied to tag the energy saving potential and first – better monitoring of indoor environment.

Acknowledgment

This research was funded by a grant (No. S-MIP-20-62) from the Research Council of Lithuania (LMTLT).

References

[1] Becerra J.A., Lizana J., Gil M., Barrios-Padura A., Blondeau P., Chacartegui R., *Identification of potential indoor air pollutants in schools*. Journal of Cleaner Production 2020, Vol. 242, 118420. https://doi.org/10.1016/J.JCLEPRO.2019.118420.

[2] López L.R., Dessì P., Cabrera-Codony A., Rocha-Melogno L., Kraakman B., Naddeo V., et al. *CO_2 in indoor environments: From environmental and health risk to potential renewable carbon source*. Science of The Total Environment 2023, Vol. 856, 159088, https://doi.org/10.1016/J.SCITOTENV.2022.159088.

[3] Wei S., Tien P.W., Chow T.W., Wu Y., Calautit J.K., *Deep learning and computer vision based occupancy CO_2 level prediction for demand-controlled ventilation (DCV)*. Journal of Building Engineering 2022, Vol. 56, 104715, https://doi.org/10.1016/J.JOBE.2022.104715.

[4] Guo M., Xu P., Xiao T., He R., Dai M., Miller S.L., et al., *Occupant-density-detection based energy efficient ventilation system: Prevention of infection transmission*. Journal of Building Engineering 2021, Vol. 187, 102889, https://doi.org/10.1016/j.enbuild.2021.110883.

[5] Park S., Choi Y., Song D., Kim E.K., *Natural ventilation strategy and related issues to prevent coronavirus disease 2019 (COVID-19) airborne transmission in a school building*. Science of The Total Environment 2021, Vol. 789, 147764, https://doi.org/10.1016/J.SCITOTENV.2021.147764.

[6] Li B., Cai W., *A novel CO_2 – based demand-controlled ventilation strategy to limit the spread of COVID-19 in the indoor environment*. Building and Environment 2022, Vol. 219, 109232, https://doi.org/10.1016/J.BUILDENV.2022.109232.

[7] Motuzienė V., Bielskus J., Lapinskienė V., Rynkun G., Bernatavičienė J., *Office buildings occupancy analysis and prediction associated with the impact of the COVID-19 pandemic*. Sustainable Cities and Society 2022, Vol. 77, 103557, https://doi.org/10.1016/J.SCS.2021.103557.

ANALYSIS OF ACTUAL INDOOR CLIMATE PARAMETERS OF A SUPERMARKET IN TERMS OF ENERGY EFFICIENCY

Rasa Džiugaitė-Tumėnienė, Rūta Mikučionienė

Vilnius Gediminas Technical University
e-mail: rasa.dziugaite-tumeniene@vilniustech.lt

Introduction

The increased requirements of building tightness go together with increased attention to indoor air quality (Kempton et al. 2022). The study (Du et al. 2020) shows that customers' satisfaction will improve when the indoor air quality is better in shopping malls. Commercial buildings such as shopping centres usually use BMS (Building management system) to ensure comfort indoor air parameters. However, scientists (Loomans et al. 2020), (Džiugaitė-Tumėnienė et al. 2021) indicated that actual indoor parameters often do not match BMS data. (Życzyńska et al. 2022), (Hauashdh et al. 2022) affirm that technical systems should be managed appropriately, and their performance parameters should be controlled.

Forming new and optimizing existing traditional design solutions for the engineering systems of commercial buildings, it is necessary to evaluate the influence of the functioning and management of indoor climate systems of operating shopping centres on their energy consumption intensity.

The main problems of high energy consumption intensity are the insufficient number of data and control parameters recorded by BMS in the existing objects, the problematic separation of the effect of technological equipment on energy consumption and the indoor climate of the premises, the too complicated connection between the building's indoor climate conditions and energy consumption.

Methodology

The goal of the paper is to determine the main indoor climate parameters of the premises of the existing supermarket, which influence the energy consumption of the building's HVAC systems. The authors assessed the functionality of HVAC system equipment and control solutions, the actual thermal comfort, air quality parameters, and ventilation intensity of the analyzed supermarket. The functionality and efficiency of HVAC systems are evaluated according to these aspects:

1. Actual energy efficiency of the existing HVAC equipment.
2. Is the capacity of the installed heating/cooling equipment sufficient?
3. Are the indoor climate parameters ensured (actual temperature, relative humidity, CO_2) in winter/summer?
4. Is the current control of the HVAC equipment effective?
5. HVAC control complexity level (manual/automatic/mixed).

Results

Analysis and evaluation of the actual indoor climate data of the investigated supermarket determine the main parameters that influence the energy consumption of the building's HVAC systems.

As seen in Figure 1, the variation in air temperature and CO_2 concentration of the supermarket's sales area does not meet the limits of the Building Management System (BMS) settings. It means that the control of the central ventilation system is not based on the indoor climate parameters of the sales area.

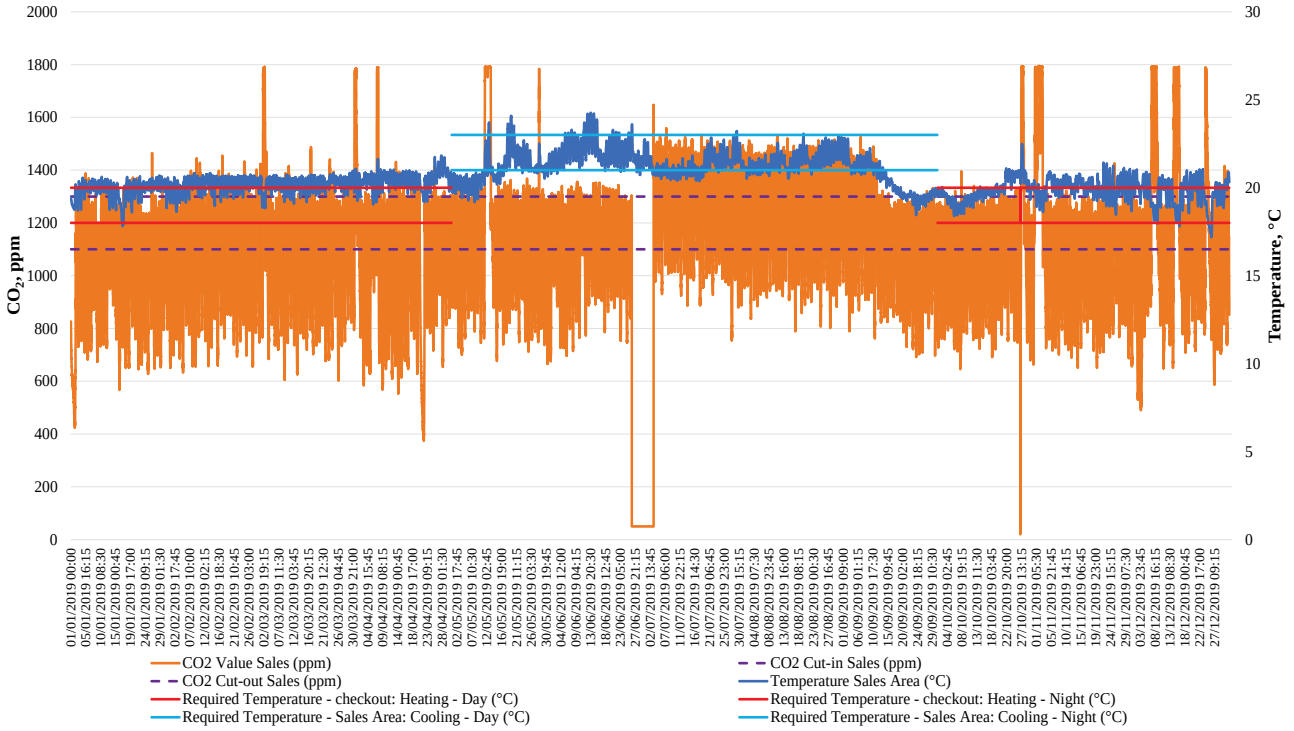

Figure 1. *The variation of air temperature and CO_2 concentration in the supermarket's sales area during the surveyed period.*

The sales area's indoor climate parameters analysis shows that the supplied air temperature during the winter (including March) usually varied in the range of [+29; +31]°C to ensure the required air temperature. During the spring, the supplied air temperature varied in the range of [+21; +24]°C. During the summer, the temperature of the air supplied during the supermarket's working hours varied in the range of [+13; +17]°C to cool the sales area, and during non-working hours [+22; +24]°C. During the autumn period, it varied in the range of [+20; +24]°C. However, in September, cooling of the sales area is still required, so the supplied air temperature is lowered in the range of [+13; +16]°C. The authors found that the supplied air temperature varies considerably (i.e. [+8; +33]°C) to ensure thermal comfort (from +17°C to +24°C) in the supermarket's sales area during the surveyed period of the year. Therefore, such a significant difference in the temperature of the supplied air indicates inappropriate control strategies of the central ventilation system.

The sales area's indoor climate parameters analysis shows that the indoor temperature reaches +20°C during the winter. A slight decrease in temperature to +19°C indicates that the indoor air temperature does not decrease by more than one degree at night. During the spring period, the air temperature of the trading hall varied in the range of [+20; +21]°C. During the summer, the indoor air temperature mainly varied [+21; +23]°C range. However, as the outside air temperature rises, the indoor air temperature exceeds +24°C. The indoor temperature of the sales area varied in the range of [+20; +21]°C during the autumn period. When the outside air temperature is in the range of [0; +10]°C, the indoor temperature decreases up to +17°C.

The central ventilation system of the sales area during the winter usually provided sufficient (from 950 ppm to 1150 ppm) and low (above 1350 ppm) air quality levels. During the spring and autumn periods, the CO_2 concentration usually varied in the range of [1134; 1294] ppm. The authors noticed that the air quality in the sales area was low during the most intensive work hours. During the summer, the CO_2 concentration usually changed in the range of [950; 1490] ppm. The authors noted that 11 stops (failures) of the ventilation system occurred per year. Most of the time, the proportion of outdoor air supplied to the trade hall is from 0% to 26% per year, resulting in sufficient or low air quality levels in the sales area of the supermarket.

Conclusions

The authors showed that the air temperature of the sales area of the supermarket is ensured during the analyzed period. The premises' thermal comfort is provided by higher energy consumption because of the central ventilation system's inappropriate control of the supplied air temperature. The authors indicated that the electricity consumption of the HVAC systems of the analyzed supermarket is the highest for the heating and cooling when heating/cooling coils (VRF type) of central ventilation system have been used to heat and cool the supplied air the whole year. In order to save energy, the Facility Manager runs the central ventilation system in partial or complete recirculation in winter and summer. Therefore, sufficient or low air quality levels are maintained in the sales area of the supermarket during working hours.

References

[1] Kempton L., Daly D., Kokogiannakis G., Dewsbury M. (2022), *A rapid review of the impact of increasing airtightness on indoor air quality*, Journal of Building Engineering 57(March): 104798. DOI: 10.1016/j.jobe.2022.104798.

[2] Du X., Zhang Y., Lv Z. (2020), *Investigations and analysis of indoor environment quality of green and conventional shopping mall buildings based on customers' perception*, Building and Environment 177(April): 106851. DOI: 10.1016/j.buildenv.2020.106851.

[3] Loomans M.G.L.C., Mishra A.K., Kooi L. (2020), *Long-term monitoring for indoor climate assessment – The association between objective and subjective data*, Building and Environment 179(May): 106978. DOI: 10.1016/j.buildenv.2020.106978.

[4] Džiugaitė-Tumėnienė R., Mikučionienė R., Streckienė G., Bielskus J. (2021), *Development and analysis of a dynamic energy model of an office using a building management system (Bms) and actual measurement data*, Energies 14(19). DOI: 10.3390/en14196419.

[5] Życzyńska A., Suchorab Z., Majerek D., Motuzienė V. (2022), *Statistical Analysis of the Variability of Energy Efficiency Indicators for a Multi-Family Residential Building*, Energies 15(14). DOI: 10.3390/en15145042.

[6] Hauashdh A., Jailani J., Rahman I.A., AL-fadhali N. (2022), *Strategic approaches towards achieving sustainable and effective building maintenance practices in maintenance-managed buildings: A combination of expert interviews and a literature review*, Journal of Building Engineering 45 (August 2021): 103490. DOI: 10.1016/j.jobe.2021.103490.

INTELLIGENT BUILDINGS

Borys Basok, Tetyana Belyaeva, Maryna Khybyna

Institute of Engineering Thermophysics of the National Academy of Science of Ukraine,
2a, M. Kapnist str, Kyiv, 03680, Ukraine

Introduction

An intelligent building is a set of organizational, engineering and technical measures and software tools aimed at creating a highly efficient economic infrastructure for servicing the complex that best meets the needs of users and owners of this building [1]. The concept of smart buildings implies the presence of an automated control system in the premises that controls what is happening inside the building and outside; reacts in the most efficient way to ensure a comfortable and safe stay in the room, minimizing the consumption of energy and resources. Users are provided with simple and affordable system management tools [2].

Certification of smart buildings

Until recently, there was no certification assessment for intelligent buildings. In November 2021, UL (Underwriters Laboratories – an American company for standardization and certification in the field of safety technology) and TIA (Telecommunications Industry Association) announced the possibility of evaluation (certification) of SPIRE™ smart buildings [3]. SPIRE certification provides a comprehensive assessment and rating of the building. To award UL's Verified SPIRE Smart Building Rating, UL experts conduct an in-depth audit of the facility's technologies and processes and virtual discussion meetings. The process focuses on six key categories of building evaluation criteria: capacity and energy, health and well-being, safety of life and property, communications, cybersecurity and sustainability. Upon successful assessment, the building receives a UL-verified SPIRE Smart Building Rating and a plaque displaying the building's overall performance score across the six categories of the rating system's criteria. The UL SPIRE Smart Building Rating was announced at a time when businesses are assessing smart building needs to get back to work amid the COVID-19 pandemic. According to the World Green Building Council, buildings account for 36% of global energy consumption and 39% of energy-related carbon dioxide emissions. Reducing energy consumption and automating temperature and lighting monitoring remain important. The pandemic has set new priorities in the search for a smart building system to help with employee spread tracking, physical distancing, contactless entry, employee temperature reading, ventilation and other efforts to keep employees and residents safe. The SPIRE rating reflects the operational qualities of a smart building, focus on health care and providing comfortable working (living) conditions for employees (residents).

Each of the smart building examples demonstrates innovation in certain key areas: heating, ventilation, air conditioning, lighting, office design (especially in the wake of the COVID-19 pandemic), and analysis of occupancy and energy efficiency data – all of which support different smart building options today. The value of different smart building options can change over time. For example, just a few years ago, the CABA Monetization of Intelligent Buildings (2018) survey of building operations ranked improving indoor air quality and improving space utilization as relatively low-priority options. Today, these same opportunities are among the most popular due to the transition to hybrid workplaces [4].

History of creation

The "Throne House" of Japanese professor Ken Sakamura in Tokyo, built in the late 1980s, is considered the first demonstrative intellectual building in the world. The housing was maximally

automated with the help of the developed climate sensor system TRON, which responded to changes in the weather. The sensors transmitted data with the microclimate parameters of the premises to the central control panel. Depending on their values, windows were automatically opened or closed; heating and air conditioning systems were turned on or off, etc. [5].

Examples of intelligent buildings

The Xanadu 2.0 house built in the USA (Redmond) for Bill Gates, the creator of Microsoft Corporation, became the most famous and most expensive intelligent house in the world. The house is located on the shore of Lake Washington, occupies an area of 83 thousand m^2 [6]. The "Pacific Lodge" style house is a super high-tech residential complex, most of which is underground. The house was built for 7 years. Each guest is given an RFID (Radio Frequency IDentification) keychain, which allows you to create a unique audio-video-light environment depending on the time of day and mood. RFID readers installed throughout the house provide information to a central computer that controls the lighting of all rooms in the house. In the house, much attention is paid to the ventilation system, heat exchange and air purification from dust and bacteria. The heated air passes through the heat exchanger and gives heat to the fresh air, which is supplied to the premises according to the schedule. The entire building is heated and cooled through a heat exchanger laid at the bottom of the lake and on the minus 5th floor. Temperature, humidity and light sensors are installed in each room. The read information allows you to create an optimal climate in the house. The computer monitors the temperature of the heated floor. The system of uninterrupted power supply allows you to maintain the efficiency of the house for an unlimited time. There is a special water purification and regeneration system. Thus, the house can function autonomously even during global cataclysms.

Rockefeller Center and the UN building in New York are among the most famous intellectual buildings in the USA. The Mall of America intellectual building, the largest shopping center in the USA (Bloomington, Minnesota), is located on an area of 12 hectares. The total operational area of the building is about 500,000 m^2. The Infinity system serves about 1,700 executive controllers and 4 operator posts. The system's tasks include temperature and air pressure management in the building, lighting, smoke control, admission control, and traffic management in the huge parking lot [7]. The Edge building in Amsterdam has been named one of the smartest buildings by Bloomberg and RCR Wireless News. The Edge is a 40,000 m^2 office building designed for the anchor tenant of the international financial company Deloitte. In an intelligent building, information technologies are used to create a working environment and space with efficient use of resources. Especially for the Edge, Philips has made efficient LED panels, which can be powered by the same cables that transmit data for the Internet. The panels are also equipped with motion, light, temperature, humidity, and infrared sensors. In total, the Edge has about 28,000 sensors installed. On days when fewer workers are expected, an entire section of the building can be shut down, reducing heating, cooling, lighting and cleaning costs. In the summer months, warm water is pumped to a depth of more than 125 m into the aquifer under the building, in winter it is withdrawn and used for the heating system. This system is the most efficient storage of heat energy in an aquifer in the world. Solar panels are installed on the south wall and roof. The Edge uses 70% less electricity than a typical office building, but when the panels were installed on the roofs of some nearby buildings, more electricity was produced than the building consumed. The day for employees at the Edge begins with a smartphone app developed in collaboration with the building's anchor tenant, consulting firm Deloitte. About 2,500 Deloitte employees work at 1,000 desks. This concept is called "hot desking" and encourages new relationships and efficient use of workspace. Tables are used only when needed. Each employee is connected to the intelligent building systems through an application on their smartphone. With the help of the program, employees can find parking spaces, free desks or other colleagues, report problems to the maintenance team, and navigate around the building. Employees have the ability to adjust the temperature and light level anywhere in the building where they want to work via a mobile app. A small robot patrols the area at night [8].

Oakland City Center (California) is known for its advanced variable airflow (VAV) system developed by Siemens. The system collects temperature and humidity data and studies changes in demand. An AI-based algorithm then evaluates the operating data and sends setpoints to the building's heating, ventilation, and air conditioning system to provide increased occupant comfort at the lowest cost. Another advantage of this dynamic system is its ability to effectively control air quality in different conditions, which is especially valuable during a pandemic. The general "green mode" setting optimizes temperature, pressure and humidity in a normal environment, but when a virus is introduced, its disinfection mode helps to minimize virus transmission by increasing the temperature and accelerating the decay of the virus. This is one of the features that made it possible to reopen safely the building for any work that requires the physical presence of employees [9].

Microsoft together with Bentley Systems and Schneider Electric presented a smart building project – Frasers Tower regional office in Singapore. The data, designed to demonstrate new ways of working, is collected using 179 Bluetooth radio beacons in conference rooms, as well as 900 real-time light, air quality and temperature sensors. The data, designed to demonstrate new ways of working, is collected using 179 Bluetooth radio beacons in conference rooms, as well as 900 real-time light, air quality and temperature sensors. With the help of sensors, the use of facilities, energy and utilities are monitored. Operators optimize the use of space, adjust air conditioning and lighting. All this provides a comfortable and productive space for employees, while increasing overall energy efficiency. Employees and staff use Smart Building CampusLink, an application that is fully integrated with Microsoft Outlook and Microsoft Office 365, to easily find directions, determine room occupancy and reserve facilities in real time. Microsoft's new Frasers Tower office is 12,500 square meters over six floors and has over 1,400 employees [10].

The Glumac office building (2011) in Shanghai (China) became the first to receive Living Building Challenge certification. It has an air monitoring system that allows workers to see its toxicity, humidity, saturation on their mobile phones Glumac has five air purification systems and a green wall to create a healthy climate inside the building [11].

In 2020, Vodaphone Group (London, England) won the Verdantix Smart Building Innovation Award in the Corporate Headquarters Modernization category for its innovative collaboration with General Electric [11]. Together, they designed and deployed a multi-sensor network that collects data on everything from air quality and energy use to human movement, noise levels and space use. In an office with different types of workspaces – for joint work, quiet work, etc. – employees use this data to find available workspace that meets their needs.

The Corning Optical Communications Headquarters building (Charlotte, North Carolina) has become a pilot for evaluation according to the SPIRE smart building criteria. The building features high-performance fiber optic connectivity, digital health tools (sensors that monitor spaces for overcrowding and air quality issues), data collection and processing technologies (to regulate energy consumption), and updated cybersecurity systems. The building meets LEED, Fitwel and WELL building standards [12].

The Institute of Engineering Thermophysics of the NAS of Ukraine has developed a concept for creating an experimental energy-efficient house and carried out its construction. The house was created as a scientific, technical and technological thermophysical laboratory. An automated measuring system has been created, including automated continuous measurements of temperature fields, heat fluxes, humidity, pressure, external climatic parameters, etc. [13].

Conclusions

The intelligent buildings and houses of tomorrow will not only include more lighting and temperature control systems; they may differ in greater individuality, the presence of means of control and combating the spread of viruses. Employees can come to work, check their workspaces, and automatically adjust them according to their preferences. They are surrounded by IoT sensors that will not only make the working environment more comfortable, but also improve the energy efficiency and maintenance of the building. This will ultimately reduce costs.

References

[1] Tabunshchikov Yu.A., *Intelligent buildings*. AVOK. 2001. No. 3 (in Rus.). https://www.abok.ru/for_spec/articles.php?nid=125&version=print.

[2] Tabunshchikov Yu.A., *The building must think*. ABOK. 2016. No. 1 (in Rus.).

[3] UL And TIA Announce SPIRE™ Smart Building Verifications Now Available, https://tiaonline.org/press-release/ul-and-tia-announce-spire-smart-building-verifications-now-available/

[4] Key Examples of Smart Buildings, https://www.caba.org/examples-of-smart-buildings/

[5] Top 10 most intelligent buildings, https://architime.ru/specarch/top_10_smart_house/smart_houses.htm

[6] Bill Gates smart building, http://stroikov.pro/blog/ekodom-bill-gejtsa/ (in Rus.).

[7] The Smartest Building in the World, https://www.bloomberg.com/features/2015-the-edge-the-worlds-greenest-building

[8] The Edge – The World's Smartest Office Building, https://www.rs-online.com/designspark/the-edge-the-world-s-smartest-office-building

[9] The Edge, Amsterdam, https://www.breeam.com/case-studies/offices/the-edge-amsterdam/?cn-reloaded=1

[10] A smart building blueprint is now ready for Microsoft's Singapore HQ 2020. The Silicon Review, https://thesiliconreview.net/microsoft/microsoft-singapore-hq-smart-building

[11] Smart Buildings in China: Creating a smart city ecosystem, https://daxueconsulting.com/smart-buildings-in-china-creating-a-smart-city-ecosystem/

[12] 5 Modern Intelligent Building Examples You Should Know, https://www.iofficecorp.com/blog/intelligent-building-examples

[13] Dolinsky A.A., Basok B.I., Nedbailo O.M., Belyaeva T.G., Khybyna M.A., Tkachenko M.V., Novitska M.P., *Conceptual foundations of the creation of an experimental house of the zero-energy type*. Building constructions, collection of scientific works. Vol. 77, 2013, pp. 222-227 (in Ukr.)

INVESTIGATION OF THE GEOMETRIC CHARACTERISTICS INFLUENCE ON PRESSURE LOSSES IN THE THERMOPRESSOR

Halina Kobalava

Admiral Makarov National University of Shipbuilding, Heroes of Ukraine Avenue, 9, Mykolayiv, 54025, Ukraine
e-mail: g.lavamay@gmail.com

A modern way to increase the efficiency of power plants is cooling of the working fluid. The different types of heat exchangers can be used for cyclic air cooling of gas turbines [1, 2], charge air cooling of internal combustion engines [3], removing superheating of vapor in refrigeration plants [4]. A promising method for cooling the working fluid is to use a two-phase jet apparatus, which is called a thermopressor [5]. Due to the evaporative cooling in the thermopressor, the effect of thermo-gas-dynamic compression takes place, that is, an increase in air pressure, as a result of the instantaneous evaporation of water, which is injected into the accelerated air flow.

A hydrodynamic analysis of typical models was carried out by using CFD simulation software ANSYS Fluent to determine the design thermopressor parameters (Fig. 1) at various air mass flow and for a number of relative air velocity values in the evaporation chamber [6, 7].

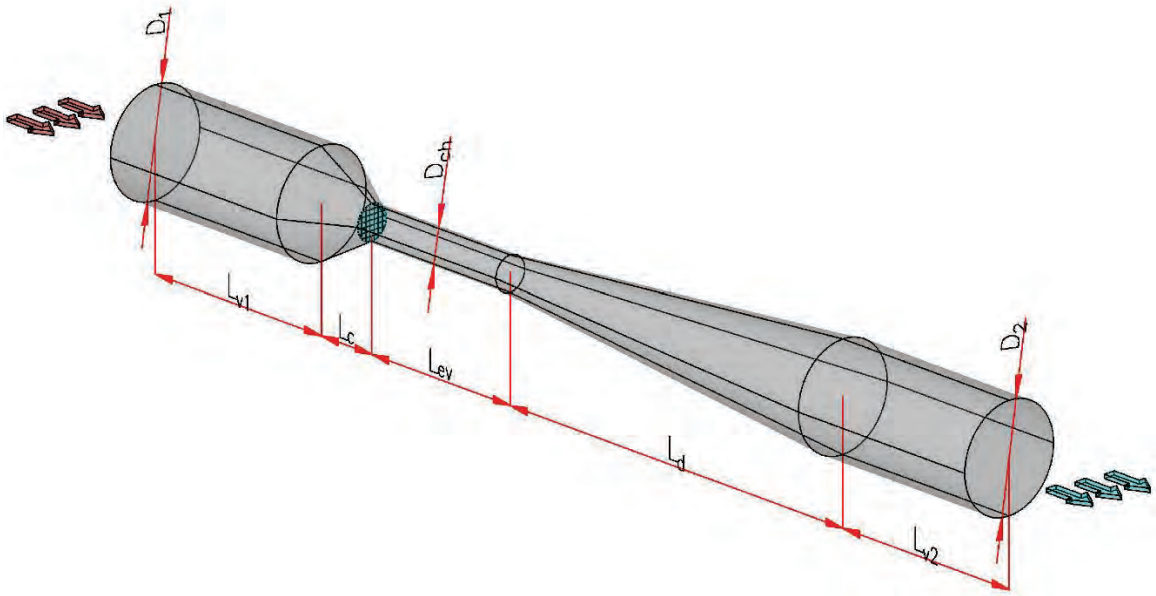

Figure 1. *3D thermopressor model.*

The experimental thermopressor was developed to study the working processes in order to determine the rational geometrical and regime parameters. The initial parameters were following: pressure P_{tp1} and temperature T_{tp1}, corresponding to the cycle air parameters of gas turbines and charge air of internal combustion engines.

To carry out numerical modeling, the finite volume method was used, which is implemented in the ANSYS Fluent software package. A calculation method was defined based on the Pressure-Based solver, a turbulence model *k-ε* Realizable was used. The calculation of the air flow parameters (total pressure, dynamic pressure, velocity, temperature, turbulent kinetic energy, etc.) in the thermopressor was carried out for a number of confusor and diffuser taper angles, as well as for a number of relative air velocity values in the evaporation chamber M = 0.4-0.8.

To determine the local resistance coefficients for the diffuser and confuser, classical methods of fluid flow mechanics were used [7].

The value of local resistance coefficients for the diffuser (divergent angle β = 6°; 8°; 10°; 12°) and confuser (convergent angle α = 30°; 35°; 40°; 45°; 50°) were determined. The initial parameters at the confuser inlet were following: inlet pressure P_{tp1} = 3·10^5 Pa; temperature T_{tp1} = 453 K, air velocity w_{air1} = 35 m/s. It should be noted that the nature of the change in velocity along the length of the thermopressor flow part was fairly uniform.

It was to compare the calculated data with the experimental data obtained in the study. It can be seen that the obtained equation for the local resistance coefficient in the diffuser gives a value with an acceptable error (δ = ±20%) in the range of divergent angles β = 4-12° (Fig. 2). At divergent angles β = ≥ 12°, the calculated values significantly exceed the experimental ones.

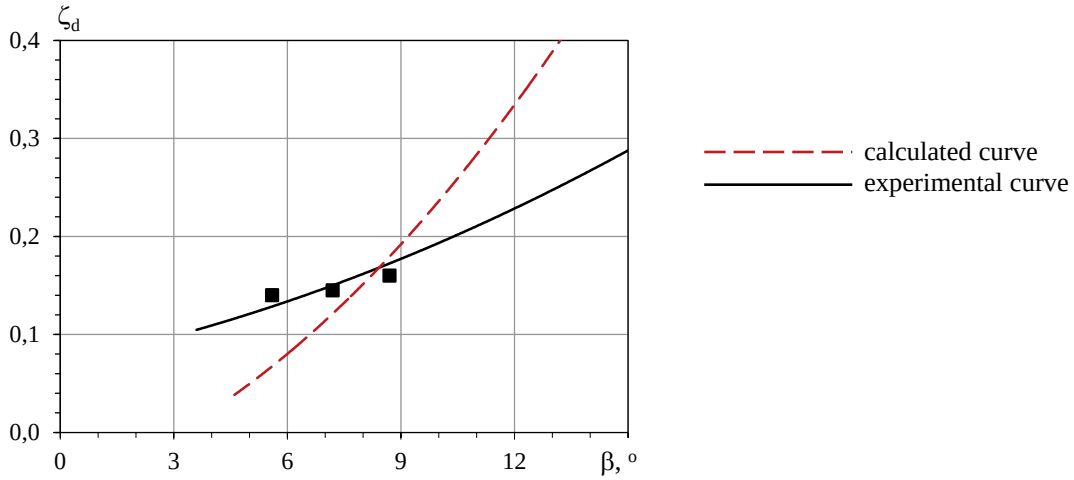

Figure 2. *Comparison of the obtained local resistance coefficient for the diffuser (ζ_d) with the calculated ones depending on the divergent angle β.*

Analysis of the calculated data shows that the total pressure loss in a "dry" thermopressor (without liquid injection for evaporation) was ΔP_{loss} = 0.05-1.00·10^5 Pa (2-31%) at a fixed confuser convergent angle α = 40° and variable diffuser divergent angles β = 4-12°. The total pressure loss was ΔP_{loss} = 0.05-0.40·10^5 Pa (1-12%) at a fixed diffuser divergent angle β = 6° and variable confuser convergent angles α = 30-50°. In this case, it is possible to recommend angles for the thermopressor flow parts (air mass flow G_{air} by to 1 kg/s): confuser convergent angle α = 30° and diffuser divergent angle β = 4°, which correspond to the minimum pressure losses ΔP_{loss} = 1.0-9.5%, and, consequently, to the maximum pressure increase as a result of thermo-gas-dynamic compression.

Conclusions. Determination of the main air flow parameters has been carried out for a number of taper angles of a confuser α and a diffuser β. The empirical equations for determining the local resistance coefficients of the confuser ζ_c and diffuser ζ_d of the thermopressor (air mass flow G_{air} up to 1 kg/s) have been determined.

The local resistance coefficients for the confuser and diffuser were determined by using computer CFD simulation: confuser local resistance coefficient ζ_c = 0.02-0.08 and diffuser local resistance coefficient ζ_d = 0.08-0.32.

It was recommended angles for the thermopressor flow parts: confuser convergent angle α = 30° and diffuser divergent angle β = 4°, which correspond to the minimum pressure losses ΔP_{loss} = 1.0-9.5%, and, consequently, to the maximum pressure increase as a result of thermo-gas-dynamic compression.

References

[1] Yousef S.H., *Novel inlet air cooling with gas turbine engines using cascaded waste-heat recovery for green sustainable energy*. Yousef S.H., Najjar A.M., Abubaker A. El-Khalil F.S. Energy, No. 93, 2015, pp. 770-785.

[2] Konovalov D., *Research of characteristics of the flow part of an aerothermopressor for gas turbine intercooling air*. Konovalov D., Radchenko M., Kobalava H., Radchenko A., Radchenko R., Kornienko V., Maksymov V., Proc. of the Inst. of Mech. Eng., Part A: Journal of Power and Energy, Vol. 236(4), 2021, pp. 634-646.

[3] Iyer A.A., *Experimental Study on the Effect of Water Injection in an Internal Combustion Engine*. Iyer A.A., Rane I.P., Upasani K.S., Bhosale Y.P., Gawande S.H., International Review of Mechanical Engineering, No. 11(6), 2017, pp. 379-386.

[4] Radchenko A., *Innovative turbine intake air cooling systems and their rational designing*. Radchenko A., Trushliakov E., Kosowski K., Mikielewicz D., Radchenko M., Energies, Vol. 13 (23), 2020, 6201.

[5] Kobalava H., *Numerical Simulation of an Aerothermopressor with Incomplete Evaporation for Intercooling of the Gas Turbine Engine*, Kobalava H., Konovalov D., Radchenko R., Forduy S., Maksymov V., Integrated Computer Technologies in Mechanical Engineering. ICTM 2020. Lecture Notes in Networks and Systems, Springer, Cham, 2021, Vol. 188, pp. 519-530.

[6] *ANSYS Fluent Tutorial Theory Guide Release 17.0.* ANSYS, Inc. Canonsburg, 2016.

[7] Bergman T.L., *Fundamentals of Heat and Mass Transfer*. 7th Edition. John Wiley & Sons, New Jersey, 2011.

FIRE SAFE STORAGE AND PRELIMINARY DEHYDRATION OF WOOD WASTE WITH DIAMETER < 30 MM FROM FINAL FELLING AND FOREST CARE FELLING, AS A SEMI-FINISHED PRODUCT FOR THE PRODUCTION OF SOLID FUEL

Vyacheslav Kremnov, George Belyaev, Konstantin Zhukov, Natalya Korbut, Leonid Shpilberg, Valentina Stetsuk

Institute of Engineering Thermophysics National Academy of Science of Ukraine
2a, Marii Kapnist Str., Kyiv, 03057, Ukraine
e-mail: kremnev@ukr.net

Introduction

Involvement in the fuel use of waste from felling for forest care and main use requires the organization of safe storage of large volumes of wet wood resources. The category of waste, in accordance with the regulatory documentation of Ukraine, includes tops of trunks and branches with a trunk diameter of <30 mm. According to the rules, these resources are subject to destruction by burning with using of liquid fuel in specially designated places. For fire safety reasons, this is done in the fall. In addition to the destruction of such waste by burning, it is allowed to grind it into wood chips and scatter it between trees for natural, gradual degradation. This method of destruction is considered undesirable due to wood chips disrupting natural biological processes in the forest floor, which plays an important role in the forest biocenosis. Currently, there is no established system of cooperation and coordination between forestry and energy in Ukraine. In our opinion, such a system is very necessary and must necessarily have a synergistic, mutually beneficial character – that is, promote the development of both forestry and energy. Wood fuel fully meets modern environmental requirements, is a promising renewable resource, but requires large volumes of raw material storage. For example, compared to coal, taking into account the difference in calorific value, bulk mass and humidity, the volume of wood in warehouse cubic meter exceeds the volume of coal by approximately 20 times, assuming the same thermal energy potential.

At the Institute of Engineering Thermophysics, within the framework of the topic "Research of heat and mass transfer processes and the development of new energy-efficient methods and technological equipment for the production of biofuel from forestry waste", the harvesting of small-diameter wood together with green leaves was carried out, as well as the storage of this wood for 16 months.

So, the storage of small-diameter wood in the three most common ways was researched, namely: in its natural form – in a pile and a fragment of a stack, and also after chopping wood – in the form of wet "green" chips. The first and second methods are considered safe in terms of self-ignition, so the main task of researching these methods was the effect of long-term storage on the moisture content of wood. The third method – in the form of wet wood chips is considered dangerous in terms of self-ignition, and this especially applies to "green" chips obtained by the method of chopping wood together with leaves.

Characteristics of alternative methods of outdoor storage for 16 months

1. In a separate pile, in the form of whole trees with leaves: width – 1.7 m; length – 3.4 m; height – 1.5 m; bulk volume ~9 m^3.
2. In a fragment of an industrial stack: width – 5 m; height – 2 m; length – 1 m (in practice, the length is not limited, has no technological significance and is determined for organizational reasons, taking into account the size and shape of the storage area); bulk volume ~10 m^3.

3. A fragment of the stack of crushed wood together with "green" leaves (of the "green" chips). Stack dimensions: height – 2 m; width: at the mark "0" – 5 m, at the mark "2" – 3 m; length – 1 m; bulk volume ~5.5 m^3.

The conception (idea) of the research was based on the following:

- Pile storage was organized on a 1:1 scale and is a full-scale experimental and industrial test.
- Storage of freshly cut "green" wood in a stack is organized in the form of a 1 m long fragment with a cross-section on a scale of 1:1, which had the shape of a rectangle, 5 m wide and 2 m high. The fragment of the stack was formed between two parallel heat-insulated flat fences.
- The research of wet "green" chips was aimed, first of all, at determining the technical conditions that prevent spontaneous combustion, which has repeatedly occurred in practice and was confirmed by researchers from different countries.

When choosing the shape and cross-sectional dimensions of the stack for storing wood chips, we took the following into account:

- Self-ignition requires a temperature level that cannot be achieved only through purely biochemical processes. Reaching the temperature necessary for self-ignition indicates the participation of exothermic chemical reactions (probably hydrocarbon oxidation reactions in the presence of flammable gases).
- Flammable gases can be formed during the activity of facultative microflora, which operates at an oxygen concentration insufficient for aerobic microflora, which produces only non-flammable gases – water vapor and carbon dioxide.

The above considerations indicate a huge unevenness of conditions in the massif of "green" wet cod. Similar problems associated with insufficient aeration occur during composting of biomass – its biological conversion by fermentation under the influence of aerobic microflora. In field composting technology, this problem is solved by mixing and aerating biomass with specialized mechanisms. Therefore, we decided to organize the storage of wet "green" wood chips in a fragment of an elongated stack with cross-sectional dimensions that would allow, if necessary, processing of the stack with commercially available mixer-aerators.

A 1 m long stack fragment was arranged between two parallel heat-insulated flat fence walls with a cross-section in the form of a trapezoid. Section dimensions: height – 2 m; width: at the "0m" mark – 5 m, at the "2m" mark – 3 m; length – 1 m.

During the entire period of storage, the temperature was measured at different points of the internal volume of the wood using a specially designed probe. It was established that the temperature in the massif of the heap was almost no different from the ambient temperature; in the stack fragment it reached 40°C; the maximum temperature in the chips massif reached 62°C, after which it gradually decreased to the ambient temperature over the course of 2 months.

During the storage period of the raw material, its moisture content decreased on average:

- in a pile ~5 times (from 1 kg of moisture per 1 kg of completely dry wood to 0.2 kg of moisture per 1 kg of completely dry wood);
- in a stack fragment – 4.3 times (from 1 kg of moisture per 1 kg of completely dry wood to 0.23 kg of moisture per 1 kg of completely dry wood);
- in a fragment of a stack of "green" wood chips ~2.5 times (from 1 kg of moisture per 1 kg of completely dry wood to 0.4 kg of moisture per 1 kg of completely dry wood).

Conclusions

1. All researched storage methods are safe with respect to spontaneous combustion.
2. Long-term storage (≥16 months) provides significant dehydration; when stored in a pile and stack, it is practically provide that the air-dry state is reached, and the fuel semi-finished

product does not require further dehydration. Storage in the form of fuel chips requires further drying of the semi-finished product.

3. Dehydration during storage in the form of wet "green" wood chips is ensured mainly due to the process of biological conversion of shredded leaves and small wood particles. We formulated and received a patent for a useful model for stacking wet wood chips in elongated stackes of a defined cross-section, which is sufficient for fire-safe storage and significant preliminary drying without stirring [3]. In addition, acceleration (if necessary) of conversion and drying by mixing and aeration was proposed.

References

[1] Kremnev V., Lyashenko A., Korbut N., Shelimanova E. (2019), *Development of a method of fire-safe long-term storage and partial dehydration of wood chips*. Enerhetyka i avtomatyka, 6, pp. 202-213, http://dx.doi.org/10.31548/energiya2019.06.202 (Ukr).

[2] Kremnev V., Timoshchenko A., Korbut N., Shelimanova E. (2019), *Organized long-term storage and pre-driving of nonliquid wood (twigs and shrub) in open air under the influence of natural factors*. Enerhetyka i avtomatyka, 6, pp. 111-121, http://dx.doi.org/10.31548/energiya2019.06.111 (Ukr).

[3] Kremnev V., Timoshchenko A., Shpilberg L., Zhukov K., Korbut N. (2020), A *method of long-term storage of wet fuel wood chips made of thin gauge wood*. Patent of Ukraine for useful model. F26B 9/00 C10L 5/00 C10L 5/40. No. 142712, declared 11.12.2019; published 25.06.2020, No. 12. (Ukr).

HARVESTING BY-PRODUCTS OF CORN AND SUNFLOWER AS SOLID BIOFUELS

Alvian Kuzmych, Serhii Stepanenko

Institute of Mechanics and Automatics of Agroindustrial Production
of the National Academy of Agrarian Sciences of Ukraine
e-mail: akuzmich75@gmail.com

Introduction

A decrease in the world's oil and gas reserves, as well as an increase in the cost of their extraction and processing, prompts the search for alternative energy sources. One of the most attractive areas is the use of plant residues of grain and oilseeds, in particular corn and sunflower, for energy purposes. A strong argument in favor of using these crops is their significant sown area of cultivation in Ukraine [1].

According to the State Statistics Committee, the area of corn and sunflower cultivation in Ukraine in 2021 amounted to about 11.9 million hectares, which in the structure of sown areas is 40.2%. Given the existing acreage of these crops in Ukraine, taking into account the scientifically grounded share (30-40%) of plant residues that can be used for energy production, the potential for using the by-products of corn and sunflower for energy purposes reaches up to 24 million tons.

Results

The analysis of recent studies suggests that at the present stage there are no scientifically substantiated technological collection processes and effective technical means that are able to ensure the production of high-quality raw materials from by-products of corn and sunflower for energy purposes in the required quantity [2].

The existing harvesting technologies and technical means for harvesting the non-grain part of the harvest of grain crops, which can be used for harvesting corn and sunflower, have significant limitations regarding their use for harvesting by-products of these crops for energy purposes.

The Institute of Mechanics and Automatics of Agroindustrial Production has developed a project for a technological process for harvesting by-products of sunflower for energy purposes, which provides for the following operations: desiccation of crops before harvesting; mowing the plants, threshing the mass, collecting seeds in the tank, and by-products of sunflower in the trailed hopper; loading the biomass from the stack into the dosing device of the baler; dosing the mass and forming packs or rolls; transportation of packs or rolls to the place of their storage. The scheme of the technology is presented in Figure 1.

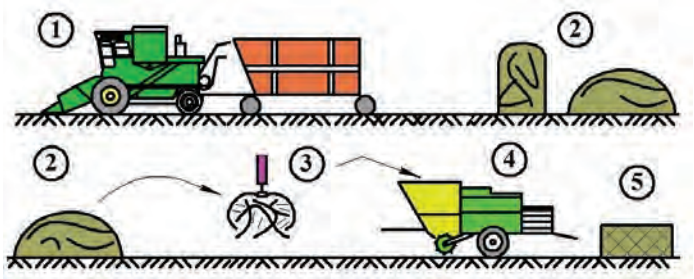

Figure 1. *The scheme of the technology for harvesting by-products of corn and sunflower: 1 – harvesting grain and non-grain part of the crop; 2 – storage of the non-grain part of the crop; 3 – loading of the non-grain part of the harvest; 4 – pressing of the non-grain part of the crop; 5 – storage of packs of the non-grain part of the crop.*

The harvesting of by-products of sunflower is carried out by combine harvesters with trailed hoppers. For the purpose of forming bundles or rolls of stalks, the design of the press pick-up device was developed for dosed feeding of crushed mass into them. Loading and transporting the pressed mass is carried out by the forklifts and the existing vehicles.

The technological process provides for streaming harvesting of by-products and unloading it at the edges of the field when the combine turns and enters the next run. Thus, a large part of the field (more than 90%) immediately after harvesting is freed up to carry out tillage operations for the next crop. The processing of headlands can be performed upon completion of the formation and removal of the packs.

The collection of plant materials that can be used for energy purposes involves the formation of packs from it to facilitate next transportation and use for storage or processing. Balers are high-performance machines, therefore (working on the collection of the mass) the swath must have a running mass of more than 4 kg per meter. With an insignificant running mass, the part of lost raw materials will increase. Especially significant losses can occur when collection raw materials such as sunflower stalks [3].

The essence of this technology is to feed the mass directly into the baler, without putting it into a swath. For this, the round baler is equipped with an accumulation and metering device shown in Figure 2. To implement the technology, the design of a roll-type baler for dosed feeding of the crushed stalk mass has been developed. A feature of the development is minimal interference in the design of the baler, which can be used with or without a metering device.

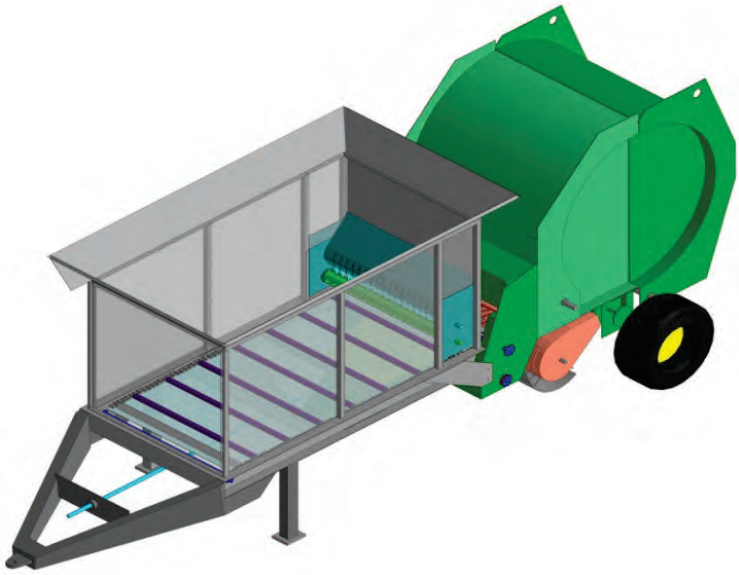

Figure 2. *The design of a roll-type baler with accumulation device for dosed feeding of the crushed stalk mass.*

The results of laboratory and field investigations proved the integrity of the formed bales from the crushed mass of the sunflower seed mass which was primarily ensured by the presence of long fibrous parts of the stalks.

Checking the consumer characteristics of bales made of crushed sunflower stalks as a solid biofuel was carried out by burning them in a heat generator of a grain dryer (Fig. 3). The results of the tests showed an increase in the thermal characteristics of the bales of crushed sunflower stalks by 5-10% when compared with bales of grain straw.

Figure 3. *Loading a bale of crushed sunflower stalks into the heat generator of the grain dryer.*

Conclusions

As a result of the research, it was found that at a level of yield of sunflower seeds in the range of 25-30 center per ha, the volume of collection of the crushed stalk mass is 7.5-8.5 center per ha with a moisture content of 18-24% and a density of rolls within 75-90 kg per cube meter. Direct operating costs for the collection of pressed by-products of sunflower are 570-680 UAH per ton.

The use of non-grain part of the crop of sunflower and corn for energy purposes will reduce greenhouse gas emissions and the cost of energy received in comparison with fossil hydrocarbons.

References

[1] Geletukha G.G., Zhelezna T.A., Dragnev S.V., Bashtovy A.I. (2020), *Potential and prospects of energy use of agrobiomass in Ukraine*, Teplofizyka ta Teploenerhetyka [Thermophysics and thermal power engineering], Vol. 42, No. 1, pp. 42-49, https:doi.org/10.31472/ttpe.1.2020.5 [in Ukrainian].

[2] Adamchuk V.V., Kuzmenko V.F., Kuzmych A.Y., Maksimenko V.V. (2019), *Aspekty procesiv zbyrannya nezernovoyi chastyny vrozhayu kukurudzy ta sonyashnyku yak tverdogo biopalyva* [Aspects of non-grain part harvesting for corn and sunflower as solid biofuels]. Mexanizaciya ta elektryfikaciya silskogo gospodarstva – Mechanization and electrification of agriculture, 9(108), pp. 10-20, DOI: 10.37204/0131-2189-2019-9-1 [in Ukrainian].

[3] Sheychenko V.O., Kuzmych A.Ya., Shevchuk M.V., Shevchuk V.V., Belovod O.I. (2019), *Research of quality indicators of wheat seeds separated by pre-threshing device*. INMATEH – Agricultural Engineering, Vol. 57, Issue 1, pp. 157-164.

COMBUSTION OF PLANT PELLETS IN A HOUSEHOLD BOILER

Borys Basok[1], Oksana Lysenko[1], Hanna Veremiichuk[1]
Oleksandr Siryi[2]

[1]Institute of Engineering Thermophysics of the National Academy of Science of Ukraine
2a, Marii Kapnist (Zhelyabova) Str., Kyiv, 03057, Ukraine

[2]National Technical University of Ukraine "Igor Sikorsky Kyiv Polytechnic Institute"
6, Politehnichna str., Kyiv, 03056, Ukraine
e-mail: lisenko_oks@ukr.net

Introduction

Today, bioenergy accounts for about a tenth of the total volume of primary energy in the world and it is the largest renewable source of heat. Modern bioenergy accounted for more than two-thirds of global renewable heat consumption in 2018, mostly in industry and the residential sector. Bioenergy is expected to increase the volume of renewable heat: its use will increase by 12% during 2019-2024, of which almost two-thirds is in industry [1]. According to the Net Zero Emissions scenario, it is necessary to increase the production of electricity from bioenergy [2]. Policies to support bioenergy development are improving around the world, but greater efforts are needed to ensure policy goals are met and production growth rates are maintained. The world experience of the energy use of agricultural waste and agrobiofuel is not so great, compared to the use of wood biofuel. At the same time, technologies have already reached a commercial level and certain countries have been successfully developing this direction for many years, but most countries are only at the beginning of this path, like Ukraine. Therefore, developing technologies and improving equipment for burning plant pellets is an urgent task. It is due to the need to involve alternative and renewable energy sources in the energy sector due to the increase in prices for the main traditional energy carriers and their exhaustion.

Results

In the Institute of Engineering Thermophysics of the National Academy of Sciences of Ukraine, an experimental installation of a solid fuel boiler with an automated pellet burner was developed and implemented to study the features of pellets combustion. The experimental installation includes a Viadrus boiler with a nominal capacity of 25 kW and a torch type burner. In Figure 1 shows a boiler with a burner, front view and side view. The burner is a metal pipe, which is a combustion chamber. A screw mechanism is installed in it, which ensures the supply of pellets to the firebox and it is driven by an electric drive. The flame is blown out of the pipe horizontally and directed to the wall of the firebox opposite the burner.

The torch pellet burner is suitable for burning wood pellets, agropellets from husks, sunflower, straw, crushed corn cobs and other agricultural waste. It is compact, easily integrated into any household boiler. Including in a boiler with a small combustion chamber. The temperature measurement in the furnace space of the boiler was carried out using a chromel-alumel comb of thermocouples, located at different distances from the outlet cross-section of the burner.

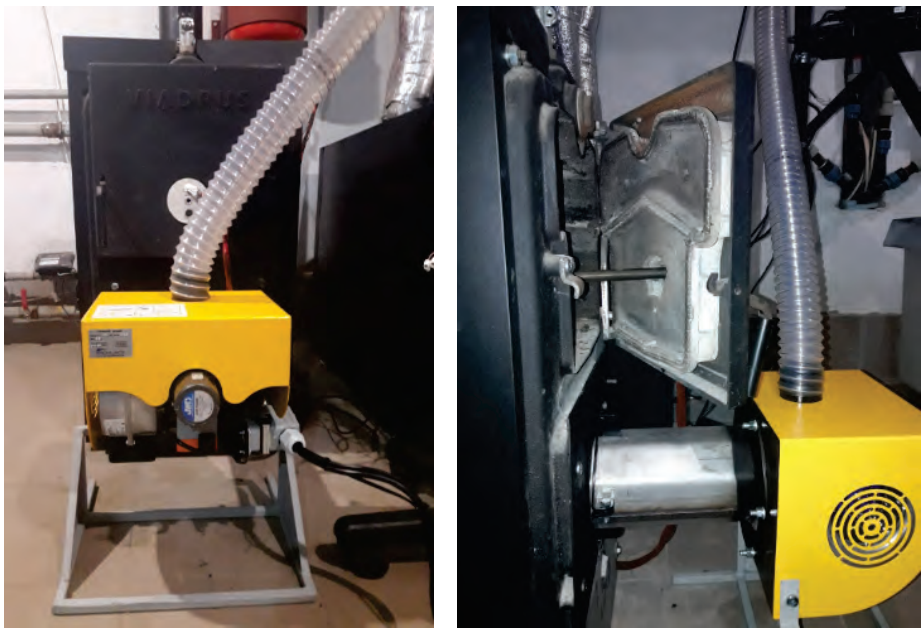

a) b)

Figure 1. *Solid fuel boiler with pellet burner: a) front view, b) side view.*

Samples of wheat straw pellets were used in the experimental research. In Figure 2 shows the change over time in the temperature state of the volume of the boiler at the stage of ignition of pellets, their burning and extinguishing.

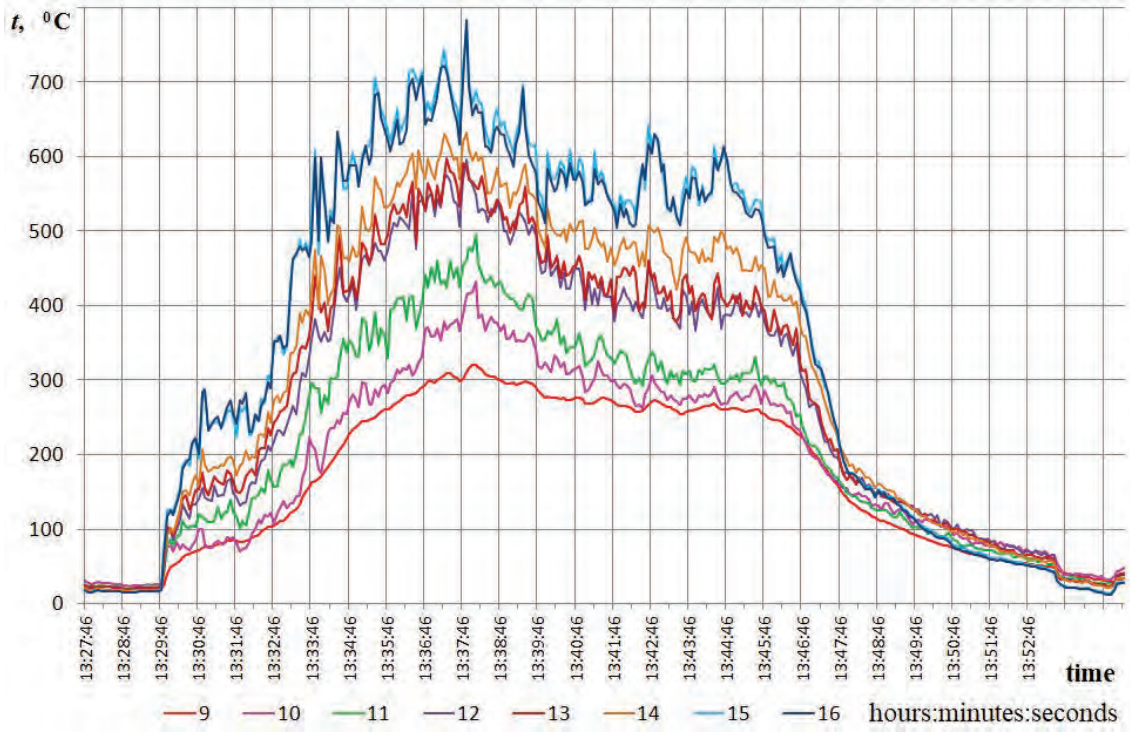

Figure 2. *Dependences of thermocouples temperatures on time during the burning of wheat straw.*

The ignition of the pellets from the igniter took place very quickly, within 2 minutes, as can be seen from the graph. After ignition, the pellets begin to burn, and the temperature values in the volume of the boiler begin to gradually increase. The largest increase in temperature occurs near the wall of the boiler, which is opposite to the burner. At the time moment of 10 minutes from the beginning of the experiment, the temperature near the opposite wall of the boiler rises to 785°C

(Fig. 2, thermocouple No. 16). From the 10th to the 18th minutes of the experiment a stable burning process of straw pellets takes place. The average temperature of flue gases is 270°C. During this time, there was an automatic periodic supply of pellets from the bunker according to a programmed algorithm. At the same time the temperatures of thermocouples No. 12-16 ranged from 380°C to 700°C, the temperature of thermocouple No. 11 ranged from 300°C to 430°C and the temperature of thermocouple No. 10 ranged from 280°C to 420°C. Temperature fluctuation occurred as a result of the periodic burning of a portion of biofuel in the burner and the arrival of a new portion of pellets from the bunker. After 18 minutes from the beginning of the experiment the burner is extinguished using the corresponding function in the controller. As can be seen from the graph (Fig. 2), a gradual decrease of temperatures in the boiler chamber and flue gases begins. At the same time, it is possible to turn on the ventilator to accelerate the burning of fuel residues.

Conclusions

Experimental studies of the combustion of plant pellets were conducted to determine their features burning in a boiler with a pellet burner. Research results have shown that wheat straw pellets are an effective biofuel.

References

[1] Bioenergy Association of Ukraine. https://uabio.org.

[2] International Energy Agency: IEA. https://www.iea.org.

NEUROMODEL OF FORECASTING ENERGY INDICATORS ENTERPRISES

Vasyl Kalinchyk, Olexandr Meita, Vitalii Pobigaylo, Olena Borychenko, Vitalii Kalinchyk

National Technical University of Ukraine "Igor Sikorsky Kyiv Polytechnic Institute", Kyiv, Ukraine,
e-mail: vkalin@i.ua

Introduction

One of the most effective ways to reduce grid losses, as well as to improve its quality at the terminals of electrical receivers, is the compensation of reactive power, which is carried out with the help of various compensating devices. Cosφ, the value of which is set in advance, can be an indicator of the economically beneficial value of the level of reactive energy consumption. It is preferable to focus on those methods that are based on the study of forecast estimates, which constitute the initial information for making management decisions to regulate the mode of operation of compensation units. In this regard, it is expedient to comprehensively solve the problem of reactive power regulation by combining control of compensating devices and regulation of voltage regimes in the system [1].

Until recently, the statistical approach was the main technique for solving the problem of forecasting. Within the framework of static models, the tasks of forecasting, detection of hidden periodicity in data, analysis of dependencies, assessment of risks in decision-making, etc. are solved. A general disadvantage of statistical models is the difficulty of choosing the type of model and selecting its parameters. One of the promising methods of forecasting in various fields of industry are methods based on non-parametric models, in particular on artificial neural networks, which are able to comprehensively process information and highlight hidden dependencies between input and output data [2-3].

The purpose of this paper is to create a neural network model of the enterprise with the function of forecasting the level of the reactive power to be consumed by the enterprise.

To achieve this goal, the following objectives are addressed in the paper:

- Evaluation of indicators characterising the enterprise's consumption of reactive power and establishment of their averaging intervals.
- Justification of the type and configuration of the artificial neural network for creating a model of reactive power consumption by the enterprise.
- Prediction of reactive power indicators and evaluation of the quality of neural models.

Object of research: graphs of changes in indicators characterising the consumption of reactive power of the enterprise.

Subject of research: characteristics of neural models that determine the forecast consumption of reactive power by the enterprise.

Presentation of the main research material

The paper predicts the power consumed by the enterprise and the power and reactive power coefficients using artificial neural networks of the MLP type. The input data are represented by graphs of changes in active and reactive power and graphs of changes in power factor and reactive power factor. The samples cover a time interval of 10 days, or 480 observations. Values were averaged at 30-minute intervals. Network training and prediction will be performed on the basis of 432 observations (9 days), and the last day's data will be used as a test sequence.

The simulation uses a multilayer perceptron (MLP) model, which will be trained according to the BFGS algorithm (Broyden – Fletcher – Goldfarb – Shanno algorithm). In the MLP structure, 48 input neurons are assumed, which were determined by periodograms, one neuron in the output layer, which corresponds to the prediction task, and a variable number of neurons in the hidden layer from 2 to 48. We use linear, hyperbolic and exponential activation functions of neurons.

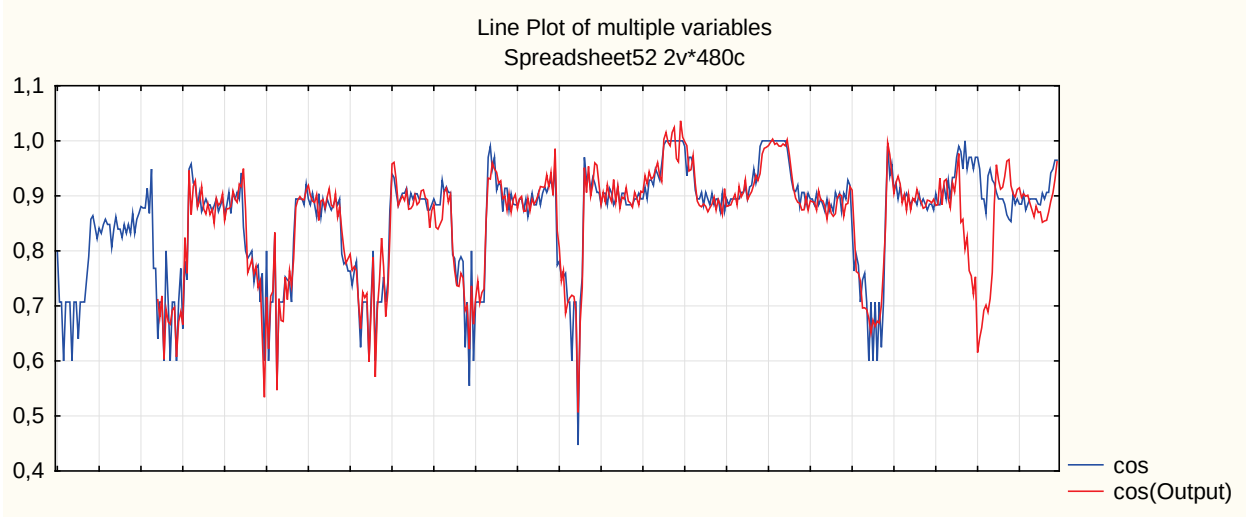

Figure 1. *Graphs of changes in cosφ power factor indicators for input data and a neuromodel with a 1-day forecast.*

The analysis of the results shows that even with sufficiently large values of network productivity (over 95% on the test sequence and 89% on the test sequence), the forecast values for the daily interval have significant discrepancies. Therefore, cosφ and tgφ indicators were predicted on the basis of the values of active and reactive powers predicted according to the graph with the accumulation of values.

Table 1. *Results of the training on sequence data with accumulation of indicators from active and reactive power meters*

Net. name	Training perf.	Test perf.	Training error	Test error	Training algorithm	Error function	Hidden activation	Output activation
Network to forecast active power								
MLP 48-39-1	0.975521	0.985453	0.000042	0.000071	BFGS 100	SOS	Identity	Identity
Network to forecast active power								
MLP 48-46-1	0.971145	0.982892	0.000065	0.000067	BFGS 81	SOS	Identity	Identity

The values of cos*φ* and tgφ are calculated based on the MLP 48-39-1 and MLP 48-12-1 network. As the networks were building a graph with accumulation, to determine the indicators, the values were recalculated into a number of absolute power values.

$$P_i^{'} = \left| P_{i+1} - P_i \right|$$

$$Q_i^{'} = \left| Q_{i+1} - Q_i \right|$$

where: $P_i^{'}, Q_i^{'}$ – absolute values of consumed active and reactive power; P_i, Q_i – modelled according to the schedule with the accumulation of active and reactive power values.

The average value of the absolute error in the forecast interval was 5.3%.

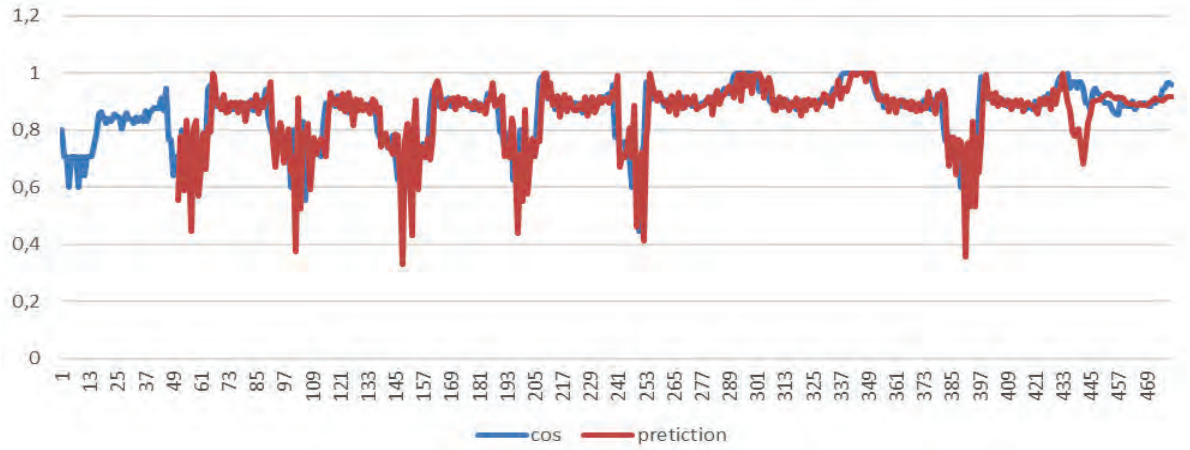

Figure 2. *Comparison of the input graph with the predicted graph.*

Conclusions

It is advisable to use artificial neural networks, in particular multilayer perceptrons, to build predictive models of the function of changes in reactive load indicators.

The graphs of active and reactive loads and their indicators with half-hourly averaging data determines the observation period and the required number of neurons (48) in the input layer, because predicting a decrease in the number of neurons will worsen the quality of the model due to period mismatch, and increase will complicate the model.

The average value of the relative error for the predicted cosφ graph is 5.3%, and exceeds 10% for the tgφ graph. Therefore, it can be concluded that, when assessing the level of reactive power consumption, it is advisable to use the forecast values of active and reactive power meter readings and the cosφ value calculated from them to determine the need for reactive power compensation.

References

[1] Aoki K., *Optimal reactive power planning considering many power flow conditions*. Electrical Engineering in Japan, 1988, Vol. 108, No. 2, pp. 31-40.

[2] Kalinchyk V., Pobigaylo V., Kalinchyk V., Skosyrev V., *Reactive power contro*l. Bulletin of NTU "KhPI". Series: Problems of Electrical Machines and Apparatus Perfection. The Theory and Practice, 2 (6) (December 2021), pp. 36-39.

[3] Rudenko O., Bezsonov O., Romanyk O., *Neural network time series prediction based on multilayer perceptron*. Development Management, 2019, Vol. 17, No. 1, pp. 23-34.

[4] Yakovyna V.S., *Software failures prediction using RBF neural network*. Odes'kyi Politechnichnyi Universytet. Pratsi, 2015, No. 2, pp. 111-118.

MICROSCALE DOMAIN PERMEABILITY CALCULATIONS OF FIBER REINFORCEMENT STRUCTURES BASED ON THE LATTICE BOLTZMANN METHOD

Maryna Novitska[1, 2], Miro Duhovic[1], David May[1]

[1] Leibniz-Institut für Verbundwerkstoffe GmbH, Technische Universität Kaiserslautern, Erwin-Schrödinger-Straße 58, 67663 Kaiserslautern, Germany

[2] Institute of Engineering Thermophysics, NAS of Ukraine, Kyiv, Ukraine

Introduction

Porous structures can be found in many industrial applications including structural materials, heat-insulating materials [1], soils in geothermal technologies [2] and filtration in gas and oil production. They can also be found in composite production in the form of rovings, which consist of thousands of clustered and arranged fibers, and textiles made of rovings. To manufacture composites these fiber structures are subsequently impregnated with resin [3-6], which after solidification forms the matrix. For proper manufacturing process design, the analysis of fluid or gas motion in such materials is extremely important. The pore sizes in such media are usually several orders of magnitude smaller than the size of the object under study (i.e. the part to be manufactured), which greatly complicates the creation of a computational grid for modeling engineering problems. For proper manufacturing process design, the analysis of fluid or gas motion in such materials is extremely important. One of the important characteristics in this approach is the prediction of permeability, which is a measure of the porous media's ability to transmit fluid and can be calculated using Darcy's law as given in Eqn (1):

$$\overline{u} = -\frac{K}{\mu}\Delta P \tag{1}$$

where: ΔP – pressure difference; K – permeability; μ – kinematic viscosity; $\overline{u}$ – average velocity.

Many different methods can be found in the literature for determining permeability, these include: semi-analytical approaches [3, 5], experimental approaches [4, 7], CFD simulations [5, 8], and prediction using machine learning methods [6, 9]. All of these approaches have their respective advantages and disadvantages. In reference [3], semi-analytical solutions for the permeability of a porous structure for the idealized case of parallel cylindrical fibers evenly distributed in space is given, providing an efficient way of initially evaluating the validity of numerical simulations. The dependence of permeability on the fiber volume content and fiber radius is given, both for the case of fiber direction and transverse to fiber direction permeability as given in Eqn's (2) and (3):

$$K_{\parallel} = \frac{8R^2}{c}\cdot\frac{\left(1-V_f\right)^3}{V_f^2} \tag{2}$$

$$K_{\perp} = C_1\left(\sqrt{\frac{V_{f\max}}{V_f}}-1\right)^{5/2}\cdot R^2 \tag{3}$$

where: c and C_1 – constants given in Table 1; R – radius of the cylinder (fiber); V_f – fiber volume content; $V_{f\max}$ – maximum theoretically achievable fiber volume content, at which further flow of the liquid is no longer possible.

Table 1. *Parameter values in Equations (2) and (3) [3].*

Fiber arrangement	C_1	$V_{f\,max}$	c
Quadratic	$\frac{16}{9\pi\sqrt{2}}$	$\frac{\pi}{4}$	57
Hexagonal	$\frac{16}{9\pi\sqrt{6}}$	$\frac{\pi}{2\sqrt{3}}$	53

The aim of this work is to evaluate the possibility of numerical permeability calculations based on the lattice Boltzmann method implemented in the open source solver Palabos [10].

Model

The derivation of the lattice Boltzmann equation for fluid dynamics problems is given in [11]. This equation can be derived by simplifying, hypothetical molecular dynamics approaches where space, time and particle velocities are discrete. The equation can be written as shown in Eqn. (4):

$$\frac{\partial f}{\partial t} + e \cdot \nabla f = \frac{f - f^{eq}}{\lambda} \tag{4}$$

where: f – particle distribution function; e – particle velocity; λ – relaxation time due to particle collision; f^{eq} – equilibrium Boltzmann-Maxwell distribution function.

An extended numerical scheme for modeling fluid flows using the lattice Boltzmann method, implemented in the open source software Palabos, can be found in [12]. The method's main idea is that the position of particles is considered discrete, meaning that a particle can occupy a position only in the nodes of a given lattice. The essence of the method is the molecular description of the fluid based on the Boltzmann equation.

To describe the array, the notation D_nQ_i is used, where n is the dimension of the grid and i the number of speed channels. In this work we used a three-dimensional array with 19 high-speed channels D3Q19.

The lattice Boltzmann method has proved to be an alternative approach (to solving the Navier Stokes equations) for CFD problems. The calculations presented in this paper are implemented on the basis of the open source lattice Boltzmann solver Palabos [10]. Calculations in Palabos are performed in relative units. The transition from real units to relative Palabos units occurs with the help of characteristic scales which is determined by the size of the characteristic objects relative to the number of voxels used to model the objects.

Geometry of the computational domain and boundary conditions

The calculation of the permeability within a microscale domain for the case of uniformly distributed parallel cylindrical fibers with fiber radius R, cross-sectional area of the sample A and length L is considered as shown in Figure 1a. The sample has a cubic shape i.e. $A = L^2$. A fluid medium with a volume flow rate Q moves through the sample due to the presence of a pressure difference ΔP. Permeability has been determined in all three directions X,Y,Z of the structure. As boundary conditions on the sides perpendicular to the axis through which the permeability was calculated, a pressure difference ΔP = 1 Pa was set. Periodic boundary conditions were applied on the other sides. The results have been compared to the semi-analytical solutions in reference [3] for the same ideal arrangement of cylindrical fibers.

Calculation of results

The results of the velocity field calculation in the computational domain are presented in Figure 1b-1d. To determine the convergence criterion, a series of calculations were performed on a geometry with a fiber radius of 4 μm. The calculations were carried out for the convergence criterion values $\varepsilon = 0.1; 0.01; 0.001$. A convergence criterion value of 0.0001 could not be achieved due to the stabilization of the solution and the velocity field variation, therefore the criterion $\varepsilon = 0.001$ was deemed sufficient for the calculations.

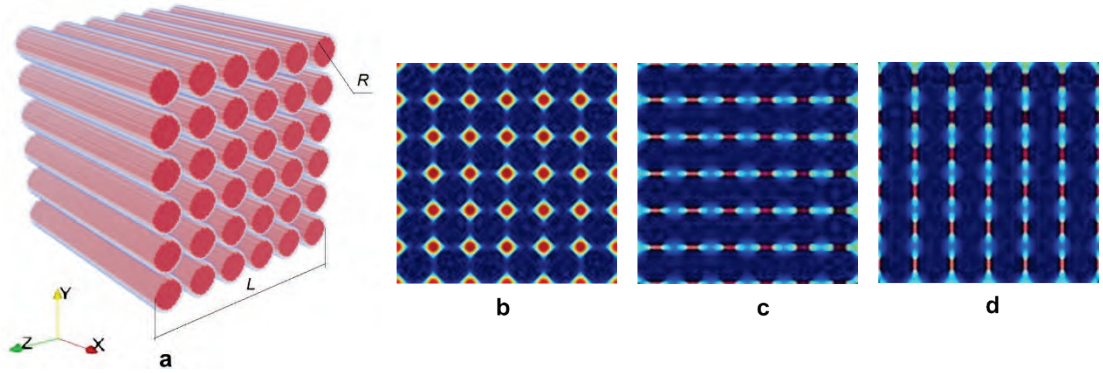

Figure 1. *a) Geometry of the computational domain and velocity field in the central cross-section of the computational domain for the case V_f = 61%, radius 4 μm and fluid motion in the directions b) X, c) Y, d) Z.*

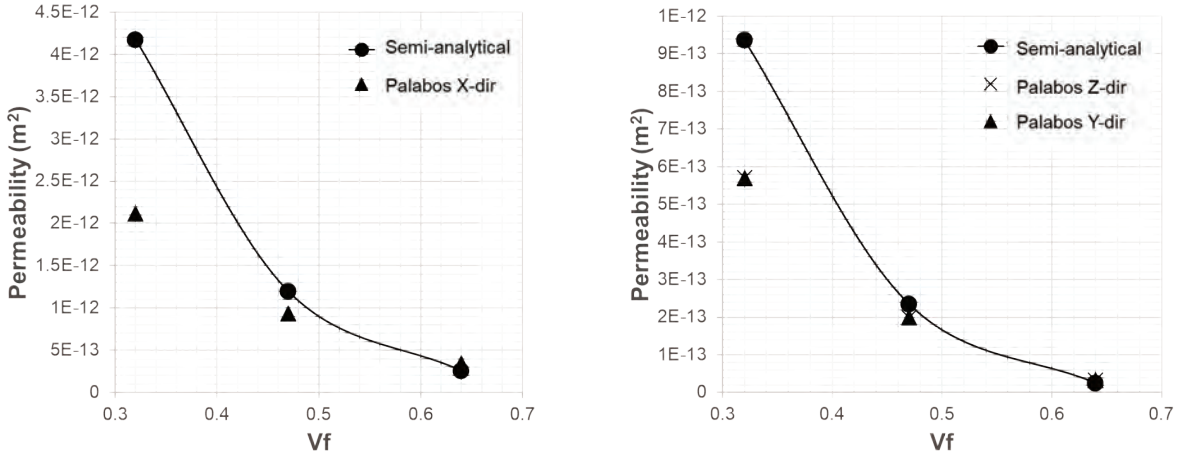

a) b)

Figure 2. *Dependence of permeability on fiber volume content in a) X – along fiber direction and b) Y, Z – transverse to fiber direction.*

Figures 2a and 2b shows a comparison of the permeability calculations carried out in Palabos to the calculations using the semi-analytical formula. The large deviations at lower fiber volume fractions can be explained by the assumptions made in Gebart's work which assume validity in the range of very close-packed fibres.

Conclusions

1. The Lattice Boltzmann method was used to calculate microscale permeability and validated using a simple geometry and semi-analytical models.
2. Based on the calculations, it was found that the Lattice Boltzmann method is a suitable alternative for carrying out microscale permeability calculations.

Acknowledgements

This work has been supported by the Volkswagen stiftung program "Funding for refugee scholars and scientists from Ukraine" at the Leibniz-Institut für Verbundwerkstoffe GmbH.
The authors also express gratitude and appreciation to Prof. Dr. Boris Basok, and Dr. Andrey Tyrinov for their helpful advice and valuable insights during this article writing.

References

[1] Basok B., Davydenko B., Pavlenko A., *Numerical Network Modeling of Heat and Moisture Transfer through Capillary-Porous Building Materials*. Materials 2021, 14, 1819, https://doi.org/10.3390/ma14081819.

[2] Basok B., Davydenko B., Koshlak H., Novikov V., *Free Convection and Heat Transfer in Porous Ground Massif during Ground Heat Exchanger Operation*. Materials 2022, 15, 4843, https://doi.org/10.3390/ma15144843.

[3] Gebart B.R., *Permeability of Unidirectional Reinforcements for RTM*. Journal of Composite Materials. 1992, 26(8), 1100-1133, http://doi.org/10.1177/002199839202600802.

[4] Rieber G., Jiang J., Deter C., Chen N., Mitschang P., *Influence of textile parameters on the in-plane Permeability*, Composites Part A: Applied Science and Manufacturing, Vol. 52, 2013, pp. 89-98, https://doi.org/10.1016/j.compositesa.2013.05.009.

[5] Nabovati A., Llewellin E.W., Sousa A.C.M., *A general model for the permeability of fibrous porous media based on fluid flow simulations using the lattice Boltzmann method*, Composites Part A: Applied Science and Manufacturing, Vol. 40, Issues 6-7, 2009, pp. 860-869, https://doi.org/10.1016/j.compositesa.2009.04.009.

[6] Caglar B., Broggi G., Ali M.A., Orgéas L., Michaud V., *Deep learning accelerated prediction of the permeability of fibrous microstructures*, Composites Part A: Applied Science and Manufacturing, Vol. 158, 2022, 106973, https://doi.org/10.1016/j.compositesa.2022.106973.

[7] May D. et al., *In-plane permeability characterization of engineering textiles based on radial flow experiments: A benchmark exercise*, Composites Part A: Applied Science and Manufacturing, Vol. 121, 2019, pp. 100-114, https://doi.org/10.1016/j.compositesa.2019.03.006.

[8] Schmidt T., Schimmer F., Widera A., May D., Motsch-Eichmann N., Bauer C., *A Novel Simulative-Experimental Approach to Determine the Permeability of Technical Textiles*. Key Engineering Materials. (2019), 809. Pp. 487-492. 10.4028/www.scientific.net/KEM.809.487.

[9] Cassola S., Duhovic M., Schmidt T., May D., *Machine learning for polymer composites process simulation – a review*, Composites Part B: Engineering, Vol. 246, 2022, 110208, https://doi.org/10.1016/j.compositesb.2022.110208.

[10] Latt J., Malaspinas O., Kontaxakis D., Parmigiani A., Lagrava D., Brogi F., et al., *Palabos: Parallel Lattice Boltzmann Solver*. Computers & Mathematics with Applications 2021, Vol. 81, pp. 334-350, https://doi.org/10.1016/j.camwa.2020.03.022.

[11] Tu J., Yeoh G.-H., Liu C., Chapter 9 - *Some Advanced Topics in CFD*, Editor(s): Tu J., Yeoh, G.-H. Liu C., Computational Fluid Dynamics (Third Edition), Butterworth-Heinemann, 2018, pp. 369-417, ISBN 9780081011270, https://doi.org/10.1016/B978-0-08-101127-0.00009-X.

[12] Bhatnagar P.L., Gross E.P., Krook M. (1954), *A Model for Collision Processes in Gases. I. Small Amplitude Processes in Charged and Neutral One-Component Systems*. Physical Review 94, pp. 511-525. https://doi.org/10.1103/PhysRev.94.511.

HEAT AND MASS EXCHANGE PROCESSES DURING DRYING OF COMPOSITE MIXTURE FROM PEAT WASTE AND CORN STALK

Zanna Petrova, Vadim Paziuk, Anton Petrov, Yuliia Novikova

Institute of Engineering Thermophysics National Academy of Sciences of Ukraine
e-mail: bergelzhanna@ukr.net

Introduction

One of the main problems of the modern world is the search for and supply of renewable energy resources that could compete with oil and natural gas.

Biofuel is an alternative type of fuel obtained as a result of the processing of animal or vegetable raw materials, as well as organic industrial waste and household products. Alternative energy considers biofuel as an option to replace traditional – coal, oil, natural gas, etc.

Among the non-traditional types of solid fuels known in Ukraine, it is worth paying attention to peat – an organic rock formed as a result of incomplete biochemical decomposition of dead marsh plants in conditions of excess moisture with a lack of oxygen, which contains up to 50% of mineral components on a dry matter basis.

Peat contains a large number of humic substances. Because of this, peat has significant energy and agrochemical potential and is used as a local fuel, as well as raw material for the production of greenhouse and consumer soils and organic fertilizers. Peat fuel is the cheapest and most efficient when transported over short distances. The cost of a unit of energy obtained from peat is 3 times cheaper than the cost of the same energy obtained from natural gas [1].

If humic substances are removed from it, and the rest is burned, then this unique natural resource can be used more rationally. The main method of obtaining humic substances is an alkaline reaction with ammonia solutions or potassium or sodium hydroxides. Such processing turns them into water-soluble salts – potassium or sodium humates with high biological activity. The composition of functional groups and the structure of molecular fragments of humic acids depends on the method of their production.

In the production of humic liquid or solid fertilizers, the humic component is extracted from peat [2]. After extraction, a solid residue remains, which can be used more rationally in the future. The creation of new compositions based on peat or its residues after extraction give a positive result when it is burned.

Materials and methods

Suitable materials, such as milled peat and nutritious corn stalk, were used for research. Milled peat has an initial moisture content of 13.18% and an ash content of 27.23%. Corn stalk have a moisture content of 8.45% and an ash content of 9.8%.

The resulting mixture of peat residues after extracting fertilizers and nutritious corn stalk was dried on an experimental stand with an automatic system for collecting experimental data and processing it. The automated data acquisition system reads data at a rate of 7 values per minute. During the drying process, data on the time of the experiment, the temperature in the middle of the drying chamber and the mixture, and the change in the mass of the material were read [3].

Results

Figure 1 shows the change in the moisture content and drying temperature of the mixture based on the solid residue of peat after the extraction of the humic component with crushed nutritious corn stalk at temperatures of 70°C and 100°C. As can be seen from Figure 1 increase in the temperature of the coolant from 70°C to 100°C intensifies the drying process by 1.8 times.

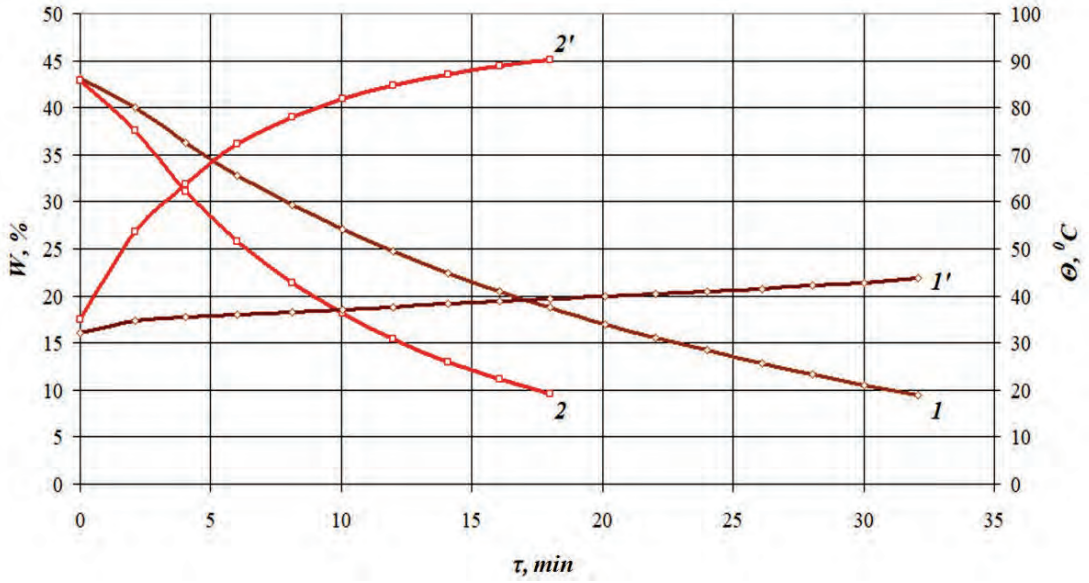

Figure 1. *Change in moisture content (1, 2) and temperature in the middle of the layer (1', 2') of the mixture based on the solid residue of peat after extraction and crushed corn stalk ratio 1:1 over time, V = 3 m/s, h = 10 mm, particle size ≥ 0.5 mm: 1, 1' – 70°C; 2, 2' – 100°C.*

Figure 2 shows the change in the presented change in the drying speed of the mixture based on the solid residue of peat after the extraction of the humic component with crushed nutritious corn stalk at temperatures of 70°C and 100°C. As can be seen from Figure 2 drying speed at a temperature of 70°C – 1.9%/min, and at a temperature of 100°C – 3.4%/min.

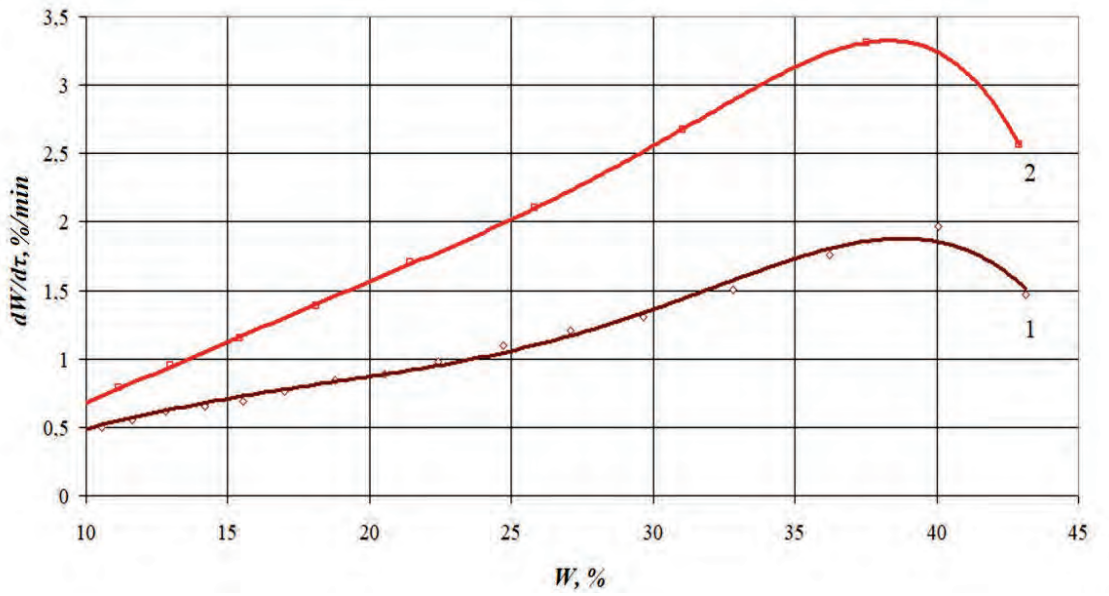

Figure 2. *Change in the speed of the mixture based on the solid residue of peat after extraction and crushed corn stalk ratio 1:1, V = 3 m/s, h = 10 mm, particle size ≥ 0.5 mm: 1 – 70°C; 2 – 100°C.*

The nature of the drying process, which is depicted on the curves of drying kinetics, drying speed and temperature curves, is determined by the physic-chemical and structural-mechanical properties of the material, which affect the form of moisture connection with it, the diffusion nature of the phenomenon, as well as the method of heat introduction, otherwise regularity of interaction of the body with the environment. A variety of factors and their interrelation makes it difficult to obtain analytical dependences of material drying kinetics. Therefore, when describing the drying process, empirical dependences are used. The most similar method of calculating the kinetics of

drying is a method based on the study of the general regularities of the process, which brings the theory and practice of drying closer together [4].

According to the appropriate methods, the kinetics of heat-moisture exchange during drying of the composite mixture was calculated [4, 5].

To study the kinetics of drying, composite mixtures were taken based on the solid residue after the extraction of humic substances from peat and nutritious residues of corn in a ratio of 1:1. After calculation according to the given method, generalized drying kinetic curves and drying speed curves were obtained.

Analysing the generalized drying curves, we can say that all drying modes fit on one curve with an error of no more than 10% (Fig. 3).

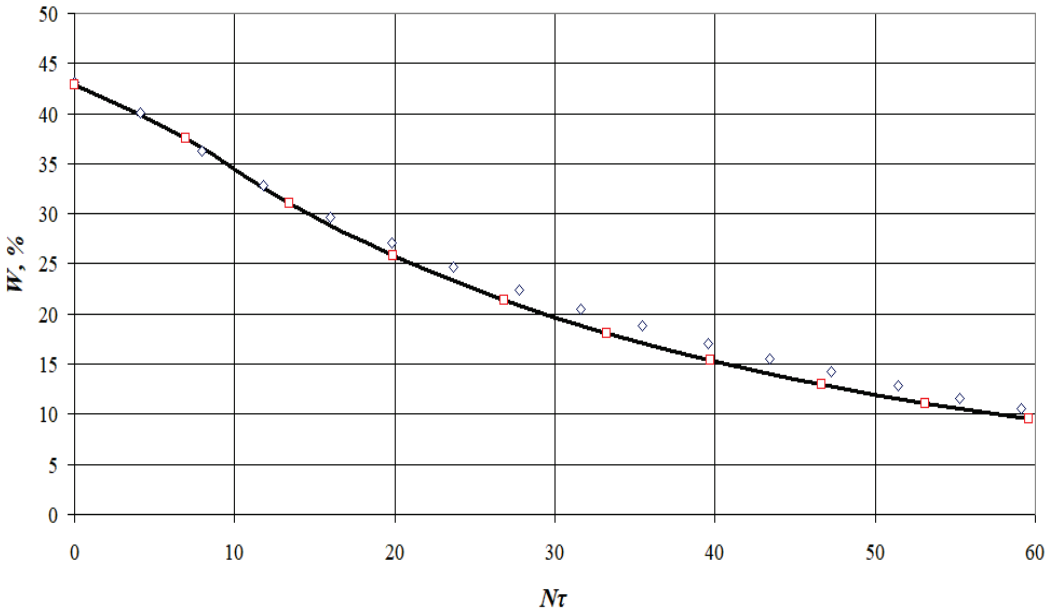

Figure 3. *Generalized drying curves of the mixture based on the solid residue of peat after extraction and crushed corn stalk in the coordinate system W – N τ.*

Carrying out graphical differentiation of the generalized curve of drying kinetics, presented in Figure 3, obtained the generalized curve of the drying speed of the composite mixture, which is presented in Figure 4.

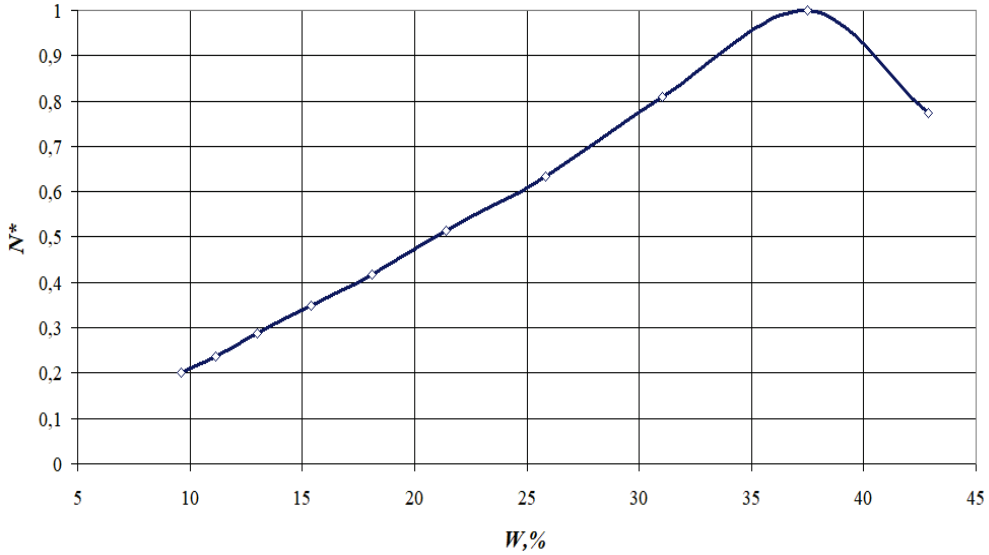

Figure 4. *Generalized curves of the drying speed of the composite mixture based on the solid residue of peat after extraction and crushed corn stalk.*

The total duration of the process in the absence of the first drying period:

$$\tau_T = \frac{1}{N}\left(\frac{1}{\chi_1}\lg\frac{Wk_1}{Wk_2} + \frac{1}{\chi_2}\lg\frac{Wk_2}{W_k}\right) = \frac{1}{N}\left(\frac{1}{0.011}\lg\frac{40}{11.6} + \frac{1}{0.010}\lg\frac{11.6}{9.5}\right) =$$

$$= \frac{1}{N}(48.89 + 8.2) = \frac{57.09}{N}$$

Conclusions

The drying kinetics of the composite mixture based on the solid residue of peat after extraction and crushed corn stalk were investigated, and effective drying modes were determined. The kinetic regularities of convective drying of the composite mixture based on the solid residue of peat after extraction and crushed corn remains were determined and summarized.

References

[1] Sniezhkin Yu.F., Petrova Zh.O., Korinchuk D.M., *Effective thermal technology of processing peat into fuel and fertilizer*. Renewable energy and energy efficiency in the XXI century: materials of the XX international scientific and practical conference, May 15-16, 2019, Kyiv: Interservice, 616 [in Ukrainian].

[2] Sniezhkin Yu.F., Petrova Zh.O., Korinchuk D.M., *Method of obtaining organo-mineral fertilizers based on humic substances*. Patent of Ukraine No. 117651 from 27.08.2018 [in Ukrainian].

[3] Sniezhkin Yu., Petrova Zh., Novikova Yu., Petrov A., *Technology of complex processing of peat. Energy and automation*, 2020, No. 5, 32-41, http://dx.doi.org/10.31548/energiya2020.05.032/

[4] Sniezhkin Yu.F., Paziuk V.M., Petrova Zh.O., Chalaiev D.M., *Heat pump grain dryer for seed grain*. Kyiv: Polygraph Service LLC, 2012 [in Ukrainian].

[5] Snezhkin Yu.F. Petrova Zh.O., *Energy-efficient thermal technologies of functional raw materials processing*: monograph. Kyiv: Naukova dumka, 2018 [in Ukrainian].

PREDICTION OF THE LEVEL OF REACTIVE POWER CONSUMPTION OF AN INDUSTRIAL ENTERPRISE USING ARTIFICIAL NEURAL NETWORKS

Vasyl Kalinchyk, Olexandr Meita, Vitalii Pobigaylo, Olena Borychenko, Vitalii Kalinchyk

National Technical University of Ukraine "Igor Sikorsky Kyiv Polytechnic Institute", Kyiv, Ukraine
e-mail: vkalin@i.ua

Introduction

The study bears relevance due to the tasks of improving the quality of electricity in load centres, where reactive power compensation is an influencing factor. At the same time, the development and research of the reactive power compensation control system to improve the quality of electricity allows to establish measurement parameters and adjust them, when the load operation mode changes [1].

Computational intelligence methods, namely artificial neural networks, are an alternative to statistical methods. A significant advantage of neural networks is that they are able to learn and generalize the accumulated knowledge. The network can also be easily used to predict output parameters due to its ability to solve complex calculations that are difficult to solve with other methods [2, 3].

The purpose of this paper is to create a neural network model of the enterprise with the function of forecasting the level of reactive power.

To achieve this goal, the following objectives are addressed in the paper:

- Determining indicators of the enterprise and establishment of averaging and forecasting intervals.
- Selecting the type and configuration of the artificial neural network to describe the enterprise as a consumer of reactive power.
- Prediction of the level of reactive power consumed by the enterprise and assessment of the quality of the neural network for the predictive model.

Presentation of the main research material

The paper builds a neural network to predict the level of reactive power consumed by the enterprise based on three sequences of data that describe the level of reactive power consumed by the enterprise. The input data is represented by a table of meter readings of the reactive power and two sequences of values that characterize the values of the consumed reactive power averaged over 1 hour $Q_i = f(t)$ and reactive power coefficient $\cos\varphi_i = f(t)$. To verify the accuracy of the model, forecasting will be based on 336 observations (14 days), and the rest of the sampling data will serve as a control sequence. Processing of graphs and creation of a model is performed using the "STATISTICA" package.

According to the constructed periodogram for the graphs of changes in reactive power and coefficient of reactive power, the period of these graphs is 24 hours. The number of observations accepted as input data for the network shall be not less than the period of the series. A multi-layer perceptron was selected as the model for the predictive model, the number of inputs of which was set according to the periodograms of the graphs. The multilayer perceptron (MLP) network is an example of nonlinear multilayer forward propagation networks and is a universal approximator [4]. As the paper considers a prediction problem, one output neuron is sufficient for the output layer. In the hidden layer, the number of neurons is set in the range from 2 to 48. The final number of neurons in the hidden layer shall be determined by the quality of the obtained model. Linear, hyperbolic,

exponential, hyperbolic and sinusoidal threshold activation functions are used. 1000 neural networks with randomly accepted initial weights were used for the training, out of which ten were chosen to evaluate the quality of the training. Productivity on the training and control sequences is 91.99% and 92.94%, respectively. We compare the results of forecasts of selected networks with real data (Figs. 1-2). The analysis indicates that there are significant deviations when forecasting extremes, which imposes significant restrictions on the use of these models for forecasting periodic series.

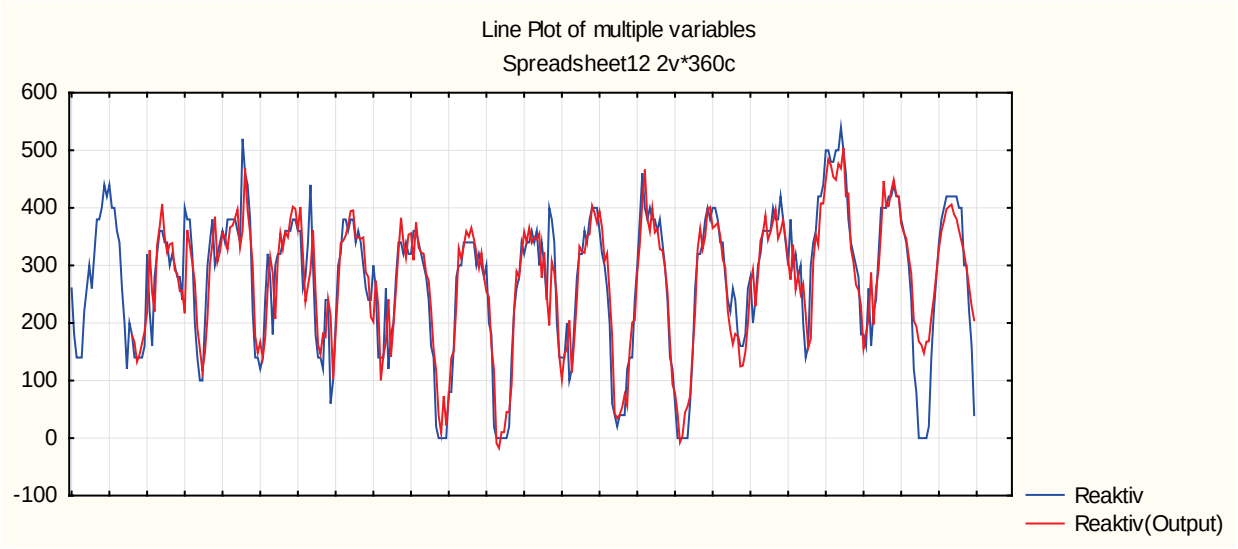

Figure 1. *Comparison of actual and forecast graphs of reactive power.*

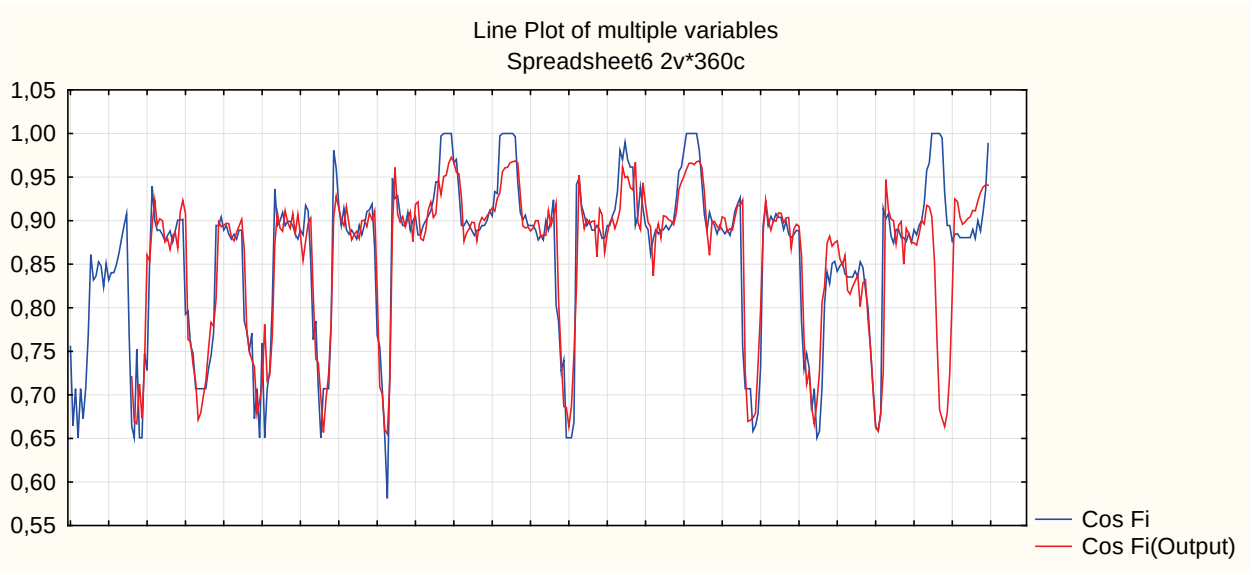

Figure 2. *Comparison of actual and forecast graphs of the power factor.*

The third variant of forecasting is performed on the basis of a schedule with the accumulation of counter indicators. Because the cumulative graph has only an increasing trend and no period, the same number of input neurons will be used to build the predictive neural model as for the previous models. 1000 neural networks with randomly accepted initial weights, with the same activation functions as previously, were used for the training. According to the results of the training, top 5 have been selected.

All models have virtually identical indicators on the study and control sequences make up and make up not lower than 99.02% and 99.17%, respectively. For these networks, the relative error was determined for each observation on the test sample, which was constructed based on the data of the 15th day of observations (Fig. 3) and its average value is determined. The best result was determined in the MLP 24-4-1 network amounting to 0.57%.

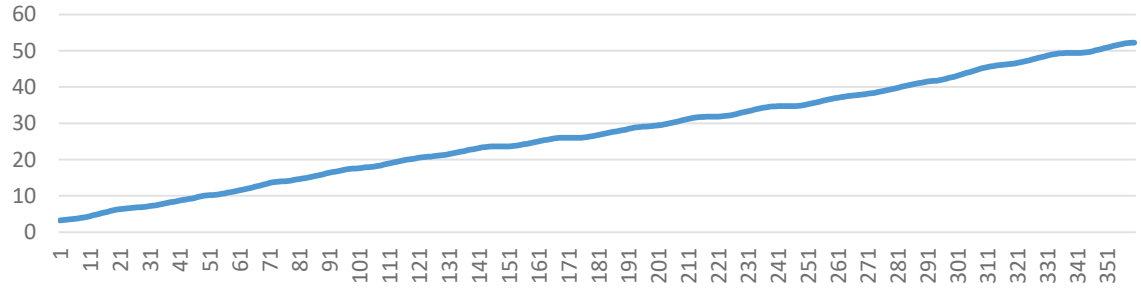

Figure 3. *Graph of accumulated reactive power consumption.*

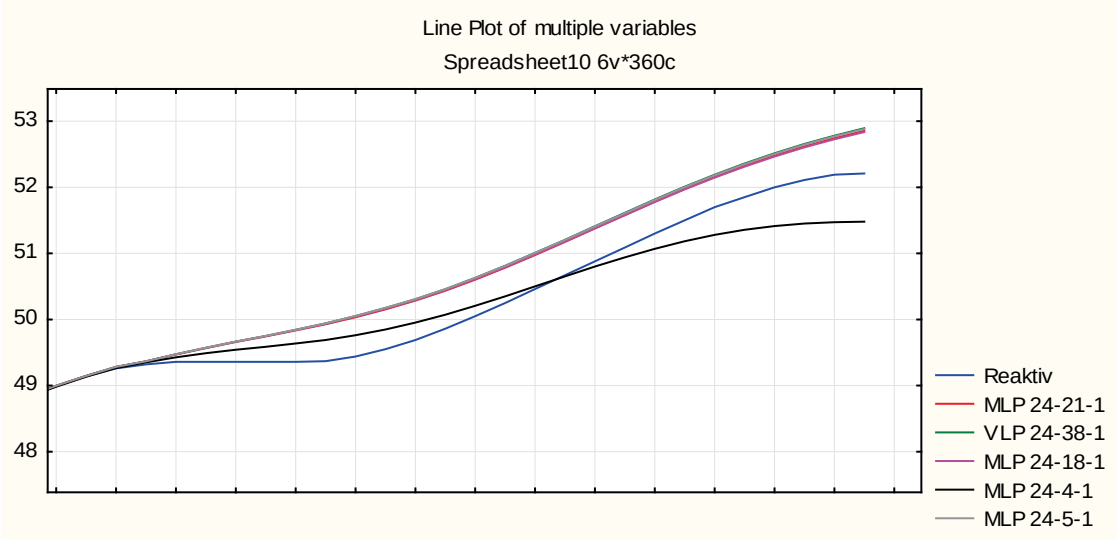

Figure 4. *Comparison of the input graph with the predicted graph.*

Conclusions

According to the results of the research, the sequence with the accumulation of the power meter was deemed as the most suitable for the creation of high-precision models for predicting reactive loads. The least accurate forecast data is obtained on the basis of power factor data. To simplify the forecasting model, it is advisable to use the conversion of periodic data with a trend into a growing sequence. Based on the numerical values of the training sequences, artificial neural networks of the MLP type were trained. The number of neurons and the type of activation function in the hidden layer did not have a significant impact on the quality of the model and the accuracy of the forecast, therefore, to simplify calculations, preference should be given to models with a smaller number of hidden neurons.

References

[1] Vlasova E.P., Botalov A.N., *Development of a model of automatic regulation of reactive power compensation for the oil and gas industry*. Oil and Gas Studies, no. 6 (March 2020), pp. 176-83.

[2] Rudenko O., Bezsonov O., Romanyk O., *Neural network time series prediction based on multilayer perceptron*. Development Management. 2019, Vol. 17, No. 1, pp. 23-34.

[3] Thakial S., Arora B., *Neural Network Based Prediction Model for Job Applicants*. Journal of Computational and Theoretical Nanoscience. 2019, Vol. 16, No. 9, pp. 3867-3873.

[4] Haykin S., *Neural networks: full course*, 2nd edition: Transl. from English, M.: Williams Publishing House, 2006, 1104 p.

THE INFLUENCE OF GROUNDWATER FLOW ON THE EFFICIENCY OF THE VERTICAL GROUND HEAT EXCHANGER

Borys Basok[1], Borys Davydenko[1], Anatoliy Pavlenko[2], Hanna Koshlak[2]

[1]Institute of Engineering Thermophysics of National Academy of Sciences of Ukraine

[2]Kielce University of Technology, Poland

Introduction

Currently, ground source heat pumps are widely used in municipal energy. Their use as elements of a premises heating system makes it possible to reduce the consumption of fossil energy carriers such as gas and coal. Ground heat exchangers are either horizontal or vertical types. The advantages of vertical heat exchangers are that they require less land and can still provide efficient operation of the heat pumps systems [1].

The main element of the vertical ground heat exchanger is a U-tube in which the heat carrier (water or an aqueous solution of polypropylene glycol) moves. The heat carrier with temperature lower than the temperature of the soil mass, moves in the heat exchanger tube, and extracts heat from the soil. The heat exchanger tube is usually placed in a vertical cylindrical borehole. The space inside the borehole is filled with grout material to ensure better heat transfer by thermal conductivity from the soil to the U-tube and prevent possible contamination of groundwater [1]. The thermal resistance of the material inside borehole can provide a significant influence on the efficiency of the ground heat exchanger and the heat pump system as a whole [2]. If there is a groundwater flow in the soil mass, heat from the soil to the heat carrier in the tube will be transferred not only by thermal conductivity, but also by convection.

The movement of groundwater is one of the factors affecting the performance of the heat exchanger. This movement can be carried out both due to natural and forced convection. The natural convection of groundwater arises due to the presence of a temperature gradient, which caused by the operation of the heat exchanger itself [3, 4]. Forced convection occurs when there is a pressure drop along the soil mass. Most of the numerous models used to determine the thermal characteristics of soil heat exchangers take into account only the heat transfer by thermal conduction in the soil mass. Models that do not take into account the convection heat transfer may, in some cases, not accurately predict the thermal regimes of ground heat exchangers.

Since the soil is a porous medium, the movement of groundwater is filtration. The intensity of this movement depends both on the conditions that cause it and on such properties of the porous material as porosity and permeability. If the material filling the space in the borehole has a porosity and permeability significantly less than the soil, the movement of groundwater in this material is practically absent. In this case, groundwater will flow around the borehole, and not the heat exchanger tubes.

The purpose of this study is to determine the effect of the material filling the borehole and surrounding the U-tubes of heat exchanger on the efficiency of its operation in the presence and absence of groundwater movement. To do this, the results of calculations of heat transfer from the soil massif to the heat exchanger tubes in the presence and absence of a borehole filled with impermeable material are compared. In the second case, it is assumed that the U-tube heat exchanger is located directly in the ground and directly contacts with groundwater flow.

Statement of the problem

The Darcy-Brinkman-Forheimer model is used for numerical simulation of groundwater movement in the soil mass and heat transfer. According to this model, the fluid flow in a ground porous medium is described by a system of equations including continuity equation; momentum

equations and energy equation. For the heat carrier flow in U-tube heat exchanger channel the approximate energy balance equation is used. For the heat transfer in borehole material the heat conductivity equation is used. On the boundaries of heat exchanger tube and on the borehole material surface the conjugate boundary conditions are sets. The statement of this heat transfer problem is described in more detail in [4, 5]. System of differential equations with boundary conditions is solved by finite-difference method.

The process of heat transfer is considered in the computational domain of the rectangular parallelepiped form. This parallelepiped with sides x_{max} = 3.5 m; y_{max} = 3.5 m; z_{max} = 17 m covers a section of the soil massif with a vertical U-tube heat exchanger. The heat exchanger channel is represented by two straight vertical sections connected by a horizontal section. Channel sections are considered square in cross section. The length of the sides of the square is a = 0.1 m, and the thickness of the channel walls is δ = 2 mm. The total length of the heat exchanger channel L = 32.8 m. The flow of groundwater is caused by the pressure gradient along the 0Y axis. Pressure drop along the computational domain is Δp = 10000 Pa. The heat carrier flow rate is $G = 0.25 \cdot 10^{-3}$ m^3/s. Heat carrier temperature at the inlet to the heat exchanger – t_0 = 5°C. The temperature of groundwater entering the area observed is t_∞ = 10°C. Heat transfer coefficient in the heat exchanger channels – α_c = 145.7 W/m^2/K; porosity of the ground – φ = 0.4; ground particle diameter – d_p = 0.25 mm. The values of thermophysical properties of the components, taking part in heat transfer process, is taken from [3].

Results

Comparison of the results of calculation of the temperature regime of the ground heat exchanger for four variants is carried out. In the first and second variants, the heat exchanger tube is in direct contact with the ground. In the first variant, there is a groundwater flow due to longitudinal pressure drop, and in the second variant, this flow is absent. In the third and fourth variants, the heat exchanger tube is placed in a borehole filled with a material with the specified properties. The permeability of this material is practically zero. Therefore, there is no filtration flow of groundwater through this material. In the third variant, there is a flow of groundwater in the soil surrounding the borehole, and in the fourth variant, this flow is absent. The distribution of groundwater flow velocity and temperature in a horizontal section of a porous ground massif for these four variants is shown in Figure 1.

As can be seen from the figure, in the presence of groundwater flow, there is an intensive heat transfer by convection in the soil mass in the direction of the flow (Figs. 1a and 1c). If the heat exchanger tubes are in direct contact with the groundwater flow (Fig. 1a), the temperature gradients around the heat exchanger tubes are greater than if there is a borehole filled with impermeable material around the heat exchanger (Fig. 1c). In this case, the heat transfer to the heat exchanger tubes is carried out only by thermal conductivity through the material filling the borehole, and the convective heat transfer occurs outside the borehole. Therefore, when the tubes of the heat exchanger are in direct contact with the ground water flow, the heat transfer intensity is increased and the operation efficiency of the ground heat exchanger is also increased. In the absence of groundwater flow (Figs. 1b and 1d), heat transfer from the ground to the heat exchanger tubes is carried out only by heat conduction. In this case, heat transfer is less intense compared to the case of the presence of a groundwater flow. Comparing Figure 1c and Figure 1d, it can be seen that the temperature distributions inside the borehole differ insignificantly. Therefore, the influence of groundwater flow on the performance of the ground heat exchanger is not as significant as in the absence of borehole material (Fig. 1a).

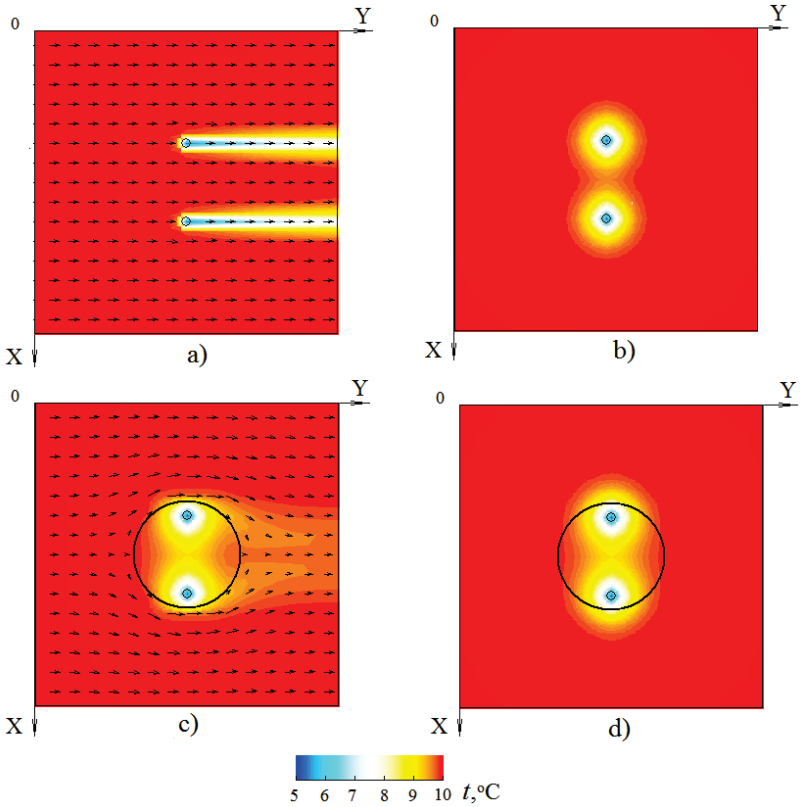

Figure 1. *Velocity and temperature distribution in the horizontal section of soil massif: a); c) groundwater flow is present; b); d) groundwater flow is absent; a); b) borehole filled material is absent; c); d) borehole filled material is present.*

Temperature changes along the length of the channel for the four conditions considered are presented in Figure 2.

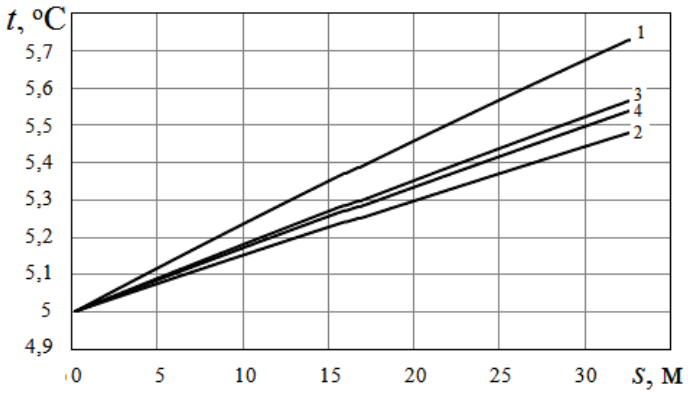

Figure 2. *Change in the temperature of the heat carrier along the length of the heat exchanger channel: 1; 3 – groundwater flow is present; 2; 4 – groundwater flow is absent; 1; 2 – borehole filled material is absent; 3; 4 – borehole filled material is present.*

As can be seen from the figure, the heat carrier in the heat exchanger channel is heated most of all in the presence of a groundwater flow in the absence of impermeable material filling the borehole (curve 1). Heat transfer to it from the ground is carried out both by thermal conductivity and convection. The heat carrier heats up least of all in the heat exchanger, when there is no impermeable borehole material and no groundwater flow (curve 2). The degree of heating of the heat carrier in the heat exchanger tube surrounded by impermeable borehole material is less than in case 1, but greater than in case 2. Heating of the heat carrier in the heat exchanger in the fourth case will be higher than

in case 2, since the thermal conductivity of the material filling the borehole is higher than the thermal conductivity of the porous ground filled with water. At the same time, this heating is only slightly lower than in case 3.

The considered results refer to stationary heat transfer modes, in which both groundwater and the heat carrier temperature at the inlet to the heat exchanger channel do not change with time. Of interest is also the periodic mode of operation of the heat exchanger, in which for 45 minutes of each hour the temperature of the heat carrier at the inlet to the heat exchanger is $t_0 = 5°C$, and for the next 15 minutes the temperature of the heat carrier at the inlet is $t_\infty = 10°C$, which corresponds to the groundwater temperature at the inlet to the area under study. The change in time of the temperature of the heat carrier at the inlet to the heat exchanger and at the outlet of the heat exchanger is shown in Figure 3. The results refer to option 1, when the heat exchanger tubes are directly in the ground and there is groundwater flow. On Figure 4 shows the differences between the temperature of the heat carrier at the outlet of the heat exchanger for this option 1 and the temperatures of the heat carrier calculated for the conditions corresponding to variants 2, 3 and 4. As can be seen from the figure, the indicated values Δt are grater then zero.

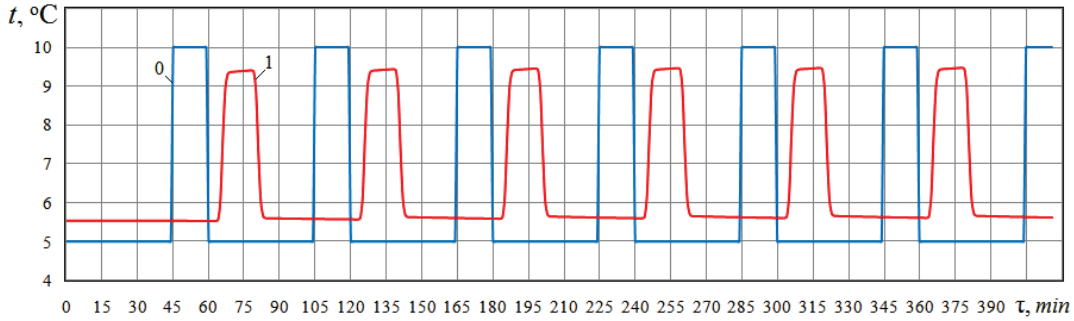

Figure 3. *The change in time of the temperature of the heat carrier for the variant when the heat exchanger tubes are directly in the ground and there is groundwater flow: 1 – inlet to the heat exchanger; 2 – outlet from the heat exchanger.*

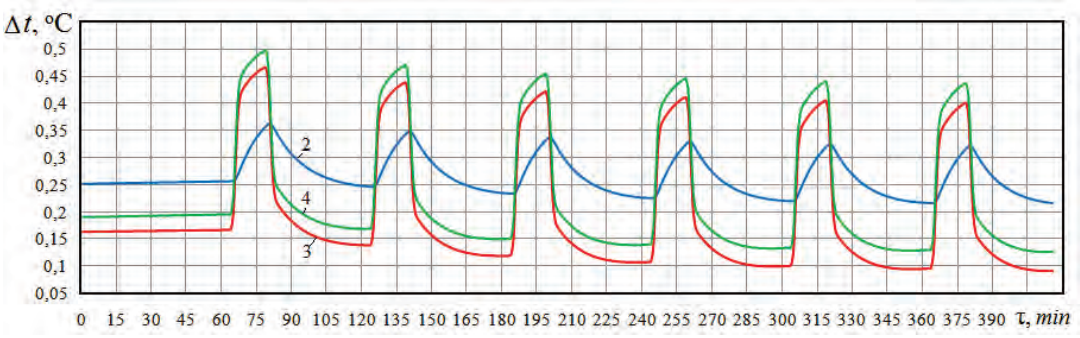

Figure 4. *Differences between the temperature of the heat carrier at the outlet of the heat exchanger for variant 1 and the outlet temperatures of the heat carrier calculated for the conditions corresponding to variants 2, 3 and 4.*

Conclusions

It follows from the presented results that, both in stationary and non-stationary conditions, the highest temperature at the outlet of the heat exchanger will be in the case when the heat exchanger tubes are in direct contact with porous soil and there is a groundwater flow. In the presence of a borehole with impermeable material, the temperature at the outlet of the heat exchanger will be lower than in option 1, both in the presence of a groundwater flow and in its absence. At the same time, when filling the borehole with impermeable material, the flow of groundwater contributes to an increase in the temperature of the heat carrier at the inlet from the heat exchanger.

References

[1] Diao N.R., Zeng H.Y., Fang Z.H. (2004), *Improvement in Modeling of Heat Transfer in Vertical Ground Heat Exchangers*. HVACR Res. 10, 459-470.

[2] Serageldin A.A., Radwan A., Sakata Y., Katsura T., Nagano K. (2020), *The Effect of Groundwater Flow on the Thermal Performance of a Novel Borehole Heat Exchanger for Ground Source Heat Pump Systems: Small Scale Experiments and Numerical Simulation*. Energies. 13, 1418.

[1] Ghoreishi-Madiseh S.A., Hassani F., Mohammadian A., Radziszewski P.A. (2013), *Transient Natural Convection Heat Transfer Model for Geothermal Borehole Heat Exchangers*. J. Renew. Sustain. Energy. 5, 043104.

[2] Basok B.I., Davydenko B.V., Koshlak H.V., Novikov V.G. (2022), *Free Convection and Heat Transfer in Porous Ground Massif during Ground Heat Exchanger Operation*. Materials. 15, 4843.

[3] Basok B.I., Davydenko B.V., Pavlenko A.M., Koshlak H.V. (2022), *Influence of Groundwater Filtration Flow on the Thermal Efficiency of Underground Heat Exchanger*. Vidnovliuvana Energetyka/Geothermal Energy. 2 (96), 71-80.

POSSIBILITIES FOR THE PRODUCTION AND USE OF HYDROGEN AS A FUEL IN EXISTING BOILERS

Oleksandr Sigal, Dmytro Paderno, Nataliia Nizhnyk

Laboratory of thermophysics processes in boilers, Department of heat-physical problems of heat supply systems
of the Institute of Engineering Thermophysics of the National Academy of Sciences of Ukraine
2A, M. Kapnist str., Kyiv, 03057, Ukraine
e-mail: sigal@engecology.com; paderno@engecology.com; niznikn27@gmail.com

Using of hydrogen at present is a key priority to achieve the European Green Deal and Europe's clean energy transition [1], and application of it as a fuel for at least partial replacement of the fossil fuels is one of the essential components to support the EU's commitment to reach carbon neutrality by 2050 and for the global effort to implement the Paris Agreement while working towards zero pollution [2].

In spite of the obvious environmental advantages, such using creates a number of currently unresolved problems due to the peculiarities of the hydrogen characteristics as a fuel, which stipulates the necessity for changing of the modes of its combustion, of the construction of fire chambers, heat-receptive elements, etc. The problems for hydrogen practical use in combustion processes in the existing boiler equipment are pointed out in [3], and maybe the main problem is that the adiabatic hydrogen combustion temperature in air is high, about 260° higher than the adiabatic combustion temperature of usually used natural gas.

However, this peculiarity may be quite useful for processes where the combustion temperature is usually insufficiently high, and must be increased.

Such a process is, in particular, the thermal processing of the municipal solid waste (MSW).

The world's leading countries consider solid waste as an alternative local energy resource that is constantly generated and is very convenient logistically – in populated areas, close to energy consumers.

At present in Ukraine, especially under conditions of military aggression against our country, one of the largest threats to national security is Ukraine's energy dependence on imported natural gas; reducing of this dependence is a priority task for ensuring the stable operation of Ukraine's energy system. The special State targeted economic program for the energy recovery of MSW at enterprises – heat energy producers is now under development in Ukraine, the purpose of which is to attract the energy potential of MSW due to its energy recovery to the country's energy balance, as well as to solve the problem of sanitary cleaning of cities due to the utilization of a significant share of MSW.

According to the EU legislation [4], which is now under implementation to the Ukrainian legislation, waste incineration plants shall be designed, equipped, built and operated in such a way that the temperature of combustion even under the most unfavourable conditions must be kept at least at 850°C for at least two seconds.

With taking into account the quite low calorific value of usual MSW (about 1650 kcal/kg) and even of the Refuse derived fuel (RDF) made from MSW (2000-4000 kcal/kg), keeping of such temperature often requires an additional high calorific fuel.

The possible solution is using the hydrogen as such additional fuel. The proposed process for realizing this technique is schematically presented at Figure 1.

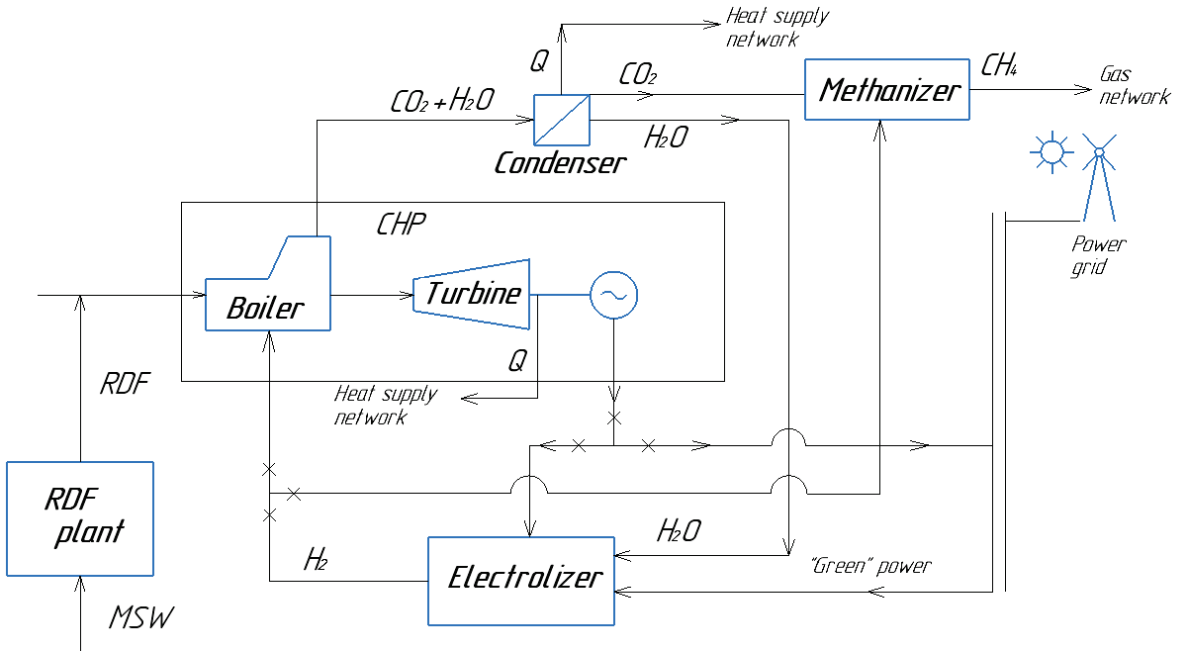

Figure 1. *Process sheme for using hydrogen at waste incineration.*

Hydrogen is generated by electrolysis with using “green” power from renewable sources (solar, wind, etc.) or own produced at the CHP, and is fed partly to the fire chamber of boiler combusting RDF, causing increasing of the combustion temperature, and partly is fed to the methanizer.

The water vapour contained in flue gases is condensed to liquid water, and carbon dioxide is fed to the methanizer.

During the reaction of interaction of hydrogen with carbon dioxide from flue gases of boilers, synthetic methane is formed in the methanizer, the formed methane-hydrogen mixture (up to 10% hydrogen) may be used practically as the usual methane, in particular may be used in existing natural gas firing boilers, or fed to a local natural gas network.

The carbon dioxide formed during the subsequent burning of such a mixture is no longer counted as a greenhouse gas emission.

The above process idea is at the stage of obtaining a patent.

Such process is proposed by the authors for implementation in the heat supply schemes for cities of Kyiv (at the heat supply station ST-1) and Odesa (at the region boiler-house Pivdenna-1), developed with participation of the authors.

References

[1] The European Green Deal. URL: https://ec.europa.eu/info/strategy/priorities-2019-2024/european-green-deal_en.

[2] Communication from the commission to the European parliament, the council, the European economic and social committee and the committee of the regions. A hydrogen strategy for a climate-neutral Europe. URL: https://eur-lex.europa.eu/legal-content/EN/TXT/?uri=CELEX:52020DC0301.

[3] Nizhnyk N., Sigal A., Plashykhin S., Safiants A., *Influence of hydrogen on the toxic substances formation process during co-incineration with natural gas*. International Science Journal of Engineering & Agriculture. Vol. 1, No. 4, 2022, pp. 19-26, doi: 10.46299/j.isjea.20220104.05.

INFLUENCE OF HEATING AND VENTILATION MODES ON THE ENERGY CONSUMPTION OF UNIVERSITY EDUCATIONAL BUILDINGS UNDER QUARANTINE CONDITIONS IN UKRAINE

Valerii Deshko, Inna Bilous, Tetyana Boiko

National Technical University of Ukraine «Igor Sikorsky Kyiv Polytechnic Institute»,
37 Prospekt Peremogy, Kyiv, 03056, Ukraine

Introduction

Since the end of 2019, humanity has faced an unprecedented phenomenon for the modern world – the global pandemic COVID-19, which has dramatically changed the lives of each of us. First of all, the changes for people concerned the usual modes of work for them – most organizations introduced remote modes of work for their employees, or – semi-remote, when employees partially visited their jobs. The same changes have taken place in the field of education. Educational institutions, particularly in Ukraine, have switched to remote or mixed mode. In March 2020, the World Health Organization declared the COVID-19 outbreak a global pandemic. At the same time, it was indicated that social distancing, sufficient ventilation of enclosed spaces and personal hygiene are the main measures that can prevent the spread of COVID-19 [1]. Therefore, to avoid crowds, most countries have introduced partial or complete closure of educational institutions, commercial and industrial companies [2]. In Ukraine, in the field of education, some institutions continued their work in a blended learning mode, while some completely switched to remote mode to prevent the spread of coronavirus disease.

Methods

For creating a building model in the DesignBuilder software, the educational building of the Igor Sikorsky Kyiv Polytechnic Institute was used as the object of the study. It was built in 1969. The building is located in Kiev. The bearing layer of the outer walls of the building is made of expanded clay concrete. For external walls U-Factor with Film – 1.021 $W/m^2 \cdot K$. The subject of the study is the consumption of heat energy by the building for the heating season under quarantine and normal conditions. During quarantine, less than 10% of the heated rooms of the educational building are used. The ventilation is provided at the level of 0.7 ac/h; another 0.3 ac/h is provided by the infiltration component (due to the looseness of the enclosing structures). Thus, the total air exchange is 1 ac/h. The hourly climate data used for the simulation is an IWEC hourly file for a typical year for Kiev conditions [3]. The energy consumption of the building was analyzed, for the normal mode of operation of the building and premises used during quarantine, under constant temperature 20°C and steady air exchange. Unused premises temperature was 14°C.

Results and conclusions

According to the results of modeling partial use of the building during quarantine allows to reduce the consumption of heat energy during the heating season by 61.32%. At the same time, the specific consumption to the total heating area is reduced by the equivalent value. However, if we compare the specific consumption of heat energy in heated to the appropriate level rooms in use, this value increases by 68.86%, compared to the normal mode, under the influence of heat exchange with unused premises.

References

[1] Sun C., Zhai Z., *The efficacy of social distance and ventilation effectiveness in preventing COVID-19 transmission*. Sustainable cities and society, 62, 2020, 102390, https://doi.org/10.1016/j.scs.2020.102390.

[2] Ivanko D., Nord N., Ding Y., *Heat use profiles in Norwegian educational institutions in conditions of COVID-lockdown*. REHVA Journal of Building Engineering, 43, Nov, 2021, https://doi.org/10.1016/j.jobe. 2021.102576.

[3] EnergyPlus. URL: https://energyplus.net/weather-location/europe_wmo_region_6/UKR.

THE INFLUENCE OF THE BUILDING'S BASEMENT DEPTH ON THE HEAT TRANSFER CHARACTERISTICS OF THE INTERNAL WALLS AND BASEMENT FLOOR

Boris Basok, Boris Davydenko, Vladimir Novikov

Institute of Engineering Thermophysics National Academy of Sciences of Ukraine

Introduction

Almost every modern building is connected to the ground in one way or another. Structurally, these can be basements, the walls of which form the foundation, floor slabs of the structure, piles and other structures directly connected to the earth (soil). However, the temperature of the soil is not always taken into account when evaluating the thermal characteristics of the building. At the same time, soil temperature is a factor that affects the heat exchange results of buildings with the environment, especially in ground buildings. Thus, it is necessary to assess this impact through the interaction of the soil with the building.

The results known to us [4] indicate that, when the influence of the soil is taken into account in the thermal analysis, the internal temperature of underground rooms increases to 8.9% in summer and decreases to 5.4% in winter, which in turn affects the overall thermal balance of the building in general.

Most of the works known to us, for example [3, 4], to calculate the effect of the soil on the thermal state of the building, used numerical solutions of the heat conduction equation in the calculation area, which included the walls of the basement and part of the soil that is in direct contact with those walls. The convective component of heat flows in the interior of the basement and on the surface of the earth was taken into account by the corresponding coefficients of heat transfer.

In this work, the thermal state of the components of a separate building is considered in a two-dimensional formulation using CFD modeling. The thermal analysis included: soil, basement, first floor, air in the basement and on the first floor, environment Figure 1.

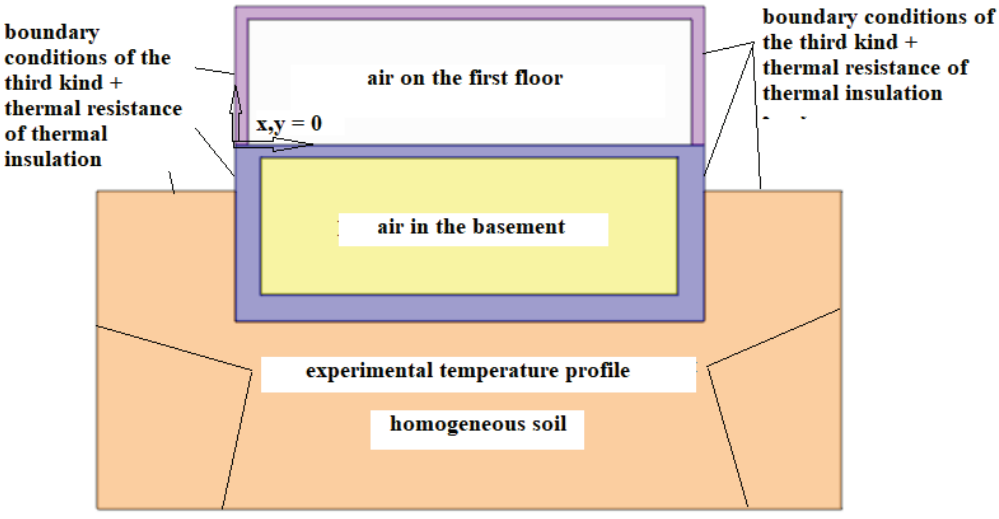

Figure 1. *Configuration of a rectangular basement in contact with a homogeneous soil and the first floor of a building.*

The width of the basement is 6 m, the height of the basement, from floor to ceiling, is 2 m, the height of the first floor is the same as that of the basement. The thickness of the walls and floor of

the basement is 0.38 m, the thickness of the floor of the basement and the walls of the first floor is 0.17 m. When the model was created, the depth of the soil massif and its width were calculated in accordance with the recommendations [1]. To analyze the thermal state of the system in Figure 1, depending on the depth of the basement immersion in the ground, three CFD models were created: 1) the basement is completely in the ground; 2) the basement is immersed in the soil by three quarters; 3) the basement is half submerged in the ground. The dimensions of the model correlate with the dimensions of the TOET energy-efficient house.

Physical and mathematical formulation

The problem of heat transfer in the above system is solved in a two-dimensional setting under stationary conditions of the external environment that correspond to the conditions of the city of Kyiv in July and December. In the model, the air in the basement and on the first floor is considered as an ideal gas, the behavior of which is described by the corresponding equation of state, the air flow regime is laminar in the field of gravity. The solid elements of the system: the soil, walls and floor of the basement, walls and floor of the first floor are considered as solid bodies with constant thermophysical properties. The material of the basement walls is considered to be concrete, the walls of the first floor are brick.

Heat transfer in the given system is described by Navier-Stokes equations, energy equations, thermal conductivity equations, and the equation of an ideal state for air. Numerical methods included in the Star CCM CFD package were used to solve the specified system.

Initial and boundary conditions

The ambient air temperature was assumed to be T_{out} = 26°C in July, and T_{out} = -10°C in December. The initial air temperature on the first floor was set at T_{ff} = 21°C, in the basement T_{bas} = 15°C. At the beginning of the calculation, the temperature fields in the soil are set for the months of July and December, respectively [2] (Fig. 2).

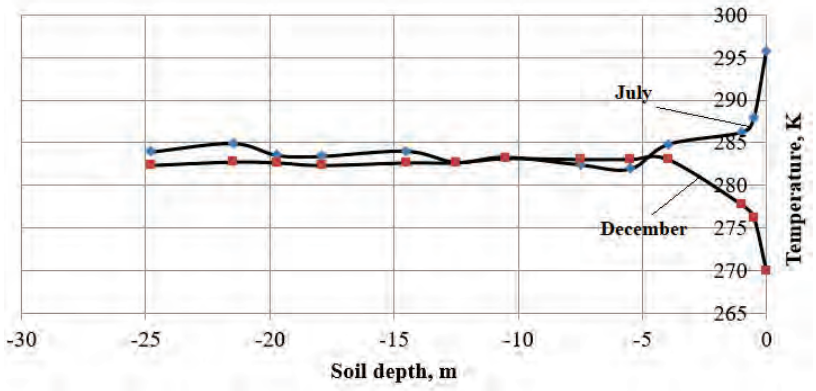

Figure 2. *Experimentally obtained temperature distributions along the soil depth.*

For modeling, the experimentally obtained temperature distributions along the soil depth were approximated by polynomials of the fourth degree:

$$Ts = -0.0003x^4 - 0.0174x^3 - 0.3618x^2 - 2.9634x + 270.26 \text{ – December}$$

$$Ts = 0.0004x^4 + 0.0221x^3 + 0.4622x^2 + 3.717x + 295.77 \text{ – July}$$

The results presented in Figure 2 indicate that the temperature of the soil starting from a certain depth does not depend on the season or the time of day. However, the temperature distributions depending on the depth will be different for different regions. In the places of contact of the air of the basement and the first floor with the corresponding walls and floors, as well as the contact of the

outer surfaces of the walls of the basement and the soil, the conjugate conditions are set. Boundary conditions of the third kind are set on the surfaces of the soil, the surfaces of the walls of the basement and the first floor, which are in contact with atmospheric air. The following values of the heat transfer coefficients on the surfaces of the walls of the basement and the first floor, which are in contact with the atmosphere, were set: the surface of the side walls of the basement and the first floor – α_w = 5 W/(m^2·K); soil surface – α_s = 5.7 + 3.8V, W/(m^2·K), where V is the speed of atmospheric air [3]. In addition to the boundary conditions of the third kind, a thermal resistance of Rt = 3.3 m^2 K/W was additionally set for the walls of the building in contact with atmospheric air.

Results of numerical studies

In Figures 3 and 4 show the fields of temperatures and velocities for a basement completely immersed in the soil.

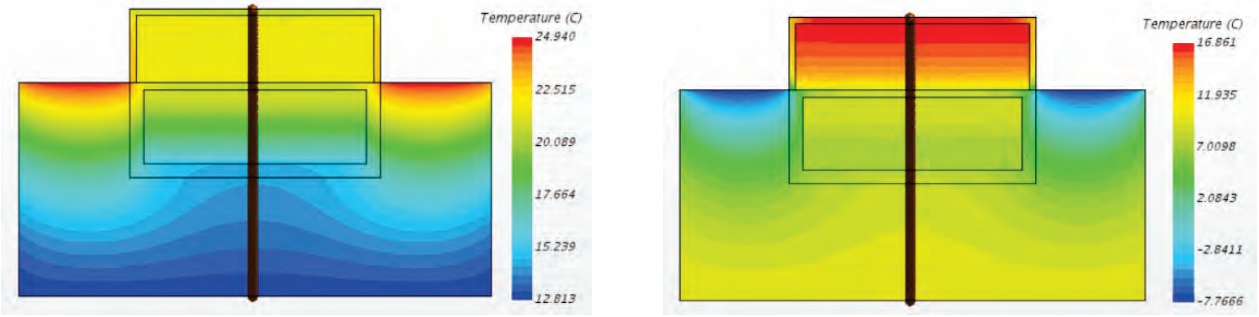

a) b)

Figure 3. *Fields of temperatures: a) July; b) December.*

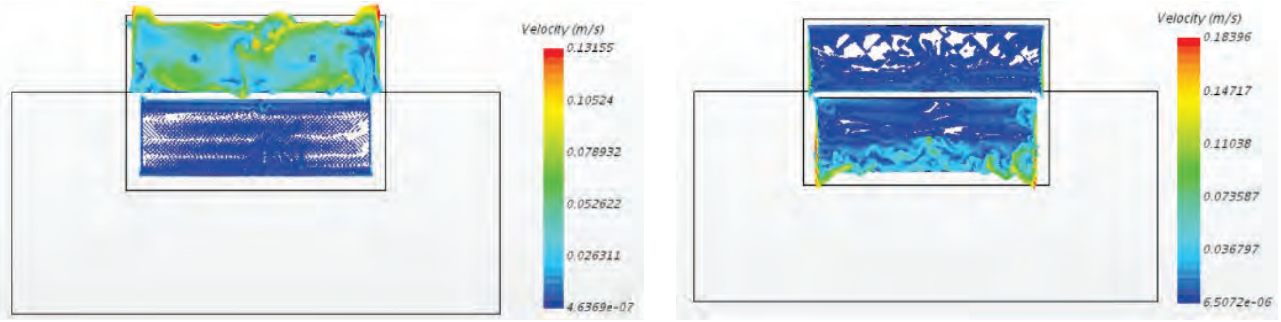

a) b)

Figure 4. *Velocity fields: a) July; b) December.*

The data shown in Figure 3 shows that the soil massif in the summer plays the role of a passive "air conditioner" that cools both the basement and the first floor. In winter, the soil massif looks like a powerful heat accumulator that maintains a certain temperature in the basement and on the first floor. Velocity fields in this case are formed under conditions of natural convection and determine a part of the convective component in the general thermal balance of the building.

In Figure 5 shows temperature distributions along the vertical line present in Figure 3.

It should be noted that when constructing the graphs in Figure 5, the coordinate system is related to the basement overlap. Comparing the temperature distribution with the soil temperature graph shows that in winter, a relatively warm basement significantly affects the thermal state of the soil. In summer, this influence is significantly less. The simulation results presented in this work indicated a very interesting fact related to the temperature in the basement. Basement walls that are in contact with the ground are without thermal insulation, but when they protrude above the surface of the ground, they have the same thermal insulation as the walls of the first floor. This

circumstance leads to the fact that the temperature in the basement remains practically constant along its height (Fig. 5) when part of the basement is in the atmosphere.

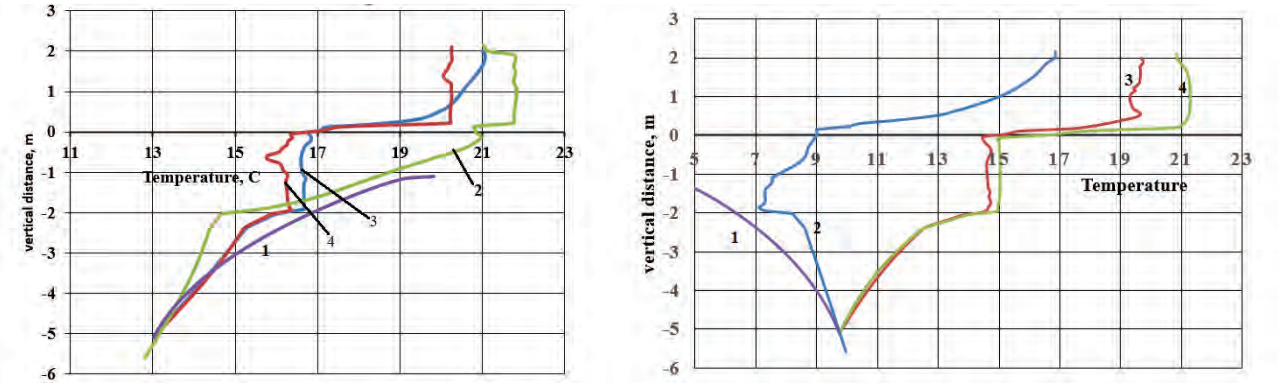

a) b)

Figure 5. *Temperature distributions: a) July; b) December: 1 – temperature distribution in the soil without the influence of the building; 2 – temperature distribution for a building whose basement is completely below the ground surface; 3 – the basement is 0.5 m above the ground; 4 – a basement of 1.0 m comes out from under the ground.*

Worthy of attention is the value of the heat transfer coefficient on the basement floor obtained as a result of modeling, its value is $\alpha bf = 8.03 \cdot 10^{-2}$. It should be noted that the indicated value of the heat transfer coefficient is significantly different from the corresponding values of the heat transfer coefficient $\alpha bf = 6.13$ W/m^2·K, which are used in works known to us to calculate the thermal state of basement rooms [3]. Such a significant discrepancy can be explained by the lack of ventilation in the built models. Forced air movement in the basement can increase this coefficient, but not so significantly.

References

[1] Sterling R.L., *Assessment of apparent soil thermal conductivity*. Thermal Performance of the Exterior Envelopes of Buildings V, 1992, pp. 147-157. Atlanta: American Society of Heating, Refrigerating and Air-Conditioning.

[2] Belyaeva T.G., *Experimental approbation of the measuring complex at the facility of a ground heat accumulator with vertical downhole heat exchangers*. Prom. heat engineering 2013, Vol. 35, No. 4, pp. 45-50.

[3] Choi S., Krarti M., *Effects of Layered Soil on Basement Heat Transfer*. Thermal Envelopes VII/Thermal Analysis of Building Systems-Principles. 1997, pp. 553-560.

[4] Resende B.C., et al., *Analysis of the influence of soil in the thermal performance of subterranean rooms in a ground-level building in Sao Paulo, Brazil, via EnergyPlus*. Ingeniare. Revista chilena de ingeniería [online]. 2020, Vol. 28, No. 1, pp. 164-177.

TORREFACTION OF COMPOSITE BIOFUEL IN THE ATMOSPHERE OF ITS OWN GASEOUS ENVIRONMENT

Viacheslav Mykhailyk, Tetiana Korinchevska, Valery Dakhnenko

Institute of Engineering Thermophysics of National Academy of Sciences of Ukraine
2a, Marii Kapnist Str., Kyiv, 03057, Ukraine
e-mail: mhlk45@gmail.com

Introduction

At peat deposits in Ukraine, actively used for many years, the ash content often exceeds the standard established for peat as a fuel. Its thermal characteristics can be improved by creating a composite with plant materials [1] and by performing granulation. However, this does not solve the problems of high hydrophilicity and biological damage. The use of biofuels and peat in energy sector requires a more significant increase in calorific value and the creation of conditions for effective dispersion. Torrefaction is among the well-known methods of increasing the energy properties of biofuel. It is a thermochemical process in an inert or limited oxygen environment, where the biomass is slowly heated to a predetermined temperature and maintained for a specified time [2, 3].

The main components of plant biomass are hemicellulose, cellulose and lignin. Coniferous wood contains 48-56% cellulose, 26-30% lignin, and 23-26% hemicellulose. These components are much less in lowland type peat. The total content of hemicellulose and cellulose residues in it is on average about 27.6%, and 12.3% lignin. However, peat contains ~40.2% humic acids, ~15.5% fulvic acids, and ~4.2% bitumen.

The temperature range of torrefaction is from 200°C to 300°C [4]. During torrefaction, most of the hemicellulose and amorphous cellulose decomposes, while crystalline cellulose and lignin undergo less decomposition [5, 6]. The content of low-calorie components decreases and the content of cellulose and lignin increases, the calorific value of which is much higher. As a result of torrefaction, the carbon content increases, which leads to an increase in the heat of combustion of the fuel [7].

Another important aspect of the torrefaction conditions is the oxygen concentration in the reactor. It was found [8] that the presence of a small amount of oxygen has a beneficial effect on the course of the process. During torrefaction biomass loses its fibrous structure, becomes brittle, grinds easily, and does not lose its properties to form granules without auxiliary binders [9]. Due to the destruction of OH groups, the fuel loses its hydrophilicity. This simplifies the conditions for its transportation and storage and provides protection against biological degradation [2]. Torrefaction makes it possible to bring the properties of the fuel as close as possible to the properties of thermal coal and to burn it in pulverized coal boilers [2–4].

The creation of an inert environment complicates and increases the cost of torrefaction technology. Therefore, it is relevant to study the possibility of carrying out the torrefaction process in a gaseous atmosphere, which occurs in a limited volume during the thermal decomposition of organic fuel substances.

Materials and methods

Pellets from a mixture (1:1) of lowland peat and crushed pine wood (composite fuel), 8 mm in diameter and 30-40 mm long, were subjected to torrefaction. Wood pellets were subjected to torrefaction for comparison. The torrefaction took place at atmospheric pressure in a non-hermetic steel cylindrical container with a volume of 0.5 l, which was densely filled with pellets. The

container was placed in a muffle furnace preheated to a given temperature (250°C, 270°C or 290°C). The countdown of the torrefaction time was started after the pellets reached the furnace temperature. The temperature of the furnace and the pellets in the container was measured using thermocouples. The wires of the thermocouples were inserted into the container through a small hole, which simultaneously served as a channel for the exit of excess gases formed during the torrefaction process.

Fuel samples were subjected to thermal analysis in the "Q-1000" derivatograph, in the range of 20-1000°C at a heating rate of 7.4 K/min. Data collection and processing was carried out with the help of the applied computer program "Derivatograph", created at the Institute of Engineering Thermophysics of National Academy of Sciences of Ukraine.

Measurement results and discussion

Pellets of composite fuel acquire a lower degree of decomposition compared to wood pellets under the same conditions of torrefaction due to the different content of biopolymers (Table 1).

Table 1. *Torrefaction conditions and degree of decomposition of granulated fuel.*

Temperature in the furnace, °C	Torrefaction time, min	Degree of decomposition, %	
		Composite	Wood
250	60	14.62	17.06
270	30	17.64	22.98
290	60	37.62	44.64

Thermal destruction of non-torrefied composite fuel begins with the removal of bound water in the range of 20-178°C (Fig. 1). The decomposition of organic substances is accompanied by a sharp change in mass and active gas formation. This process reaches its maximum rate at 324°C. The active phase of gas evolution in composite fuel ends at a lower temperature (375°C) than in wood (387°C). The decomposition of composite fuel is completed at 637°C, and pine wood at 606°C. An endothermic process of thermal dissociation of $CaCO_3$ is observed in the composite fuel in the range of 637-729°C. $CaCO_3$ is present in peat in the form of remains of shells of molluscs.

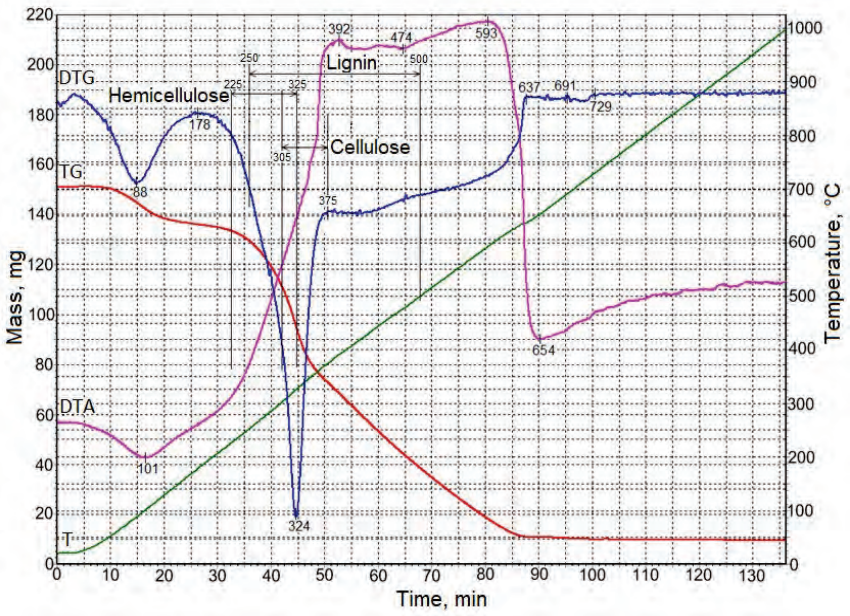

Figure 1. *Derivatogram of non-torrified composite fuel.*

The temperature of the beginning of thermal decomposition of organic substances in composite fuel torrefied at 250°C is higher (205°C) than that in non-torrefied (178°C) and slightly shifts towards higher temperatures (207°C) with an increase in the torrefaction temperature to 290°C (Figs. 2 and 3). The increase in thermal stability is a consequence of the destruction of thermolabile components, primarily hemicellulose.

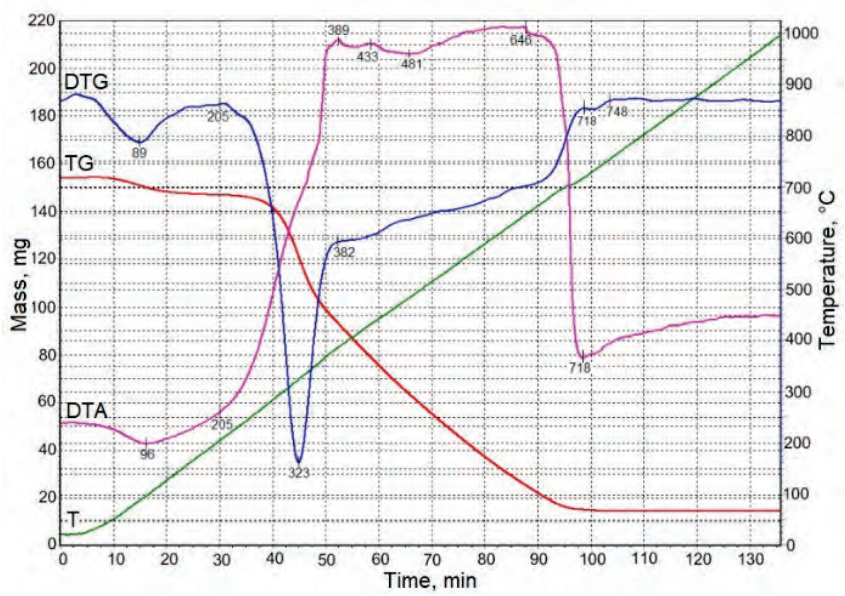

Figure 2. *Derivatogram of composite fuel after torrefaction at 250°C.*

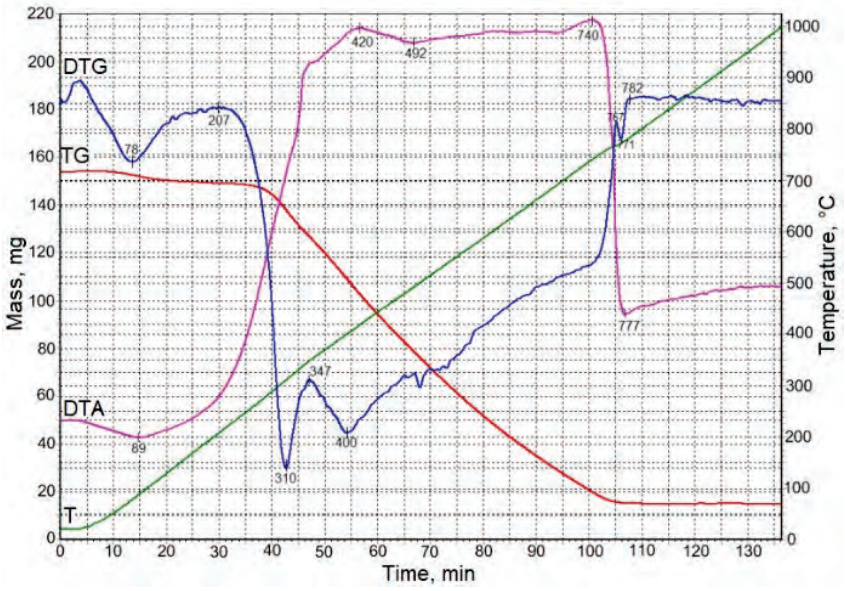

Figure 3. *Derivatogram of composite fuel after torrefaction at 290°C.*

Torrified fuel has a wider temperature range of thermal decomposition. The temperature interval of thermal decomposition of non-torrified composite fuel is in the range of 138-637°C (Fig. 1). Increasing the heat treatment temperature from 250°C to 290°C increases the temperature range of its decomposition from 205-718°C to 207-767°C (Figs. 2 and 3). Extending the range and increasing the thermal decomposition temperature indicates an increase in the carbon content in the fuel.

Torrefaction caused an increase in the hydrophobicity of fuels, which was manifested in a decrease in equilibrium moisture content (Table 2) as a result of the destruction of biopolymers and a decrease in the number of hydrophilic active centers.

The equilibrium moisture content of pellets torrefied at 250°C is more than two times lower than that of non-torrefied ones. Increasing the torrefaction temperature to 290°C leads to deeper changes in the composition and structure of biofuels, which leads to an increase in their hydrophobicity. The equilibrium moisture content of composite fuel pellets is somewhat higher than wood pellets in both non-torrified and torrified states due to the presence of peat.

Table 2. *Thermal characteristics of fuels*

Fuel	Moisture content, %	Ash content, % to DM*	Heat effect, mB·s/mg DM*	Increase in thermal effect, %
Composite fuel pellets				
Non-torrified	9.94	6.92	369.7	–
Torrefied at: 250°C	4.55	9.87	426.8	15.4
270°C	4.60	8.63	442.3	19.6
290°C	3.06	10.01	484.9	31.2
Pine wood pellets				
Non-torrified	7.33	0.76	325.3	–
Torrefied at: 250°C	3.16	1.43	389.1	19.6
270°C	3.20	1.35	413.1	27.0
290°C	2.65	1.84	535.0	64.5
* DM – dry mass				

Ash content of torrefied fuel is higher compared to non-torrefied fuel due to unchanged mineral composition and a decrease in dry mass. A decrease in the dry mass of the fuel also leads to an increase in the ash content in it with an increase in the heat treatment temperature (Table 2).

An estimate of the heat of thermal decomposition showed that the used torrefaction modes cause an increase in the heat of decomposition. Thus, the specific heat of thermal decomposition of torrified composite fuel increases from 15.4% to 31.2% compared to non-torrified fuel with an increase in the torrefaction temperature from 250°C to 290°C. The specific heat of thermal decomposition of wood increases from 19.6% to 65.4% under the same conditions of torrefaction (Table 2).

The decrease in the thermal effect of decomposition for composite fuel is associated with peat, the torrefaction conditions of which still need to be studied. Considering that the thermal decomposition of biofuels in the derivatograph takes place in the air atmosphere, there is a direct relationship between the specific heat of thermal decomposition and the calorific value of the fuel.

The time of heat treatment affects the results of torrefaction. It can be seen from the thermal analysis data (Tables 1 and 2) that heat treatment at 270°C for 30 min is insufficient. The obtained results on the degree of decomposition, equilibrium moisture, ash content and heat of decomposition are either worse or the same as for fuel torrefied at 250°C for 60 min.

Torrified fuels have the properties of a brittle solid. They are easily crushed to a powdery state, which is the key to effective dispersion in ball or hammer mills of power plants.

Conclusions

Thermal analysis of torrefied pellets made from a mixture (1:1) of pine wood with lowland peat and pine wood showed that the degree of their decomposition directly depends on the temperature and time of heat treatment.

The specific heat of thermal decomposition of torrefied biofuels depends on the degree of decomposition of fuels. Pine wood pellets showed 2 times increase in the specific heat of decomposition compared to composite fuel pellets under equal torrefaction conditions. This fact requires future studies of peat torrefaction conditions.

Biofuel significantly loses its hydrophilic properties as a result of heat treatment. This is manifested in a decrease in its equilibrium moisture. Ash content of torrefied fuel increases due to a decrease in dry mass.

Studies of the method of torrefaction of biofuels at atmospheric pressure in a gaseous environment formed during the partial thermal decomposition of organic substances have shown its effectiveness and the possibility of application without the use of inert gases.

References

[1] Mykhailyk V.A., Snezhkin Yu.F., Korinchuk D.M. (2014), *Termichne rozkladannia hranul palyva na osnovi torfu ta derevyny*. Promyslova teplotekhnika. 36(2), pp. 11-19.

[2] Tumuluru J.S., Sokhansanj S., Hess J.R., Wright C.T, Boardman R.D. (2011), *A review on biomass torrefaction process and product properties for energy applications*. Industrial Biotechnology. 7(5), pp. 384-401, https://doi.org/10.1089/ind.2011.7.384.

[3] Granados Morales D. (2017), *Studies of the Torrefaction of Sugarcane Bagasse and Poplar Wood, thesis*. Universidad Nacional de Colombia, Sede Medellín Facultad de Minas, Escuela de Procesos y Energía.

[4] Bergman P.C.A., Boersma A.R., Zwart R.W.R, Kiel J.H.A. (2005), *Torrefaction for biomass co-firing in existing coal-fired power stations "Biocoal*", Report ECN-C-05-013. Petten, The Netherlands, Energy Research Center of the Netherlands.

[5] Shafizadeh F. (1985), *Pyrolytic reactions and products of biomass*, in: Overend R.P., Milne T.A., Mudge L.K. (Eds.), Fundamentals of Biomass Thermochemical Conversion: Elsevier, London, pp. 183-217.

[6] Ciolkosz D., Wallace R. (2011), *A review of torrefaction for bioenergy feedstock production*. Biofuels, Bioprod. Bioref. 5, pp. 317-329, https://doi.org/10.1002/bbb.275.

[7] Muafah A.A., Khalik M.S., Yoshimitsu U., Lukman I.A. (2012), *Study on Torrefaction of Oil Palm Biomass*. Journal of Applied Sciences. 12(11), pp. 1130-1135, https://dx.doi.org/10.3923/jas.2012.1130.1135.

[8] Basu P. (2013), *Torrefaction*, in: Basu P. (Ed.), Biomass Gasification, Pyrolysis and Torrefaction, second ed. Academic Press, Boston, pp. 87-145, https://doi.org/10.1016/B978-0-12-396488-5.00004-6.

[9] Phanphanich M., Mani S. (2011), *Impact of torrefaction on the grindability and fuel characteristics of forest biomass*. Bioresource Technology. 102, pp. 1246-1253, https://doi.org/10.1016/j.biortech.2010.08.028.

COMPARATIVE COMPUTATIONAL ANALYSIS OF THE SELECTION OF BATTERY ENERGY STORAGE FOR CIVIL OBJECTS AND PARKING WITH PHOTOVOLTAIC PLANTS

Petro Zinkevych, Serhii Baliuta, Iuliia Kuievda

National University of Food Technologies, 68 Volodymyrska str., 01601 Kyiv, Ukraine
e-mail: petrozinkevich@gmail.com

Introduction

Energy production from PPS has a number of advantages and disadvantages. One of the disadvantages is that PPS does not produce electricity at night, so they cannot support the load of consumers. To solve the problem of stability of electricity supply at night battery energy storage (BES) are used [1]. BES in combination with a solar power plant is called a battery energy storage system (BESS). This system absorbs and releases energy in different periods. There is no doubt that the additional investment and operating costs of BESS will affect the cost-effectiveness of the PPS.

Materials and Methods

In this study, the selection of the BES and the simulation of the operation modes of the PPS, which is installed on the roof of civil facilities and a parking lot, are carried out. The system consists of PPS, charge controller, inverter and BES. SAM software was used for research.

The structural diagram of the power supply system with PPS and BES is shown in Figure 1.

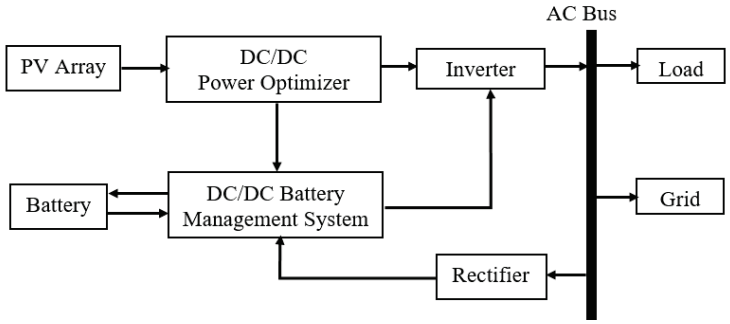

Figure 1. *Model of BESS [2].*

The principle of operation of BESS is that the energy produced in the PPS charges the BES, and then, when there is no solar insolation, the storage is discharged. At the same time, energy can be used to supply electricity to public housing facilities (parking lots) or can be fed into the electrical grid [3].

The selection of an EE storage unit for an existing PPS involves the following stages:

1. Determining the load capacity of public transport facilities (parking lots).
2. Based on the data on the installed capacity of the PPS, the forecast of the annual EE generation.
3. Calculation of the peak annual load in the SAM software.
4. Calculation of the power and capacity of the BES based on the peak annual load.
5. Choice of BES type: lead-acid or lithium-ion.
6. Selection of the mode of use of the BES.
7. Modeling of BESS operating modes in the SAM software to determine the value of the generated energy of the PPS and evaluate the efficiency of using the BES.

8. Economic analysis and evaluation of the economic performance of the hybrid system using the SAM software, taking into account the daily, monthly and annual volumes of electricity generated by the PPS, BES data and electricity consumed by the facility.

Results and Discussions

It was calculated studies of efficiency using BES for power supply of objects using PPS were carried out. The research objects are located in the city of Kyiv (latitude: 50.4; longitude: 30.45).

Using the calculated parameters of the peak load, the capacity of the BES is determined. The storage was selected taking into account the condition that the peak load should be less than the nominal power of the PPS. A Vipow lithium-ion (lithium-iron-phosphate) battery with a capacity of 50 Ah and a voltage of 3.2 V was selected for the designed PPS. For each object of research using the SAM software, the selection of the choice of BES, the time of operation at maximum power and the capacity BES.

With the use of SAM software, the following modes of operation of the BES were simulated by programming the drive dispatch controller:

1. Mode 1: BES charge during the day, feeds the load in the evening.
2. Mode 2: At night (11:00 p.m. – 7:00 a.m.) it does BES fully charge from the power grid (low electricity tariff), in the morning (7:00 a.m. – 8:00 a.m.) it gives electricity to the electric grid, and then charges from the PPS.

Such working periods are BES defined:

Period 1. All energy from the PPS is directed to battery charging.

Period 2. Discharge of BES and power supply of consumers.

Period 3. Charging of the battery from the electrical grid and subsequent return of energy from the BES to the electrical grid.

It was calculated parameters of BESS, an economic assessment of projects of electricity supply of research objects with the use of PPS was performed.

Analyzing the final data, the results showed that the project with the use of PES for power supply of the parking lot in mode 1 for A4 with a payback period of 10.5 years has the greatest economic efficiency. For civilian objects, the most effective project is the residential building B4-19 with a payback period of 11.3 years and a cost of 219,431 dollars.

Conclusions

1. For the most efficient use of the power supply system with PPS and storage throughout the year, it is advisable to use mode 1, which involves charging the BES during the day, and feeding the load in the evening.
2. Mode 2 should be used to cover the load only during the spring-winter-autumn period, when the generation electricity from the FES is not sufficient.

References

[1] Salkuti S.R., *Comparative analysis of storage techniques for a grid with renewable energy sources*. Salkuti S.R., Chan M.J., International Journal of Engineering and Technology 2018, Vol. 7, Iss. 3, pp. 970-976.

[2] Pirthi T., *Performance analysis of pv and bess based hybrid system for residential load volume*. Pirthi T., Tanu P., International Journal of Current Engineering and Scientific Research 2020, Vol. 7, Iss. 3, pp. 18-22.

[3] Feisal A., *Application of behind the meter battery storage system integrated with net metering in Indonesia*. Feisal A., Sudiarto B., Setiabudy R., IOP Conference Series: Earth and Environmental Science 2020, pp. 1-6.

FORMATION OF RISK PROFILE FOR THE INTEGRATION OF RENEWABLE ENERGY SOURCES INTO THE ELECTRICITY SUPPLY SYSTEM

Anatolii Zamulko, Yurii Veremiichuk, Vitalii Stepanenko

National Technical University of Ukrain Igor Sikorsky Kyiv Polytechnic Institute,
37 Peremogy avenue, Kyiv, Ukraine
e-mail: y.veremiichuk@kpi.ua

Ensuring reliable, stable and efficient operation of electricity distribution networks is becoming increasingly challenging. The reason for this is the uncontrolled increase in the number of renewable energy sources (RES), in particular solar power plants (SPP), connected to distribution networks.

The growing number of renewable energy sources causes a variety of risks of their integration into power grids, in particular regarding the organization of planning, operation and management of power grids. The negative consequences of such integration are the deterioration of the quality of electricity, the need for unscheduled modernization of power grids, the occurrence of higher harmonics and an increase in the volume of reactive power flow, as well as the introduction of non-market methods for using the constraint management system [1].

Therefore, there are issues of finding the optimal location of RES capacities with the necessary technical characteristics. At the same time, the determining factors should be not only the climatic factors of RES location, but also the operating parameters of the power grid at the point of connection. The solution to this problem can be realized through the use of risk management methodology.

The risk of RES integration is understood as an event, or condition or state that may or may not occur in the future and adversely affect the effectiveness of RES as a set of desired results achieved by the successful integration of RES into the electricity supply system. The emergence of possible risks is due to the presence of causes (processes or phenomena) that contribute to their occurrence and explain why the risk is inevitable. Such phenomena are called risk factors.

The fundamental issue in solving the problem is to ensure the simultaneous consideration of a set of risk factors. Thus, there is a question of forming a risk profile of RES integration into the power grid, which is considered as a description of a set of risk indicators (criteria with predefined parameters), which is the result of collecting, analyzing and systematizing information.

The formation of a risk profile for the integration of RES into the electricity supply system can be organized in several stages:

Stage 1. Definition of risk indicators.
This stage is based on the analysis, identification and assessment of risks, also with the use of information technologies, and includes: 1) identification of conditions and factors that affect the occurrence of risks; 2) identification of risk areas; 3) identification of risk indicators; 4) assessment of the probability of risks and possible damage in a case of their occurrence.

Stage 2. Formalization of the risk profile.
The following parameters can be used as primary risk indicators:

- indicators of the quality of electricity at the border of the balance sheet between the distribution system operator and the consumer. These indicators under normal operating conditions must comply with the parameters specified in DSTU EN 50160:2014 [2];
- characteristics of power supply voltage and their normalized values;
- indicators of power supply reliability.

Indicators that can be used in the formation of a risk profile have different origins and different procedures are used to obtain them. Thus, the risk assessment procedure is often implemented in a poorly formalized environment [3].

Stage 3. Determination of the algorithm for calculating the degree of risk according to the risk profile and, depending on the degree of risk, of adequate measures necessary to prevent or minimize risks, if the need to determine such measures is provided for by the risk profile.

Within the framework of the study, it is determined that fuzzy logic algorithms are one of the most acceptable for solving the problems of modeling risk avoidance in the integration of renewable energy sources into the power supply system. Here are the main advantages of using the fuzzy logic model [4]:

– fuzzy logic methods make it possible to qualitatively, verbally describe risk factors by introducing the concepts of linguistic variables, the meaning of which is clear to the expert, which are determined not by numbers, but by fuzzy concepts;
– the use of fuzzy sets allows formalizing more flexible relationships between the factors of each of the studied risks, which is more consistent with the nature of the studied real interactions in the power industry, in particular in the power supply system;
– fuzzy methods make it possible to make decisions under conditions of incomplete information by synthesizing and analyzing qualitative values, what is important for making a generalized decision when connecting RES to the power supply system.

Stage 4. Generalization of risk analysis results and formation of risk management system at strategic, tactical and operational levels.

At the same time, at the strategic level of risk management, priority areas for the development and implementation of risk management measures are determined, at the tactical level – specific (actual) risk management measures are developed, and at the operational level – appropriate (approved) risk management tools are applied.

Practical implementation

To form a profile of risks arising from the integration of RES into the grid, modelling was carried out using fuzzy logic methods in the MATLAB environment.

To describe the set of risk indicators, we used the number of factors that directly reflect the problem of effective integration of RES into the electricity system. This category includes the following factors: higher harmonics (*Ku*), voltage deviation from *Un* (ΔU) and reactive power flow ($\cos\varphi$).

According to the algorithm, the selected factors were analyzed and a scale for evaluating linguistic variables was formed. For each output indicator, we propose to use three term sets of linguistic variables: "low", "medium" and "high" (Table 1).

Table 1. *Scale for evaluating linguistic variables*

Factors			Range	Scale for evaluating indicators		
				low (L)	medium (M)	high (H)
Higher harmonics	*Ku*	%	0-10	0.9-0.94	0.92-0.98	0.96-1.0
		Rel. unit	0.9-1			
Voltage deviation from *Un*	ΔU	%	±15 (196-264 V)	0.85-0.91	0.88-0.97	0.94-1.0
		Rel. unit	0.85-1.0			
Reactive power flow	$\cos\varphi$		0.75-1.0	0.75-0.85	0.8-0.95	0.9-1.0

Using the functionality of the selected software, it is possible to obtain the output surface of our system, that is, the entire possible range of the integration index based on the range of the input set of risk factors (Fig. 1).

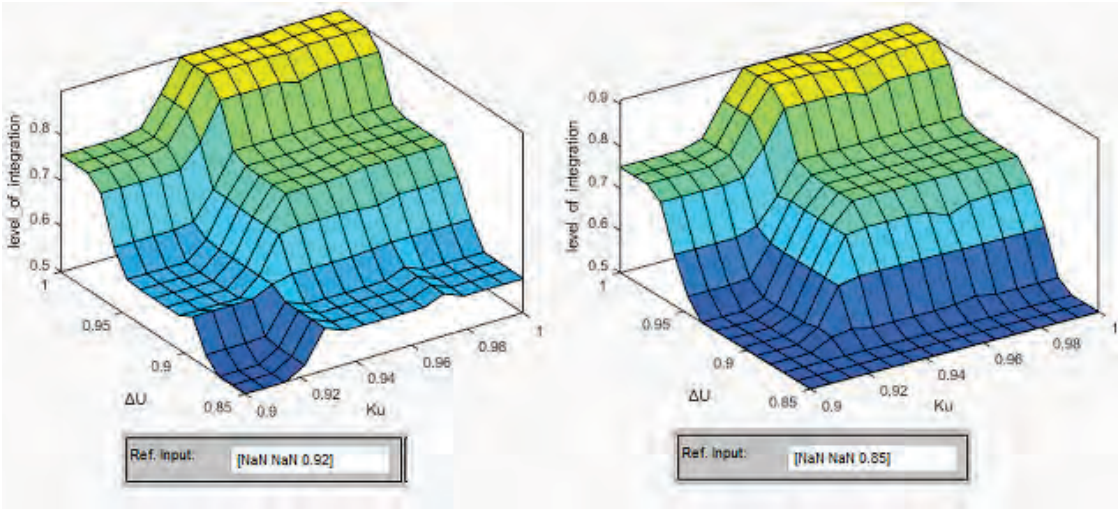

a) b)

Figure 1. *The surface of the fuzzy conclusion at the input parameters ΔU, Ku at cosφ = 0.92 (a) and cosφ = 0.85 (b).*

Thus, we have formed a risk profile of RES integration into the power grid based on such factors as higher harmonics, voltage deviation from *Un* and reactive power flow. The resulting model makes it possible to visually assess the probabilities of the situation, which may lead to the connection of the relevant RES installation to the power grid; and to decide on the feasibility of such connection.

Conclusions

In the course of the study, the concept of "risk profile of RES integration into the power grid" was defined, the stages of risk profile formation were proposed. The Mamdani fuzzy logic algorithm was used for a comprehensive assessment of risk profile formation and planning of possible solutions.

The obtained results provide an opportunity to develop a methodology for the controlled and efficient development of renewable energy and to determine the appropriate requirements for the parameters of the electrical installation in accordance with the formed risk profile at the stage of connection to the power supply system.

References

[1] Stepanenko V., Zamulko A., Veremiichuk Y., Nakhodov V., *Assessment of risk for the integration of renewable energy sources into the electricity supply system*. POWER ENGINEERING: economics, technique, ecology. 2022. No. 2, pp. 64-74. ISSN 1813-5420 (Print). URL: http://energy.kpi.ua/article/view/261372.

[2] DSTU EN 50160: 2014 Characteristics of power supply voltage in general purpose electrical networks (EN 50160:2010, IDT).

[3] Zadeh L.A., Aliev R.A., *Fuzzy Logic Theory and Applications*, World Scientific, Singapore, 2018.

[4] Zamulko, A. Veremiichuk Y., *Evaluation of efficient usage of methods of the electric power consumption control under the conditions of uncertainty*. Visnyk of Vinnytsia Polytechnical Institute" #2, pp. 16-21. URL: https://visnyk.vntu.edu.ua/index.php/visnyk/article/view/1097.

THERMODYNAMIC ANALYSIS OF THERMAL DESALINATION SYSTEM WITH OPEN AND CLOSE AIR CYCLE

Volodymyr Sereda, Andrii Solomakha, Natalia Prytula, Nazar Shvets

National Technical University of Ukraine «Igor Sikorsky Kyiv Polytechnic Institute»,
37 Prospekt, Kyiv, 03056, Ukraine

Introduction

The demand for clean drinking water is growing both in Europe and the whole world due to the population growth, the increased rate of urbanization, industrialization, agricultural activity and social and economic development [1]. The potential technical solutions to solve water scarcity are: water reuse, desalination, saving water, increasing productivity in agriculture and industry, reducing leakages in public water supply, using brackish water, wastewater, seawater [2, 3].

Membrans and thermal humidification-dehumidification (HDH) process are most often used for small scale fresh water production [4]. Advantages of the HDH process: the possibility of operation due to the use of renewable and low-temperature energy; simple installation and low operating cost. In spite of significant benefits of this technology, it has a key drawback – high thermal energy consumption [5]. In this study, the authors aim to develop a mathematical model for the cycle of air humidification-dehumidification, to carry out a thermodynamic analysis of a thermal desalination system based on salt water heating in an intermediate heater and to determine the system operation conditions to obtain the maximum performance with minimum energy consumption.

Methods

The diagram of the desalination system based on the working principle of open air – close water with water heating (OAOW-WH) is shown in Figure 1.

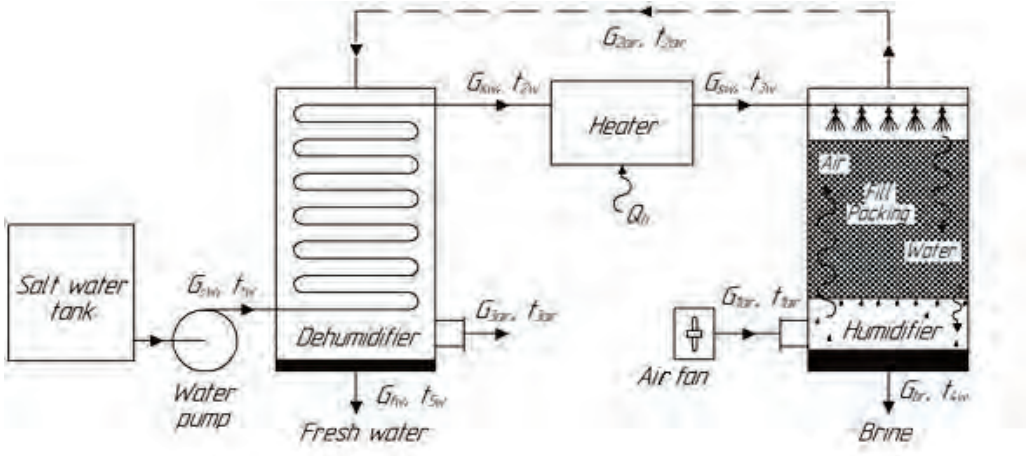

Figure 1. *Desalination system working on the air humidification-dehumidification principle (OAOW-WH).*

Air and salt water move in the open circuits. Salt water is pumped to the dehumidifier at the temperature t_{1w}. Then, the salt water circulates through the dehumidifier tubes, being heated up to the temperature t_{2w} removing heat from the saturated air, which is dried by cooling in the tube space of the dehumidifier. Ambient air with the temperature t_{1air} and humidity d_{1air} is supplied to the humidifier by the fan. In the humidifier, the air is heated to the temperature t_{2air} and humidified

by direct contact with the salt water heated in a heater up to the temperature t_{3w}. Hot water is sprayed through the nozzles for efficient heat and mass transfer. Some of the water evaporates into the air, while the rest is released as a brine into the lower part of the dehumidifier. At the outlet of the humidifier, the air humidity can reach 100%. Next, the saturated air is supplied to the dehumidifier, where water vapor condenses from the air to produce fresh water. Cooled air with the temperature t_{3air} is removed to the atmosphere.

System shown in Figure 1 can work according to the scheme of closed air – open water (CAOW-WH). In this case, the air will move along a closed circuit (it will not be released into the atmosphere). Air thermodynamic properties at the entrance to the humidifier and at the exit from the dehumidifier will be the same.

The desalination system model is a theoretical model developed on the basis of mass and energy balances applied to each of the cycle components, following the laws of thermodynamics [6] with subsequent thermodynamic analysis. The model is calculated with the help of PTC Mathcad engineering software, using CoolProp package to determine the properties of moist air and salt water [7]. The following parameters are then calculated:

1. Gain output ratio (GOR) is the main indicator of the desalination system performance evaluation. It shows how much heat energy is consumed in the desalination process. It numerically equals the ratio of fresh water mass flow rate (G_{fw}), multiplied by the latent heat of vaporization (r), to the thermal energy supplied during the cycle (Q_h):

$$\mathrm{GOR} = G_{fw} r / Q_h \tag{1}$$

2. Recovery ratio (RR) is the ratio of fresh water mass flow rate obtained in the system to the salt water consumption (G_{sw}):

$$\mathrm{RR} = G_{fw} / G_{sw} \tag{2}$$

3. Mass flow rate ratio (MR) is the ratio of the salt water mass flow rate to the mass flow rate of the input air (G_{1air}):

$$\mathrm{MR} = G_{sw} / G_{1air} \tag{3}$$

Results

The effect of salt water temperatures at the inlet and outlet of the dehumidifier on the main parameters of the desalination system is shown in Figures 2 and 3. GOR increases along with increasing salt water temperature at the dehumidifier outlet. In addition, for the same t_{2w}, the value of GOR is higher at the lower t_{1w}. The values of GOR and RR do not depend on the method of air circulation and change according to the laws established in [8].

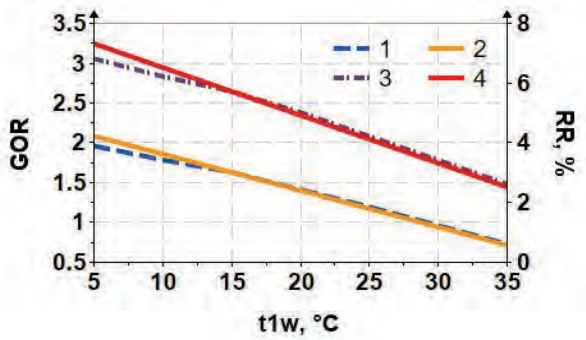

Figure 2. *Dependence of GOR and RR on t_{1w}: 1 – GOR for CAOW; 2 – GOR for OAOW; 3 – RR for CAOW; 4 – RR for OAOW.*

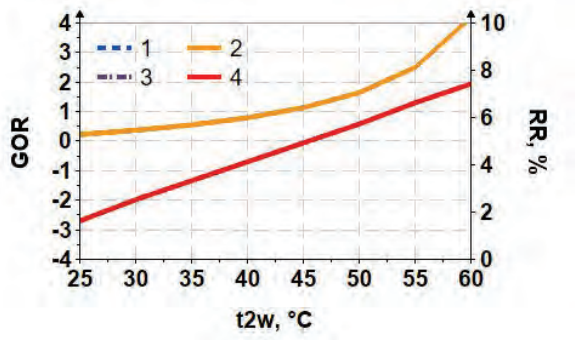

Figure 3. *Dependence of GOR and RR on t_{2w}: 1 – GOR for CAOW; 2 – GOR for OAOW; 3 – RR for CAOW; 4 – RR for OAOW.*

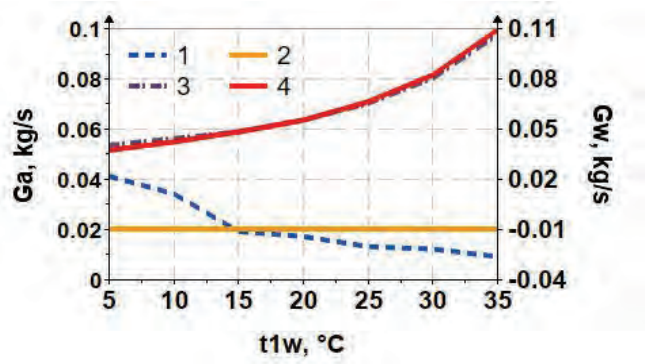

Figure 4. *Dependence of G_a and G_w on t_{1w}: 1 – G_a for CAOW; 2 – G_a for OAOW; 3 – G_w for CAOW; 4 – G_w for OAOW.*

As we can see in Figure 4 at $t_{1w} \approx 15$°C, the air flow rate for both schemes is the same. Below this value, it is better to use an OAOW-WH scheme (lower air flow rate, and therefore lower electricity consumption on the fan; higher efficiency of the humidifier, correspondingly smaller geometric dimensions of the heat exchanger). Accordingly, the values of GOR and RR will be slightly higher (see Fig. 2). If value of t_{1w} is more than 15°C, it is more profitable to use a CAOW-WH scheme.

Conclusions

The main factors limiting further increase in GOR and RR are the limitations of the maximum values of t_{3w} and Δt_{sw}. This necessitates the use of a heater with external heat supply in the cycle.

The difference between a CAOW-WH and OAOW-WH scheme is in the "hard" fixation of air temperature and humidity at the inlet and outlet of the heat exchangers in the case of closed air circulation. As a result, in order to obtain maximum performance in a closed circuit, it is necessary to regulate the air flow in case of changes in the temperature of salt water at the inlet and outlet of the dehumidifier. This leads both to a sharp change in the efficiency of the heat exchangers and to an increase in the air temperature in them.

It is advisable to use an OAOW-WH scheme in case of a change in the temperature of the incoming water up to 15°C. At higher temperatures, the use of CAOW-WH becomes effective.

The most effective way to increase GOR is to use the renewable energy sources (sun, recycled heat, etc.) to heat salt water in the heater. This solution will significantly reduce the cost of thermal energy in the heater and increase the system efficiency (GOR).

References

[1] Nature-based solutions for water. UNESCO, Paris, France, 2018 [Electronic resource]. Access mode, https://unesdoc.unesco.org/ark:/48223/pf0000261424.

[2] Dhakal N., Salinas-Rodriguez S., Hamdani J., Abushaban A., Sawalha H., Schippers J., Kennedy M., *Is desalination a solution to freshwater scarcity in developing countries*. Membranes. 2022, 12, 381. https://doi.org/10.3390/ membranes12040381.

[3] The Problems of Water Stress [Electronic resource], Access mode, https://www.eea.europa.eu/ publications/92-9167-025-1/page003.html.

[4] Subrumani A., Jacangelo G., *Emerging desalination technologies for water treatment: a critical review*. Water Research, 2015, Vol. 75, pp. 164-187.

[5] Mohamed A. et al., *Desalination process using humidification – dehumidification technique: a detailed review.* Int. J. Energy Res., 2020, Vol. 45, No. 3, pp. 3698-3749.

[6] Kudelia P., Dubovskyi S., *Energy and exergy approaches to problem of rational energy use.* Enerhetyka: ekonomika, tekhnolohii, ekolohiia, 2020, Vol. 2, pp. 7-16.

[7] *C++ library of properties for 122 components*, CoolProp.org. [Electronic resource], Access mode, http://www.coolprop.org.

[8] Sereda V., Solomakha A., Prytula N., Zabolotny O., *Thermodynamic analysis of thermal desalination system with humidification–dehumidification cycle*, KPI Science News, No. 4, pp. 105-112, 2021, https://doi.org/10.20535/kpisn.2021.4.250663.

FAST SYNTHESIS OF GAS HYDRATES

Anatoliy Pavlenko[1], Hanna Koshlak[1], Borys Basok[2]

[1]Kielce University of Technology, al. Tysiąclecia Państwa Polskiego 7, 25-314 Kielce, Poland
e-mail: apavlenko@tu.kielce.pl

[2]Institute of Engineering Thermophysics of National Academy of Sciences of Ukraine
2a, Marii Kapnist Str., Kyiv, 03057, Ukraine

Global demand for energy resources is expected to increase significantly in the coming decades and although the share of renewable energy in the overall balance is steadily growing, the amount of energy generated may still be far from enough to meet the high energy demand.

By 2040 more than 76% of energy is predicted to be generated from carbon-based sources (gas, oil and coal). Among these, demand for natural gas will increase at the highest rate (up to 2% per year). However, we should also expect CO_2 emissions to worsen.

Nearly 80% of the world's natural gas consumption is met by conventional sources, while unconventional sources such as tight gas, shale gas, and coal bed methane have become increasingly common in recent years. Gas hydrates are a very promising source of natural gas, with an energy resource several times greater than all proven deposits of carbon fuels. Therefore, technologies of gas extraction from natural gas hydrates are currently of great interest to researchers all over the world. In this paper we propose a new fast gas synthesis, such as mine methane, natural gas and CO_2, which can be used to form gas hydrate blocks and their subsequent storage or transportation. CO_2 hydrate can be safely buried at fuel extraction sites. We also propose a theoretical framework to assess stability of gas hydrates фтв apply to the development of technologies for gas extraction from natural hydrate deposits. The paper analyses thermodynamic conditions in fast synthesis of hydrates and proposes an optimization criterion for thermodynamic and heat and mass transfer parameters for effective implementation of a new fast synthesis technology.

U USE OF GROUND ACCUMULATORS FOR MUNICIPAL HEAT SUPPLY

Borys Basok, Tetyana Belyaeva, Maryna Khybyna

Institute of Engineering Thermophysics of the National Academy of Science of Ukraine

Environmental and energy problems of our time require the need for a transition to environmentally friendly waste-free and low-temperature technologies. Solar radiation is a universally available environmentally friendly energy resource that meets these requirements. For municipal thermal power engineering, this is the use of solar radiation for heat supply to buildings. The difficulty lies in the fact that the greatest intensity of solar radiation falls on the warm season, and the maximum need for warmth – on the cold period. The only way out is to accumulate excess solar energy during the warm period with its subsequent use during the heating period.

Municipal thermal power stations (TPS) operate at nominal capacity only during the heating season. After the end of the heating season, due to a significant decrease in heat consumption, problems arise in the rational use of heat produced by municipal TPS. The problem of excess heat can be solved by accumulating it for the purpose of further use during the heating season.

When extracting heat from the accumulator, the required temperature is maintained by heat pumps. Thus, an interacting technological system arises: "TPS – accumulator – heat pump", the operation of which must be mutually coordinated.ts.

For a number of years, ITTF NAS of Ukraine has been conducting research on the organization of a thermal accumulator in a natural soil massif. The method of organizing a ground accumulator, developed under the guidance of Professor A.I. Nakorchevsky, is based on an analysis of the joint operation of a system of ground heat exchangers and methods that reduce the temperature difference between the coolant and the ground mass and prevent the expansion of the accumulation area [1, 2].

Accumulators of large thermal capacity are organized in a natural ground massif by a system of vertical heat exchangers located in wells. As a result of accumulation, a main area with a volume V_0 with the highest temperature T_0, conditionally limited by the external contour of the heat exchanger system, and a buffer area are created. It is formed as a result of thermal interaction of the main area with the surrounding soil massif with temperature T_m = const. The temperature in the buffer region varies from T_0 to T_m. The accumulation efficiency increases with a decrease in the size of the buffer region and a uniform temperature distribution over the volume of the main region. This is achieved by using the same type of heat exchangers with the same heat load, constant step L of their location in the system, the same potential of the intermediate heat carrier and a small difference in its temperatures $T_w = \left(T_{w.in} - T_{w.out}\right) \sim 1$°C, respectively, at the inlet and outlet of each heat exchanger and a number of other reqвuirements. An extremum study of the ratio of the volume of the buffer area to the volume of the main one found that the minimum corresponds to the cubic shape of the main accumulation area ($X = Y = Z$) [3].

The size of the buffer area can be reduced when creating the top heat shield layer. At the same time, the depth of drilling of wells decreases and there is no need to insulate the inlet and outlet pipelines. The cost of building a foam concrete shield with a thickness of 0.1-0.3 m is much less than the cost of drilling. Calculations have shown that the heat loss through the shield for the year will not exceed 1% [2]. When creating the upper heat-insulating shield and the cubic shape of the main area, the optimal ratios are as follows: $X = Y$; $Z = 0.5\,X$; where: X, Y – length and width of the main area, Z its height. The volume of the accumuator with a shield is determined by the dependence:

$$V = V_o + V_b = S_o \cdot Z + \left(P_o \cdot Z + S_o\right) \cdot R_b + \pi\left(Z + 0.25P_o\right) \cdot R_b^2 + 0.667\pi R_b^3 \quad (1)$$

where: $S_o = XY = X^2$; $P_o = 2\left(X + Y\right) = 4X$; $V_o = S_o Z$; $Z = 0,5X$.

The linear size of the buffer area changes with time:

$$R_s = \sqrt{24a_m t} \quad (2)$$

The "thermal volume" of the accumuator is determined taking into account the temperature distribution in the buffer area:

$$E_a = E_o + E_b = V_o + 0,4(P_o \cdot Z + S_o) \cdot R_s + 0,2\pi(Z + 0,25P_o) \cdot R_s^2 + 0,0762\pi R_s^3 \quad (3)$$

The energy accumulated during the summer period can be written as:

$$E_a = N\tau_a \quad (4)$$

where N is storage power related to the characteristics of heat exchangers by the equation:

$$N = q_0 2\pi R_0 k_a Z \quad (5)$$

where: q_0 – heat flux density on the outer surface of the heat exchanger with radius R_0; k_a – the number of "efficiently" working heat exchangers, is determined by the size of the heat exchange surface with the heat flow directed inside the main accumulation area. To avoid large temperature differences between the intermediate heat carrier and the main storage area, q_0 = 100 W/m^2. Given q_0 equation (5) is transformed into a relation connecting k_a and R_0:

$$k_a R_0 = \frac{N}{2\pi Z q_0} \quad (6)$$

$$m = \sqrt{k_a} + 1, \quad k = m^2, \quad L = \frac{X}{m-1} \quad (7)$$

where: m – number of heat exchangers on the linear dimension; X, k – total number of heat exchangers in the accumulator; L – step between the heat exchangers. By changing the values of k_a and R_0, it is possible to determine the optimal values of the quantities presented in (7). Thus, relations (4)-(7) determine the parameters of a soil accumulator with a given capacity.

During accumulation, the temperature $T_0(t)$ will increase from the initial temperature of the soil massif T_m to some value $T_{0,\max}$, and then, when discharging, $T_0(t)$ will decrease to the initial value T_m with the full extraction of the accumulated energy. The temperature of the intermediate heat carrier T_w changes in a similar way, which, when the battery is discharged, is determined by some function descending in time:

$$T_w = T_{w.p}\varphi(t) \quad (8)$$

where $T_{w.p}$ is the value of T_w at the beginning of the discharge. The intermediate coolant, which extracts heat from the accumulator, enters the heat pump evaporator. Typically, heating networks operate with a constant heat load and require a constant operating temperature. Thus, the operation of the heat pump must meet condition (8) and the requirements:

$$G = \rho_1 \dot{V}_1 = \text{const}, \quad T_2 = \text{const} \tag{9}$$

where: G – mass flow rate of the working fluid of the heat pump; ρ_1 – density of the working fluid; V_1 – volume flow rate of the working fluid of the compressor on the evaporator side. It is assumed that due to the low thermal resistances of the heat pump heat exchangers, the temperatures on both sides of the heat exchange surface are practically the same $(T_{w1} \approx T_1; T_{w2} \approx T_2)$, in the indices, the number 1 indicates the parameters in the evaporator, the number 2 indicates the parameters in the condenser. We assume that the thermophysical characteristics of the working fluid in the evaporator and condenser meet the saturation conditions.

Then, respectively:

$$\rho_1 = \frac{G}{V_1(t)} = \frac{\rho_1}{RT_1}; \ \rho_1 = \psi(T_1); \ \rho_2 = \psi(T_2) = \text{const} \tag{10}$$

where R is gas constant of the working fluid of the heat pump. Therefore, the volumetric efficiency of the compressor should change as:

$$\dot{V}_1(t) = \frac{G}{\rho_1(t)} = \frac{GRT_1(t)}{p_1(t)} \tag{11}$$

fulfillment of conditions (7), (9), (10) can be easily implemented in a piston-type compressor with a variable engine speed $n(t)$:

$$n(t) = \frac{G}{\rho_1(t)\xi S l} \tag{12}$$

where: ξ – transmission coefficient; S – piston area; l – stroke length. The constancy of the pressure in the condensation chamber p_2 is maintained almost automatically by the discharge valve. The theoretical power used to compress the gas is defined as:

$$N_T = \frac{m}{m-1} GR(T_2 - T_1) \tag{13}$$

where m is polytropic index. Taking into account the effective efficiency heat pump, taking into account the energy losses due to friction in the compressor, in the drive and the deviation of the process from the theoretical one, the required power will be [1]:

$$N_{TH} = 1.852 \frac{T_2 - T_1}{T_2 + 273} N \tag{14}$$

where N is power taken from the ground accumulator.

The calculation of the annual cycle of operation of the system "TPS – ground accumulator – heat pump" with a thermal power of $N = 1.16 \cdot 10^6$ W was carried out. The maximum temperature of the hot heat carrier was assumed to be 96°C. The parameters of the ground accumulator were as follows: soil – clay (λ = 0.8 W/(m·K), $\rho_m c_m$ = $1.512 \cdot 10^6$ J/(m^{3}K)); geometric dimensions of the heat exchanger – Z = 120 m, R_0 = 0,15 m, step L = 1.6 m.

It was obtained that the total number of heat exchangers in the system will be k = 240, the number of operating heat exchangers during accumulation k_a = 210, during extraction – k_p = 184,

the size of the area occupied by the heat exchangers – $L_m \times L_n = 24 \times 22.4$ m^2, the volume of the main area storage V_0 = 0.645·105 m^3, the volume of the buffer area at the end of accumulation (τ = 180 days) $V_{b.a}$ = 0.259·10^6 m^3, the volume of heat-insulating plates V_{iz} = 497 m^3 (blocks of perlite sand with a thickness of δ = 0.3 m, λ = 0.05 W/(m·K). The heat flux density on the outer surface of the heat exchangers during accumulation q_{0a} = 48.8 W/m^2, during discharging q_{0p} = 56.4 W/m^2. During accumulation, the accumulated energy monotonically increases and reaches the value of E_a = 0.18·10^{14} J on the 180th day. At the same time, the ground temperature in the main accumulation area is $T_{e,\max}$ = 88°C, the coolant temperature is T_{w1} = 95.4°C, the linear size of the buffer area is $R_{b.a}$ = 14.1 m. When heat is extracted (accumulator is discharged), the functions T_0 and T_{w1} change to the opposite: now T_{w1} is less than T_0. We assume that the constant temperature of the network heat carrier is maintained by the heat pump, for example, $T_{w2} = T_{TH}$ = 80°C, then the amount of energy E_{TH} supplied to the pump from an external source on the 180th day of discharging will be 23.3% of E_a. During the calculation, the energy losses through the upper insulating shield were controlled, and they did not exceed 0.6% of E_a. Final value $R_{b.r}$ = 19.9 m.

Let us consider one more case of efficient use of ground heat storage for heating and hot water supply of a village of several thousand inhabitants [4].

In such a village, there is usually a school or village stadium. The territory of a football field of about 100×100 m^2 can be used for underground placement of heat exchangers. Ordinary solar collectors allow you to get the temperature of the working water not higher than 60°C. Therefore, during accumulation, the maximum achievable temperature in the main region, V_0, will be of the order of $T_{c,\max}$ ~ 50°C. With a significant thermal resistance of a typical ground massif, the heat flux density during accumulation will be of the order of q_0 ~ 300÷400 W/m^2 at the beginning of the process with a gradual decrease, providing the final potential of the massif $T_c \approx$ 50°C. Since the soil resistance is the limiting element of heat transfer, it is irrational to maintain high values of α_0 ~ 10^5 W/m^2 and a transition from turbulent to viscous-gravitational flow of the intermediate coolant is necessary. The positive side of the latter solution is a significant reduction in water consumption in the circulation circuit.

Parameters of the heat exchanger system on the site 100×100 m^2: $m = n$ = 51; L = 2.0 m; $\eta_{t.bush}$ = 0.961. Thermal properties of soil: ρ_m = 1.84·10^3 kg/m^3; λ_m = 1.42 W/(m·K); c_m = 1.15·10^3 J/(kg·K); T_m = 10°C. The accumulation of heat at q_0 = 380 W/m^2 at the beginning of the process and a gradual decrease in q_0 by 20 W/m^2 every 10 days (decade) led to a temperature change in coolant temperature T_w from 37.07°C (at the beginning of the first decades) to 50.87°C (at the end of the eighteenth decade) with a maximum value of 56.99°C falling on the tenth decade. Indicators at the end of the 18th decade: linear parameter R_s = 26.55 m, temperature T_c = 49.24°C; the amount of accumulated energy E_i = 0.1361·10^{15} J.

When extracting the accumulated heat from the soil mass, in order to maintain a uniform temperature distribution in the main area V_0, peripheral heat exchangers are not operated and the number of workers with the same heat load (q_0 = idem) will be: $k_p = m \cdot n - 2(m+n) + 4$.

As in the case of accumulation, during the first one or two hours of heat extraction, the heat exchanger radii will come into contact, and, starting from this moment, heat will be extracted from V_0 at $R = R_c$ = const.

The dynamics of continuous extraction (at $q_0 = 53$ W/m^2 = const) of heat previously accumulated in the ground massif is shown in Figure 1. The difference ($T_c - T_w$) was within 4°C and the coolant temperature decreased from 45.32°C to 5.88°C. The R_s parameter during discharge increased by 4 m and reached a value of 30.91 m. The "quality" of the received energy, characterized by the coefficient of performance ε of the heat pump, turned out to be high.

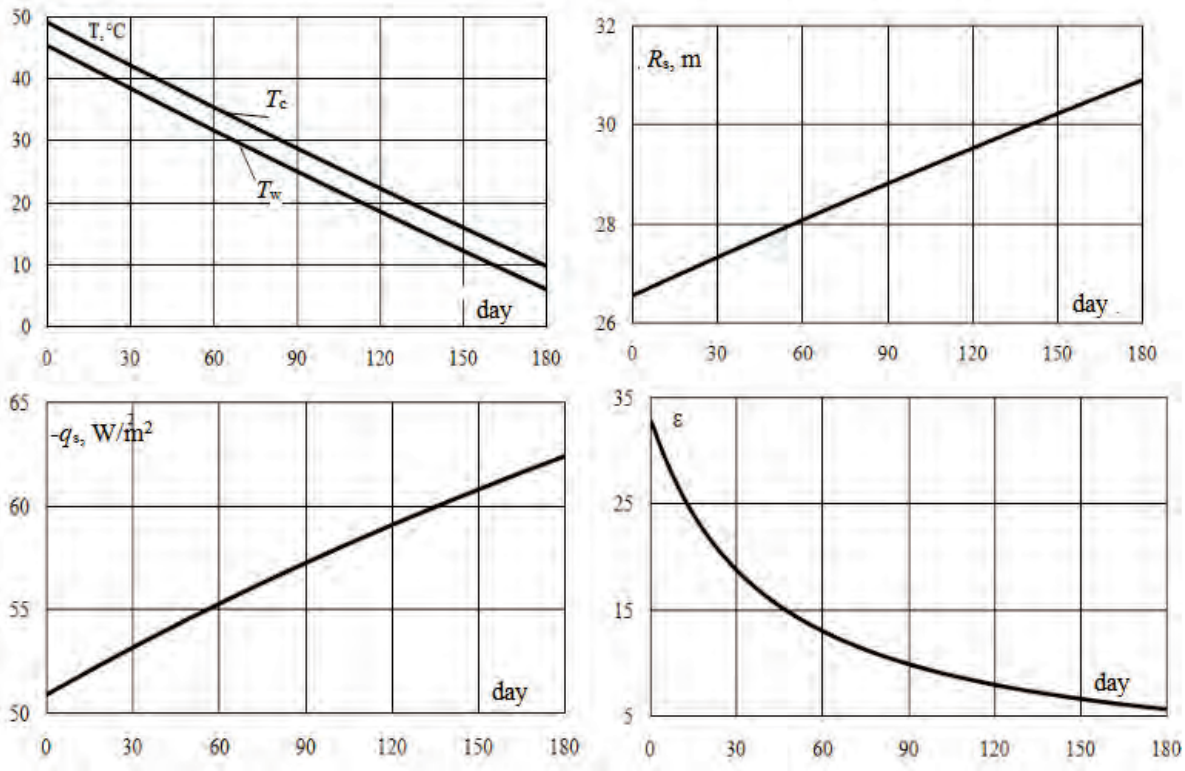

Figure 1. *Change in parameters when extracting heat from a ground accumulator by a system of heat exchangers*

The data presented indicate the prospects for solving the problems of heat storage-extraction by a system of heat exchangers and the use of a ground accumulator for decentralized municipal heat supply.

References

[1] Nakorchevskiy A.I., *Ground heat accumulators and modernization of communal thermal power engineering*. Kyiv: Naukova Dumka, 2010, 256 p.

[2] Nakorchevsky A.I., Basok B.I., Belyaeva T.G., *Problems of soil heat storage and methods of their solution*. Prom. heat engineering 2003. Vol. 25. No. 3. pp. 42-50.

[3] Nakorchevskiy A.I., Basok B.I., Belyaeva T.G., T*echnological indicators of various schemes of soil heat storage*. Teploenergetika. 2006. No. 3. pp. 29-35.

[4] Nakorchevskiy A.I., Basok B.I., Belyaeva T.G., *Some aspects of using the heat of solar radiation for municipal heat supply*. Izvestiya RAN. Energy. 2006, No. 4, pp. 94-103.

EXPERIMENTAL STUDIES OF BURNING PELLETS IN A BURNER UP TO 30 KW

Hanna Veremiichuk

Institute of Engineering Thermophysics, National Academy of Sciences of Ukraine, Kyiv, Ukraine
e-mail: averemiichuk@gmail.com

Given the current trends in agricultural biofuel use, Ukraine has a certain potential to develop this direction at the expense of a significant resource base [1, 2]. The assessments show that today biomass of agricultural origin (straw of grain crops and rape, side products of maize production for grain and sunflower, sunflower husk) remains the main component of the energy potential of biomass in Ukraine.

Taking into account the relevance of research of the process of burning of biofuel in the Institute of Engineering Thermophysics of the NAS of Ukraine the experimental installation of solid fuel boiler with pellet fuel for heating of experimental house of passive type (Kyiv, 2 Bulakhovskogo St.) [3, 4]. The main purpose of this research is to determine the main regularities of the combustion process of agricultural pellet and to study the influence of regime parameters on the distribution of temperatures in the combustion chamber, as well as to study the productive characteristics of biofuel raw materials.

The heating system of the closed type has in its composition boiler rated capacity of 30 kW Combustion of biomass occurs directly in the furnace of the boiler, and the released heat is transferred to the coolant partly in the furnace itself, and partly from the combustion products, which in the furnace, thanks to their movement, come into contact with the convective heat exchange surfaces (convective heat exchanger) and gradually give off heat to the coolant. The facility implements a combined combustion technology that combines the ignition in a layer with fluidization. The burner device is an automated element of the fuel system with automatic fuel supply, regulation of the oxidant (air) supply and the moving element – a scraper on the surface – for periodic cleaning from the ash of the column platform.

The fuel supply speed is set manually to obtain continuous operation with a small amount of combustible elements in the remainder.

It is also important to control the air flow that comes to the combustion chamber from the outside, with a fan with frequency regulation of productivity. At the initial stage, the combustion chamber is not yet heated to sufficient temperature. Therefore, increased air consumption during ignition, which enters the combustion chamber, can significantly slow down the combustion process. The air flow is controlled by the variable speed fan mounted inside the burner. The boiler has an airtight combustion chamber and it is believed that the filtered air penetration is insignificant.

The consumption of pellets coming from the hopper to the combustion chamber is regulated by the electronic control unit of the solid-fuel boiler. It also allows to adjust a number of parameters of the boiler operation: the boiler capacity, maximum and minimum fan capacity, the operating time of the inner auger in the burner when lifting the pellet into a high temperature zone, parameters of cleaning by the moving scraper of the fuel lift.

Variations of physical and chemical properties among used pellets are relatively large. It has been found that mechanical strength and mass are lower than the limit values. This can cause problems with the transportation of pellets and the pollution of the palm. The latter may cause problems with the operation of the finger.

Ash content for agropelets ranged from 4.4% to 7.6%.

When burning wood pellets ignition occurred during the first 300 seconds. Fuel ignition is realized from a special burner. After the pellets are burned, the temperature in the boiler volume

starts to increase gradually. The greatest increase in temperature occurs near the front wall of the boiler, which is opposite to the burner. At the time of 2550 s from the beginning of the experiment, the maximum temperature values are 680°C (Fig. 1).

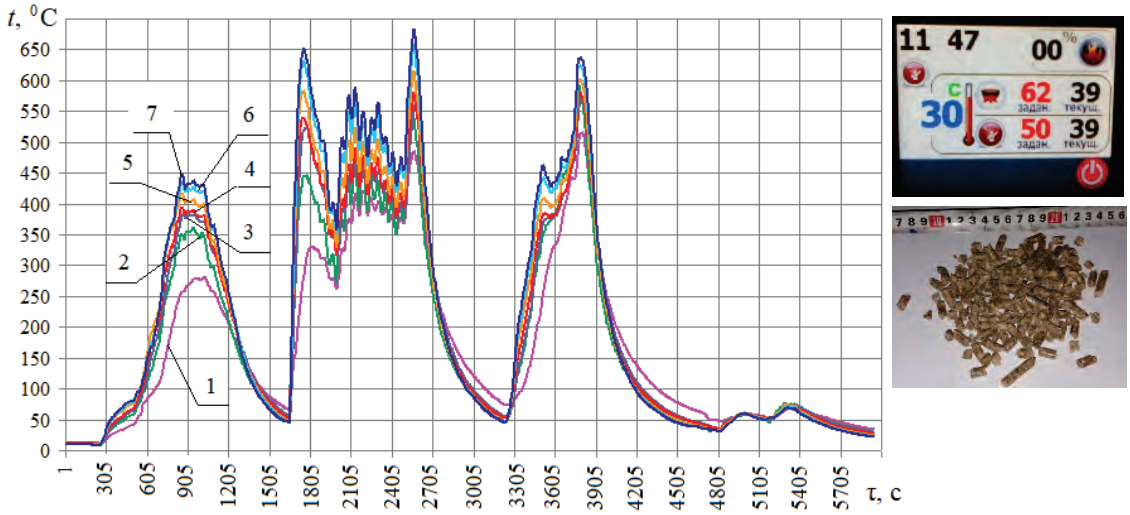

Figure 1. *Temperature of combustion products in the high temperature zone of the combustion chamber when burning wood pellets: 1-7 – temperature values measured by thermocouples.*

From 2105 s from to 2500 s with the experiment there is a stable process of burning wood pellets. The average temperature of the flue gases is 260°C. During this time the automatic periodic feed of pellets from the bunker on the programd algorithm was carried out. At that, the temperature was fluctuating within the following limits:

– Thermosteam No. 4-8 – 400...590°C;
– Thermosteam No. 2-3 – 350...450°C.

Temperature fluctuations occur as a result of the periodic burning of biofuel in the palm and the arrival of a new pellet from the hopper. The burner is extinguished by selecting the "Extinguishing" menu item in the controller. As can be seen from the graph, a gradual decrease in temperature in the chamber of boiler and flue gases begins. After extinguishing, the corresponding symbol appears on the controller display.

Similarly, as in the previous experiment with burning of wood pellets, the results of the research of burning of agropellet from the rapeseed straw (Fig. 2).

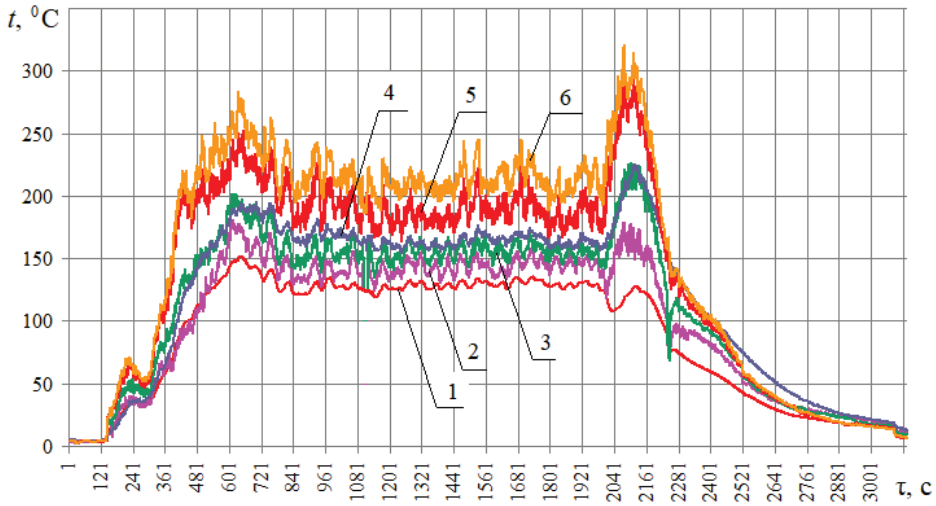

Figure 2. *The temperature of combustion products in the high-temperature zone of the combustion chamber during rapeseed burning: 1 – temperature of the flue gases; 2-6 – temperature values measured by thermocouples No. 2-6, respectively.*

In this case, a lower temperature level (thermocouple No. 2-6) is realized compared to wood fuel. The measured values are in the range of 120…250°C at the established combustion mode (720-2000 s).

Execution of gas analysis was carried out at burning of wood pellets. The selection of combustion products was done in the wild immediately after the boiler. As a result, the NO_x and CO concentrations of the appropriate temperature were obtained at the sample site. The change in the time of concentration of these substances in the flue gases is shown in Figure 3.

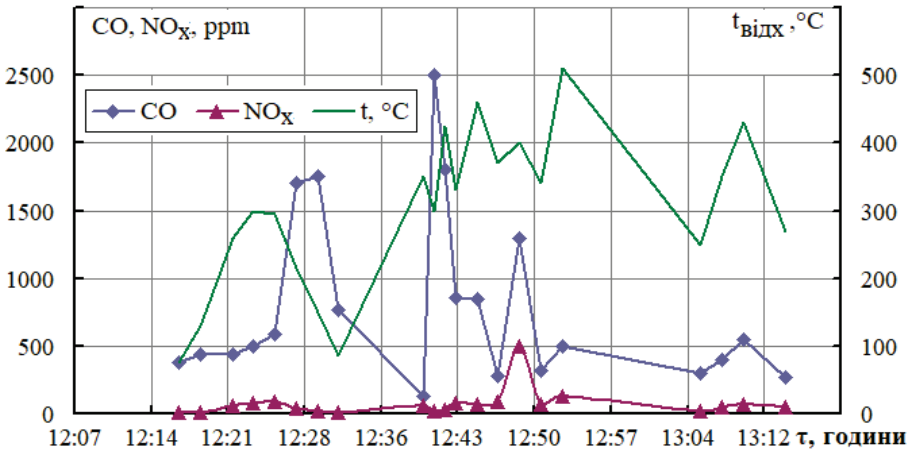

Figure 3. *Concentrations of NO_x and CO in the exhaust gases when burning wood.*

Nitrogen oxide concentrations should be considered moderate, which cannot be argued for the concentration of carbon monoxide. This picture is typical for the process of low-temperature combustion with the presence of a significant chemical underburning. It was obtained that the significant concentration of CO is realized in the transition phases of fuel supply, fuel release and extinguishing. Maximus concentrations correspond to the transient processes between the ignition and the process of settled combustion. In general, concentration of CO as the main component of chemical underburning have an excessive level and need further adjustment by setting up working regimes of the fuel system and, if possible, introducing additional constructive measures.

Conclusions

When combined with a solid-fuel boiler and a proposed burner (low power – up to 30 kW), a wide range of pellets of plant origin can be burned. The results of the research can be used to increase the efficiency of combustion process at burning of biofuel and modernization of fuel-inflammation systems of boilers of low power of municipal and industrial heat power, social-budget sphere, individual-household sector, etc.

References

[1] Geletukha G., Zheliezna T., Drahniev S., *Analysis of barriers to the production of energy from agribiomass in Ukraine*. Bioenergy Association of Ukraine, No. 21, https://uabio.org/materials/uabio-analytics/.

[2] Lysenko O., Veremiichuk A., Siryi O., *Research of burning of agricultural pellets in boilers with capasity up to 25 kW*. Thermophysics and thermal power engineering. 2022. Vol. 44, No. 3, pp. 21-25, https://doi.org/10.31472/ttpe.3.2022.11.

[3] Basok B., Davydenko B., Kuzhel L., Lysenko O., Veremiichuk A., *Experimental studies of burning plant pellets in a domestic boiler*. Ventilation, Illumination and Heat-Gas Supply. 2021. Vol. 37, pp. 13-23, https://doi.org/10.32347/2409-2606.2021.37.13-23.

[4] Basok B., Goncharuk S., Priemchenko V., Lysenko O., Veremiichuk H., *Research of thermotechnical characteristics of domestic boiler with a mechanical pellet burner*. Environmental safety and natural resources. 2021. No. 4 (40), pp 60-72, DOI: 10.32347/2411-4049.2021.4.60-72.

ACTUAL PROBLEMS OF THERMAL AND RENEWABLE ENERGY IN METALLURGY

Ladislav Lazić[1], Anatoliy Pavlenko[2]

[1]University of Zagreb, Faculty of Metallurgy, Aleja narodnih heroja 3, 44 000 Sisak, Croatia

[2]Kielce University of Technology, Faculty of Environmental, Geomatic and Energy Engineering, al. Tysiąclecia Państwa Polskiego 7, 25-314 Kielce, Poland

Industrial production has been driven by the requirements of maintaining or improving product quality and minimization of production costs. Within these requirements the overall energy management plays important roles. It is a known fact that the improving fuel utilisation efficiency is the key to good financial and environmental practice. To meet the higher requirements it is necessary to improve existing furnace by optimising the energy efficiency and by reducing the pollutant production of burners and combustion chambers. In the introduction of the article, the efficiency improvement opportunities for fuel- based process heating systems in metallurgical practice are listed. Thereafter, some of the solutions for increasing the energy efficiency for metallurgical furnaces in the Republic of Croatia are briefly described.

Efficiency improvement opportunities for fuel-based process heating systems can be grouped into five categories [1]:

- Heat generation: discusses the equipment and the fuels used to heat a product.
- Heat containment: describes methods and materials that can reduce energy loss to the surroundings.
- Heat transfer: discusses methods of improving heat transferred to the load or charge to reduce energy consumption, increase productivity, and improve quality.
- Waste heat recovery: identifies sources of energy loss that can be recovered for more useful purposes, and addresses ways to capture additional energy.
- Enabling technologies: addresses common opportunities to reduce energy losses by improving material handling practices, effectively sequencing and scheduling heating tasks, seeking more efficient process control, and improving the performance of auxiliary systems.

Actual furnace operational issues in metallurgical practice can be listed in the following order:

- Energy efficiency and operating cos;
- GHG emissions;
- Combustion efficiency;
- Emissions control;
- Product quality;
- Integrity/life and reliability parts of plants;
- Maintenance cost;
- Safety.

Within this requirement the energy efficiency plays important roles. First of all, solutions to optimize the furnace energy efficiency with substantially reduced pollutant emissions should be sought in improving the governing processes in open-flame furnaces:

- Fuels and combustion;
- Burner and furnace aerodynamics;
- Heat transfer.

In this connection, it is especially important to pay attention to the operating conditions such as:

- Excess Air;
- Pressure Control;
- Oxygen Enrichment;
- Combustion Air Preheat;
- Load Temperature (at inlet and discharge);
- Flame Temperature and Emissivity;
- Wall Emissivity.

It is equally important to examine the possibility of replacement of the existing conventional combustion technology by the so-called ’advanced’ commercially available combustion techniques, for example High Temperature Air Combustion (HiTAC) or Oxy-Fuel combustion, under which the furnace should be operated in order to maximize the efficiency and minimize the pollutant emissions. In the process of choosing a certain technology it is essential to take into account the cost effectiveness of the investment i.e. the payback period.

But, in any case, reducing energy consumption through the application of appropriate working conditions in practice as well as investment in advanced technologies can enhance competitiveness in metallurgical production.

THERMOGASDYNAMIC AND RADIATION INTERACTION OF THE NEW SAFE CONFINEMENT BUILDING OF THE CHERNOBYL NPP WITH THE ENVIRONMENT

Pavlo Krukovskyi, Vladyslav Oliinyk

Institute of Engineering Thermophysics National Academy of Sciences of Ukraine (Ukraine)

Introduction

The melt down of the Reactor Unit 4 of Chernobyl Nuclear Power Plant (ChNPP) that happened on 26 April 1986 is the worst accident in history in terms of resulting deaths, health issues, environment and costs. It is one of only two accidents classified as a level 7 event (the other being the Fukushima Daiichi nuclear disaster in 2011).

The sarcophagus or Shelter Object (SO) (Fig. 1) was designed and built in November 1986 to limit radioactive contamination of the environment, by encasing the most dangerous area and protecting it from climate exposure [1-3]. It is located within a large restricted area known as the Chernobyl Exclusion Zone. Inside the SO there still remains about 95% of the fuel, which was in the reactor at the moment of the accident.

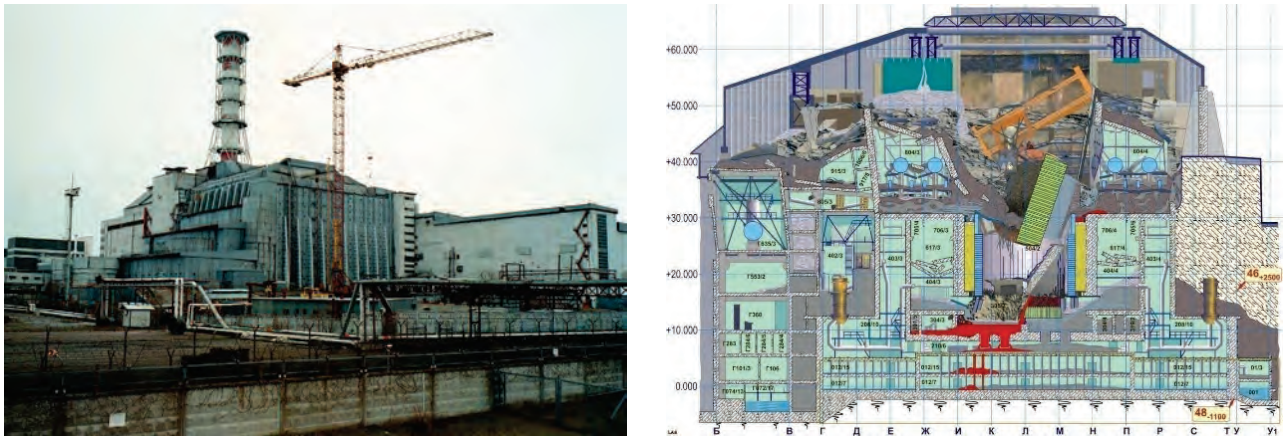

a) b)

Figure 1. *The Shelter Object (a) and destroyed reactor #4 (b).*

During the last 30 years some of SO bearing constructions became unstable and were strengthened and repaired. Metal light roof of the SO was sealed but for today there still remain about 120-150 m^2 of cracks and holes, through which a large amount of radioactive aerosols can get to the environment.

A decision to enclose the SO by a so called New Safe Confinement (NSC) was taken, and a project to reconstruct the enclosure has been completed. It is a complex of engineering solutions, designed in the form of the Arch, covering the SO (Fig. 2). Main purpose of the NSC is the protection of the environment from radiation and radioactive aerosols (RA) during the SO dismantling and the 100 years operation of the NSC. It also contains the equipment for extracting the nuclear fuel remains from the destroyed unit, to transform it to an environmentally safe system ensuring the safety of personnel and environment. The NSC has been built for 5 years near the SO and was slid to its design position over the SO NSC in November 2016 (Fig. 2b). Its height is 110 m, width – 250 m, length – 160 m and weight of about 36,000 tones. Its frame is a huge lattice construction consisting of tubes, supported by two longitudinal concrete beams (Fig. 2a, poz. 5).

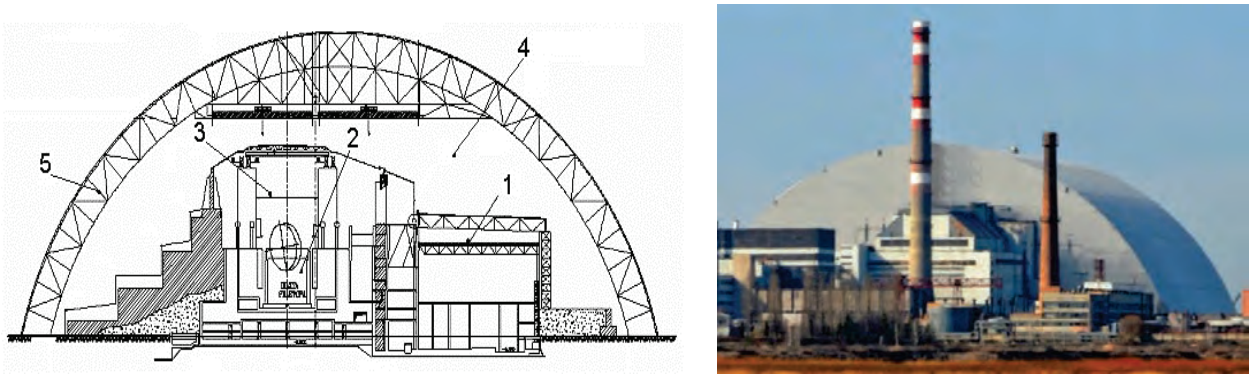

a) b)

Figure 2. *The scheme of the SO and the NSC cross-section (a) and the photo of NSC and SO after NSC sliding over the SO (b); 1 – turbine hall, 2 – destroyed reactor, 3 – central hall, 4 – main volume, 5 – annular space of the NSC.*

The comparative sizes of the New Save Confinement are such a huge size of the NSC that it could cover the Statue of Liberty in USA (height 93 m) and a Colosseum in Rome, Italy (length 188 m). The NSC as a barrier between destroyed reactor and environment was designed with several design goals:

1. Transform the destroyed ChNPP Unit 4 into an environmentally safe system (i.e. preserve the radioactive materials at the site to prevent further environmental contamination).
2. Reduce corrosion and weathering of the existing shelter and the Unit 4 reactor building.
3. Mitigate the consequences of a potential collapse of either the existing shelter or the Unit 4 reactor building, particularly in terms of retention the radioactive dust that would be produced by such a collapse.
4. Enable safe dismantling of unstable structures (such as the roof of the existing shelter) by providing remotely operated equipment.

Problem Formulation

To ensure the 100-year lifetime of the NSC, its bearing steel constructions are enclosed into the outer and inner claddings (annular space in Fig. 2), between which the relative humidity is maintained below 40% under different weather conditions. Special ventilation system was designed for this purpose, which heats up, recirculate and dry the air of the annular space between the NSC claddings.

Purpose of the ventilation system:

1. Maintenance of humidity in the Arch annular space below 40% and pressure about 50 Pa.
2. Maintaining the pressure in the main volume of the NSC at about -5 Pa.

Such requirements should be fulfilled in following range of climatic conditions: temperature -22°C to +31°C, relative humidity 0% to 100% and wind speed 0 m/s to 25 m/s.

To verify the ventilation system operability engineering and construction company VINCI Construction Grands Projects/Bouygues Travaux Publics NOVARKA ordered the work on the 3D CFD (Computation Fluid Dynamic) modelling of thermalgasdynamic and humidity state of the NSC-SO, which has been completed. For this, the model has to consider the following properties and physical processes outside and inside of the NSC and SO:

1. 3-D and unsteady state of the NSC and SO.
2. The thermal inertia of the NSC and SO in the annual cycle consideration.
3. Consideration of external as well as internal movement of air.
4. Accounting for the work of basic engineering equipment (ventilation, dehumidification, heating, etc.).

5. Main heat sources in the NSC and the SO.
6. Consideration of non-tightness of NSC claddings.
7. The radioactive aerosols distribution inside and outside the NSC.

Methodology

The general idea of the work is to go through the following steps: development of separate SO model, then its calibration after which united model of SO and NSC will be developed and applied too. The SO model calibration is identification (estimation) of its parameters using experimental data. Parameters can be divided into groups: hydraulic resistances of the SO roof and volumes and source terms of radioactive aerosols inside the SO. In model, it is possible to assign properties of porous media to volumes of SO roof and internal volume of chimney. It makes possible adjusting airflows through each opening in the model that is extremely important for aerosol leak rates. Parameters of hydraulic resistances have been estimated using the information on average airflows through the SO roof and chimney.

SO and NSC+SO models creation. Numerical models consider all main geometric parts of the NSC+SO (Fig. 2a) models and have been created in frame of ANSYS FLUENT software [4].

It simulates following steady and unsteady physical phenomena:

- NSC flow-around by wind at different speeds and directions;
- conjugate heat and mass transfer (heat conduction, forced and natural convection, radiative heat transfer between ground, foundation, destroyed reactor, SO and NSC and environment including the solar radiation in the light time and radiation to the sky-space at night;
- humidity distribution in all of the volumes of the SO, NSC and environment;
- air and humidity leakages through the small gaps of the NSC claddings and gaps between the vertical NSC walls and existing buildings;
- radioactive aerosols distribution, either as a second phase or as particles, moved by the airflows.

Model has allowed checking the operability of the ventilation system under various weather conditions and also in cases of different failures of ventilation equipment. NSC+SO model analysis/ Since developed NSC+SO model can simulate the 3D flows of the air, it also can simulate the radioactive aerosol emission from the destroyed heat-generating reactor, either as a second phase or as discrete particles, transferred by the airflows for different scenarios. The mass transfer is simulated in the units of kg/m3, and concentration distributions are recalculated through the weight activity Bq/kg for 1 kilogram of RA.

The analysis shows that the NSC is not an absolute barrier for radioactive aerosols between the destroyed reactor and the environment. Small amount of RA can penetrate to the environment along with air flow (Figs. 3 and 4) through the outer cladding and gaps between the western and eastern walls of the NSC walls and building structures (Fig. 4). To take into account such phenomena, specific features have been implemented and built into the model, part of which is not included into the software used. Among such features is considered the heat and mass transfer through the inner and outer non-hermetic claddings of the NSC under small pressure gradients and large hydraulic resistances.

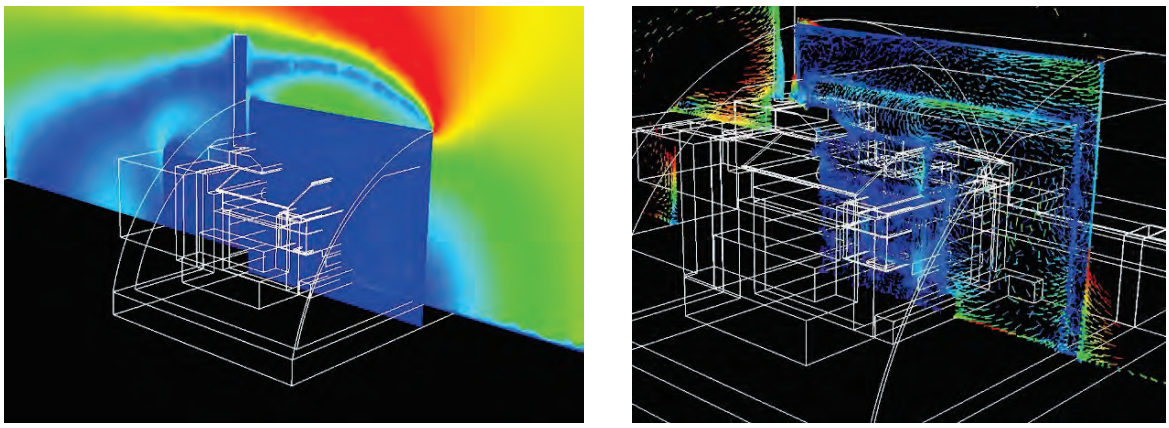

a) b)

Figure 3. *Velocity (a) field and (b) vectors distribution in longitudinal cross section of NSC+SO model and surrounding area.*

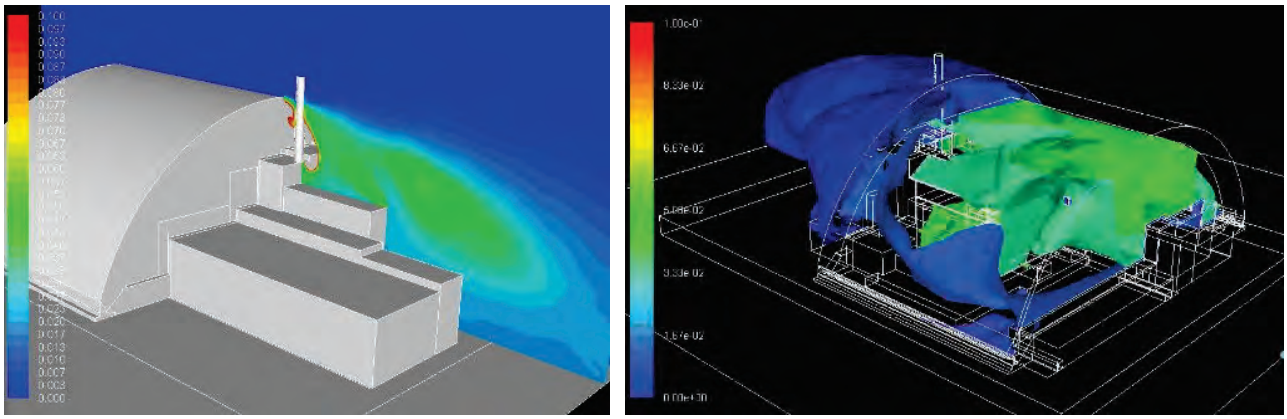

a) b)

Figure 4. *RA concentration distribution, Bq/m^3, outgoing from NSC to the environment (a) and isosurfaces of RA concentrations inside and outside the NSC (b).*

Preliminary results of the model show that workers, being under the NSC using various protective equipment, can gain the maximum permissible radiation dose of 20 mSv/year for NPP personnel (1 Sv = 100 R, 1 Bq = 0.18 mSv) for various time intervals

Conclusion

This paper has discussed the purpose and the design of the New Safe Confinement (NSC), which was built and slid over "Shelter" Object (SO) and Destroyed Reactor of the Chernobyl nuclear power plant. Was justified the necessity of analysis and forecasting of the conjugate thermal, gas dynamic and humidity transfer processes in the SO and NSC, which determine the 100-year lifetime of the NSC. For this a 3D CFD-computer model has been developed, which allows analyzing the abovementioned phenomena as well as the radioactive aerosols distribution in the SO and NSC volumes and their leakages to the environment.

References

[1] *Chernobyl Sarcophagus*. Chernobyl International. Retrieved 2010-11-30.

[2] *Conceptual design of the New Safe Confinement, Chernobyl Nuclear Power Plant – Block 4*, State Specialized Enterprise "Chernobyl Nuclear Power Plant (SSE ChNPP)", Kyiv region, Ukraine 2003.

[3] *A Second Shelter for Chernobyl*. Proceedings of the Institution of Civil Engineers, February 1997, Paper 11133.

[4] ANSYS FLUENT 12.0/12.1. Documentation.

MATHEMATICAL SIMULATION OF THE KINETICS OF MELTING OF LUCK FUSIBLE MATERIALS

Anastasiia Pavlenko, Mykhailo Babenko

Dnieperovskii State University, Ukraine
e-mail: mvbab@ukr.net

The introduction of materials of different chemical and granulometric composition into liquid steel is an effective resource-saving technology for refining, microalloying and finishing the chemical composition of steel. The currently used modes of introducing lumpy materials (conditionally cylindrical or spherical shapes) into the melt are not always accompanied by their predictable melting under the melt layer and uniform distribution of the additive, but by its ascent to the "slag-metal" boundary.

The determining processes that affect the technological parameters in the production of steel are heat and mass transfer processes in metallurgical units. Conducting experiments in industrial conditions is always associated with high material costs, especially in metallurgy, where there are additional difficulties due to high temperatures and the opacity of the media under study.

These shortcomings are devoid of mathematical modeling, the availability of which is due, among other things, to the modern development of computer technology, which makes it possible to sufficiently fully take into account the defining characteristics of thermophysical processes in mathematical models. Therefore, the development of mathematical models that make it possible to study the melting processes of lumpy additives of various compositions, shapes and properties, which are used at different stages of steel production, is an urgent scientific and technical task. The presence of such a mathematical apparatus will make it possible to predict the assimilation of additives depending on the conditions of introduction into the metal melt and form a search direction in increasing the efficiency of using not only expensive, but also imported materials.

The study of heat transfer processes in systems of bodies with moving internal or external boundaries is relevant for a number of branches of modern technology. Physical and chemical processes, the course of which is accompanied by the movement of phase boundaries, include, for example, a change in the state of aggregation, dissolution, chemical interaction, a change in crystalline modification, mechanical processing, etc. The problems of heat conduction for systems with moving phase boundaries are usually called problems Stephen. The solidifying metal contains three regions – liquid, solid and two-phase located between them. In the two-phase region, the transition of the metal from the liquid to the solid state (during solidification) occurs and all the main determining processes are concentrated. The theory of a two-phase zone is essentially a thermophysical theory of crystallization of a metal alloy.

Melting or solidification is an integral part of most technological processes for the production and processing of metals and alloys. These processes, as physical phenomena, have certain general patterns that characterize them. These include, first of all, the absorption or release of latent heat of a change in the state of aggregation of a substance. Another common feature of these processes is that the absorption or release of the latent heat of phase transformation occurs at a well-defined temperature (for pure crystalline substances) or within a temperature range (for alloys). The phase transformation temperature (or temperature range) depends on the physical nature of the substance.

With all the variety of melting processes, they have in common the appearance of a layer of solidified melt on the surface of a cold piece, which then, as the solid body warms up, melts. The time during which a layer of solidified melt exists on the surface of a solid is called the thermal period. The nature of the course of the thermal period has a significant impact on the process of

heating and melting of the body as a whole, causing, firstly, the total duration of this process and, secondly, the thermal state of the body by the time the melt and solid surface begin to interact.

Another common feature of melting or solidification processes is the presence of a moving interface between the solid and liquid phases. This boundary is expressed as an isothermal surface for pure crystalline substances characterized by a melting point. For alloys, the boundary turns into a two-phase region bounded by isothermal surfaces with liquidus and solidus temperatures for a given alloy.

The problem of determining the temperature field and the kinetics of melting bodies in the melt belongs to the class of heat conduction problems with moving phase boundaries. These problems belong to the class of essentially non-linear ones. Approximate methods, both analytical and numerical, are used to solve them. Approximate analytical methods are applicable only for simplified heat conduction problems (one-dimensional, single-phase, etc.). Their application for multiphase problems, which include the problem of melting lumpy low-melting materials in a melt, causes significant difficulties. As a rule, numerical methods are used to solve nonlinear heat conduction problems with moving phase boundaries. Numerical methods for solving heat conduction problems include, first of all, finite difference methods (mesh methods), control volume, finite elements, and boundary elements. In this work, the control volume method was used.

The control (finite) volume method (FVM, Finite Volumes Method) is based on the fact that the computational domain is divided into a set of control volumes using a grid. The nodes where the solution is sought are located at the centers of these volumes. For each volume, the laws of conservation of mass, momentum and energy must be fulfilled. That is, the change in time of the mass of the medium in the control volume can occur only due to the external mass flow entering the volume or due to the mass flow leaving the given volume.

Some of the benefits of MCOs:

- preservation of basic quantities throughout the area, such as the energy of the system, mass, heat fluxes, etc. This condition is satisfied even for a coarse computational grid;
- high calculation speed;
- ease of use for tasks with complex geometry and curvilinear boundaries;
- ease of use of different geometric types of elements – triangles, polygons, etc.

MODELING OF THE DISTRIBUTION OF WIND PRESSURES OF THE BUILDING OF THE NEW SAFE CONFINEMENT OF THE CHERNOBYL NPP

Dmytro Skliarenko, Pavlo Krukovskyi, Vladyslav Oliinyk

Institute of Engineering Thermophysics National Academy of Sciences of Ukraine (Ukraine)

Introduction

Determination of the distribution of pressure maps in buildings is necessary to determine the resistance of buildings to winds with high air velocity, the mutual influence of buildings in densely built-up areas for the design of the supply ventilation system of premises, for emergency buildings with particularly valuable or hazardous substances inside it, the air exchange of which depends on the pressure distribution maps on the outer surfaces of buildings through a large number of small gaps. Because due to the difference in pressure inside and outside, air from the windward side enters the building, and from the in 2016, the NSC was built over the destroyed ChNPP Unit 4, which was built using modern technologies and design standards, but it could not be completely sealed. There are many small gaps between the NSC walls and the rest of the ChNPP Unit 4 structures through which air can flow both inside and outside the NSC, therefore, to analyze and control the release of unorganized air exchange and radioactive aerosols (RA) from the main volume (MV) of the ChNPP NSC into the environment (EE), information on the distribution of wind pressures on the NSC outer surface and on the Shelter building structures is required. Such maps of pressure distribution on the NSC outer surface can be obtained by means of full-scale or computational experiment.

For this purpose, a small-scale physical model of the NSC at a scale of 1:300 (Fig. 1a) was tested in a wind tunnel during NSC design and maps of wind pressure distribution on the outer surface of the NSC model were obtained for all directions of air blowing from 0° to 360° with a step of 10 degrees [1] in order to determine the stability of NSC arch structures against wind with a wind speed of 23 m/s, both during construction and during NSC operation.

The pressure maps are the values of pressures in 197 separate sections of the western, eastern and cylindrical surfaces of the NSC of the small-scale physical model of the NSC (Fig. 1a), which did not include all structures under the walls and near the NSC. During operation, these wind pressure distributions were used to perform the above task, the results of which showed that these pressure maps qualitatively and quantitatively do not correspond to the literature experimental and calculated data. An alternative way to obtain pressure maps is to build a computer model using CFD (Computational fluid dynamics) technology (Fig. 1b).

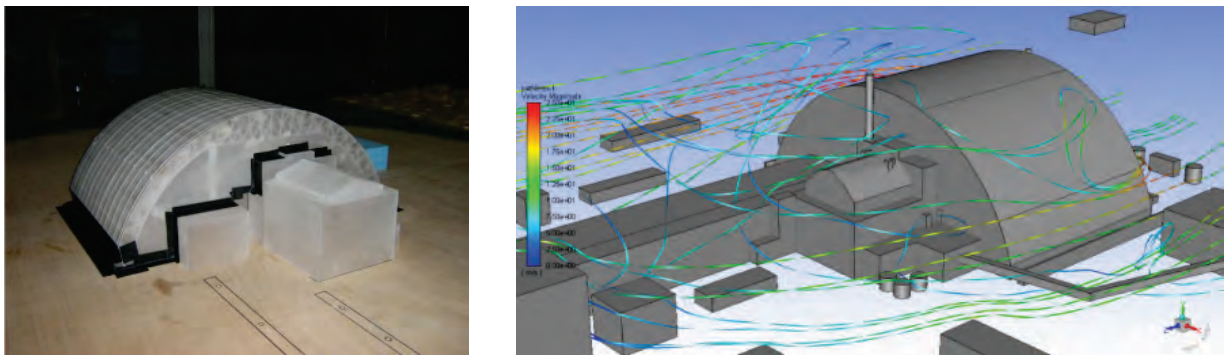

a) b)

Figure 1. *The NSC and the Shelter: a) photo of a small-scale physical model in the wind tunnel channel from the southeast angle; b) full-scale modeling of the external aerodynamic flow of the NSC and adjacent buildings from the northeast angle.*

Defining the goal and objectives of the study

The purpose of the work is to build a three-dimensional full-scale 1:1 computer CFD model of the NSC external air flow (Fig. 1b) for arbitrary rotation angles and wind speeds and to pre-tune the model according to the literature and experimental data of the ChNPP, which includes all structures under the walls and near the NSC to obtain the pressure distribution on the NSC outer surface and building structures of the Shelter during air flow.

The geometric, physical, and mathematical models

The paper considers a three-dimensional full-scale 1:1 computer model of the NSC external airflow (Fig. 1b) for the same rotation angles and arbitrary velocity range, which was pre-tuned according to the literature and experimental data of the ChNPP, containing all structures under the walls and near the NSC. The geometric model has dimensions of 3.5x3.5 km, up to the upper limit of 800 m. The computational grid of such model consists of about 4 million cells (polyhedral mesh). Thickening of cells (Fig. 2a) was carried out to obtain the result of acceptable in time and stable calculation results in the CFD model of the NSC external flow.

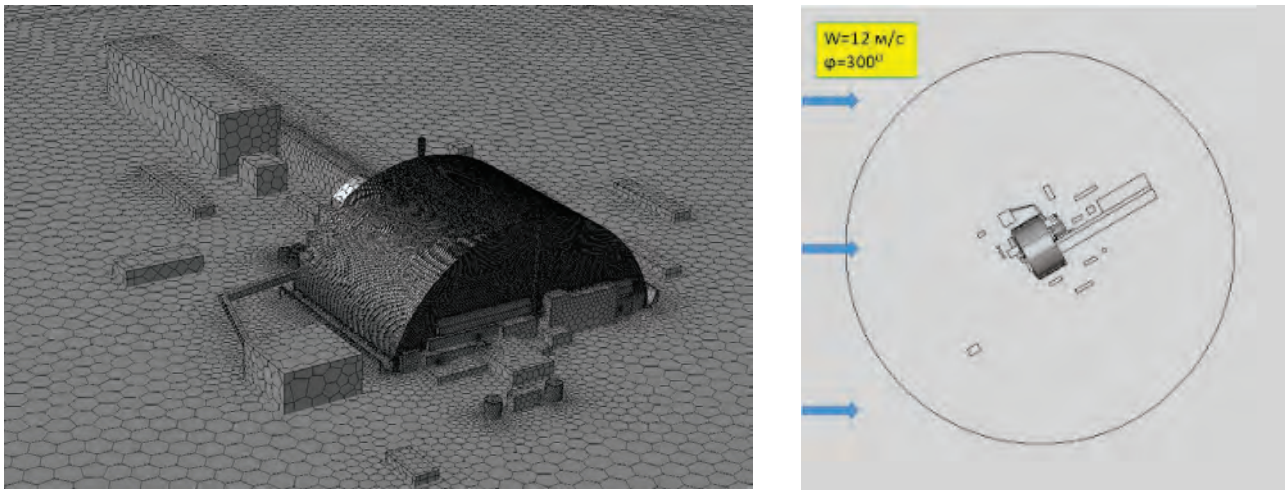

a) b)

Figure 2. *Computational grid of the NSC air flow model and the area of the computer model of the NSC and the environment that is rotated relative to the wind direction (direction 300° is indicated).*

To properly take into account the wind flow, the distance from the NSC to the lateral edge of the computational domain was chosen to be at least 1,0 km, taking into account the NSC height of about 110.0 m, as well as the atmospheric pressure at the remote P_∞ = 10^5 Pa and the air temperature T_∞ = 15°C. The wind direction was taken into account by rotating the internal volume of air with the geometry of the NSC with a radius of 1.0 km (Fig. 2b), the dimensions of which are selected in accordance with the literature [2-4] to simulate the external air flow around the buildings. At the input boundary of the computational domain, the wind direction and speed are set, the distribution of which in height corresponds to the power law for the terrain of type III with the power law index m = 0.31.

When setting up the CFD model of the NSC, the variable profile of wind speed in height, surface roughness, intensity and scale of turbulence at the entrance to the computational domain, turbulence model and its parameters, ground temperature, as well as the geometry of buildings at the ChNPP industrial site were adjusted.

Research results

In contrast to the small-scale physical model, the full-scale computer model allows obtaining continuous pressure distributions over the entire NSC surface (Fig. 3), which is 87.6 thousand m^2, as opposed to 197 values in individual sections of the small-scale physical model of the NSC.

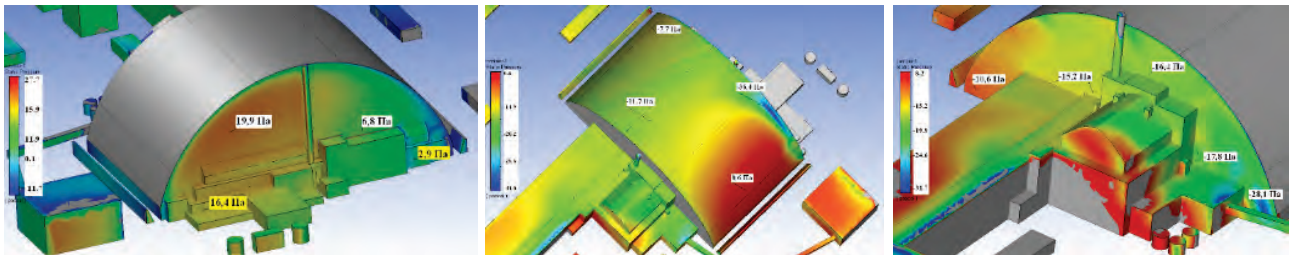

a) b) c)

Figure 3. *Distribution of static pressure on NSC surfaces and Shelter structures.*

Maps of pressure distribution on the outer surface of the NSC and building structures of the Shelter were obtained for different wind directions, which qualitatively and quantitatively coincide with the literature data [2-4] on the external flow of buildings and greenhouses.

The obtained pressure distributions on NSC surfaces were calculated for all wind directions from 0° to 360° through 10° at wind speed of 3.8 m/s. For other wind speeds, the pressures obtained with the help of physical and computational models are recalculated using dependence [1]:

$$P_c = P_b \cdot \left(\frac{V_c}{V_b} \right)^2 \qquad (1)$$

where: P_c – pressure for the current (c) value of wind speed; V_c – current value of wind speed; P_b – pressure for the base (b) value at the base wind speed V_b = 3.8 m/s.

As a result, the obtained maps of wind pressure distribution on the NSC outer surface and Shelter building structures can be used during scientific support as information support, monitoring and forecasting of air flow rate Q (m^3/s) of radioactive material outlet to and inside the NSC and control of the NSC ventilation system in order not to exceed the maximum permissible level of radioactive material release from the NSC [5].

Conclusions

The paper presents a three-dimensional full-scale 1:1 computer model of the external air flow around the New Safe Confinement (NSC) for different rotation angles and an arbitrary range of wind speeds. The results of calculations of wind pressure distribution on the NSC outer surface are in good agreement with the literature and ChNPP experimental data. Wind pressure distributions on the NSC outer surface are used to solve an important task of controlling the release of unorganized air exchange with radioactive dust from the NSC into the environment.

References

[1] Wind tunnel test results: (Report), 2009. NOVARKA, SIP-N-TE-22-B102-RPT-001-01, c. Slavutych, Ukraine (In Russian).

[2] Valger S.A., Fedorov A.V., Fedorova N.N. (2013), *Modeling of incompressible turbulent flows in the vicinity of poorly streamlined bodies using ANSYS Fluent*. Computing Technologies. 18, #5, 27-40 (In Russian), https://elibrary.ru/item.asp?id=20345326 (accessed October 28, 2022).

[3] CEN. Eurocode EN 1991-1-4: Actions on Structures-Part 1-4: General Actions-Wind Actions; European Committee for Standardization: Brussels, Belgium, 2010.

[4] Maraveas C. (2020), *Wind Pressure Coefficients on Greenhouse Structures*. Agriculture 10(5), 149, pp. 1-21, https://doi.org/10.3390/agriculture10050149.

[5] Krukovskyi P.G., Skliarenko D.I., Diadiushko E.V., Kondratenko S.A., Kuzmenko V.G., *Analysis and management of low air emissions from a new safe confinement into the environment*. Proceedings of the VI International Online Conference "Problems of Decommissioning of Nuclear Power Facilities and Environmental Restoration", INUDECO 2021, April 27-29, 2021, Slavutych, Ukraine, 137-140. ISBN 978-617-7932-10-8 (In Ukrainian) https://inudeco.pro/wp-content/uploads/2022/04/2021.pdf (accessed October 28, 2022).

PROVISION OF SPECIAL MICROCLIMATE CONDITIONS IN THE CONSTRUCTION OF THE NEW SAFE CONFINEMENT CHERNOBYL NPP

Dmytro Smolchenko, Pavlo Krukovskyi

Institute of Engineering Thermophysics National Academy of Sciences of Ukraine (Ukraine)

Introduction

The New Safe Confinement (NSC) above the destroyed reactor and Shelter Object (SO) of the Chernobyl NPP (Fig. 1) is an additional protective structure for extracting materials containing nuclear fuel in the destroyed reactor and converting the SO into an environmentally safe system for personnel, the public and environment [1]. The NSC is a steel structure in the form of an Arch, consisting of steel bearing structures located in the annular space of the Arch, outer and inner shells, under which are the main volume (MV), the Shelter Object and the destroyed reactor.

Figure 1. *Photo of the New Safe Confinement from the sides of the western wall.*

The NSC arch is made of about 7.5 thousand ferrous metal pipes with a diameter of 0.4 m to 1 m. It is possible to ensure the corrosion resistance of NSC load-bearing steel structures by maintaining humidity in the volume of the AS no more than 40% during the entire service life. To maintain the desired humidity in the AS, a complex ventilation system is provided (Fig. 2) [2]. This ventilation system should provide an increased air pressure relative to the main volume (MV) at a level of 10-30 Pa.

To maintain such pressure levels in the volumes of the AS and the RO with sizes of about 1 million m^3 of the AS and 1.5 million m^3 of the RO, 3 ventilation unit (VU) 1 ventilation units are continuously operating to blow dry air into the AS with a total capacity of 75 thousand m^3/h and 3 VU11 ventilation units with a total capacity of up to 140 m^3/h for extracting air from the MV outside the NSC through horizontal channels 11-13, HEPA filters RA and a vertical ventilation pipe up to a height of 111 m (mixing) of air in the AS in order to ensure the most uniform humidity in terms of volume, the local values of which depend on local temperatures in the AS volume and places where moisture penetrates from the environment due to the non-density of the NSC outer shell. The total power of all VU of the ventilation system is about 1 MW.

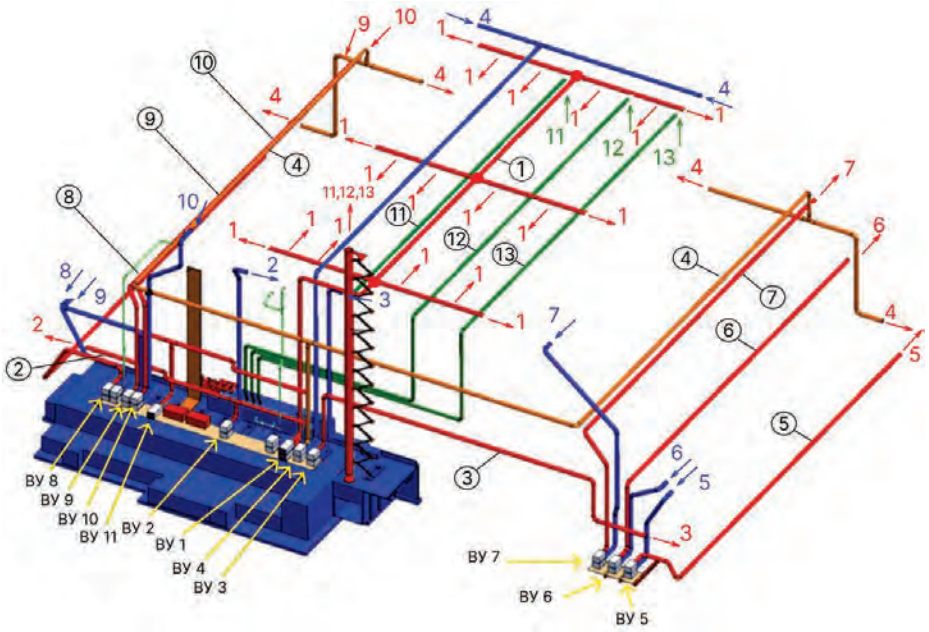

Figure 2. *NBK ventilation scheme. In the figure: Numbers 1 indicate the locations of 18 dry air injection nozzles from a 3-row collector, circuit 2-3 – ventilation of the western wall, circuit 4 – ventilation of the eastern wall with 2 suction and 4 injection nozzles, 5 – southern and 8-10 northern parts of the cylindrical part of the circular space.*

In the process of designing the NSC and the ventilation system, it became necessary to analyze the unevenness of humidity in the volume of the AS under various climatic conditions and the number of ventilation units that pump dry air into the AS, which are special microclimatic conditions. ***This work is devoted to answering these important questions, which are the purpose of this work.***

Such an analysis can only be performed using the technology of three-dimensional CFD (Computational Fluid Dynamic) models, the physical and computer components of which are described below.

Physical model of the NSC

The microclimatic (temperature-humidity) state in the AS of the NSC and in the main volume is formed as a result of the interaction of aerodynamic and heat and mass transfer processes. These include heat conduction through the elements of building structures, forced outside and free-convective and radiative heat transfer inside when wind flows around the NSC with different speeds and directions. There are various sources of heat in the MV, one of which is heat release from fuel materials in the Shelter Object.

Computer model

To perform work in the ANSYS FLUENT software environment, a 3D CFD model was created, which includes both all parts of the NSC Arch and all objects under the Arch, including the Shelter Object with a destroyed reactor, a turbine hall, a deaerator stack, a technological building and soil with foundations to a depth of 15 m. The computational grid of the model consists of 1 million computational cells, of which about 0.4 million cells accounted for the annular space.

Simulation results

The 3D CFD model briefly described above made it possible, on the basis of a detailed analysis of the obtained temperature and relative humidity fields in the volumes of the AS and MV (Fig. 3), to determine the distribution of humidity in the AS of the NSC for different wind speeds, the

number of operating VU, to regulate the level of humidity to ensure the corrosion resistance of bearing steel structures, assess the time to reach 40% humidity in the control room in case of failure of the ventilation equipment.

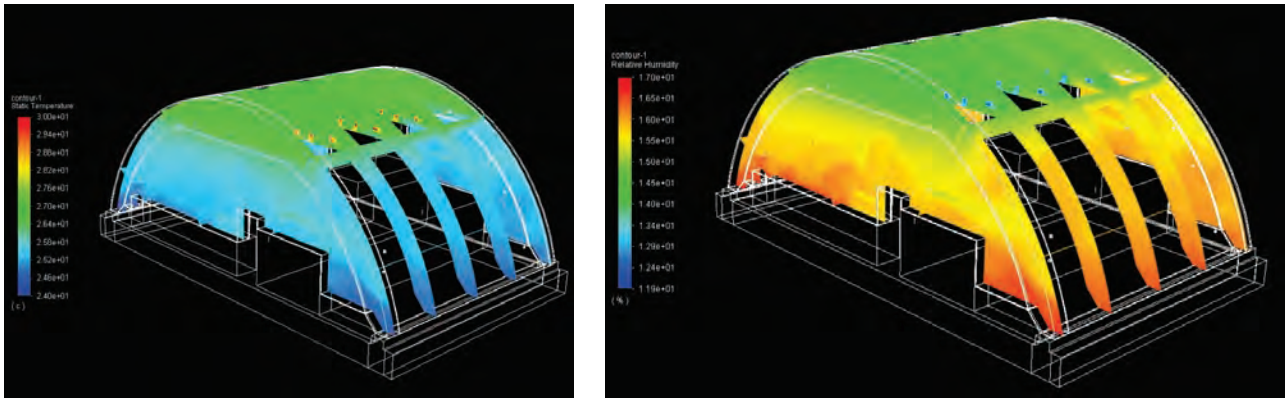

a) b)

Figure 3. *Typical distributions of temperature (a) and humidity (b) fields in the cross sections of the AS.*

Table 1 shows the results of the analysis of the heat and humidity state of the NSC volumes and the levels of energy saving depending on the number of ventilation units injected into the AS, operating recirculation and external west wind speeds of 3.8 m/s, 7.3 m/s and 25 m/s. It can be seen that with all three VU operating for the injection of dry air into the AS with a total flow rate of 75,000 m^3/h, a wind speed of 3.8 m/s, and recirculation turned on, the average humidity is 15.2%; the average humidity is 15.2% at a temperature of 26.1°C (Option 1).

Table 1. *Heat-moisture state of NSC volumes depending on the number of ventilation units (VU) injected into the AS, operating recirculation and external wind speed.*

Variant No.	n-r VU	Total flow VU, m^3/h	Recycling	Wind speed, m/c	Annular space (AS)		Main volume (MV)	
					Temperature, °C	Humidity, %	Temperature, °C	Humidity, %
1	3	75000	є	3.8	26.1	15.2	23.2	32.7
2	2	50000	є	3.8	23.7	19.7	21.3	39.1
3	2	50000	є	7.3	23.3	23.3	20.7	44.3
4	2	50000	є	25	21.7	36.0	18.5	66.7
5	2	50000	–	3.8	24.02	19.14	21.77	39.88

In this main volume, the temperature is lower, and the humidity is higher, since colder (15°C) and more humid (100%) air from the environment enters there.

Table 1 also shows the average values of humidity over the entire volume of the AS, although since there are uneven temperatures in the air of the AS, they lead to uneven humidity, which was also studied using simulation. With a fully operating ventilation system (option 1), the distribution of temperatures, humidity and their maximum values are shown in Figure 3.

For variant 1 (Table 1) temperature differences were 11°C humidity up to 7% with a maximum humidity of 17% and a minimum of 10%. When the air recirculation system was turned off, the temperature drops were 9°C, and the humidity was up to 12% at a maximum humidity value of 22%, which does not differ significantly from the values with the recirculation turned on.

Conclusions

1. The problem of providing a microclimate in the NSC with the help of a complex ventilation system for pumping dried air and recirculating it in the annular space is considered, which is analyzed using the developed three-dimensional CFD model of the thermal state of a complex arched configuration of the NSC volumes for the selected design parameters of the conditions.
2. The CFD model made it possible to show that, under the considered design parameters of ventilation operation, the detailed distributions and maximum temperature drops in the NSC annular space do not exceed 9°C, humidity drops do not exceed 7% during normal operation of the dry air injection and recirculation system. It is also shown that with the considered parameters of ventilation operation, the maximum value of humidity in the AS is 17%, which is much lower than the limit value of 40%, which makes it possible to reduce the performance of the dry air injection and recirculation system.

References

[1] Krukovskyi P.G., et al., *New Safe Confinement of the Chernobyl NPP (computational and experimental analysis during design and operation)*, Kyiv. 2019. 300 p., ISBN 978-966-97864-7-0.

[2] Smolchenko D.A., Dyadyshko Y.V., Sklyarenko D.I., Krukovskyi P.G., *Analysis of Ways to Improve the Energy Efficiency of the Ventilation and Humidity Control System in the New Safe Confinement of the Chernobyl NPP*. Renewable Energy and Energy Efficiency in the 21st Century: materials international science-practical. online conf. 19-20 may. 2022 p., Kyiv: NTUU KPI, 2021. p. 85-88.

OPTIMIZATION OF COMBUSTION PROCESSES IN VORTEX HEAT GENERATORS

Valerii Fedoreiko, Roman Zahorodnii, Mykola Rutylo, Nazar Burega

V. Hnatiuk Ternopil National Pedagogical University,
2 Maxyma Kryvonosa Str., Ternopil, 46027, Ukraine
e-mail: zagoroman@ukr.net

Fact-based research shows that the replacement of traditional fuel with renewable biological wastes of local origin contributes to a significant reduction (by 5-7 times) of gas consumption, creates almost zero burden on the environment, as well as provides additional work places.

Our state agricultural sector annually produces a technically available volume of biowastes in the amount of 25 million tons. Given that 2.5-3.0 tons of these wastes replaces 1000 m^3 of natural gas, the implementation of diversification efforts in primary heat generation systems can make up a value equivalent to the import of 9-10 billion m^3 of gas [2].

The study provides comprehensive automation of the processes of heat energy production from uncertified fuels based on artificial intelligence systems, controlled by adjustable asynchronous electric drives, specially adapted sensors of: temperature, humidity, speed, pressure levels, etc. Given the undetermined nature of changes in technological parameters, it is foreseen the creation of process models, the development of adaptive control algorithms, software, which in complex will streamline the combustion of uncertified fuel in continuous vortex furnace, coordinate the supply of combustion products to the heat exchanger, to determine the range of air supply for heating to the required inlet temperature. It is necessary to take into account the type of fuel, its calorific value, humidity, particle size distribution for the possibility of controlling the regulated supply with the dosing fan. Adjustable fans of the vortex combustion chamber provide an optimal combustion zone for uncertified fuel, preventing its movement to the upper part of the heat generator, where the exhaust fan is primary mixing combustion products with atmospheric air and the temperature at the top of the furnace is reducing to 650-700°C, to prevent overheating of the primary chamber of the heat exchanger.

The research is aimed at the development a control system that will ensure the coordination of all the above undetermined parameters of the technological process to optimize energy-efficient heat production modes in systems of vortex combustion of uncertified fuel.

Heat generators based on vortex continuous combustion of uncertified crushed fuel are used in the research (Fig. 1). Fuel supply into them is carried out by means of the screw dispenser with the frequency-regulated asynchronous electric drive and the aspiration fan.

Figure 1. *Exploratory prototype of a 2500 kW heat generator-utilizer with the principle of vortex combustion of uncertified fuel.*

To increase the energy efficiency of heat energy production systems, an automated control system has been developed, which will take into account a number of nondeterministic factors, including that which are influencing its operation: calorific value of a fuel, temperature and humidity of the air supplied to the combustion chamber.

Studies performed show that to determining of the optimal modes of operation of heat energy production systems that use uncertified fuel, it is necessary to take into account its calorific values. The efficiency of the fuel combustion process ensures the cost efficiency of the heat generator' operation and helps to reduce environmental pollution. The process of vortex combustion requires regulation of air supply, in accordance with the humidity, heat and technical properties of the fuel, in particular, taking into account the excess air coefficient value.

In addition, for efficient combustion of solid fuel, it is necessary to ensure coordinated control of specific modules of electricity technological complex of the heat generator, in particular solving the problem of regulating the speed of electric drives of fans and a screw, which determine the dosing volumes of fuel mixture components and vortex combustion modes.

Simulation modeling theory was used to create computer models and the Matlab/Simulink software environment was used; graphical presentation of modelling results was performed using MS EXCEL and Matlab environment.

The Figure 2 presents a block diagram of the control system for technological modes of operation of the bioheat generator. It is performed by means of computer simulation modelling in MATLAB environment (Simulink).

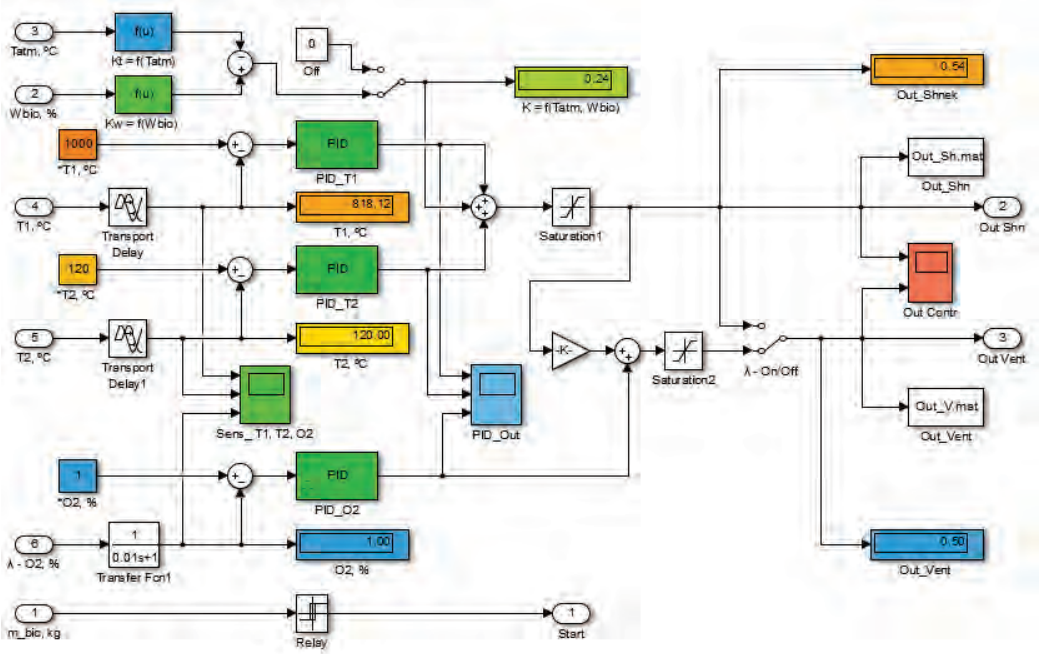

Figure 2. *Heat generator control system with three-circuit interconnected PID control.*

A specific feature of this model is the three-circuit interconnected proportional-integral-differential (PID) control of fuel and air with dispensers taking into account their humidity and ambient air temperature, as well as making corrections of productivity control of operating devices (dispensers) basing on these data.

Such an approach enables to reduce the error of regulation in the dynamic of the equipment transient operation modes, especially obvious during the occurrence of stochastic changes in humidity of uncertified fuel.

The PID_T1 controller maintains the set temperature (1000°C) in the combustion chamber (furnace) until the set temperature of the heat transfer agent T2 (120°C) is set at the exit from the heat generator, then it switches to the output value limiting mode and, thus, does not affect the

control process. The temperature in the furnace is reduced, and the temperature of the heat transfer agent (T2) is maintained constant by introducing of the controller PID_T2 into the control process. The signals from the controllers PID_T1 and PID_T2 are fed to the summing unit, which also receives the correction signals K = f(W bio, T atm), functionally related to the humidity of biofuel W bio and the air ambient temperature T atm. The corresponding control signals generated in this way are fed to the control channel of the screw dispenser Out Shn.

To ensure the completeness of the fuel combustion and, at the same time, to increase the energy efficiency of the heat generator in the system, the control of the percentage concentration of oxygen (O2) in the flue gases by using a λ-probe is foreseen. Information from this sensor is fed through the comparison element to the entrance of the PID_O2 controller and the corresponding control signals from it through the summing unit are fed to the control channel of the air fan-dispenser Out Vent. The productivity of the dispensers for the fuel mixture components is controlled by the frequency-regulated asynchronous electric drives with energy consumption optimization functions.

Conclusions

1. The efficiency of rational dosing of combustion components with the use of regulated operational modes of the fuel supplying screw and fans is substantiated for the first time, which will increase the energy efficiency of solid fuel heat generators, reduce harmful emissions into the atmosphere, ensure safe fuel supply into the combustion chamber.
2. Rational modes of dosing the fuel mixture components are determined, experimental researches of energy-efficient heat generation processes in the systems of the vortex combustion of uncertified fuel were carried out. The research results are used in the process of setting up the technology control system based on the fuzzy logic.

PROSPECTS OF BIOMETHANE PRODUCTION IN UKRAINE

Georgii Geletukha

Institute of Engineering Thermophysics of the National Academy of Sciences of Ukraine,
Marii Kapnist street, 2a, Kyiv, 03057, Ukraine
e-mail: geletukha@uabio.org

Introduction

Biomethane as a close analogue of natural gas can be used for the production of heat and electricity, as a fuel for transport as well as raw materials for the chemical industry. In addition, the production of biomethane is in line with the idea of circular economy as it converts agricultural by-products or household waste into energy ensuring the recycling of nutrients to agricultural land. The common opinion of experts in biogas sector is that "biomethane is the future of biogas".

Prerequisites and advantages of biomethane production in Ukraine

Ukraine has the largest area of agricultural land in Europe, and, accordingly, one of the world´s best potentials of agricultural raw materials for biomethane production. Highly developed existing natural gas supply network in Ukraine (both main pipelines (GTS) and distribution networks (GDS)) with all necessary infrastructure compatible for biomethane transmission as technically close analogue of natural gas. That includes storage facilities, pipelines, valves, regimes of operation, operator instructions, automatics, and personnel qualification. Connection of existing main gas pipelines of Ukraine to the European hubs creates possibility for biomethane export to the EU.

Biomethane is ready for injection into the gas network today unlike hydrogen. No investment is required in the modernization of gas networks (GTS and GDS) and gas equipment (gas burners, engines, turbines, valves etc.). Biomethane can help to load the Ukrainian GTS after the termination of the contracts with Russia.

Biomethane plants, in addition to biomethane, generate digestate, which can become the main organic fertilizer needed for the revival of Ukrainian soils.

Investments in biomethane plants are close to investments in biogas plants with electricity generation (approximately 2.5-3.0 thousand EUR/kW_{el}). The approximate calculations are as follows: a biomethane plant with a capacity of 10 million m^3/year of biomethane, is an analogue of a biogas plant with a capacity of 4 MW_{el}, and it will cost about 10 million Euros. Accordingly, to deliver one billion m^3 of biomethane into the natural gas network, Ukraine needs 100 plants of 10 million m^3/year. Accordingly they will cost one billion Euros in total.

The roadmap for the development of bioenergy in Ukraine until 2050 provides for the introduction and growth of biomethane production in Ukraine to 1.7 billion m^3/year in 2035 and up to 3 billion m^3/year in 2050 (Geletukha et al. 2021).

By author's estimates the total biogas production could reach 1.6 billion m^3/year CH_4 in 2030 (Geletukha et al. 2022). The significant part of that biogas could be upgraded to biomethane. Total biomethane production could be 1.0 billion m^3/year in 2030. It is expected that biomethane could partly (0.2 billion m^3/year) be exported to the EU. The rest could be utilized locally for combined heat and electricity generation in CHP units (0.5 billion m^3/year), heating and industry applications (0.23 billion m^3/year) and for transportation purpose (0.08 billion m^3/year). In such a way biogas sector could serve the growing demand in sustainable and clean energy from the transport and industry sectors.

Feedstock for biomethane production

A variety of organic materials can potentially be used for biogas production, including specially grown crops, by-products and wastes from plant and animal products, animal husbandry wastes, and other anthropogenic wastes. Due to the limited statistical data available to serve as input data for further estimation of waste volumes only main types of wastes and by-products are covered by this assessment including the following organic materials:

1. Animal husbandry wastes, including cattle manure, pig manure, poultry litter, sheep and goat manure formed during animal keeping at the enterprises.
2. Maize silage, specially grown.
3. Crop residues of major crops, including wheat, rye, barley, maize, sunflower, soybean, rapeseed and sugar beet.
4. Food & beverage industry by-products and wastes.
5. Sewage sludge from municipal treatment facilities.
6. Organic fraction of solid waste.

Results and discussion

The estimated biomethane potential from the most prospective feedstock types described above amounts to 9.73 billion m^3 CH_4 a year, as on 2020 (Fig. 1).

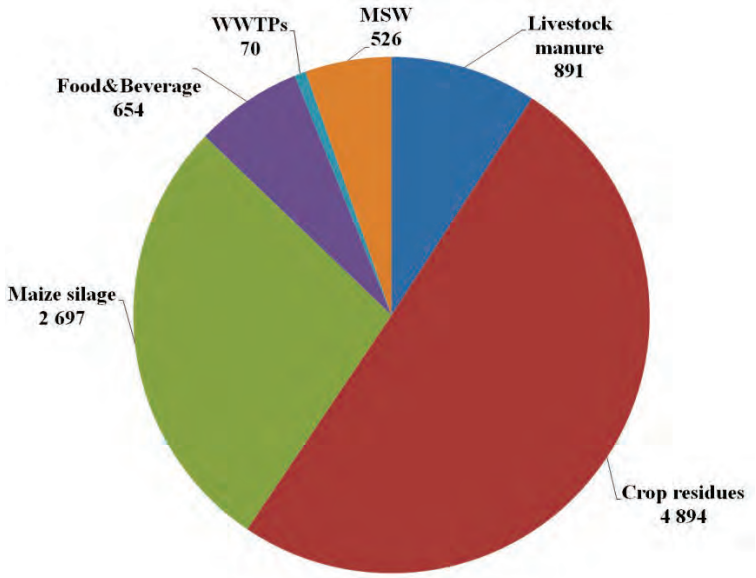

Figure 1. *Biomethane potential in Ukraine by feedstock type as on 2020, mln m^3CH_4 a year (2020).*

Half of this potential is related to crop residues and one third to maize silage production. Animal husbandry wastes can contribute by 9.2%. Food & beverage industry can contribute by 6.7%.

Organic fraction of MSW and wastewater sludge could contribute together by additional 6.1%. The potential of biogas production from municipal sewage sludge amounts to only 69.6 mln m^3CH_4 per year. The overall potential related to temporarily occupied territories of Ukraine amounts to 467 mln m^3CH_4 per year or 4.8%.

The most valuable potential among food&beverage by-products belongs to sunflower oil industry and sugar production. The overall potential that oil by-products could contribute amounts to 0.32 billion m^3CH_4 a year, whereas oil press cake only can give 203 mln m^3CH_4 a year. Sugar beet press can contribute 205 mln m^3CH_4 a year. The rest accounted types of by-products amounts to the little shares, however in total can contribute up to 35% to food & beverage biomethane potential. Estimated biomethane potential from food&beverage by-products related to TOT contribute only 0.4%.

In 2050, the total production potential of biogas/biomethane may increase to 17 billion m^3/year. A significant increase in capacity is projected due to the growth of industrial production, expansion of the raw material base for biogas/biomethane production, consolidation of livestock enterprises and the transition from solid waste disposal to the use of mechanical and biological treatment technology.

Regional level

At the level of regions of Ukraine, almost a half of the potential for biomethane production is concentrated in 6 regions of Ukraine (Vinnytsia, Kyiv, Cherkasy, Poltava, Dnipropetrovsk and Donetsk) (Figs. 2 and 3).

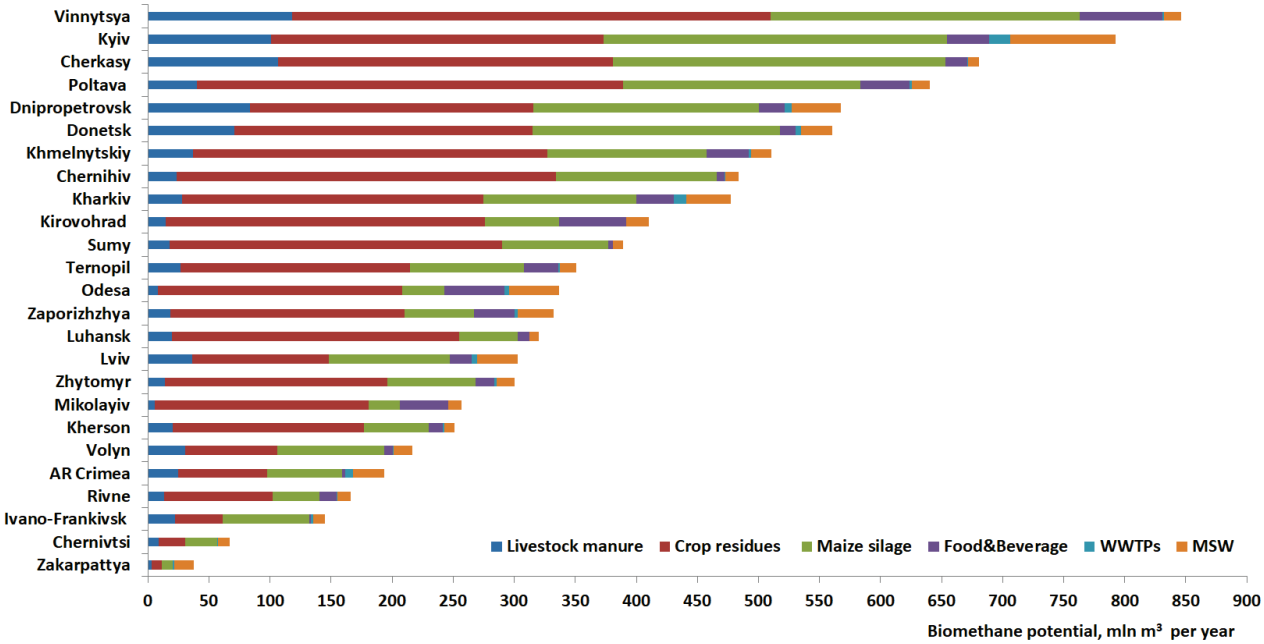

Figure 2. *Biomethane potential by regions and by feedstock type (2020).*

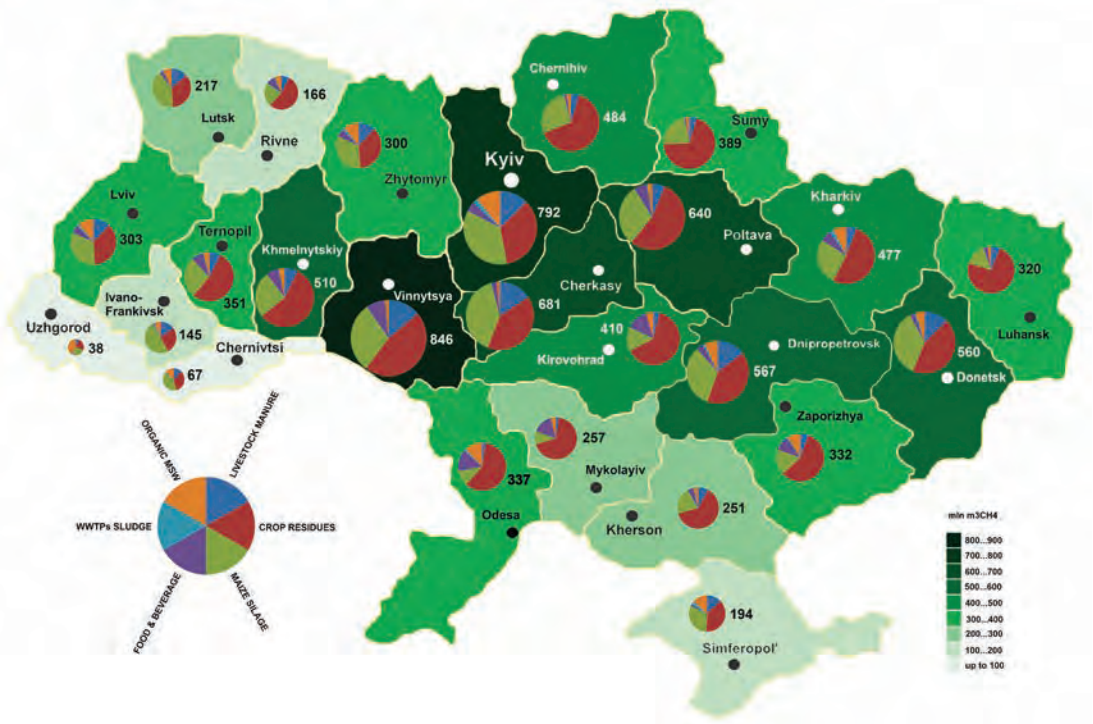

Figure 3*. Mapping biomethane potential by regions and by feedstock type, mln m^3CH_4 a year (2020).*

The highest potential estimated in Vinnytsya region, while the lowest in Zakarpattya region. Biomethane potential by regions ranges from 38 mln m^3CH_4/year to 846 mln m^3CH_4/year, averaged at 385 mln m^3CH_4/year by region.

Conclusions

Current Ukraine's Energy Strategy sets an ambitious goal of achieving 11 Mtoe of biomass, biofuels and waste in the total supply of primary energy in 2035. It corresponds to 11.5% of the total primary energy supply. Biogas and especially biomethane will play important role in this development.

Production of biomethane with biogas upgrading to the quality of natural gas can significantly increase the energy efficiency of biogas utilisation. The main advantage of biomethane compared to green hydrogen is the possibility of its transportation using the existing gas infrastructure without modernisation.

We believe that in the coming years after the adoption of legislation to support the development of biomethane production, the most of biomethane produced will be exported to EU countries, which have created more favorable conditions for its consumption. As Ukraine's economy grows, more and more of the biomethane produced will remain for domestic consumption.

References

[1] Geletukha G., Zheliezna T. (2021), *Prospects for Bioenergy Development in Ukraine: Roadmap until 2050*. Ecological Engineering & Environmental Technology. 22(5), pp. 73-81, http://www.ecoeet.com/Prospects-for-Bioenergy-Development-in-Ukraine-Roadmap-until-2050,139346,0,2.html.

[2] Geletukha G., Kucheruk P., Matveev Y. (2022), *Prospects and Potential for Biomethane Production in Ukraine*. Ecological Engineering & Environmental Technology. 2022, Vol. 23, Issue 4, pp. 67-80, http://www.ecoeet.com/Prospects-and-Potential-for-Biomethane-Production-in-Ukraine,149995,0,2.html.

APPLICATION OF PHASE CHANGE MATERIALS IN VENTILATION SYSTEMS – A REVIEW

Beata Galiszewska

Kielce University of Technology, al. Tysiąclecia Państwa Polskiego 7, 25-314 Kielce, Poland
e-mail: bgaliszewska@tu.kielce.pl

Heat losses caused by ventilation systems significantly affect energy consumption in buildings. Therefore, it seems reasonable to look for solutions to improve the efficiency of heat recovery and storage in ventilation systems. One example of such solutions are thermal energy storage systems using phase change materials (PCM), which can be a way to improve the thermal performance of a building. Utilizing the increased energy absorption capacity of phase transition temperatures through phase change materials, increases the efficiency of energy accumulation and subsequent release. The use of sensible and latent heat of PCM materials can significantly affect the efficiency of heat recovery and storage in ventilation systems. The paper presents an overview of various applications PCM in ventilation systems. The study presents the method of conducting selected research and the results achieved.

TEMPERATURE DISTRIBUTION ANALYSIS ON THE SURFACE OF THE RADIATOR WITH AN INFRARED CAMERA AND THERMOCOUPLES

Dagmara Kotrys-Działak, Katarzyna Stokowiec

Kielce University of Technology, al. Tysiąclecia Państwa Polskiego 7, 25-314 Kielce, Poland
e -mail: ddzialak@tu.kielce.pl

The aim of the work was to perform experimental tests of the thermal analysis on the outer surface of the radiator. For this purpose, a localized test stand was used in one of the lecture rooms in Kielce University of Technology. The experiment concerned the isothermal character of a radiator during its operation. Temperature distribution was verified with two different methods: thermocouples and thermovision camera. The radiator was divided into 8 measuring fields and temperature was measured in each of them. The experiments were conducted for different supply flow rates of the medium. The results were presented by means of diagrams comparing both methods of temperature survey.

VI International
Scientific-Technical Conference

Book of abstracts

ACTUAL PROBLEMS OF RENEWABLE ENERGY, CONSTRUCTION AND ENVIRONMENTAL ENGINEERING

The time and place of the meeting: 24-27 November 2022
Faculty of Environmental, Geomatic and Energy Engineering,
Kielce University of Technology, Poland